UNIVERSITÀ DEGLI STUDI DI PADOVA

Sede Amministrativa: Università degli Studi di Padova
Dipartimento dei Beni Culturali: archeologia, storia dell'arte, del cinema e della musica (dBC)

CORSO DI DOTTORATO DI RICERCA IN: Storia, Critica e Conservazione dei Beni Culturali
INDIRIZZO: Archeologico-scientifico
CICLO XXIX

TRACING PROVENANCE OF MESOLITHIC AND NEOLITHIC POTTERY ALONG THE NILE RIVER BY TRACE ELEMENTS AND Sr ISOTOPE ANALYSIS

Tesi redatta con il contributo finanziario di INPS Gestione Dipendenti Pubblici - Progetto Homo Sapiens Sapiens

Coordinatore: Ch.mo Prof. Vittoria Romani
Supervisore: Ch.mo Dott. Lara Maritan
Co-Supervisori: Ch.mo Dott. Sandro Salvatori
Ch.mo Dott. Giancarlo Cavazzini

Dottorando : Elisa Gravagna

CONTENTS

Summary..... 1

Sommario 4

INTRODUCTION 7

FIRST CHAPTER
PREHISTORY OF CENTRAL-NORTHERN SUDAN: A BRIEF OVERVIEW

1.1 Introduction 13

1.2 The archaeological problem 16

1.3 Al Khiday archaeological sites 18

1.4 Al Khiday: the pottery assemblage 22

1.4.1 Site 16-D-5 23

1.4.2 Site 10-W-4 25

1.5. Pottery from other archaeological sites 26

1.5.1. The Blue Nile: Wadi Soba area..... 26

1.5.2. The Wadi Howar region..... 27

SECOND CHAPTER
CENTRAL-NORTHERN SUDAN: GEOLOGICAL AND HOLOCENE ENVIRONMENTAL CONTEXT

2.1 Geology of Central-Northern Sudan..... 29

2.2 The Nile River..... 31

2.3 Location of archaeological sites from environmental and geological viewpoints..... 33

THIRD CHAPTER
PROVENANCE STUDIES AND TECHNIQUES

3.1 Pottery and provenance studies..... 41

3.2 Petrographic analysis..... 43

3.3 Chemical analysis and statistical treatment of data (XRF) 47

3.4 Mineralogical analysis and statistical treatment of data (XRPD) 50

3.5 Microstructural analysis (SEM) 51

3.6 Thermal analysis of clay materials (TGA and DSC) 52

3.7 Sr isotope analysis (Thermal ionization mass spectrometry) 54

FOURTH CHAPTER
DESCRIPTION OF THE SAMPLES

4.1 Clay samples and other raw materials..... 61

4.2 Pottery samples..... 65

4.2.1 Quartz-tempered pottery 66

4.2.2 K-feldspar tempered pottery..... 69

FIFTH CHAPTER
RAW MATERIALS ALONG THE NILE RIVER: CLAY, SAND AND ROCK SAMPLES

5.1 Preparation of the samples..... 72

5.2 Petrographic analysis..... 72

5.3 Mineralogical analysis and statistical treatment of data (XRPD) 78

5.4 Chemical analysis and statistical treatment of data (XRF) 80

5.5 Microstructural analysis (SEM) 93

5.6 Thermal analysis (TGA and DSC) 98

5.7 Sr isotope analysis (TIMS) 103

5.8 Discussion and conclusion..... 110

SIXTH CHAPTER
MESOLITHIC AND NEOLITHIC POTTERY FROM CENTRAL-NORTHERN SUDAN

6.1 Preparation of the samples..... 113

6.2 Petrographic analysis..... 113

6.3 Chemical analysis and statistical treatment of data (XRF) 117

6.4 Microstructural analysis (SEM) 128

6.4.1 Secondary phases..... 131

6.4.2 Biological inclusions..... 134

6.5 Sr isotope analysis (TIMS) 136

6.6 Discussion and conclusion..... 141

CONCLUSIONS..... 145

APPENDIX..... 149

REFERENCES..... 161

Summary

The aim of this research is to define the provenance of Mesolithic and Neolithic pottery found in some prehistoric sites in Central-Sudan. The study focuses on the analysis of both local raw materials (clay and temper) and ceramic artefacts. In particular, this research is orientated towards the application of Sr isotope analysis ($^{87}Sr/^{86}Sr$) to pottery characterised by similar pastes in terms of bulk chemical and petrographic composition. Moreover, the possibility of using Sr isotope analysis in provenance studies of pottery in Central Sudan is here investigated.

The analysed samples have been found in several Mesolithic and Neolithic sites located along the Nile River across Central-Sudan and on an area located western of the river, in ancient times connected to the Nile by a tributary. The full set of samples includes both raw materials and pottery sherds. A total of 29 clays have been collected between 2013 and 2014 along the Nile system, covering a distance of nearly 1600 km, while during 2015 campaign six more samples have been added to the set of samples. Raw materials are described by a total of 35 geological samples, including clays, sands and rocks. As regards pottery, the initial selection criteria have been discussed with the archaeologist, Sandro Salvatori, and lead to the creation of a set of samples made by Mesolithic sherds found at Al Khiday (16-D-5) characterized by both quartz-tempered paste and decorative motifs that have a wide spatial-temporal distribution in Central Sudan (Rocker stamp dotted zigzag and Rocker stamp plain zigzag). Later, the set have been increased by adding Neolithic quartz-tempered pottery coming from both Al Khiday (16-D-5) and other regions where the same decorative motifs have been found, and in particular from: i) the Wadi Soba area, located along the Blue Nile and particularly the sites of Sheikh Mustafa and Al Mahalab supplied four sherds; ii) the Wadi Howar region lies in southern fringe of the Sudanese Eastern Sahara, and three samples from the site of Ennedi Erg have been studied. Lastly, the study was integrated with the analysis of K-feldspar-tempered pottery that has been found in several prehistoric archaeological sites of central Sudan, included Al Khiday. While raw materials and quartz-tempered pottery have been ground as is usual, pastes of K-

feldspar-tempered pottery were micro-drilled in order to collect only the fine matrix and remove the K-feldspar inclusions. The issue regarding K-feldspar provenance is still under debate: it is usually found in combination with specific ceramic decorations (*incised wavy line, rocker stamp dotted zigzag packed, alternating pivoted stamp*) but its geological origin is attributable to outcrops of granite-like rocks (granite, syenite, and related ring complexes) that lies only in relatively small areas far away from Al Khiday sites (about 80-100 km), as the nearest location where they outcrop. Therefore, movement of raw materials or finite objects? The answer to this issue is very important to define social structure, relationships and exchange patterns within Mesolithic hunter-gatherer-fisher communities of central Sudan.

As regards pottery studies, usually the localisation of the supply zone (the zone where people had direct access to the source of raw material/s) and therefore the definition of the provenance area are based on the presence of specific minero-petrographic markers if the ceramic production is committed to coarse pastes. If the pastes are of fine manufacture, the supply zone is identified by geochemical characteristics belonging to specific reference groups (e.g. production wastes). Nevertheless, in many cases the lack of specific traits of both lithological and geochemical nature prevents the resolution of important issues concerning pottery provenance. In the particular case study of Al Khiday, the presence of abundant quartz in the pastes causes a strong dilution effect also on trace elements potentially useful as markers of provenance. In cases where the coarse fraction of a ceramic is composed entirely of quartz (SiO_2), which does not contains significant amounts of Rb or Sr, the Sr isotopic composition of the ceramic is derived almost entirely from the clay fraction. For this reason, the region of Central-Sudan is a suitable area where to apply this analytical method. The application of Sr isotopic analysis in ceramic provenance study rests on the premise that the geological origins of the minerals in ceramic pastes are not entirely obscured by processes associated with ceramic production.

The comparison between the isotopic fingerprint of clays deposited by the Nile River across the central-Sudan and that of pottery coming from aforementioned prehistoric archaeological sites helped in the interpretation of provenance and production. Some supply zones have been excluded while others turned out to be more than plausible. Nevertheless, the study of pottery through Sr isotope analysis must face also the fact that the ceramic vessels were used in daily life and were subject to contamination by solid and liquid food. The comparison of Sr isotope signatures obtained from clay and pottery yielded information about the mixing processes of Nile sediments along the

areas of interest and about some possible supply zones for raw materials used in pottery production. Because of the contamination of the sherds, which is evident analysing the bulk Sr contents, it is possible to make only some hypothesis about pottery provenance but all this information considerably contributed to the reconstruction of the material culture of Mesolithic and Neolithic populations of central Sudan.

Sommario

Scopo di questo progetto è lo studio di provenienza di ceramiche antiche rinvenute in alcuni siti archeologici del Sudan centrale, inteso come analisi sia delle materie prime locali che delle produzioni ceramiche. Nello specifico il lavoro è stato rivolto all'applicazione dell'analisi degli isotopi dello Stronzio ($^{87}Sr/^{86}Sr$) allo studio di manufatti ceramici che presentano impasti analoghi in termini di composizione petrografica e chimica di bulk, con la possibilità di utilizzare tale metodo per la determinazione della provenienza. I frammenti ceramici oggetto di studio provengono da diversi siti Mesolitici e Neolitici situati lungo il corso del Nilo che attraversa il Sudan centrale e in un'area posta ad ovest di questo, attraversata da uno dei suoi antichi affluenti. Il set di campioni analizzati include sia argille che ceramiche. Un totale di 29 argille è stato campionato tra il 2013 ed il 2014 coprendo una distanza di circa 1600 km, mentre nella campagna del 2015 ne sono state aggiunte sei, per un totale di 35 campioni geologici, tra argille, sabbie e rocce. Per quanto riguarda le ceramiche, dopo un confronto con l'archeologo Sandro Salvatori, per iniziare sono stati selezionati campioni provenienti dai siti di Al Khiday (16-D-5) appartenenti al periodo Mesolitico, decorati secondo uno stile ben distribuito nell'arco spazio-temporale relativo al Sudan Centrale (Rocker stamp dotted zigzag e Rocker stamp plain zigzag) e caratterizzati da impasto temperato a quarzo. Successivamente il set di campioni è stato ampliato aggiungendo ceramiche, sempre temperate a quarzo, appartenenti al periodo Neolitico provenienti sia dal medesimo sito di Al Khiday (16-D-5) che da altre zone in cui è stato rinvenuto lo stesso tipo di ceramica decorata con il medesimo motivo: la regione di Wadi Soba lungo il Nilo Blu, nello specifico i siti di Sheikh Mustafa e Al Mahalab; i siti della regione di Wadi Howar nel nord-ovest del Sudan, più precisamente dall'Ennedi Erg. Infine il quadro è stato completato con lo studio degli esemplari di ceramica temperata a feldspato potassico rinvenuta in numerosi siti archeologici, compreso quello di Al Khiday. Da questi impasti è stata meccanicamente prelevata unicamente la matrice fine e sono stati rimossi gli inclusi di feldspato potassico, la cui presenza determina delle importanti variazioni composizionali rispetto a quelle dell'argilla utilizzata. L'ipotesi della provenienza di questo smagrante

è ancora dibattuta: si trova principalmente abbinato a specifici motivi decorativi (*incised wavy line, rocker stamp dotted zigzag packed, alternating pivoted stamp*) ma la sua origine geologica è imputabile ad affioramenti di rocce di tipo granitico che si trovano solo in determinate aree a molti chilometri di distanza (almeno 80-100 km) dai siti di Al Khiday. Questa parte del lavoro è stata rivolta alla risoluzione della questione se il feldspato venisse importato nei centri produttivi e mescolato con le argille locali di queste aree, o se i manufatti ceramici venissero prodotti in vicinanza delle zone di affioramento del feldspato e poi diffuse regionalmente. Pertanto, circolazione di una materia prima o di prodotti finiti? La risposta a questo quesito rappresenta un elemento importante nella definizione delle relazioni e della struttura sociale delle comunità di cacciatori-raccoglitori-pescatori Mesolitici.

Per quel che riguarda i materiali ceramici, la presenza di markers minero-petrografici in produzioni ad impasto grossolano e specifici caratteri geochimici riferibili a gruppi di riferimento, cioè a produzioni di sicura origine locale (scarti di cottura, materiali di fornaci) o a materiali argillosi per le produzioni ad impasto fine, costituiscono il miglior vincolo nella definizione delle aree di approvvigionamento delle materie prime, e pertanto della provenienza. In molti casi però, l'assenza di elementi peculiari, siano essi litologici o geochimici, impedisce di risolvere importanti problematiche di provenienza delle ceramiche. Negli impasti presi in esame, inoltre, la predominanza di smagrante quarzoso determina anche un forte effetto di diluizione degli elementi in traccia, che quindi non consente di fornire indicazioni sulla provenienza delle argille. Per questo motivo il territorio del Sudan centrale preso in esame rappresenta una zona adatta per sperimentare questa indagine scientifica e, proprio in questo caso, l'analisi dei rapporti isotopici dello stronzio potrebbe rivelarsi decisiva; nei casi in cui viene utilizzato uno smagrante quarzoso, il quale non contiene quantità significative di Rb o Sr, la composizione isotopica dello stronzio nella ceramica è derivata per lo più dalla frazione argillosa/limosa.

Il confronto tra l'impronta isotopica delle argille deposte dal Nilo lungo il suo corso attraverso il Sudan centrale e quella delle ceramiche provenienti dai siti sopracitati ha fornito una chiave di lettura per definire la provenienza di manufatti nei quali l'assenza di markers petrografici ne impedisce invece la collocazione. Alcune aree di approvvigionamento sono state escluse mentre altre sono risultate essere più plausibili. Tuttavia, lo studio del rapporto isotopico dello Sr in manufatti ceramici deve fare i conti con il fatto che questi oggetti erano parte integrante della vita quotidiana

di queste popolazioni ed erano legati alla preparazione e alla consumazione del cibo, sia solido che liquido.

Il confronto dei rapporti isotopici dello Sr di argille e ceramiche ha fornito informazioni sia riguardo ai processi di mescolamento dei sedimenti lungo il corso del Nilo nel Sudan centrale che ad alcune possibili zone di approvvigionamento di materie prime per la produzione delle ceramiche prese in esame. Ma, a causa della contaminazione dei frammenti ceramici, la quale si manifesta principalmente nell'analisi del contenuto in Sr, è possibile abbozzare solo alcune ipotesi sulla provenienza di queste ceramiche, sulla unica base isotopica. Tuttavia queste informazioni hanno contribuito in modo considerevole alla ricostruzione della cultura materiale delle popolazioni Mesolitiche e Neolitiche del Sudan centrale.

INTRODUCTION

Pottery artefacts represent the group of archaeological findings more widely and extensively studied to improve the knowledge of ancient populations. Several aspects of pottery production come into play in order to define socio-economic systems and they can range from provenance and supply zones to exchanges of materials and expertise. Usually, the archaeological research is based on the study of decorations, fabrics, shapes, chronology and typology. Lately, archaeometry supplied an interdisciplinary approach in order to complement the information obtained by archaeologists with the aim of provide a scientific characterization and to solve questions mainly concerning their provenance, production technology, use in relation to the food processing and storage, and alteration for conservation purposes and post-depositional environmental reconstruction.

In this context of interdisciplinary approach, the Italian archaeological mission directed by Donatella Usai and Sandro Salvatori has always looked for scientific collaborations in order to disclose the social, ideological and material production complexity of the prehistoric communities of central Sudan. The first to write about Mesolithic in central Sudan was A.J. Arkell (1947, 1949) who excavated the Mesolithic site of Khartoum Hospital, characterized by the presence of decorated ceramics, with a great variability in decorative motifs, bone instruments, a peculiar chipped-stone industry and a consistent number of grinding stones and grinders. The finding of the same decorative motifs in different sites far away one from each other suggest intensive and recurrent contacts and movement, both of materials and people. Moreover, the Mesolithic groups of central Sudan were characterized by a semi-sedentary way of life relied on hunting, gathering and fishing.

The study of Khartoum Mesolithic culture had to face several issues concerning the environmental context: the territory has been subjected to a gradual process of desertification that is strictly related to a series of climatic crises starting with the 8200 cal. BP one (Zerboni, 2013) driving strong wind and water erosion phenomena (Cremaschi and Zerboni, 2009). These important climatic changes caused the progressive dry, from the end of the VII but more intensively from the middle of the V

millennium BC, of the Saharan and sub-Saharan regions, including also Upper Nubia and central Sudan, previously characterized by a humid environment. Nearby the sites, archaeological materials have been scattered for several tens of meters but they were already lying right underneath the surface level. This disturbance of the archaeological sequence is mainly due to the building of Meroitic, Post-Meroitic, Christian and Muslim graves whose construction usually reshuffle the earth primarily digging the burial chamber, then gathering the earth to shape a tumulus (Salvatori et al, 2011; Salvatori, 2012).

The importance of the work of the Italian archaeological mission in Central-Sudan relies on the fact that the Al Khiday sites provide the first well-preserved, quite continuous Mesolithic stratigraphic sequence of the whole region. The sequence of events that occurred in this area on the western bank of the White Nile started from the occupation of the Pleistocene banks of the Nile River at the beginning of the VII millennium BC (Salvatori et al, 2011; Salvatori, 2012; Zerboni, 2011). The rising banks were suitable for the settlement placement because the proximity of the seasonal floods of the river was not a danger for the settlement itself during the Holocene. The repeated seasonal occupation caused the accumulation of materials but after the Neolithic period, the disturbance activities started to compromise the archaeological layers causing the loss of stratigraphy (Salvatori et al, 2011).

One of the most abundant findings coming from Mesolithic and Neolithic layers at Al Khiday is pottery. It is mainly composed by clay mixed with quartz-rich sand, which was added as a temper in order to improve the mechanical and physical properties (Salvatori, 2012; Dal Sasso et al, 2014). The paste type, with other aspects of the manufacture, including the decoration, represents one of the basic elements to identify the existence of exchange systems. The decorative system of a ceramic product can be considered an out-and-out meta-language which takes on, among other, also the identity of the community which produced it. Unfortunately, the absence of mineral and rock markers in the quartz-predominant pastes does not allow to define which decorative motifs are representative of specific groups, limiting in this sense the understanding of the social organization, of the material culture and of the changes which interested the transition from Mesolithic to Neolithic in central-northern Sudan, as well as possible exchanges of materials between also far away regions. Since on the basis of the minero-petrographic composition of inclusions it is not possible to constraint the provenance of the pottery with this type of paste, and considering the monotony of the Nubian Desert sand in terms of petrographic composition, different

methods are required to define if the pottery was locally produced or was imported/exchanged from other areas/communities. Moreover, the occurrence of abundant quartz inclusions causes a strong dilution effect also on those trace elements that in other cases can be used for provenance studies of pottery on a chemical base. In this frame, the possibility of using Sr isotopes ratio can be decisive in provenance studies. In ceramic pastes in which inclusions and added temper are Sr-free or very low (like quartz sand), the $^{87}Sr/^{86}Sr$ ratio is constant, being independent from the inclusions content, and therefore is representative of the used base-clay.

Since the beginning of the research planning, northern and central Sudan appeared to be a suitable region for the experimental application of this new analytical method. Nile and its tributaries are characterized by different isotope signatures in relation to the different rock types outcropping in the respective hydrographic basins of White, Blue and Main Nile and Atbara, and in particular to the Tertiary basalts, Mesozoic clastic sedimentary sequences (mainly sandstone) and Precambrian basement (metamorphic rocks and granitic and syenitic intrusions) (Padoan et al, 2011; Garzanti et al, 2015). In this situation, pottery obtained from silt and clayey materials, more or less rich in quartz sand, preserves the Sr isotopic ratio of the area in which they were produced. Therefore, the possibility of using Sr isotopes ratio by comparing the isotopic signature of the raw material (clay) and the clayey matrix of the ceramic can here represent a decisive method in pottery provenance studies.

It is important to point out that there are two published studies on the use of Sr isotope for tracing the pottery provenance (Carter et al, 2011; Li et al, 2005). They deal with two different types of pottery (coarse and fine, respectively) for which other provenance markers (lithic inclusions and bulk geochemical composition, respectively) already defined the different origin of the subset of materials. In particular, the study of Carter et al. (2011) clearly indicates how the Sr isotopic ratio is directly related to the different minero-petrographic composition of inclusions occurring in the prehistoric Grey-ware from the Grand Canyon (USA), being the isotopic signature related to the coarse-sized fraction of the ceramic paste. The study of Li et al. (2005), on the other hand, showed the potentiality of Sr isotope ratio analysis to constrain the provenance of IX-XI century Chinese stoneware, therefore of fine pottery, the isotopic ratio of which fundamentally depends from those of the type of base-clay. Specifically, the Sr isotopic ratio was crucial to distinguish ceramic materials obtained by a kaolinite-base clay, characterized by a low Rb/Sr ratio, from those produced using a

sericite-base clay, with a higher Rb/Sr ratio, which in any case showed also different bulk chemical composition, as also pointed out by the authors.

Therefore, the research here proposed would represent an important contribute to define the effective possibility of a multianalytical approach, comprising also Sr isotope analysis, for pottery provenancing.

In order to define the provenance of the pottery, a set of clay materials from various segments of the Nile river system and some of its tributaries were collected. Obviously, it was necessary to compile an appropriate clay sampling to better define how to differentiate the Nile sediments and therefore divide the river system into "segments" each with specific geochemical and specifically Sr isotope ratios. Over a span of three years, three dozens of geological samples have been collected along the course of the Main Nile and its tributaries, involving as well areas near other archaeological sites of interest, like Wadi Howar region in the Southern Libyan Desert (Klein et al, 2004) and Wadi Soba area along the Blue Nile (Fernández et al, 2003). Clay materials from the river banks of White Nile, Blue Nile, Main Nile north of Khartoum (after the confluence of White and Blue Nile), along the Atbara, and along the Main Nile after the Atbara confluence to the second cataract, and from some tributaries (although some of them are now evanescent rivers: *wadi*) have been analysed. The statistic provided by Padoan et al. (2011) and Garzanti et al. (2015) for the central Sudan is very limited and does not take into account confluence areas, in which the geomorphological situation is complex, also in relation to the hydrographic evolution over the time (Williams et al., 2015). Moreover, the isotopic analyses they performed were carried out on the fine fraction of the deposits (< 62 micron) and not on the materials that were probably collected by ancient potters, and represented by a sandy-silty clay. For this reason, it has been decided not to make any grain-size selection on the clay materials before performing the chemical and the isotopic analysis, since the aim of this research is addressed to define possible markers to distinguish ancient pottery provenance. In fact, during the ceramic production, especially in prehistoric period but also in historic periods, any possible preparation of the clay material (levigation or tempering) was carried out according to the potters' skills and not using sophisticated separation methods as those used in laboratories.

The last part of the project focused on the analysis of a second group of materials: pottery, tempered with K-feldspar coming from a granite-like rock, that has been found at both Al Khiday and the two other regions of interest (Dal Sasso et al, 2014; Klein et al, 2004). This pottery paste is typically found in association with three

specific decoration (*wavy line, rocker stamp dotted zigzag packed, alternating pivoted stamp*) (Salvatori, 2012; Dal Sasso et al., 2014). The real issue of this granite-like rock is its geographically limited occurrence that forces the archaeologists to wonder if the movement of the pottery regarded whether raw materials or the final products. In order to analyse the $^{87}Sr/^{86}Sr$ ratio of the clayey matrix it has been necessary to eliminate by hand the added temper. Since Rb substitutes for K, the radioactive decay of ^{87}Rb in ^{87}Sr contributes to increase the $^{87}Sr/^{86}Sr$ ratio in the rocks, and this effect will be more important with increasing geological age of rocks. Therefore, the occurrence of K-rich temper (deliberately added inclusions by the potter) in the ceramic paste can considerably affect the Sr isotope signature with respect to that of the original base clay. Finally, all the Sr isotopic ratios have been compared. Results from this research, are able to validate or reformulate archaeological hypothesis, and possibly define relationships between different geographic areas in a vast territory characterized by an important river system, in different also climatic periods.

As concern the archaeological results, evidence of importation might allow to trace exchanges and contacts between different communities or the frequentation of different geographic regions. Since the potsherds analysed covered a long span time, from the Mesolithic to the Neolithic period, possible difference in terms of pottery movement and exchanges, could be defined for the more ancient pottery, relative to a society based on gartering, hunting, and fishing with respect to the Neolithic one, more residential and in which agriculture and pastoral activities were prevalent.

This research thesis is therefore articulate in a series of chapter as follow.

The first chapter introduces the prehistory of Central-Northern Sudan summarizing the main events of the Mesolithic and Neolithic periods. The archaeological sites of interest are described in order to give an accurate overview of the archaeological problem.

Chapter two illustrates the geological and Holocene environmental context in connection with the location of the archaeological sites. To complete this chapter, an important section is dedicated to the Nile River and its tributaries.

The third chapter describes the analytical methods used for this provenance study, their fundamental principles with respect to archaeometric studies of pottery, and the respective sample preparation techniques.

Chapter four is dedicated to the description of the samples. The first paragraph presents the raw materials while the second one illustrates pottery from all the archaeological sites.

The fifth chapter deals with the presentation and discussion of the analyses of the raw materials in order to give an efficient characterization of the samples.
Chapter six presents the results concerning Mesolithic and Neolithic pottery from Central-Northern Sudan and focuses on the comparison between raw materials and final products in order to lay the foundation for the final conclusions.

FIRST CHAPTER

PREHISTORY OF CENTRAL - NORTHERN SUDAN: A BRIEF OVERVIEW

1.1 Introduction

Since the first excavations conducted by A. J. Arkell and F. Debono at the Khartoum Hospital settlement site in 1944-45 (Arkell, 1947, 1949), a yet unknown early Holocene hunter-gatherer-fisher groups were discovered in central Sudan. The new culture was named by Arkell "Early Khartoum" or "Khartoum Mesolithic" because of the supposed antiquity of the cultural remains, a peculiar lithic assemblage and the absence of domesticated animal bones and domestic plant remains in the archaeological deposits. Among the main features of the Sudanese Mesolithic are an unusually large pottery production, a strong trend to permanent or almost permanent settlements, and a subsistence economy mainly based, at least during the 7th millennium BC, on the exploitation of fish resources abundantly provided by the river Nile. Typical pottery and chipped lithic of the Khartoum Mesolithic have been collected at a number of sites along the White and Blue Niles and the Main Nile north of Khartoum till the Shendi area (Salvatori, 2012) and to the west along the Wadi Howar (Jesse, 2003). Variants of the Khartoum Mesolithic pottery assemblage are known in the Debba area, south of the IV Cataract (Karmakol group: Gatto, 2006), in the Sennar area (Shabona: Clark 1989) and possibly in the area of the Gash river (Kassala: Manzo, 2016). In Upper Nubia, north of the IV Cataract, a number of sites of Early Holocene pottery bearing hunter-gatherer-fishers have been located. Since the beginning (Shiner, 1968; Nordström, 1972) this pottery production was thought to be related to the Khartoum Mesolithic pottery production and thus named Khartoum Variant on the base of very light similarities in the pottery decorative lexicon. In recent years the excavation of two key sites in the area of Kerma (El Barga and Wadi el-Arab: Honegger, 2014) provided the evidence that the Upper Nubian Mesolithic followed a different cultural trajectory well distinct from the central Sudan Mesolithic. Generally speaking, most

of the archaeological sites in the northern regions are apparently small seasonal sites while in the south settlements are wider and the archaeological deposit appears as a mound. The differential visibility of the Mesolithic sites in the north and the south of the country could possibly be explained by diverging mobility behaviours of the groups linked to different subsistence practices and/ or by different erosive processes in the two regions as suggested by the Wadi el-Arab settlement in the Kerma area (Williams, 2012).

One of the major problems affecting a deeper knowledge of the Khartoum Mesolithic processual history is due to a number of post-depositional disturbances of the prehistoric sites in central Sudan and consequently the lack of stratified deposits. In order to overstep this lack of information, most archaeologists adopted obsolete methods as artificial cuts that easily led to associate radiocarbon determinations to layers and material assemblages not related one to another. Beside this, every indication about the deposit formation processes were lost (Salvatori et al, 2011). The excavation at Khartoum Hospital inspired numerous other archaeologists that found many other sites with Early Khartoum pottery spread on their surface (Caneva, 1983a, 1988; Fernández et al. 1997; 2003a, b; Garcea and Hildebrand, 2009; Haaland and Magid, 1995; Honegger, 2005, 2010; Jesse, 2003; Khabir, 1985, 1987; Salvatori and Usai, 2006, 2008; Salvatori et al., 2011; Usai, 2001, 2006; Usai and Salvatori, 2002, 2005; Usai et al., 2010). All sites emerge as mounds running along the banks of the watercourses (Nile River or its tributaries) with a wide dispersal of archaeological material. However, the issue that combines the majority of the sites is the disturbance by post-depositional interferences both natural, as wind and water erosion, or animal tunnels, and moreover anthropic disturbances as Neolithic, Meroitic, Post-Meroitic, Christian and Muslim graves. Among these, the Post-Meroitic burial practice (earthen tumuli) was possibly the most dangerous for the prehistoric deposits. In fact, the building method of these big structures consisted in the excavation of large burial pits, in close proximity of the artificial mounds of the Mesolithic and often Neolithic older settlement areas, that after the deposition of the individuals were covered with earthen superstructures (earthen tumuli), mostly using the prehistoric deposit as building material. In the last two millennia, water and wind erosion and a related colluvial redeposition process were reshaping the tumulus-like superstructures, thus expanding the distribution of the prehistoric materials contained in the earth used to build up the funerary structures. The result of this process is the mixing of the material and thus its redistribution as colluvial deposit (Salvatori, 2012) (Figure 1.1).

This way, it is impossible to use archaeological records as comparative tools at a regional level. Actual lack of information about Sudanese Mesolithic period is due mainly to the disturbances described above that produce inconsistency between radiocarbon determinations and cultural material.

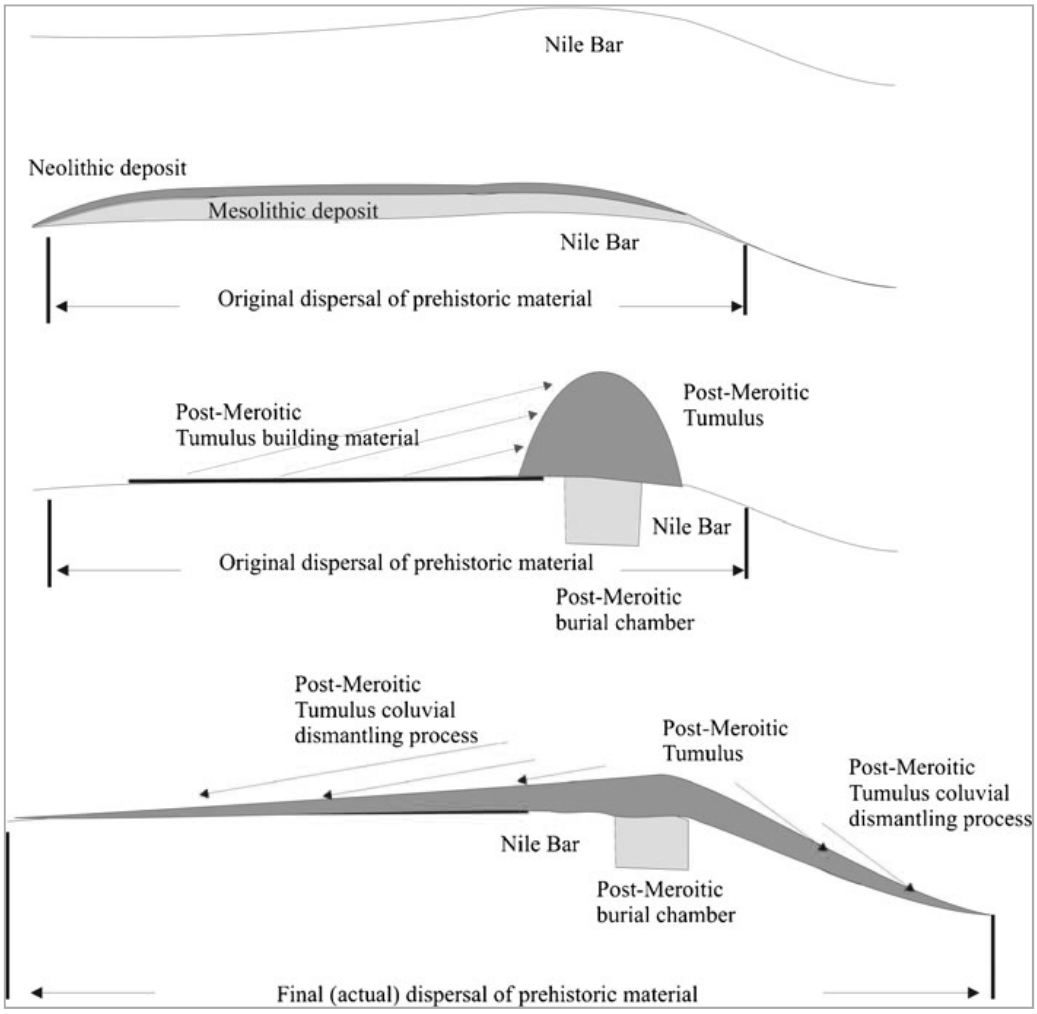

Figure 1.1: schematic process of the building and dismantling of the Tumulus. From (Salvatori, 2012)

In the past, in spite of the heavy disturbances affecting almost all excavated sites, cultural development in the Khartoum Mesolithic culture was generally associated to a change in decorative motifs. The case at hand regards the hardly demonstrable transition from incised wavy line (IWL) to impressed dotted wavy line (DWL). It is clear that the development of a whole culture cannot be restricted to a single attribute in pottery decoration. It is connected instead with pottery making practices and symbolic system (Salvatori, 2012). The latter is frequently the result of cultural

changes often due to contacts with other groups. Several issues arise as a result of this: questions regarding provenance of both raw materials and finished products, potential exchanges of materials and communication routes.
Only recently, the discovery and subsequent excavation, on the left bank of the White Nile, 25 km south of Omdurman, of a cluster of Mesolithic and Neolithic sites with at least partially preserved and stratified deposits, opened a new season of the research on the Mesolithic period in central Sudan (Salvatori et al., 2011, 2014; Usai, 2014; Zerboni, 2011).
The passage from Mesolithic to Neolithic period occurred not simultaneously in this big area of interest. In Nubia the Neolithisation process started at the end of the VII millennium BC while it reached central Sudan at about the end of the VI millennium BC (Salvatori and Usai, 2016). The causes of this chronological discrepancy are still debated but they are probably related to the persistence of more advantageous climatic conditions. Social-cultural factors cannot be excluded though. Neolithisation in central Sudan might have been the consequence of influences coming from the northern regions as Nubia and the whole mechanism could have been related to displacements of individuals from north to south. Again, one of the most critical problems regarding the study of Neolithic populations and sites is the lack of complete structures not subjected to disturbances. Again, A.J. Arkell was the first to observe this issue regarding conservation. He excavated the Neolithic site of Shaheinab (Central Sudan) where he found reworked remains of a settlement and few traces of a fireplace. These archaeological findings were associated to pottery and lithic assemblages that were clearly very different from the previous Mesolithic culture.

1.2 The archaeological problem

Actually, pottery decorative systems can be considered a meta-language containing several meanings besides the identity-making message of the originating community. Both paste typology and traits regarding the production, such as decoration, are elements that can be used in order to recognize the extent of regional relationship networks.

The case of the Al Khiday sites is now providing controlled Mesolithic pottery assemblages covering almost 1500 years and allows to tackle more complex narratives on pottery production.

There is a way to theorize pottery production groups and it lies in the idea that they simultaneously work within both communities of identity and communities of practice. Communities of identity can be considered as social networks in which potters share a group identity (Eckert, 2008, 2012). The term 'identity' is still under debate but it is used to present the idea that people preserve social groups "despite changes in membership and practice over time" (Sampeck, 2011). This membership can be emphasized in the community of identity (ethnicity, class, age, gender, lineage) when individuals move between different social situations. As the individual experiences these new situations or moves through life-cycle events, the communities of identity of the individual may change. Concerning pottery production groups, membership in a community of identity corresponds to deliberate production decisions. This system of choices might have helped to reinforce or attenuate group membership within specific social contexts and, in this framework, decorative technique (design layout, design element, colour …) could have been be played an important role since it was easily noticed by others (Bowser, 2000; Eckert, 2008; Mills, 2007).

Communities of practice can be described as social networks in which potters share a technological tradition. From an ethnographic point of view, this tradition was passed down from generation to generation (Stark, 2006). It is important to highlight that various communities of practice can exist within a single community of identity, or vice versa (Eckert, 2008, 2012; Gilpin and Hays-Gilpin, 2012).

Beyond the concepts of communities of identity and communities of practice lies the conflicting relationship among three concepts: raw materials, production tradition and provenance. While the production tradition deals with the decisions made by potters during each step of the production process, raw materials concern procurement areas used by potters. Provenance instead pertain to the origin of an item under consideration.

Although provenance of ceramic materials is usually determined according to the chemical composition of the used clays, in the case of Al Khiday the presence of abundant quartz in the pastes causes a strong dilution effect also on trace elements potentially useful as markers of provenance. Moreover, pottery pastes rich in K-feldspar (microcline-perthite), probably derived from pegmatites and often related to specific decorative motifs (Incised Wavy Line, Rocker Stamp dotted zigzag Packed,

Alternately Pivoted Stamp) have been found at Al Khiday sites, and moreover at all the Mesolithic sites of central Sudan. The closest source of this material used as temper is Jebel Seleitat, which lies near the VI cataract, about 100 km north of Al Khiday. The finding at Al Khiday of ceramic fragments characterized by K-feldspar temper might be related to the existence of long-range exchange among populations living in different areas (Dal Sasso, 2011; Dal Sasso et al., 2014). Questions arise out of whether the movement of materials through different regions regarded final products or raw materials. This study aims to define whether the pottery was imported from elsewhere or locally produced using imported temper.

1.3 Al Khiday archaeological sites

Most of the pottery for provenance studies comes from a cluster of archaeological sites in Central Sudan. The El Salha Archaeological Project (El Salha is a small village along the western bank of the White Nile) started in 2000. The project is directed by the archaeologists Donatella Usai and Sandro Salvatori and supported by the following authorities and institutions: Ministero degli Affari Esteri (2000–2011), Istituto Italiano per l'Africa e l'Oriente (2000–2011), Università degli Studi di Parma (2005–2011), Michela Schiff Giorgini Foundation (2002–2003, 2005, 2007), Università degli Studi di Padova (2010–2015) and GASID of Torino (2000–2009). The two main goals of the project are both the exploration of Sudanese Nile Valley studying Mesolithic and Neolithic cultures and the emergency excavation of large archaeological sites in danger of destruction because of the rapid urban growth of the villages located in that area. The project have always involved experts coming from different fields, highlighting the importance of having a multidisciplinary approach. The Italian archaeological mission has its base 25 km south of Omdurman, near the small village of Al Khiday. The area intensively surveyed was 5×35 km from the bank of the river to the Jebels to the west (Jebel Baroka). More than 160 sites of different periods (from the Palaeolithic to Islamic period) were located and named according to Hinkel's (1977) system (Figure 1.2). The aim of the research is to study the transition from a Mesolithic way of life, based on hunting, fishing and gathering, to a Neolithic food-producing economy. The main starting point for the study of Mesolithic period in central Sudan is the pottery production: at the beginning of the VII millennium BC,

the technique was already well developed and this must be nothing else but the result of a long phase of testing. Unfortunately, at the moment there are not enough evidences of this phase in the area. In 2004 a number of Mesolithic, Neolithic, Late and Post- Meroitic sites were identified. They were labelled as follow: 16-D-3 is a large mound-like site with Mesolithic and Neolithic pottery on the surface. 16-D-4 looks like a low mound with superficial Mesolithic and few Neolithic evidences. 16-D-4B is a very low morphologic relief with a number of Mesolithic pits. 16-D-5 appears as a relatively large mound-like site with Mesolithic and Neolithic pottery on the surface and evidences of Late or Post-Meroitic tumulus-like graves on its eastern side. 16-D-6 is a flat Neolithic site with discrete clusters of pottery and other artefacts. 16-C-2 emerge as a large Post-Meroitic cemetery with more than a hundred tumuli. Lastly, 10-W-4 looks like a late Mesolithic flat site, about 20000 m^2 large, placed on a stabilized Pleistocene dune at the border of a large *wadi* that is nowadays used as a sand quarry for building purpose (Salvatori, 2012).

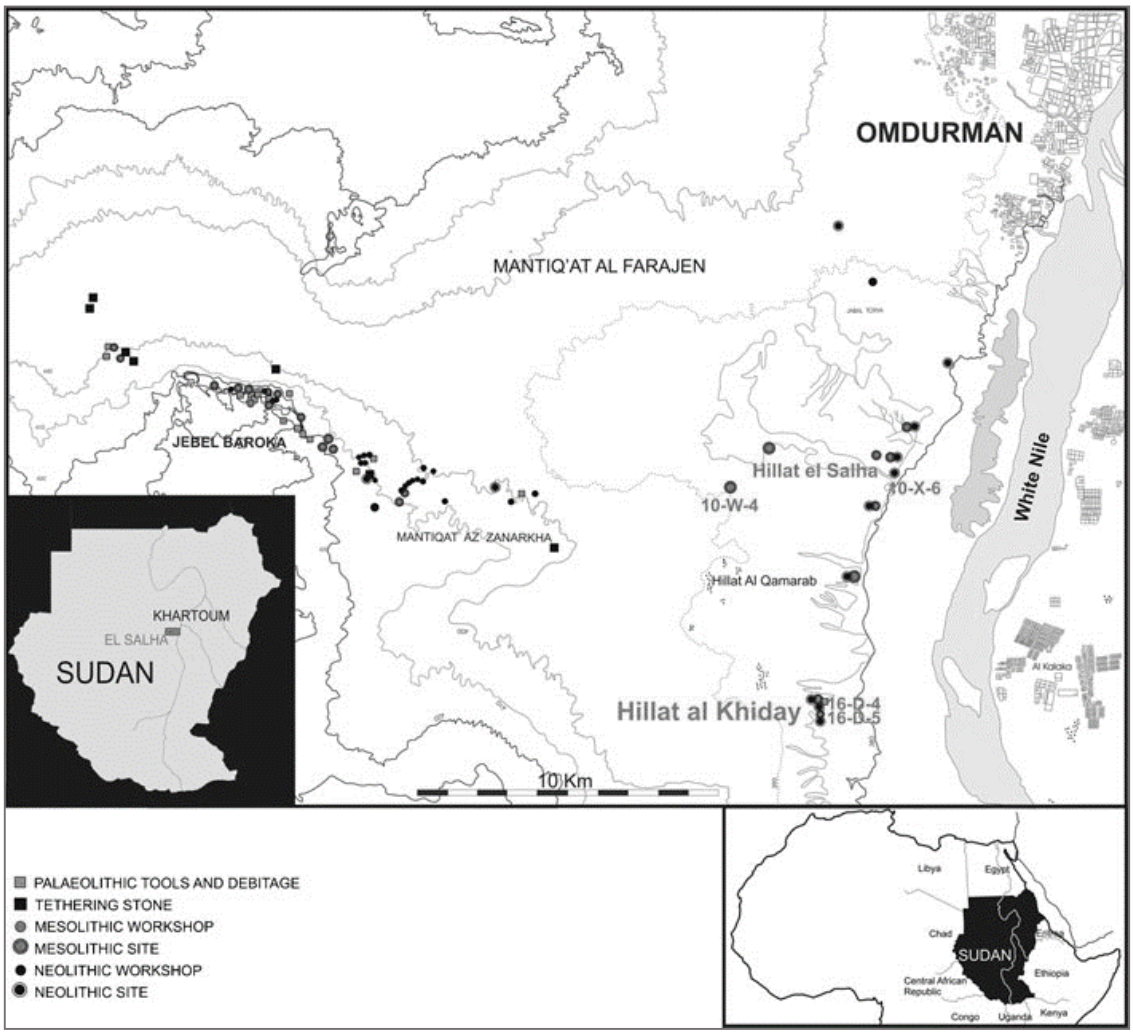

Figure 1.2: map of El Salha region and distribution of the prehistoric sites. Only the names of the Mesolithic sites are reported. From (Salvatori et al, 2011).

In this context, 16-D-5, 16-D-4, 16-D-4B, 16-D-3 and 10-W-4 are the sites of interest (see Figure 1.3). 16-D-5 is a settlement that was very lightly affected by the building of the superstructures: the earth collected to build the tumuli disturbed only the upper part of the original prehistoric deposit. The redeposited sediment (colluvium) involved only the first 10–60 cm of the surface and it was loose and organized in oblique lenses (Salvatori et al., 2011; Zerboni, 2011). The section lying under the colluvial deposit was well preserved and two different cultural phases were identified. The first was the lower and older one (Early Mesolithic, 7000-6750 BC), characterized by ashes and a fireplace containing abundant fragments of shell (mainly *Pila wernei*), fish and mammal bones, lithic and bone tools, pottery sherds and a grinding stone. The upper layer corresponding to the second and younger phase (Middle Mesolithic, 6750-6000 BC) has been further divided in two phases. In the lowest one, mud architectural remains, fireplaces, fish and mammal bones, pottery and lithic remains were identified. The upper Middle Mesolithic layer was disturbed by the superficial alteration due to the building of the tumulus. Together with the older assemblage, a pebble that preserved a black painted sketch of a boat was found (Figure 1.4). According to the associated radiometric data, this finding dates to the early VII millennium BC and this association is worth some remarks regarding the use of boats for navigation along the Nile. The boats as means of transportation open new possibilities in long-range socioeconomic exchanges. Through waterways is possible to carry heavy products and/or raw materials and this issue is particularly interesting for this research, which deals with pottery and provenance studies.

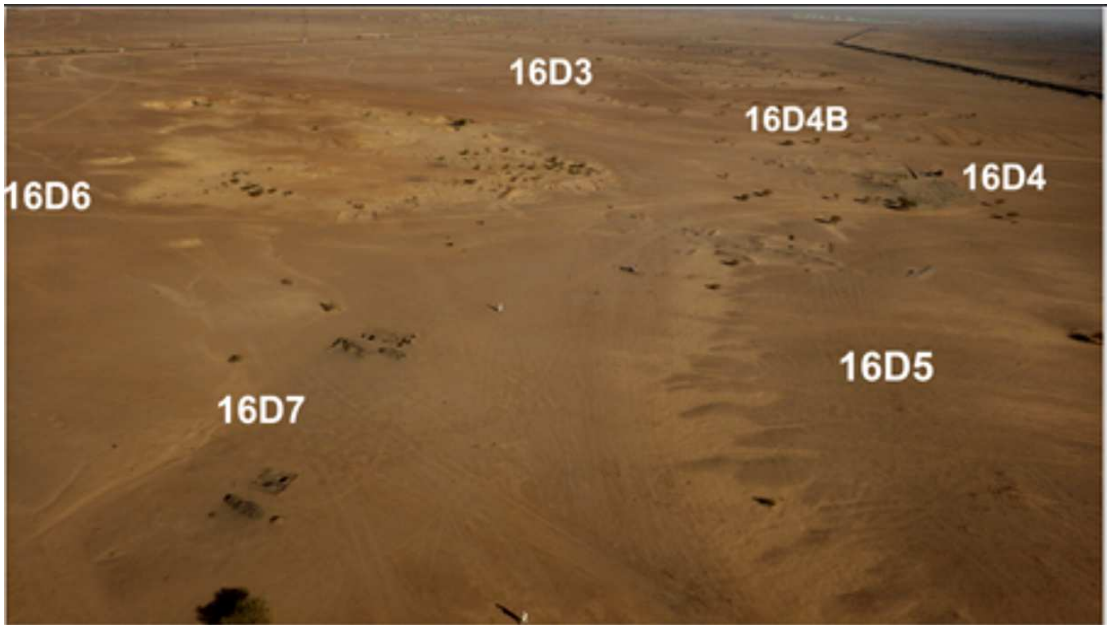

Figure 1.3: Kite view of the sites at Al Khiday (kindly provided by Donatella Usai and Sandro Salvatori)

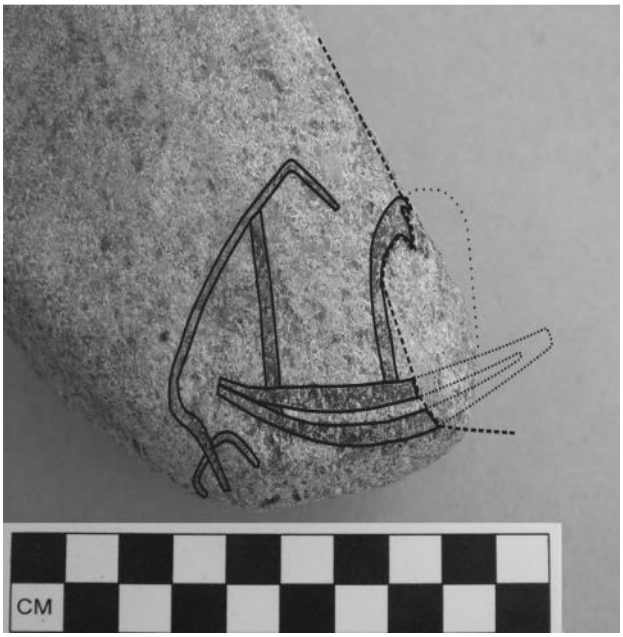

Figure 1.4: pebble with sketch of the boat and its interpretation by Donatella Usai and Sandro Salvatori. From (Salvatori and Usai, 2007)

16-D-4 and 16-D-4B are two functional areas just to the north of 16-D-5 were hundreds of pits of different shape and use have been excavated. The two areas were in use mainly during the Middle Mesolithic phases.

16-D-3 is a mound located less than hundred meters to the north-west of 16-D-5 were a sequence covering the entire VII millennium BC was excavated in 2013. The excavation brought to light impressive stockpile of gastropods (*Pila* sp.) and bivalves (*Chambardia* sp.) together with pottery and lithic tools.
The archaeological site 10-W-4 dates to the second half of the sixth millennium cal. BC (5488-5379 cal BC). It is located away from the actual course of the White Nile (~9 km) but close to a former seasonal lake and occupies nearly 20000 m^2. The excavation revealed a series of huts but the whole stratigraphy is complex because of the repeated frequentation of the area, which might have been seasonal. Fortunately, human disturbances as later burial activities did not affect the area (Salvatori, 2012). At 10-W-4, only a Late Mesolithic phase is represented and this might be the sign of a change in mobility of populations related to the deterioration of climatic conditions. Some pottery that was close to the huts was investigated together with a garbage pit inside another partially excavated hut. It included large amounts of animal bones, lithic remains and pottery sherds.

1.4 Al Khiday: the pottery assemblage

Despite the impressive amount of potsherds found at Al Khiday, it is quite challenging to outline models able to describe trends related to both pottery decorations and temper recipes. Nevertheless, it is most likely that Khartoum Mesolithic pottery was hand-made at a familiar level and intended for domestic employment. Probably, modifications of temper recipes and small stylistic modifications might be the reflection of the individual expression of each potter made on deeply rooted decorative motifs. More discrete stylistic changes in the decoration motifs that can be appreciated along the sequence can be possibly understood as the expected temporal variability of a meta-language used as a means to communicate with other groups. Differently, if we are looking for a sign of organization of pottery production at the familiar level within the society, it might be represented by the total variability (Salvatori, 2012).

Pottery from Al Khiday was classified according to Caneva (1983b; Caneva and Marks 1990). Caneva's typology for Mesolithic and Neolithic Sudanese pottery was based on a tree-like structure arranged considering techniques, tools, elements, motifs and

structures. Unfortunately, it did not contemplate stylistic variations in motif execution and in pottery fabric (Salvatori, 2012).

1.4.1 Site 16-D-5

The pottery sequence excavated at 16-D-5 and related sites represents the Early and Middle Khartoum Mesolithic Culture. It ranges from ca. 7000 to 6000 BC. Pottery both from Al Khiday and from the other Sudanese Mesolithic sites is shaped by hand with the coiling technique (*e.g.* Haaland, 1993; Caneva, 1991): a large number of fractures have been observed at the coil joints and this highlighted the attempt of a better joining by making the edge of the rings more rounded. The coiling formation commonly started from the base and the bases of this pottery were usually very thick (from 1.75 to 3 cm). Shapes vary a lot but it is very difficult to recognize recurrences because only few rims or large sections of the vessels have been found. Regarding the temper, its variability is impressively large and it is possible to identify at least 30 different recipes, which is probably the result of a domestic production (Salvatori, 2012; Dal Sasso et al., 2014). The most ancient stratigraphic units at 16-D-5 dated back to the beginning of the VII millennium BC and contained almost new decoration types. These unknown motifs named incised Lunula patterns and impressed deep dots or drops were associated with well-known types such as IWL (*Incised Wavy Line*) and impressed DWL (*Dotted Wavy Line*) (Figure 1.5). The second phase can be divided in two sub-phases. With the first sub-phase, deep dot or deep drop patterns persisted but Lunula motifs disappeared. IWL and DWL presence coexisted with various types of Rocker Stamp decoration, but IWL tended to decrease while there was an increase in Rocker stamp dotted zigzag packed (Rsdzz packed) and Rocker stamp drop motifs. The presence of DWL along the entire sequence was accounted for low percentages but it was still present at 10-W-4 (Late Mesolithic site). When decoration motifs are associated with temper recipes it is possible to detect differential behaviours that we can summarize as follow. IWL pottery was generally tempered with feldspar and quartz grains with angular edges: in the first phase, grains were >2 mm while in the second phase feldspar and quartz grains were fine (<1 mm). Other recipes were only rarely used in the first phase for IWL pottery. Throughout the second phase, sand tempers gradually increased showing the peak concentration (12 %) in the last stratigraphic unit. Decoration motif Rocker Stamp dotted zigzag (Rsdzz) revealed a

very similar trend. It was mainly associated with feldspar tempers (71,16 %) and it presented an increase of both fine feldspar grains with angular edges and sandy tempers during the second phase of the sequence. Regarding the other decorative motifs, Rocker stamp plain zigzag (Rsplzz), Rocker stamp drops (Rsdrops), Lunula type decoration and scraped sherds were typically tempered with sand blended with ochre, fragments of finely chopped straw and calcareous grains. Alternately Pivoted Stamp (APS) pottery was tempered with fine materials (feldspar and quartz grains with angular edges <1 mm) and DWL was mainly characterized by sandy tempers (73.34 %) and less frequently (26.66 %) by feldspars and quartz grains with angular edges (Salvatori, 2012).

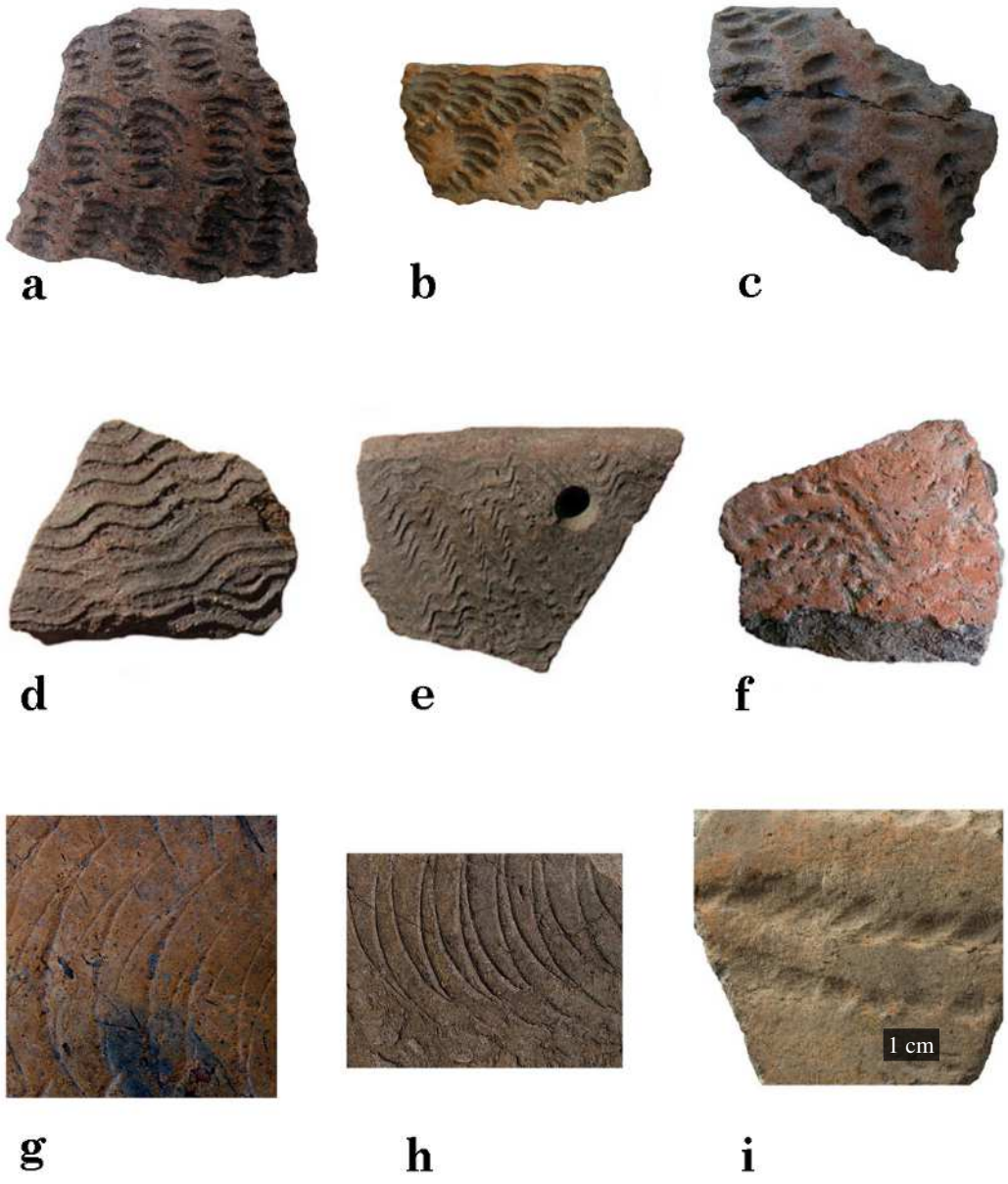

Figure 1.5: different types of decoration. a), b) Lunula; c) Rocker Stamp deep drops (Rs deep drops); d), e) incised wavy line (IWL); f) dotted wavy line (DWL); g), h) Rocker stamp plain zigzag (Rsplzz); i) Alternately Pivoted Stamps (APS). From (Salvatori, 2012)

1.4.2 Site 10-W-4

At the Late Mesolithic site 10-W-4, Rsdrops and Rsdzz were the most popular decoration motifs while the other typologies represented only < 10 %. There was only one impressed motif and it was characterized by a sequence of large oval and parallel dots (Salvatori, 2012). At 10-W-4 almost all the tempers were represented. IWL, DWL and Rsdzz showed a similar pattern: sherds were mainly tempered with feldspar and quartz grains >2 mm (40,48 %) followed by an increase (reaching 37,30 %) of fine (<1 mm) feldspar and quartz grains with angular edges. Also APS was characterized by the latter temper type and this recipe was very stable. Rsdrops and Rsplzz, which are the prevalent decorations at 10-W-4, were mainly tempered with sand (Table 1). It has also been observed that all the pottery was coiled by hand. Regarding the shapes, it was possible to count many bowls of different sizes but rare dishes.

Table 1: distribution of different tempers according to decoration type at 10-W-4. From (Salvatori, 2012)

Decoration	Feldspar + quartz (%)	Fine feldspar + quartz (%)	Sand (%)	Total (%)
IWL	36.45	42.06	21.50	100.00
DWL	4.55	50.00	45.45	100.00
Rsdzz	14.13	48.70	37.17	100.00
Rsdzz packed	10.36	47.72	41.92	100.00
Rsdrops	3.66	24.12	72.21	100.00
Rsplzz	6.25	18.75	75.00	100.00
Scraped	0.00	0.00	100.00	100.00
APS	14.58	79.17	6.25	100.00
Incised lines	0.00	80.00	20.00	100.00
Not det.	7.59	32.37	60.04	100.00

1.5 Pottery from other archaeological sites

In order to set up a comparison among Al Khiday sherds and ceramic found (and very likely produced) in other regions, some pottery samples from other archaeological sites have been selected. Discriminating parameters considered the similarities of decorative motifs and temper, in addition to the age. There were two research groups directly involved: the Spanish Archaeological Project in Central Sudan (Complutense University of Madrid) that worked in the Blue Nile area (Fernàndez et al., 2003) and the African Research Unit (Institute of Prehistoric Archaeology - University of Cologne) that was operating in northwestern Sudan and in the Egyptian western desert (Klein et al., 2004).

1.5.1 The Blue Nile: Wadi Soba area

The Spanish archaeological mission carried out five seasons of archaeological survey during the winters of 1990, 1992, 1993, 1994 and 2000. After a first unsystematic collecting (grab sample) of surface finds in all the sites when discovered, in the main sites other techniques were applied, by choosing differentiated, systematically sampled units. Each unit was randomly selected inside every 30x30-m or 20x20-m square. For the classification of pottery decoration types during the Mesolithic and Neolithic periods, they have followed Caneva's typology (Caneva, 1983: 164-183; Caneva, 1988: 83-110; Caneva and Marks, 1990). They have employed the term "Mesolithic" for the cultural period also known as "Early Khartoum" (c. 8000-5000 BC) in the central Sudan. "Early Neolithic" for the period also known as "Shaheinab" (and actually dated to 4600-4000 cal BC: Salvatori and Usai 2016). For the period called "Late Neolithic" the alternative terms are "Kadada" or "Jebel Moya" (c. 4000-3000 BC) (Fernández et al, 2003).

In particular, pottery from three archaeological sites has been considered.

a) Soba-2 (Soba-2, 6): Mesolithic to Late Neolithic site. Mesolithic sherds included DWL and rocker; late Neolithic sherds had incised triangles and impressed-incised combined decoration.

b) Sheikh Mustafa-1 (S. Mustafa 13): Mesolithic site. The surface sherds were classified in IWL (11), rocker, mostly spaced zigzags (15) and APS (7) types. Those

coming from systematic sampling were IWL (9), rocker (14) and alternately pivoting stamp (1) types.
c) El Mahalab (El Mahalab 26): Mesolithic site. Sherds included IWL (17 in the surface sampling, 4 in the systematic sampling), rocker (9, 1) and APS (10, 0).
In total, four samples have been selected:

1. two quartz-tempered Neolithic sherds from Soba-2 (BN7 and BN8)
2. one Kfs-tempered from Sheikh Mustafa-1 (BN5)
3. one Kfs-tempered from El Mahalab (BN10)

1.5.2 The Wadi Howar region

The ACACIA project (Arid Climate Adaptation and Cultural Innovation in Africa) focused in the Wadi Howar Region. It consisted of a multi-disciplinary research project of the University of Cologne. Given that almost 2000 prehistoric sites were located in that area, pottery was the most important source of data regarding cultural evolution and interactions among different populations. The working area of this research project included 5 main subareas: 1) Wadi Howar (Middle and Lower), 2) Jebel Tageru (a sandstone plateau south of Wadi Howar), 3) the Ennedi Erg (a former lake north-west of Wadi Howar), 4) Wadi Hariq (a wadi system 200 km east of Ennedi Erg), 5) the Laqiya region (situated about 150 km north-east of Wadi Hariq). During the Early and Middle Holocene, climatic conditions were favourable and the humid phase around Wadi Howar persisted until 4000 BC. At that time, the *wadi* was an uninterrupted chain of pools fed by ground water and climatic conditions along the watercourse were favourable for the growth of rich vegetation, molluscs, fishes and great mammals as well as human settlements. Since at least the beginning of the VI millennium BC, the first residents based their life on fishing, hunting and gathering and established a good network of relationships (Klein et al, 2004).
For the comparative study with the pottery from Al Khiday, only qtz-tempered samples had been analysed, since Kfs-tempered pottery was not available from these sites. As a result of XRF data analysis, three fragments turned out to be suitable for the subsequent analysis:

1. sherd No. 24 from Ennedi Erg, DWL (Dotted Wavy Line Horizon, c. 5200-4000 BC) (WH24)
2. sherd No. 25 from Ennedi Erg, DWL (WH25)

3. sherd No. 29 from Ennedi Erg, Hl (Leiterband Horizon, c.4000-2400 BC) (WH29)

SECOND CHAPTER

CENTRAL - NORTHERN SUDAN: GEOLOGICAL AND HOLOCENE ENVIRONMENTAL CONTEXT

2.1 Geology of Central-Northern Sudan

Sudan is a vast country of approximately 2.5 million square kilometres laying along the southern boundaries of the Sahara desert. It has common borders with seven countries and with the Red Sea coastline, which connects the country to the Middle East and Asia. In its territory flows the Nile River, with all its active watercourses and modern and ancient tributaries, which has formed wide depositional plains and basins. The Sudan territory is also characterised by the volcanic uplands in Darfur (western Sudan) and along the borders with Ethiopia (south-eastern Sudan). The Sudan plain consists of both dark clays and yellow to red sands and it is interrupted by rocky hills or smooth mountains (called *jebels*) that are sometimes isolated, sometimes in groups. In the North-East of Sudan occurs the long sequence of the Red Sea Hills that extend into Egypt.

The geology of Sudan is extremely differentiated with a variety of metamorphic, igneous and sedimentary rocks (Figure 2.1) (Whiteman, 1971). Its whole evolution is related to the Central Africa Rift System. The most widespread formations in Sudan are those belonging to the Basement Complex. They are dated to the Pre-Cambrian Age and consist of igneous, metamorphic and sedimentary rocks. Together with the Nubian Sandstone Formation (mainly sandstones of Lower to Upper Cretaceous age) and the Gezira Formation (*Umm Rawaba*, Tertiary to Quaternary fluvial and lacustrine clays, sands …) it covers almost all of Sudan surface.

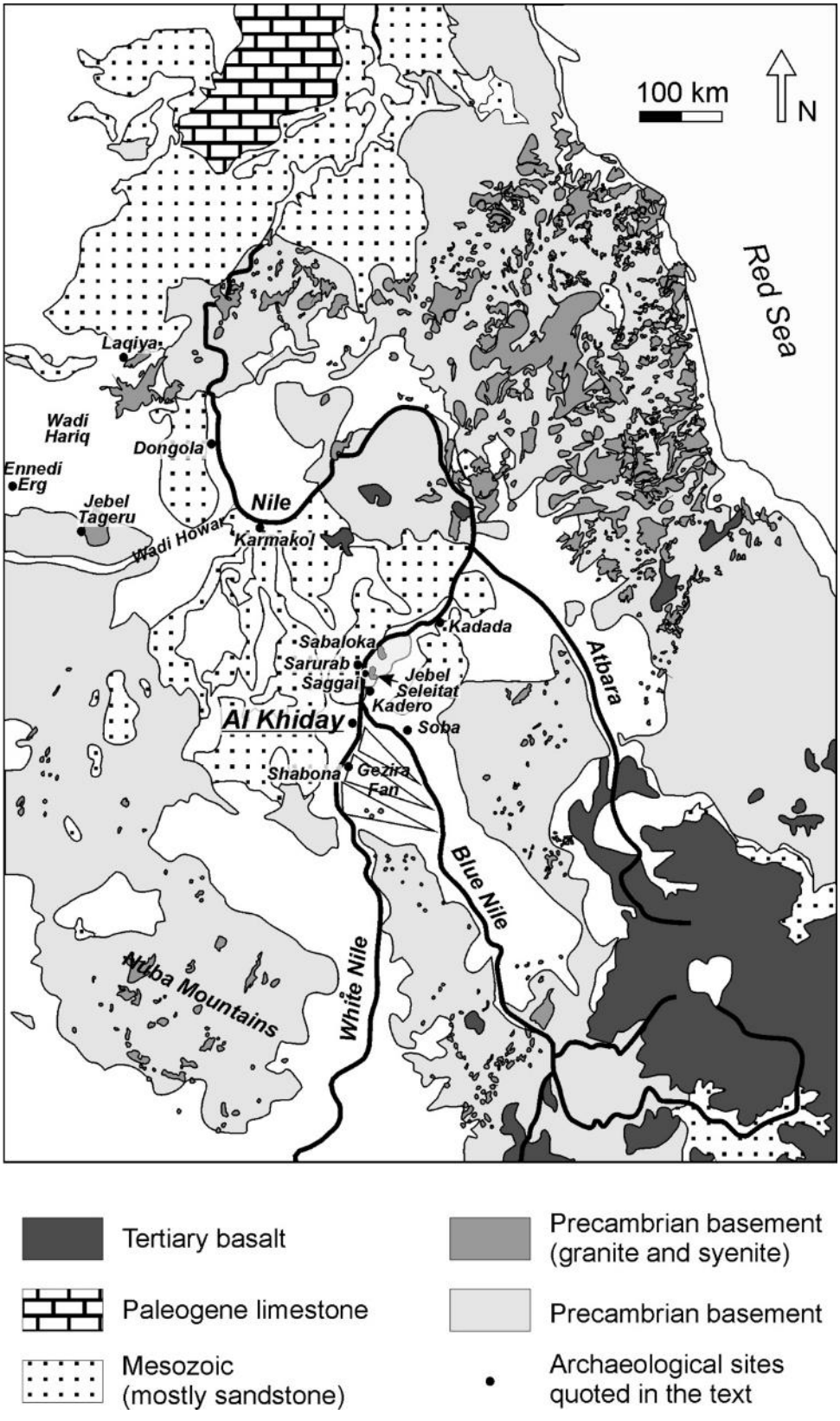

Figure 2.1: geological sketch of Sudan (modified from Dal Sasso et al., 2014)

2.2 The Nile River

The Nile and its tributaries are the main rivers of Sudan. Besides them, many desert *wadis* (small branches) flow occasionally, but only few of them reach the Nile. The basin of this great river interest an area of about $3x10^6$ km^2 and its water resources are shared by eleven countries. It flows northward for ~6800 km and follows a linear course that crosses the geological boundaries of the territory (Garzanti et al, 2015). However, there are some interruptions along the river represented by the dams. They were built in order to control the floods and plan the water supply but today sediments and water are accumulating in those artificial reservoirs damaging the local environment. Dams are located along each branch of the Nile River: White Nile (Jebel Aulia dam), Blue Nile (Sennar and Roseires dams), Atbara (Khashm el Girba dam) and Nile (Merowe and Aswan dams).

Fluvial regimes of the main branches are related to the climate. White Nile supplies the Main Nile with 83% of its low-season flow, but only 10% of its peak flow and its high flows persist from late September to January. About 85% of the Blue Nile flow is concentrated from July to October and Atbara almost dries out from December to May (Sutcliffe and Parks, 1999). The Main Nile regime reflects the summation of its main branches since it does not receive any tributary north of Atbara, and rarely any rainfall (<50 mm/a) across the Sahara (Figure 2.2). The White Nile sources from rainy highlands of Uganda, Rwanda and Burundi and passes through SUDD (Arabic word meaning "barrier" or "obstruction") where it loses half of its water (Garzanti et al., 2015; Padoan et al, 2011; Woodward et al., 2007; Williams et al., 2000). This vast treeless wetland acts as a physical filter since it consists of various meandering channels, lagoons, reed and papyrus fields (Padoan et al, 2011). Then the river flows slowly upwards bringing only a small portion of the total sediment load: in a typical year, this branch accounts for only 3 ±2% of the total sediment load that corresponds to about $\leq 10^7$ t/a overall (Woodward et al, 2015). The Blue Nile drains Ethiopian highlands and is characterized by a seasonal regime. Its mean annual sediment flux is $140\pm20x10^6$ t/a that corresponds to about 60±12% of the total sediment load (Sutcliffe and Parks, 1999; Garzanti et al., 2006). Alluvial histories of White and Blue Nile are bounded since the middle Pleistocene (>250 k.y. ago,) because of the presence of a large lake that occupied the plain that lays between the rivers (*Gezira* plan) (Williams et al., 2003; Barrows et al., 2014). The palaeolake probably received water from several sources and it was most likely 500 km long, 30–40 km wide and 5 m deep

and its volume would have amounted to 75–100 km^3 (Williams et al., 2003, 2006). The Atbara River flows within the Ethiopian plateau through volcanic and then into greenshist-facies basement rocks. It accounts for 38±7% of the total sediment load, which corresponds to 82±10 10^6 t/a of sediment flux (Sutcliffe and Parks, 1999; Garzanti et al., 2006). The Nile, called also Desert Nile after the confluence between White and Blue Nile at Khartoum, does not receive other tributaries after this last tributary confluence at Atbara.

The dominant feature of the main watercourse is the variability in the flux of water and sediments. However, sediments transported by the Blue Nile and Atbara characterize the sediment load of the Desert Nile (Garzanti et al, 2006; Garzanti et al, 2015; Padoan et al, 2011).

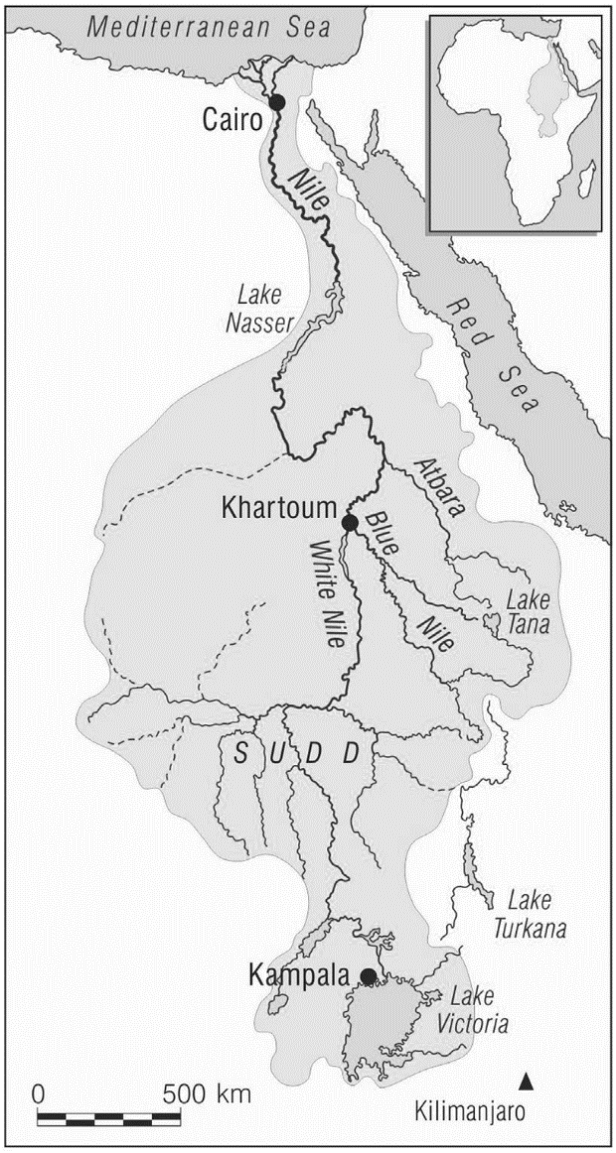

Figure 2.2: Nile basin drainage network (from Woodward et al, 2015)

Climate of Sudan varies from complete desert (northern Sudan) through semi-desert (central Sudan) to equatorial with dry seasons (southern Sudan) (Whiteman A.J., 1971; Garzanti et al., 2006). The average rainfall is seasonal and in central Sudan is generally characterized by varying intensity and duration that occurs mainly in summer: it is governed by the seasonal migration of the intertropical convergence zone from south to north and back. This movement affects the total annual precipitation and the length of the summer rain so that runoff season progressively decrease northward (from >2000 mm/a in the Baro basin, to ~1500 mm/a in much of the Blue Nile basin, to ≤1000 mm/a in the Atbara basin) (Garzanti et al, 2006; Nyssen et al, 2004; Sutcliffe and Parks, 1999). Average temperatures are naturally high: in summer around Atbara temperatures reaches 43°C while in Khartoum 47°C are often experienced. In winter mean daily temperature is about 15°C in the north and nearly 28°C in the south (Whiteman A.J., 1971).

The River Nile dynamics have always influenced regional palaeoenvironment and this is especially true during seasonal flooding of the Nile, corresponding to the wet seasons, when water filled small basins around the riverbed. On the contrary, during dry seasons the basins usually dried up. In particular, some authors (Williams and Adamson, 1980) discussed the occurrence of seasonally swamps in the western White Nile region, dated to ca 6400 and 4800 cal. yr BC. These events were related to the higher White Nile flood level in central Sudan during the Early-Mid Holocene, which was characterized by a wetter climate. Moreover, palaeohydrological records collected across the drainage basin of the Nile River show a general higher water availability related to the African monsoon, which resumed after the arid Late Pleistocene phase and contributed to a wetter period (Zerboni, 2011).

2.3 Location of archaeological sites from environmental and geological viewpoints

The Nile River always had an essential role in the development of human civilization. People living along its banks have always strived for controlling the water flow and its resources since the Mesolithic period. Numerous sites have been discovered and partially excavated along the banks and the inner lands of the Main Nile, the Blue

Nile, the White Nile, and of some Main Nile tributaries active in the Early Holocene, like the Wadi Howar and the Wadi Muqadam (Salvatori et al., 2011; Salvatori et al., 2014; Marks and Mohammed-Ali, 1991; Jesse, 2003; Caneva, 1983a; Caneva, 1991; Fernández et al., 2003a, 2003b; Clark, 1989; Cremaschi et al., 2007; Elamin and Mohammed-Ali, 2004; El-Anwar, 1981; Gatto, 2006; Haaland and Magid, 1995; Ali Hakem and Khabir, 1989; Jesse, 2000; Khabir, 1987; Krzyżaniak, 2002; Usai and Salvatori, 2005; Salvatori and Usai, 2008; Suková and Varadzin, 2012, Jesse, 2000; Shirai, 2013).

In this research project, ceramic materials coming from three areas located in different geographic areas with respect to the Nile river system (Al Khiday, wadi Soba, wadi Howar) will be analysed. Following, a description of the area on which they insist will be done, focusing on both the geological and geomorphological aspects.

The sites of Al Khiday are located in Central Sudan, 25 km south of Khartoum, along the western bank of the White Nile, between the Jebel Aulia dam and the confluence of the White Nile with the Blue Nile. The archaeological sites of interest for this research are 16-D-5 and 10-W-4 (Figure 2.3). The geological bedrock of this area is formed of Mesozoic sandstone, the Nubian Sandstone Formation (Whiteman, 1971; Williams et al., 2015), which rarely outcrop near the White Nile and are more common inland to the west, where they constitute some tens meters-high hills called Jebels.

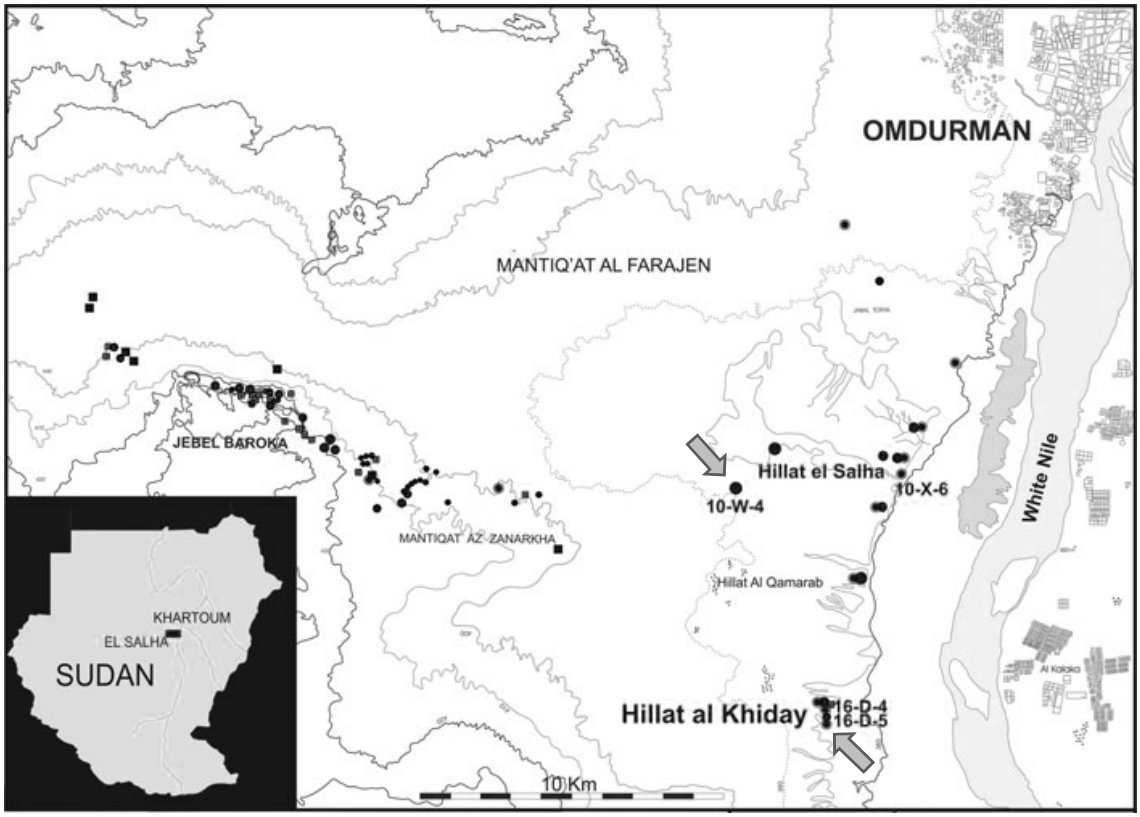

Figure 2.3: main research area along the western bank of the White Nile where are allocated the two sites from which the ceramic materials studied come form: 10-W-4 and 16-D-5 (from Salvatori et al, 2011)

With the others discovered and excavated in the area, these sites are located along a belt, which connects the western pediment surface to a terrace just few meter higher, which was excavated during the Late Quaternary by the White Nile. Since the beginning of the African Humid Period, the morphological action of the river in this territory determined the deposition of clays on its flood plain and the reworking of the late Pleistocene sands, leading to the formation of point-bars, sandy alluvial islands and mid-channel bars (Williams et al., 2000). The decrease of the White Nile water load in the Holocene determined a reduction of the flood level. Consequently, sand ridges became preferred occupation sites for groups of Mesolithic hunter-gatherer-fishers (Zerboni, 2011; Williams et al., 2015). These considerations derive from a deep geomorphological reconstruction of the Al Khiday area (Zerboni, 2011; Williams et al., 2015). Here, the sites are positioned on ridges and humps that stand from a flat lower plain. Ridges are made by plain laminated coarse-to-fine sand, interlaid by planar lenses of fine gravel, and are interpreted as parts of a complex and longitudinal system

of sandy river bars belonging to the Nile River (Zerboni, 2011). Spots of a dark sediment composed by a sandy-loamy deposit very rich in organic matter, characterize the flat area around the mounds. This dark layer corresponds to a sandy-loamy gyttja deposited by a former swamp fed by the seasonal flood of the White Nile (Zerboni, 2011) related to the monsoonal precipitations. The archaeological sites belonging to the Mesolithic period emerge like wide, low mounds and lie at about 2,5 – 4 km from the present Nile course. Most of these sites are located 4m above the level of the surrounding plain and are clustered in discontinuous alignments North-South, roughly parallel to the Nile course (Salvatori et al, 2011). The surface of the mounds is covered with archaeological material but this is not surprising because in Sudan this is closely related to the use of the top of the hillocks thanks to their elevated position (Caneva, 1983). It was the presence of the archaeological material that protected the surface from water and wind erosion. In this area, there are also tracks of palaeochannels flowing on the western bank of the present day White Nile course and these traces support the presence of sandy river bars (Fig. 2.4). Moving some kilometres western of Al Khiday, other Mesolithic sites have been discovered (Salvatori et al., 2011), some of them located near a large freshwater lake dated to the Upper Pleistocene (Williams et al., 2015) and others near small ponds along the Wadi Baroka and Wadi Abu Asheem, the freshwater deposits of which were dated to the Holocene (Williams et al., 2015; Cremaschi et al., 2007; Williams et al., 2006; Williams and Jacobsen, 2011).

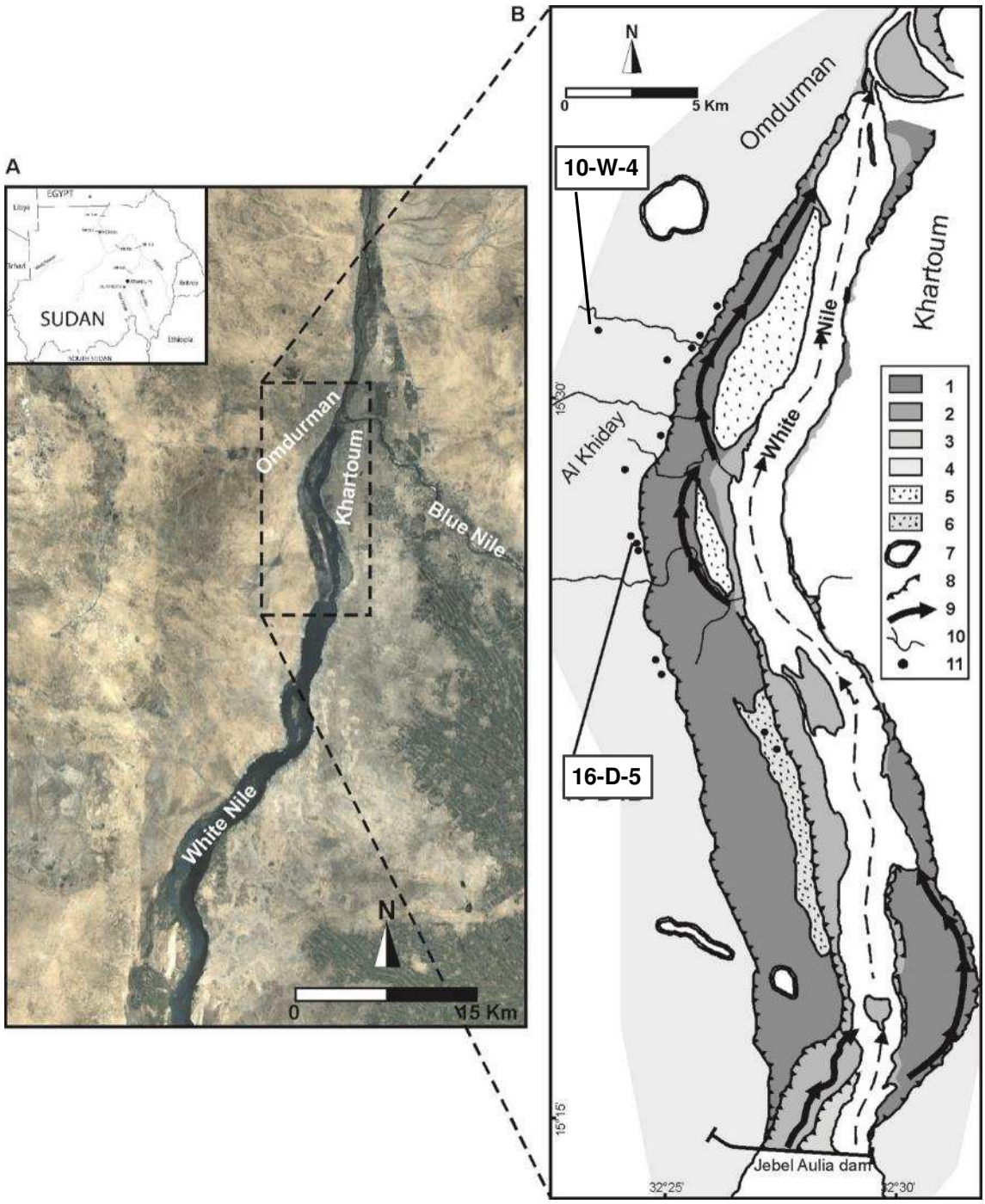

Fig. 2.4. Geomorphology of western bank of the White Nile. (A) Satellite image; its position in the Sudan is indicated in the insert. (B) Geomorphological sketch of the northern part of the western bank of the White Nile (modified after Zerboni, 2011 and Williams et al., 2015). Key: 1–3, Nile alluvium (silt); 4, glacis and slope deposits (sand to gravel); 5, longitudinal sand bar; 6, Pleistocene sand dune; 7, sandstone bedrock outcrop; 8, margin of the fluvial terrace; 9, Nile paleochannels; 10, present day ephemeral fluvial net; 11, Mesolithic sites (modified after Zerboni, 2011).

The second area of interest in this research project is located between Khartoum North and the village of Eseilat on the Blue Nile (eastern bank). It consists of a series of Mesolithic and Neolithic sites close to the area of Wadi Soba, and in particular the sites of Soba-2, Sheikh Mustafa-1 and El Mahalab (Figure 2.5) (Fernández et al, 2003a). The landscape is mostly flat, spotted with many artificial water reservoirs. Alluvial plains are now subject to agriculture so the soil and the archaeological information are unusable. Therefore, also in this case, higher areas like river terraces and banks might contain more information because it is where the accumulation of archaeological material occurs (Fernández et al, 2003b). Geological bedrock in this area (eastern bank of the Blue Nile) consists of the Nubian Sandstones Formation and Basement Complex and rocky outcrops lies at both north (Jebel Seleitat) and east (Jebel Qeili). Exposed sandstones are visible south of Wadi el Hasib and quartz pebbles coming from this region were used for making "microlithic implements" (Sedimentological and geochemical analysis, p.208, Fernandez et al, 2003). Climatic changes occurred around 8000 BC leaded to a sequential occupation and then abandonment of the area. Archaeological evidence indicates the lack of Upper Palaeolithic sites followed to the development of numerous Mesolithic sites, possibly as a consequence of the optimum climatic conditions. Before 8000 BC, the area was subject to humid conditions and the proximity of swamplands to the riverbed was not ideal for human establishment. After 8000 BC, the decrease of the flooding levels related to a reduction in humidity, led to the spreading of a Mesolithic population. Between 5400 and 4900 BC, a dry phase caused the reduction of water availability but at a later time, between 5000 and 3000 BC, another humid period occurred (Fernández et al, 2003b).

Sites Soba-2 and Sheikh Mustafa-1 are located near the eastern bank of the Blue Nile, about 50 Km south of the confluence with the White Nile, whereas site El Mahalab is on the northern bank of an ancient tributary of the Blue Nile (Fig. 2.5).

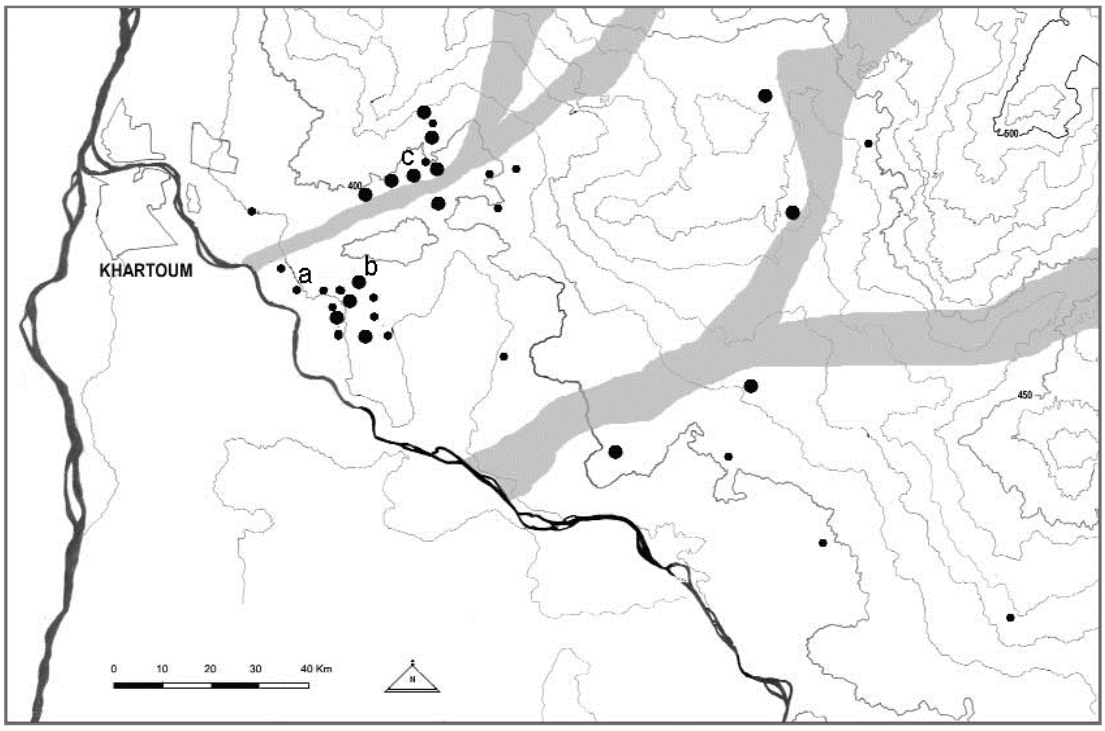

Figure 2.5: the research area in the eastern bank of the Blue Nile, southeast of Khartoum: a) Soba-2; b) Sheikh Mustafa-1; c) El Mahalab. From (Fernández et al, 2003b).

The area from which the potsherds here analysed come from lies in the southern Libyan Desert, north-western Sudan. This region is characterized by the presence of a large wadi, Wadi Howar, which originates near Jebel Marra and merge with the Nile River close to Ed Debba (Fig. 2.6). The area of interest among this group of sites is located north-west of Wadi Howar, and it is named Ennedi Erg (Figure 2.6). Here the presence of a former lake and swamp areas is attested. During prehistoric times, this area was suitable for human settlement because of its humid climatic conditions. Advantageous climate conditions prevailed from around 8300 BC, corresponding to the beginning of the Holocene, to around 4000 BC (Pachur and Kröpelin 1987; Neumann 1989, 111; Kröpelin 1993; Hoelzmann et al . 2001). Human occupation started well before the beginning of the VI millennium BC: settlements appear to be wide and situated close to the water. These elements suggest a rather sedentary / semi-sedentary way of life, based on fishing, hunting and gathering (Klein et al, 2004). Local climatic conditions changed even more dramatically around 1100 BC causing a complete disappearing of human presence in the area.

Under a geological viewpoint, the sites insist on the Precambrian basement, mainly composed of metamorphic rocks, on which some jebels formed of syenitic and granitic

rocks rise. In the area of Ennedi Erg also of Permo-Triassic sandstone occurs north-west of the sites.

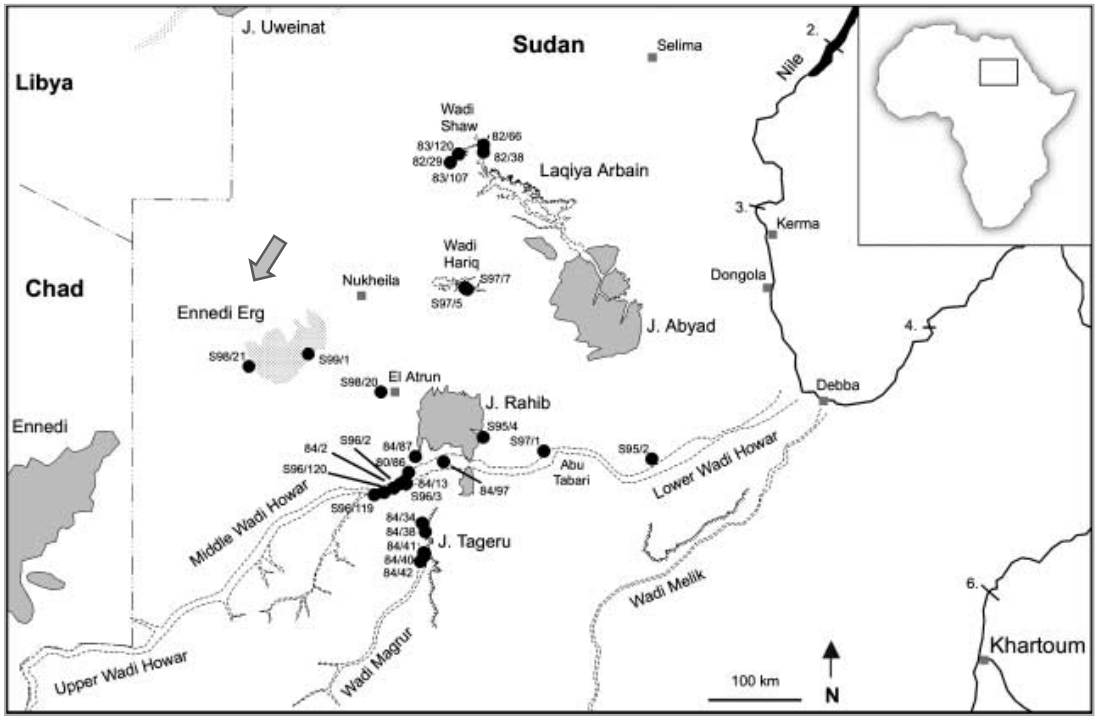

Figure 2.6: sites along the Wadi Howar area. The site indicated with the arrow is the one from which the potsherds studied in this research come from (from Klein et al, 2004)

THIRD CHAPTER

PROVENANCE STUDIES AND TECHNIQUES

3.1 Pottery and provenance studies

Pottery, raw materials and tools have been always intimately related to the inscrutable events of ancient populations, including daily life, death and relationships. The technology regarding pottery production and its development involves essentially three variables (clay, fire and need for containers) that are closely intertwined with a "complex mix of ecological, historical, economic, and social factors that differed greatly among past human societies" (Hoopes and Barnett, 1995). Specific environmental and social processes appear to be involved in the origin of pottery, since several locations sited far away attest that fired clay containers and their technology were well known since ancient times. The most ancient use of clay to produce objects is dated around 26.000 years BP in Europe (Verpoorte, 2001; Budja, 2006). The first appearance of pottery vessels is now dated to 20.000 BP in China (Xianrendong cave, Xu et al., 2012); 15.000 BP in Russia (Usti-Kyakhta); 16.000 BP in Japan (incipient Jōmon pottery, Aikens, 1995; Shelach, 2012), to the early Holocene in China (Underhill, 1997), 10.000 BP in North Africa (middle Nile valley: Jesse, 2010), 11.000 BP in central Africa (Ounjougou, Mali, Huysecom et al., 2009), and 7500 BP in South America (Pedra Pintada, Brasil, Roosevelt et al., 1996). All these archaeological findings date back to a period still characterized by a non-sedentary way of life based on hunting, gathering and fishing. At the beginning of the XIX century, the archaeological researches reported that the production and diffusion of pottery were considered as the sign of the passage from the Palaeolithic to the Neolithic period, as the evidence of the transition to agriculture and to a resident way of life. Nowadays, it is evident that it was nothing but an oversimplification of the problem, which developed differently in all the societies. Origins of pottery are still under debate but considering the complexity of processes involved in its production, it is obvious that the expertise achieved by ancient societies was the result of a series of experiments and failures.

Detailed analysis of the origin of pottery does not fall within the aim of this research, but provenance studies are strictly related to specific pottery productions. Significant amounts of early pottery found around the world show well-defined decorations and this suggests some kind of symbolic function that can be interpreted in two ways (Rice, 1999). Whereas on the one end, vessels used for serving and sharing food might be expected to be decorated with nice motifs containing information about the family or the upper social group, on the other end specific decorations might be the result of intensive socialization at a larger scale. Moreover, increasing complexity of hunter-gatherer groups and/or possible seasonal aggregations might have been associated with exchanges of products and/or technologies and might have occurred in specific and somehow sacred regions, possibly related to some natural or environmental feature (Hommel, 2016). For this reason, many recent studies including this one are focusing on provenance studies of prehistoric pottery as a key for tracing exchanges in order to study relations among groups at different levels. In order to achieve a plausible answer to this archaeological problem, specific materials and methods are required. In addition to pottery samples from different locations, it is necessary to collect raw materials (usually clay) belonging to the pertinent geographical area for comparison, as well as possible temper materials added to the ceramic paste. Later, each sample has to be characterized using the main and most suitable scientific techniques. At this regard, numerous approaches can be used, based mainly on petrographic and/or geochemical analysis, according to the ceramic paste (coarse and fine, respectively), although a multianalytical study is always preferred for the possibility of disclosing different aspect of the ceramic production and to better interpret the provenance and production technology. Lastly, it is essential to compare and crosscheck data in order to obtain an overview of the situation, which is going to integrate the archaeological panorama of prehistoric pottery.

In the frame of this research project, a series of different analytical methods largely consolidated within provenance studies of ancient pottery, like petrographic, chemical and mineralogical analyses, were coupled with new analytical method only recently and scarcely adopted in the study of ancient ceramics like strontium isotope analysis. Following are reported the methods adopted in this research with indication of the analytical procedure and preparation protocols used in the analysis of ceramic fragments and raw materials (clays and sand) collected in the area of Al Khiday and along the Nile system (for the list of samples see CHAPTER FOUR).

3.2 Petrographic analysis

The petrographic analy sis, the analytical method first applied in the study of ancient pottery (Obenauer, 1933; Shepard, 1942), represents an important tool to define the provenance, especially of coarse grained ceramics, as well as to constrain the production technology of these artefacts (Maggetti 1982; Williams 1983; Whitbread 1989, 1995; Courty and Roux, 1995; Reedy 1994, 2008; Freestone 1995; Betancourt and Peterson 2009; Quinn 2009, 2013; Ingham 2010).

In this research, optical microscopy analyses were carried out both on pottery and on briquettes obtained from the firing of the clay materials collected along the Nile system. As regards clays, they were dried out in a fan-assisted oven at 60°C for 48hrs. Then, they were crushed in an agate mortar paying special attention to the cleaning of the mortar (washing with ultrapure water - *Millipore Water purification System* - and rinsing with a small amount of the new sample). In order to prepare the thin sections from the loose materials, samples were mixed with ultrapure water and a plastic paste was prepared; they were then dried for some days obtaining what we can define a series of *briquettes* (Figure 3.1). Afterwards, half of each *briquette* was fired at 500°C for 7 hours in order to eliminate the organic matter and obtain a hard specimen that could be cut in slices to be prepared then as thin sections.

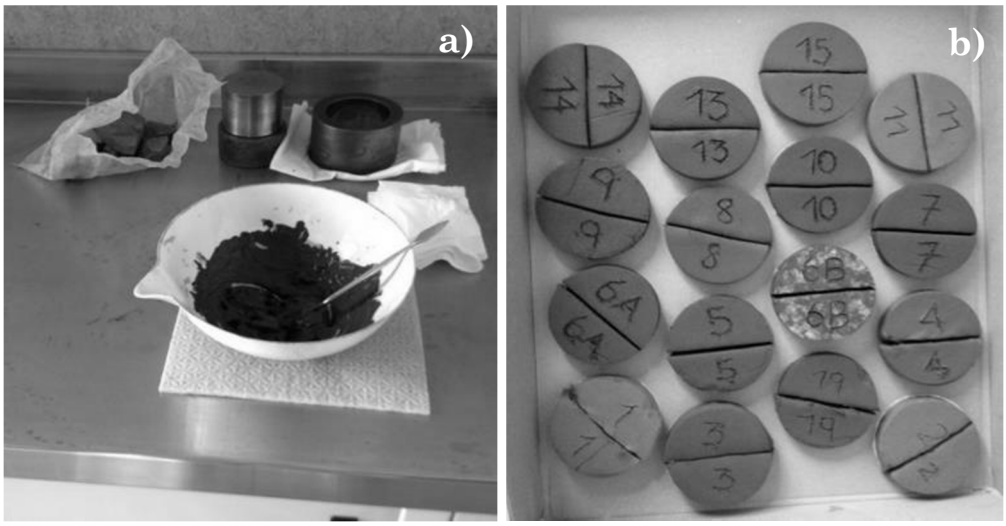

Figure 3.1: preparation of the *briquettes*: a) blending with ultrapure water. b) *briquettes*

The petrographic thin sections (30 µm thick) were prepared at the Department of Geoscience, University of Padova. Both pottery and clay samples were cut with

IsoMet® 1000 Precision Cutter in order to obtain a representative chip of the sample itself and they were then attached to a glass slide with a two-part epoxy adhesive (Araldite), grinded and polished with diamond abrasive powders until the achievement of a 30 µm thickness. Thin sections were then analysed under polarizing light microscope, with the description protocol illustrated by Whitbread (1986, 1989, 1995) and revised according to Quinn (2013). This method takes into account the main features of a paste (groundmass/matrix, non-plastic inclusions, voids/porosity) according to the following sequence.

Matrix or micromass: it is the finest constituent of the ceramic paste and represents the former clay and fine silt fraction, with particle size smaller than 10 µm. For this reason, it is not easily solvable. It is described by its homogeneity, orientation and optical state. The homogeneity describes the spatial distribution of the textural elements of the paste. Extreme heterogeneity reveals the mixing of clays, a technique adopted in some cases to obtain a more workable paste or specific aesthetic patterns (Cairo et al. 2001). Orientation is related to the preferred directions of clay minerals, pores and eventually of other mineral phases with elongated habit. It depends on the forming technique, although a univocal correspondence does not exist. In fact, the spatial arrangement (Courty and Roux 1995; Rye 1981) depends on the stress orientation (compression or shear) during the object shaping, and it is conditioned by the section orientation (Quinn 2013). The optical state indicates if the matrix under crossed polars still shows interference colours and extinctions upon rotation of the thin sections, if clay minerals and/or other fine grained grains (such as small crystallites of calcite, dolomite) are still crystalline (optically active) or decomposed determining an inactive matrix. Optically active micromass can be described in terms of birefringent fabric (b-fabric) according to Bullock et al. (1985) and the recent revision of Quinn (2013). It can be distinguished on the basis of type of minerals, size and orientation of clay domains (aggregates composed of particles with parallel orientation) in the micromass, using the same terminology adopted in micromorphological thin-section analysis: crystallitic, strial, striated and speckled.

Post-deposition processes may affect the micromass composition by precipitation of secondary phases (Quinn, 2013), such as calcite, aragonite, gypsum, and pyrite, and by oxidation, reduction or hydration of oxides (Secco et al., 2011).

Voids: in the ceramic paste they are classified by their shape, concentration and size. Concerning the shape, they are divided in four groups, according to the terminology adopted in soil micromorphology (Stoops, 2003): planar (linear in thin section but

planar in three dimensions), channels (cylindrical in three dimensions), vughs (large and irregular) and vesicles (regular shape, smooth surfaces). Increasing the firing temperature, voids tend to assume more regular shapes, switching from vughs to vesicles. The amount of pores is estimated as percentage by comparing the distribution with the diagram in Figure 3.2. Voids are also classified as primary and secondary when they are formed during the working of raw materials, or related to the decomposition of minerals and organic phases and to the shrinkage of the clay, respectively.

Secondary phases can precipitate in voids and occasionally cover also the external surfaces, testifying the post-depositional chemical-physical conditions. Secondary calcite, gypsum, pyrite, jarosite, vivianite, mitridatite, halite and crandallite are reported in literature (Freestone 2001; Cau Ontiveros et al. 2002; Maritan and Mazzoli 2004; Secco et al. 2011; Rodrigues and Costa, 2016).

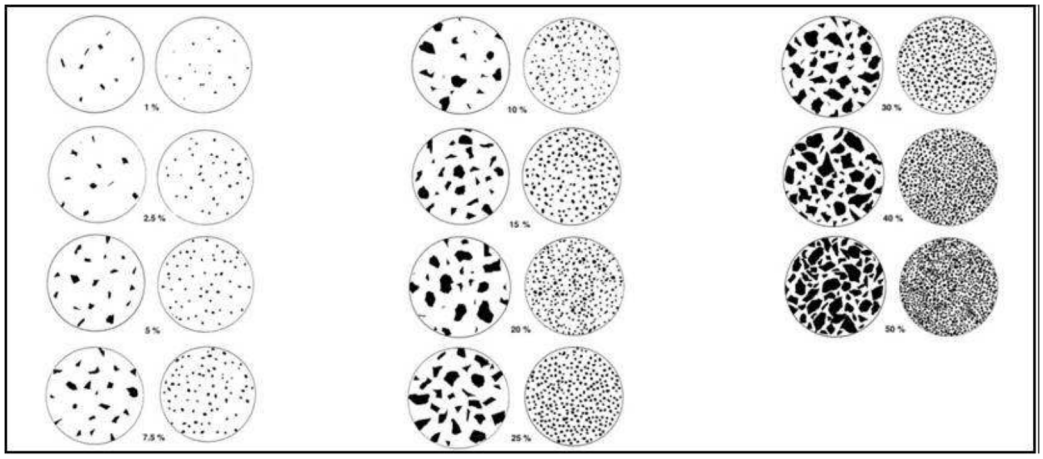

Figure 3.2: chart for the estimation of the percentage composition of the textural elements, voids included

Inclusions: they are mainly rock fragments and minerals with grains sizes bigger than 10 µm. They can be naturally present in raw materials or intentionally added by the potter (in this case named *temper*). Fundamental in the definition of pottery provenance is the occurrence in the ceramic paste of mineral and/or rock markers, specific mineral phases and/or rocks that can be univocally attributed to a specific geographic region. However, they are often very difficult to find in most of the common pottery productions, due to the absence of specific mineral phases in the lithotypes outcropping in the production area from which the clay and/or temper (deliberately

added material by the potter) were collected. Occasionally, heavy minerals can be used to constrain the provenance (Mange and Bezeczky 2007). A particular type of inclusions is represented by organic origin inclusions, mainly consisting in vegetal remains, which normally testify the deliberate addition of a temper in the clay paste to produce light ceramic materials. Due to the low decomposition temperature in oxidising conditions, vegetal remains are often burned out during firing, and large pores preserving their original shape (moldic voids) are the only attestation of their former presence. The plant temper is preserved in pottery (Jiang and Liu 2006; Tomber et al., 2011; Mariotti Lippi et al., 2011) when firing did not exceed the decomposition temperature of organic matter (less than 500-600°C), or when the process was short, or took place in reducing conditions. In some cases, types of plants added as temper can be identified on the basis of the analysis of phytoliths preserved after firing (De Paepe et al. 2003; Kreiter et al. 2014).

The distinction between naturally occurring inclusions and temper is normally defined on the basis of the grain-size distribution, shape and composition. Generally, polymodal distributions of inclusions indicate tempering with sand, when inclusions have rounded shape, or ground-up materials, when especially large inclusions are angular shaped. Moreover, some type of inclusions (such as fragments of bone, shells, chamotte, glass, chaff, straw, rice, and hair) testify the deliberate addition by the potter, since they are not natural constituent of base clays. Grog or chamotte is a particular temper composed of fired ceramic, the occurrence of which indicate recycling of such material (Whitbread 1986; Cuomo Di Caprio and Vaughan 1993).

As for porosity, in this research its amount was estimated in percentage, through the relative proportion of the coarse and fine components (c:f ratio) of the ceramic paste, respectively larger and smaller than 10 μm. The c:f distribution can be: close-spaced, single-spaced, double-spaced or open-spaced depending upon the distance between grains. The description of the inclusions takes into account the roundness of the grains (see Figure 3.3), that is to say the degree of rounding of corners and edges. Therefore, they can be: angular (A), sub-angular (SA), sub-rounded (SB), rounded (R) and well-rounded (WR).

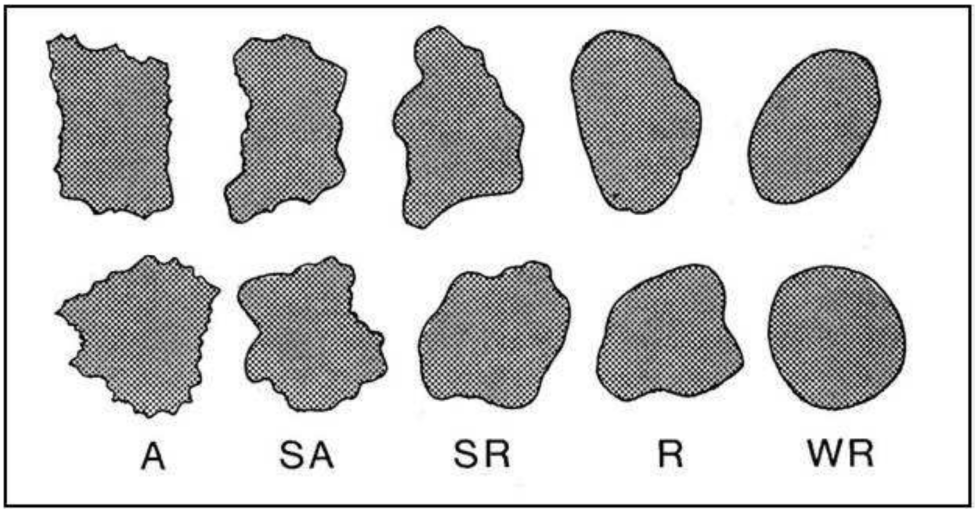

Figure 3.3: roundness classes to describe inclusions

3.3 Chemical analysis and statistical treatment of data (XRF)

The chemical composition of a potsherd can supply important information about the raw materials used and the production processes, as well as contamination effects caused during its usage and post-depositional history. Various analytical methods can be adopted to define the chemical composition, such as neutron activation analysis (NNA), atomic absorption analysis (AA), inductively coupled plasma mass spectrometry (ICP-MS) and X-ray fluorescence (XRF), being this latter the more diffused one for the easy accessibility, simple sample preparation, low cost and diffusion of the instruments worldwide.

X-ray fluorescence analysis was conducted within this research project at the Department of Geosciences, University of Padova. Pottery samples were ground in an agate mortar, after the cleaning of the pottery surfaces with a micro-drill in order to eliminate possible alterations. Qtz-tempered sherds have been broken into small pieces and then grinded in an agate mortar. Before grinding a sample, the mortar need to be washed with ultrapure water (*Millipore Water purification System*) and rinsed with a small amount of the new sample, in order not to contaminate one sample with the other. Kfs-tempered ceramics could not be grinded as quartz-tempered ones.

Grains of potassium feldspar have been eliminated through a micro-drilling carried out under the stereo microscope (Figure 3.4). The clay matrix extracted from each sample (nearly 100mg) has been then treated together with the other powdered samples. Clay samples were ground in an agate mortar applying the same cleaning procedures as for pottery samples.

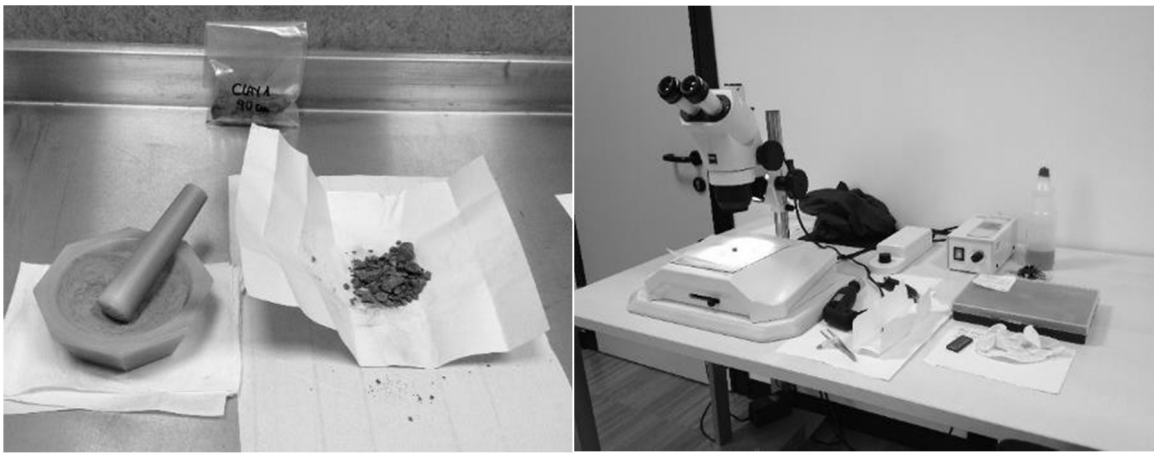

Figure 3.4: two phases of the preparation of ceramic samples: a) grinding of a qtz-tempered sherd; b) micro-drilling of the Kfs-tempered sherd under the stereo microscope

About 1g of each sample was heated in a furnace at 860°C for about 20 minutes and then at 980°C for about 2 hours for the determination of loss on ignition (L.O.I.) and therefore the measurement of the volatile elements: hydrogen, oxygen and carbon. These are not determined by XRF and are related to the occurrence of residual organic matter, water bound in clay and hydrated minerals and carbon oxides forming carbonate phases (calcite, dolomite). Samples for XRF analysis were then prepared as glass beads mixing 0,65 g of the calcined powder and the flux di-lithium tetraborate $Li_2B_4O_7$ with a dilution ratio of 1:10 and melted using a fluxer Claisse Fluxy (~1150°C). The instrument is a WDS sequential Philips PW2400 spectrometer, operating under vacuum conditions and equipped with 3 kW Rh X-ray tube, 5 analysing crystals (LiF220, LiF200, Ge, PE, TlAP), 2 detectors (flow counter and scintillator), 3 collimators (150 µm, 300 µm and 700 µm), 4 filters (Al 200 µm, Brass 100 µm, Pb 1000 µm and Brass 300 µm) and sample changer Philips PW2510 with 30 sample holders. Chemical elements analysed are: Si, Ti, Al, Fe, Mn, Mg, Ca, Na, K, P Sc, V, Cr, Co, Ni, Cu, Zn, Ga, Rb, Sr, Y, Zr, Nb, Ba, La, Ce, Nd, Pb, Th and U. Instrumental precision is within 0,6% relative for major and minor elements, and within 3% relative for trace elements. Detection limits are within 0,01% for major elements Al, Mg and Na, within

0,2% for Si, within 0,005% for Ti, Fe, Mn, Ca, K and P. Limits for trace elements are (in ppm): Sc=5, V=5, Cr=6, Co=3, Ni=3, Cu=3, Zn=3, Ga=5, Rb=3, Sr=3, Y=3, Zr=3, Nb=3, Ba=10, La=10, Ce=10, Nd=10, Pb=5, Th=3, U=3.

A set of geological standards, as analytically tested by the international scientific community (Govindaraju, 1994), was used for calibration; they were supplied by the following agencies: USGS (United States Geological Survey, Reston, USA), CRPG (Centre de Recherches Pétrographiques et Géochimiques, France), ANRT (Association Nationale de la Recherche Technique, Paris, France), GIT-IWG (Groupe International de Travail - International Working Group, France), RIAP (Research Institute of Applied Physics, Irkutsk, Russia), GSJ (Geological Survey of Japan, Japan), MINTEK (Council for Mineral Technology, South Africa) and WIHG (Wadia Institute of Himalayan Geology, India).

Essentially, compositional data are measures of proportions, percentages, parts per million (ppm), *etc.*, which sums up to a constant value, also referenced as closed data (around 100%). Such data are constrained and require a transformation to remove the constraint, thereby making them usable in context of standard statistical approaches. The chemical data were then statistically treated using both a univariate and a multivariate approach. The R Project for Statistical Computing was used to explore the compositional variation matrix, according to the method proposed by Buxeda i Garrigós (1999). Chemical data were then processed with standard statistical tools such as Principal Component Analysis (PCA) and cluster analysis (CA) on a subset of elements, excluding those with a low ratio between total variation (vt) and variance (τ.i). Raw data were standardised according to procedures designed by Vitali and Franklin (1986), Baxter and Buck (2000) and Buxeda i Garrigós (1999), by log-normal centred log-ratio transformation (Aitchison, 1986) in order to avoid misclassifications due to the different orders of magnitude and range of variation of the variables.

3.4 Mineralogical analysis and statistical treatment of data (XRPD)

The mineralogical composition of a ceramic can be defined on the basis of the X-Ray powder diffraction (XRPD) analysis. This technique has been intensively used in archaeometric studies of pottery to constrain production technologies, with particular focus on the raw materials used and the firing conditions, mainly temperature and firing atmosphere (Bimson, 1969; Heimann and Franklin, 1972; Grattan-Bellew and Litvan, 1978; Maggetti, 1982; Martin-Socas et al.,1989; Philpotts and Wilson, 1994; Tite, 1995; Maritan, 2004; Nodari et al., 2004; Papadopoulou et al., 2006; Prudêncio et al., 2006; Prudêncio et al., 2009; Charalambous et al., 2010; Velraj et al., 2010; Mangueira et al., 2011; Maritan et al., 2013). It is also used to identify and characterise possible post-depositional alterations (Heimann and Maggetti, 1981; Maggetti et al., 1984; Pradell et al., 1996; Buxeda i Garrigós, 1999; Buxeda i Garrigós et al., 2001; Maritan and Mazzoli, 2004; Buxeda i Garrigós et al., 2005; Schwedt et al., 2006; Secco et al., 2011).

XRPD analyses in this project were carried out at the Department of Geosciences, University of Padova. This analysis allows identifying mineralogical composition, which is crystalline phases in pure materials and complex mixtures. About 5 g of each sample (only clay) were ground in fine powder (less than 10 mm) with an agate mortar Retsch RM 0. The instrument used for this analysis is a Philips X-Pert PRO diffractometer (PW3710 parafocusing geometry Bragg-Brentano diffractometer) equipped with a copper anode, sample spinner, a goniometer PW3050/60 (Theta/Theta) with minimum step size 2Theta: 0,001 and a RTMS detector (X'Celerator). The analyses were conducted in the range 3–80° 2Theta using a step interval of 0.017° 2Theta, with a counting time of 100 s. The phase identification and semi-quantitative analyses were performed using the software package X'Pert HighScore Plus (3.0 version) with whom the shape of multiple peaks were closely examined. The phases' identification was gained by the comparison with the reference pattern databases PDF2 (ICDD), Panalytical-ICSD and COD (Crystallography Open Database).

Since XRPD is an easily accessible, fast and cost-effective analytical technique, it is commonly performed on large numbers of samples, the interpretation and especially the comparison of which is time-consuming. Moreover, the definition of homogeneous

groups of samples in terms of mineralogical composition is complicate, due to the complex nature of the data themselves, and the complexity of defining and quantifying differences among them. For all these reasons, XRPD patterns were statistically treated by cluster analysis according to the procedure proposed by Piovesan et al. (2013) for analysis of mortars and Maritan et al. (2015) for that of pottery.

3.5 Microstructural analysis (SEM)

The microstructural analysis of a potsherd can supply important information on the composition, structure and texture of the ceramic paste, in terms of production recipes, firing temperature, provenance and alteration processes (Tite and Maniatis, 1975; Tite et al., 1982; Maritan et al., 2012; Secco et al., 2011; Maritan and Mazzoli, 2004). In the present research project this analytical method was used to define the possible occurrence of secondary phases in the analysed potsherds, and the microstructural diversity between the micromass of pottery produced according to different recipes (quartz-rich and feldspar-tempered) and the possible corresponding clay materials.
The analyses were carried out at the Department of Geosciences, University of Padova. Samples were prepared as polished thin sections, carbon coated in order to make them conductive. SEM-BSE images were acquired with a SEM CamScan MX 2500 microscope, coupled with an energy dispersive spectrometer (EDS), equipped with a LaB_6 cathode, working in high vacuum mode (HV). Back scattered electron images (SEM-BSE) were acquired. This type of images are grey scale images where the discrimination of phases is based on the mean atomic number (Z), commonly associated to the grey hues: a "brighter" BSE intensity is correlated with greater average Z, and "darker" areas with lower average Z. The analytical parameters used during the acquisitions (luminosity, contrast, working distance, spot size,…) have been changed time by time considering the specific features of each sample. SEM analyses were carried out in order to characterize specific features like types of inclusions, matrix structures and to perform a comparative study of clay and pottery attributes.

3.6 Thermal Analysis of clay materials (TGA and DSC)

Thermal analysis has been defined by the International Confederation of Thermal Analysis (ICTA) as a study of the relationship between a sample property and its temperature as the sample is heated or cooled in a controlled manner. Thermogravimetric analysis (TGA) measures the change in mass of a material as a function of time at a determined temperature (i.e., isothermal mode), or over a temperature range using a predetermined heating rate. Essentially, a TG consists of a microbalance surrounded by a furnace. A computer records any mass gains or losses. Weight is plotted against a function of time for isothermal studies and as a function of temperature for experiments at constant heating rate. Thus, this technique is very useful in monitoring heat stability and loss of components. DSC (Differential Scanning Calorimetry) allows the detection of endothermic and exothermic transitions: the sample and reference are maintained at nearly the same temperature throughout the experiment and the heatflux is measured. The obtained plot is known as a DSC curve and shows the amount of heat applied as a function of temperature or time.

Natural clay is generally made up of a mixture of clay minerals. Some of the common clay minerals that occur in nature are kaolinite, illite, montmorillonite and nontronite. Thermal methods are well-established investigative tools in clay science.

Following are reported the main transformation which can be recorded during a thermal analysis of a clay. Drying shrinkage of clay minerals occurs due to pore water loss in the temperature range of 100–150°C. The oxidation of any organic material, commonly present in the secondary type clays, takes place in the range of 200–600°C. The oxidation of sulphides begins between 400 and 500°C. The hydroxyl water is removed from the clay minerals starting at temperatures around 500°C and continuing to temperatures approaching 900°C. The nature of the clay minerals in clays and the particle size influences the specific temperature and rate of hydroxyl loss. An endothermic reaction below about 200°C usually indicates the presence of montmorillonite or illite. A clay containing these components will have high plasticity and shrinkage. In general, the larger this fraction the higher the plasticity and shrinkage. Endothermic reactions between 300 and 500°C usually indicate a hydroxide of alumina or iron. A broad exothermic reaction between 200 and 600°C is due to the presence of an organic material. Clays yielding such thermal reactions will

frequently be very plastic. An intense endothermic reaction at about 600°C followed by a sharp exothermic reaction at about 975°C indicates the presence of kaolinite. A clay with a peak of low intensity at about 500 or 700°C followed by another endothermic reaction at about 900°C and then a final exothermic reaction may indicate the presence of illite or montmorillonite. A small endothermic break at 575°C is typical of quartz transition between the phase α to phase β. An intense endothermic peak at about 850°C, and relative loss of weight, indicates the presence of calcite, whereas a doublet of endothermic peaks at 750°C and 850°C are characteristic of the occurrence of dolomite.

Thermo-gravimetry (TG) and differential scanning calorimetry (DSC) analyses coupled with simultaneous FTIR for evolved gas analyses (EGA) were carried out by means of a Netzsch Jupiter STA449 (NETZSCH-Gerätebau GmbH, Selb, Germany) F3 apparatus coupled with a Bruker Tensor 27 (Bruker Optik GmbH, Leipzig, Germany) at the Department of Geological and Environmental Studies, University of Sannio (Benevento). Powdered samples (20–30 mg) were placed in alumina crucibles and heated up to 1150°C at 10°C/min of heating rate in an air-purged, silicon carbide furnace. The furnace was initially purged for 1 h at 40°C to remove atmospheric contamination; the weight signal was calibrated using Al_2O_3 standards to correct for buoyancy effects and beam growth drift. The FT-IR EGA was carried out with 8 cm^{-1} resolution, 32 spectra scans per minute, and 100 spectra scans for background. Netzsch Proteus 6.1.0 (NETZSCH-Gerätebau GmbH) and Opus 7.2 software (Bruker Optik GmbH, Leipzig, Germany) were used for data analysis. The possibility of coupling the thermal analysis with the infra-red spectroscopy on the gas derived from the phase decomposition, allowed to better correlate functional groups of the released volatiles with specific mass loss.

Thermal analyses were carried out in order to characterize the clay samples collected along the Nile system with the aim of combining these data with the relative mineralogical features.

3.7 Sr isotope analysis (Thermal Ionization Mass Spectrometry)

In the last decades, provenance issues on archaeological materials have been faced also through the strontium isotope ratio. Unlike other ancient materials, like obsidian (Gale, 1981), marble (Brilli et al., 2005), glass and glaze (Freestone et al., 2003; Brems et al., 2013; Ma 2014), and human remains (Price et al., 2002; Bentley, 2006), the strontium isotope ratios have been only recently investigated, though still limited to few cases (Alex et al. 2012, Knacke-Loy 1994, Pinter 2005, Carter et al. 2011; Li et al. 2005) to constrain the provenance of pottery. This is due to the fact that the isotopic signature of a ceramic depends on both that of the used clay and that of possible added temper. The pottery ceramic body is in fact composed of a clay and a silt fraction, and eventually a sandy-sized fraction of the used raw materials, constituting the micromass and the inclusions of the ceramic paste, respectively. Therefore, the isotopic ratio of a potsherd depends from the ratio between these different grain-size fractions and can be strongly affected by the presence of specific mineralogical phases or rock fragments in the raw materials.

The study of Carter et al. (2011) clearly indicates how the Sr isotopic ratios are directly related to the different minero-petrographic composition of inclusions occurring in the prehistoric Grey-ware from the Grand Canyon (USA). In this case study, the isotopic imprint results to be related to the coarse-sized fraction of the ceramic paste.

The study of Li et al. (2005) showed the potentiality of Sr isotope ratio analysis to constrain the provenance of IX-XI century Chinese stoneware, therefore of fine pottery, the isotopic ratio of which fundamentally depends on those of the base clay. Specifically, the Sr isotopic ratio was crucial to distinguish ceramic materials obtained by a kaolinite-base clay, characterized by a low Rb/Sr ratio, from those produced using a sericite-base clay, with a higher Rb/Sr ratio.

The research of Knacke-Loy (1994) was based on the combination of isotopic and geochemical data through which local and imported ceramics could be distinguished. Bulk powders of clays, loam and marl of variable grain size and geochemical composition from alluvial deposits in the surroundings of Troy in addition to locally excavated ceramic sherds were analysed. A selection of samples was isotopically investigated, including some reference pottery from Mykene, Tiryns, Cyprus, and Syria.

Pinter (2005) carried out an investigation of Early Iron Age knobbed ware of Troy and the Balkan region using petrographical, mineralogical, geochemical, and isotopic methods. Sr and Nd isotopes were combined. The samples varied significantly in Sr and Nd isotope ratios as a result of differences in the geological background of the various investigation sites.

Alex et al. (2012) investigated ceramics from the Teotihuacan Valley, Mexico, using different approaches including Sr isotope analysis. The results of the investigation suggested that clay deposits used as raw materials were derived from weathered young volcanic rocks of the Mexican volcanic belt.

In the frame of this research project, the strontium isotope analysis is explored to define if it can represent a strategic tool for pottery provenance studies when other methods (like petrographic and analysis) fail.

In the environment, strontium (Sr) is found in rocks, water, soil, plants and animals. Strontium is composed of different percentages of its four isotopes: ^{84}Sr (~ 0.56%),^{86}Sr (~9.87%), ^{87}Sr (~7.04%) and ^{88}Sr (~ 82.53%) (Faure and Powell, 1972). Among these four isotopes, only ^{87}Sr is radiogenic; it is formed by radioactive decay of rubidium (^{87}Rb), which has a half-life of ~ 4.88×10^{10} years (Faure, 1986). The strontium concentrations and isotope ratios in the soil, plants and rocks vary according to local geology. $^{87}Sr/^{86}Sr$ ratios are quite variable because of bulk composition of the surface. Concerning clay samples, the isotopic signature of sediments at a specific location can be considered as a weighted average of the isotopic signatures of end-member rocks eroded in the drainage basin. For this reason, it is possible to attempt a comparison between clays (meant as raw materials) and pottery pastes (intended as a mix between clays and possible added temper, usually a mineral or organic material). The possibility to discriminate different geographical origins within small ranges of variation of the $^{87}Sr/^{86}Sr$ isotope ratios, requires high precision of the measurement and this can be reached by the Thermal Ionisation Mass Spectrometry (TIMS) technique. Mass spectrometers are designed to separate ions (charged atoms and molecules) on the basis of their specific masses (mass/charge unit). This separation occurs because of their differential motions in magnetic fields. Most mass spectrometers basically consist of three parts: the source (that originates the beam of ions), an electromagnetic analyser (that separates the ions) and an ion collector composed of a Faraday bucket that collects the ion and converts it in an electrical signal (Faure and Mensing, 2005). Samples are normally processed under clean laboratory conditions and are sub-sampled before isotope analysis. They are subjected

to several cycles of dissolution with acids and evaporations to dryness. After the column chromatography, they are loaded on filaments and placed inside the source. The ion source consists in a chamber that operates under vacuum (10^{-7} mbar) thanks to a vacuum pump. Each filament is traversed by a current (2-3 A) that causes the heating of the filament and finally brings to the ionization of the atoms in the vapour. Only some atoms are ionized while others remain neutrals. The ratio between ionized (n^+) and neutral (n_0) atoms is named "ionization efficiency" and is given by:

$$n^+/ n_0 \propto e^{(W-I)/(kT)}$$

where W is the work function of the emitting surface, I is the ionization potential of the element which must be analysed, *k* is the Boltzmann constant and T is the temperature in Kelvin's degrees. Then, the ions are accelerated under a high voltage and collimated into a beam of ions, which enters in an electromagnetic field through a flight tube. The tube is kept under high vacuum (10^{-8} mbar or lower) in order to minimize collisions with residual molecules. The direction of the electromagnetic field is perpendicular to that of the travelling ions. The interaction between the ions and the field deflects the ions into circular paths, whose radii are determined by their mass. The ions have electric charge q and mass m and their kinetic energy E depends on acceleration due to the voltage V according to the equation:

$$E = \tfrac{1}{2}\, mv^2 = qV \qquad \text{therefore} \qquad v^2 = 2qV/m$$

where v is the particle's velocity. When the beam moves through the magnetic field B, the Lorentz's force (F = qvB) deflects its trajectory in a circular path with radius r. Since the Lorentz's force is a centripetal one, we equate the expression of the Lorentz's force with the expression of the centripetal force (mv^2/r), obtaining:

$$qvB = mv^2/r \;, \quad v^2 = B^2q^2r^2/m \quad \text{and so} \quad 2qV/m = B^2q^2r^2/m$$

If we formulate the q/m ratio in terms of intensity of the magnetic field B, radius of curvature r and electric potential V we obtain:

$$m/q = B^2r^2/2V$$

The magnetic field separates ions that have different mass/charge ratios. At the end of their path, the electric charges (ions) are detected using an ion detection system (Faraday cup) inserted in the high vacuum of the mass spectrometer. These electric charges are collected for a time span (integration time) determining a voltage at the

end of a resistor; the ion voltages are then amplified and processed in order to obtain the isotopic ratio (Figure 3.5).

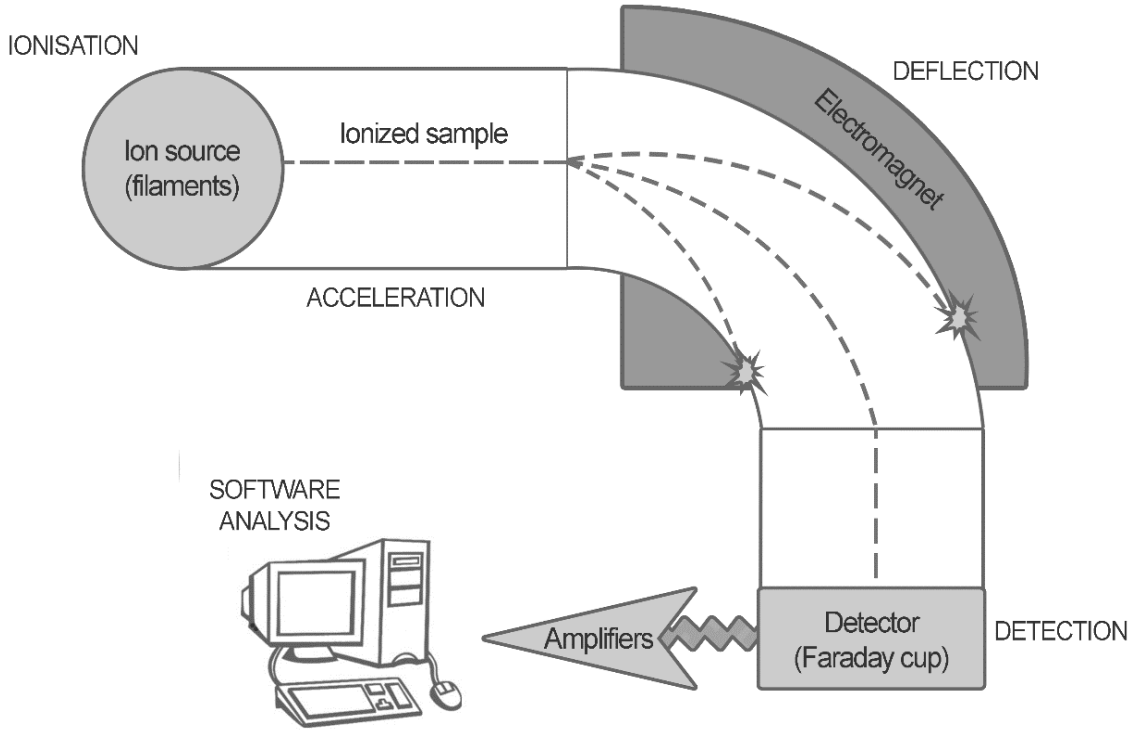

Figure 3.5: scheme of a mass spectrometer

The calculus of the $^{87}Sr/^{86}Sr$ isotopic ratio requires two corrections. ^{87}Rb is a well-known interference on ^{87}Sr peak during TIMS analyses and this interference is usually solved by chromatographic separations. Moreover, Rb has a relatively low ionization energy and it can be easily volatilized from the hot filament before the measuring of Sr. The other correction regards the mass-fractionation. The process of evaporation from the hot filament is mass-dependent. Solid-source TIMS analysis produces low fractionation effects, but the process of evaporation starts to 'use up' the lightest isotopes in the sample so that the isotopic composition of the residue becomes progressively heavier and heavier (the 'reservoir effect'). Eberhardt et al. (1964) showed that this process follows a Rayleigh fractionation law. The magnitude of this effect could yield totally unacceptable errors of up to 1% per amu in measured isotope ratio (Dickin, 2006). However, for elements with two or more non-radiogenic isotopes, an internal normalization for such mass-dependent fractionation can be performed. In the case of strontium, the fractionation of $^{87}Sr/^{86}Sr$ can be monitored using the $^{88}Sr/^{86}Sr$ ratio, since ^{88}Sr and ^{86}Sr are both non-radiogenic and the ratio $^{86}Sr/^{88}Sr$ can be

considered constant at a certain good approximation throughout the Earth and is taken to be 0.1194 by international convention (Steiger and Jäger, 1977). In order to achieve high precision data, in single-collector TIMS machines the magnetic field is 'switched' to check a sequence of peak positions. On switching to a new peak, there is a delay time of 1–2 s to allow the complete decay of the Faraday's resistor before new ion current acquisition. The signal of each mass is collected for a few seconds. The software then cycles round and round a series of peaks, baseline/background(s) and interference monitor position(s), interpolating between successive measurements of the same peak to correct for growth or decay of the beam size. The instrument used was a Micromass VG 54E single-collector mass spectrometer interfaced with an IBM computer. Shown below the electromagnetic parameters and other working conditions: accelerating potential 8 kV, magnet current approximately 3.0 A, pressure in the flight tube about 10^{-7} mbar. The data acquisition software was Analyst (Version 2.20), from Ludwig K.R. (Ludwig, 1993) The $^{87}Sr/^{86}Sr$ values were all normalized to the Nier (1938) $^{86}Sr/^{88}Sr$ value of 0.1194. Over the period of the measurements, the average value of NBS 987 was 0.7102595 +/- 0.0000080 (2σ, n = 4).

In order to measure the amount of Sr in some samples, isotope dilution technique was used. In this technique, the sample is mixed with a tracer solution or 'spike', which contains a known concentration of the analysed element, artificially enriched in the isotope which is the less abundant in nature. The resulting isotopic composition is measured by mass spectrometry and used to calculate the concentration of the element in the sample. Before use, the concentration of the tracer must be accurately determined by the same technique. In the mixture, each isotope peak is the sum of spike and natural material. Isotope dilution is a very-high-precision method. The only other sources of error in isotope-dilution analysis are incomplete homogenization between sample and spike solution, and weighing errors. The first of these can be overcome by checking for any undissolved material and repeating the dissolution steps as necessary until complete solution is achieved (Dickin, 2006). Balance calibration and calculation of evaporation rate during weighing can solve the problems regarding other inaccuracies.

Isotope analyses were carried out at Geochronology and Isotope Geochemistry Laboratory of the Institute of Geosciences and Earth Resources of National Council of Research (CNR -IGG - Padua Territorial Unit).

Sample preparation for TIMS analysis was carried out in clean lab conditions. At first, the Teflon labware was cleaned with several boilings in distilled water and acids: 1:1

HNO_3 (one time) and stilled HCl (two times) and washings with water (milli-Q water subsequently purified by slow evaporation in quartz, and by very slow evaporation in Teflon bottles). All the reactants (HCl, HF, HNO_3) used throughout the dissolution and elution procedures were purified by distillation and/or very slow evaporation in Teflon bottles. Then approximately 1 g of powder was calcined (fired in platinum crucibles at 750°C for one night). Then the samples (approximately 100 mg) were digested through repeated acid attacks: HF and HNO_3 together with HCl were used to totally dissolve the sample. In a sealed Savillex® Teflon vial, 4ml of HF were fist added to the sample. The sample was then left on a hot plate at about 100°C for one night and then the vial open, and the solution evaporated to dryness. The most part of Si was removed this way as SiF_4. In the second step of dissolution, approximately 1 ml of HNO_3 was added to 4 ml of HF and the vials have been kept at 100°C for 48 hours. After the subsequent evaporation to dryness, approximately 4 ml of 6.2 N HCl were added to the sample, and the vials were closed to completely dissolve the residue. Vials were heated at 100°C for one night and then opened to evaporate the solution to dryness. HCl dissolution and subsequent evaporation was then repeated and after the subsequent evaporation, the residue was dissolved in 2.5 N HCl. This solution was centrifuged, and processed by column chromatography in order to separate Sr from Rb. First, 3x0,1 ml of the solution were loaded on a column of cation-exchange analytical grade resin (AG 50Wx-12 BioRad) (Figure 3.6a). Then 4x0.1 ml of 2.5 N HCl were loaded for washing. In order to separate Sr, 2.5 N HCl was used: three aliquots of this eluent were added for the waste collection (10 ml, 10 ml, 7 ml) and one aliquot (15 ml) for the collection of Sr in a Teflon Becker. At the end, columns were washed three times with 6.2 N HCl and then reconditioned with 2.5 N HCl. The collected Sr was first evaporated to dryness and then repeated nitrations were carried out using 5-6 drops of ultrapure HNO_3 in order to change Sr chloride to Sr nitrate and to remove possible presence of resin. After evaporation, the sample was dissolved in 0.5 N HNO_3 and loaded on a single tungsten filament over a drop of $TaCl_5$, and dried at approximately 0.3 A (Figure 3.6b). After loading, the filament current was slowly increased to a dull red, hold for ~10 seconds.

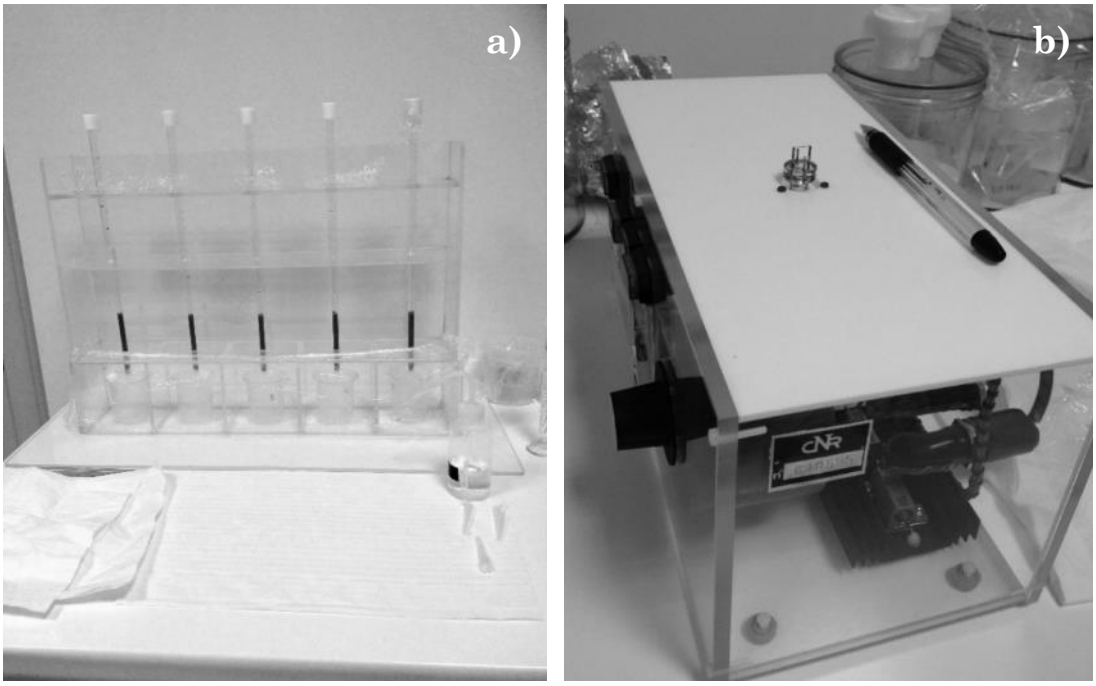

Figure 3.6: a) cation-exchange resin column for chromatography. b) loading device for the tungsten filament

FOURTH CHAPTER

DESCRIPTION OF THE SAMPLES

4.1 Clay samples and other raw materials

From 2013 to 2015, nearly 1800 km have been covered along the banks of the Nile River from central to Northern Sudan. The sampling design has been wisely planned in order to reach every branch of the river along the three main segments and active tributaries of the river (Blue Nile, White Nile, Atbara and Main Nile) and further points of interest in the proximity of recorded archaeological sites. Soil samples have been numbered from 1 to 31 (Figure 4.1) and basically they represent the Nile sediments as follows:

- ***White Nile western bank (WNw)***: clay 1, 1-35, 1-70, 1-90, 2, 11, 12 and 31 are representative of the western bank of the White Nile; clay 1 was collected near the archaeological sites of interest in this project, that is to say Al Khiday, and 1-35, 1-70, 1-90 are three parts of a core drilled in the same area, with the samples taken at a depth of 0, 30, 70 and 90 cm respectively from the surface. The White Nile mainly drains and cut rocks of the basement complex composed of amphibolite-facies to granulite-facies gneisses (Padoan et al, 2011; Abdelsalam et al., 2002; Link et al., 2010) and the clastic sediments of the Nubian Sandstone Formation. All these rocks and therefore clay sediments show the quartzose signature of Craton Interior Provenance.
- ***White Nile eastern bank (WNe)***: clay 17, 18 and 30 describe the eastern bank of the same river (WNe) (see Table 4.1), defined also as part of Gezira, an area where the White Nile sediments used to be mixed until at least the late Holocene, to Blue Niles ones (Williams et al., 2015);
- ***Blue Nile (BN)***: clay 13 and 14 were sampled along the eastern bank of the Blue Nile, whereas clay 15 and 16 along its western bank. Blue Nile sediments are largely derived from volcanic rocks and gneisses belonging to the Ethiopian highlands (Padoan et al, 2011);

- ***Main Nile "a" (MNa)***: samples belonging to the stretch of the river between Khartoum and Atbara are clay 3, 4, 5, 6A/6B and 10; generally, MNa sediments show mixed provenance as they are characterized by volcanoclastic, metamorphic and clastic assemblages (Padoan et al, 2011);
- ***Atbara (A)***: only one sample was collected along the river Atbara (clay 9) before its confluence into the Main Nile; the sediments of this tributary are very rich in volcanic constituents, as it cross the Ethiopian and the eastern Sudan sequences;
- ***Main Nile "b" (MNb)***: clays from 19 to 29 are representative of the Nile River after the confluence of the Atbara River, where the same characteristics as the MNa stretch are shown.

A total of 18 samples have been selected for the isotopic analyses and they are marked with the asterisk in Table 4.1. They roughly represent the sediments of the corresponding river branch.

The sampling method consisted in collecting the selected clay from the ground using sterile gloves, bearing in mind that it is important to choose undisturbed and workable sediments. As the disturbance may be restricted essentially to the superficial layer, near-surface samples rather than surface samples have been preferred. Moreover, the features of the hydrographic basins belonging to the main branches of the Nile River have not been subjected to any geological alteration in the last 10000 years, so we can assume that the soil samples collected lately are very similar to those present in the Mesolithic period. For the area of Wadi Soba and Wadi Howar there are not clay samples available. This is due mainly to the fact that these ancient tributaries are now completely drained and that the clay sediments underwent important modification processes (secondary mineral precipitation, especially calcite) related to the desertification of the areas. Moreover, the area of Wadi Howar is of very difficult access.

Table 4.1: clay samples with their location and GPS coordinates; "*" samples selected for Sr isotope analysis

SAMPLE ID	SELECTED	LOCATION	ACRONYM	COORTDINATES
CLAY 1	*	near Al Khiday	WNw	N 15° 25' 30" E 32° 26' 50"
CLAY 1-35	*	near Al Khiday	WNw	N 15° 25' 30" E 32° 26' 50"
CLAY 1-70	*	near Al Khiday	WNw	N 15° 25' 30" E 32° 26' 50"
CLAY 1-90	*	near Al Khiday	WNw	N 15° 25' 30" E 32° 26' 50"
CLAY 2	*	near Jebel Aulia dam	WNw	N 15° 13' 14" E 32° 26' 20"

CLAY 3	*	near Saggai	MNa	N 15° 55' 16" E 32° 33' 53"
CLAY 4	*	near Gerri	MNa	N 16° 13' 03" E 32° 36' 40"
CLAY 5		near Banqa	MNa	N 16° 30' 59" E 33° 06' 12"
CLAY 6A		Meroe	MNa	N 16° 59' 48" E 33° 42' 22"
CLAY 6B	*	Meroe	MNa	N 16° 59' 48" E 33° 42' 22"
CLAY 7		Atbara	MNb	N 17° 41' 24" E 33° 58' 06"
CLAY 8	*	Atbara	MNb	N 17° 49' 58" E 33° 58' 43"
CLAY 9	*	Atbara	Atbara	N 17° 40' 54" E 34° 01' 22"
CLAY 10		Alyab	MNa	N 17° 19' 58" E 33° 47' 02"
CLAY 11	*	near Jebel Maddaha	WNw	N 15° 23' 47" E 32° 13' 49"
CLAY 12		Wadi Mansurab	WNw	N 15° 22' 39" E 32° 20' 44"
CLAY 13	*	Soba	BNe	N 15° 30' 54" E 32° 40' 13"
CLAY 14		south Soba, Doykhra	BNe	N 15° 25' 08" E 32° 42' 57"
CLAY 15	*	El Srmir Village	BNw	N 15° 23' 50" E 32° 40' 59"
CLAY 16		west of El Srmir Village	BNw	N 15° 22' 01" E 32° 38' 26"
CLAY 17	*	Kalakla Galaa	WNe	N 15° 30' 22" E 32° 28' 43"
CLAY 18		Chinese bridge	WNe	N 15° 35' 04" E 32° 30' 18"
CLAY 19		near Sereger (V cataract)	MNb	N 18°44'54.9" E 33°33'39,1"
CLAY 20		north of Merowe	MNb	N 18°35'09" E 31°59'30,3"
CLAY 21	*	near Korti	MNb	N 18°06'06" E 31°32'48,3"
CLAY 22		near Ed Debba	MNb	N 18°02'11.3" E 30°58'10,9"
CLAY 23		near El Ghaba	MNb	N 18°10'30.4" E 30°45'26,2"
CLAY 24	*	Amara	MNb	N 20°49'13" E 30°22'58,9"
CLAY 25		between Amara and Sai	MNb	N 20°48'22" E 30°20'41,4"
CLAY 26		island of Sai (north)	MNb	N 20°44'56,5" E 30°19'45,5"
CLAY 27		III cataract	MNb	N 19°57'13" E 30°33'28,6"
CLAY 28	*	near Kerma	MNb	N 19°32'53.4" E 30°25'05,2"
CLAY 29		near Khantaq	MNb	N 18°36'18.3" E 30°34'01,9"
CLAY 30	*	near Ed Duiem	WNe	N 18°36'18.3" E 30°34'01,9"
CLAY 31		near Ed Dueim	WNw	N 18°36'18.3" E 30°34'01,9"

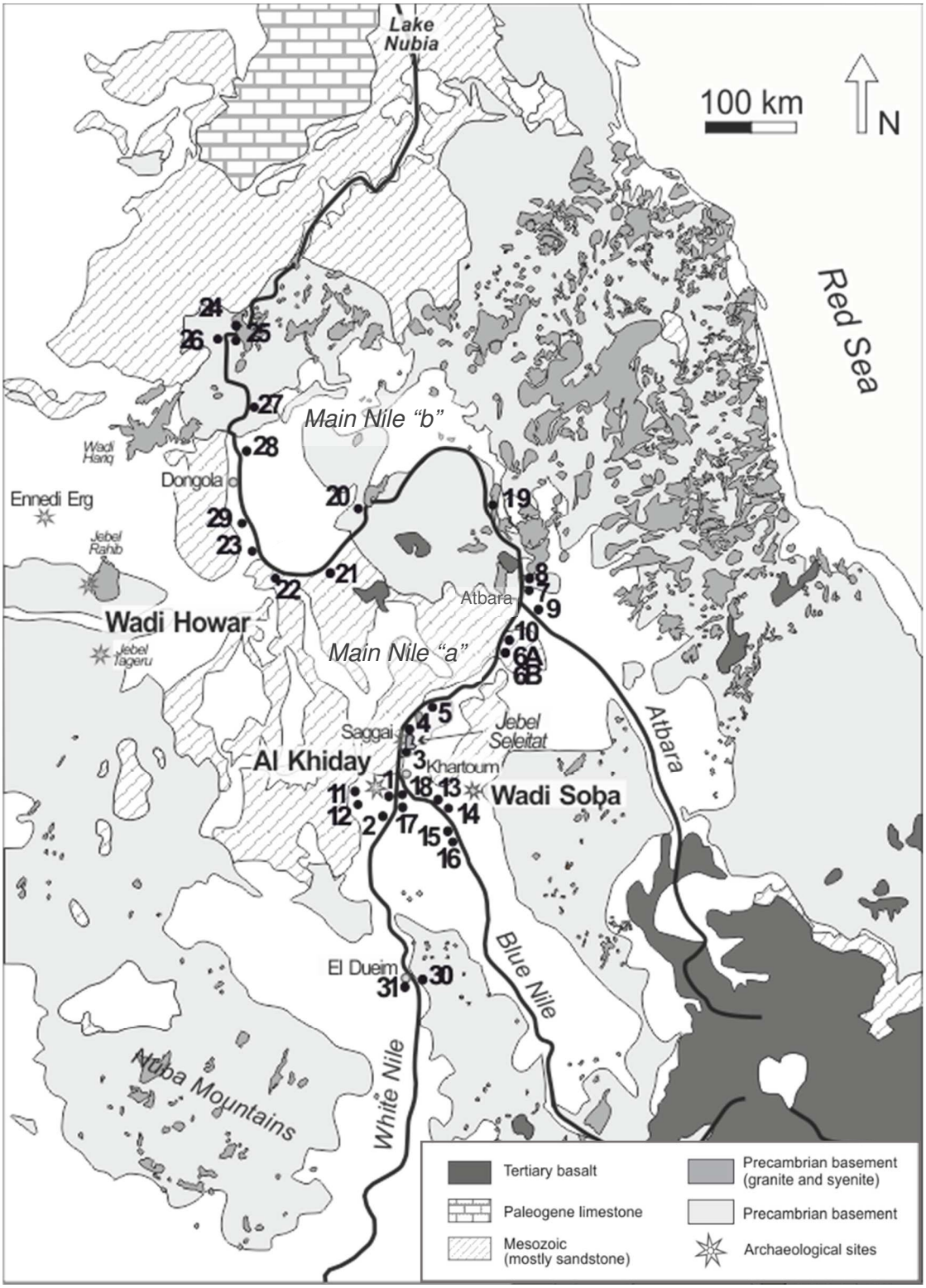

Figure 4.1: location of the clay samples collected along the Nile River and its tributaries together with the archaeological sites investigated in this research.

Samples of raw materials possibly representative of the temper used to produce the pottery at Al Khiday were also collected *in situ* for bulk chemical analysis and $^{87}Sr/^{86}Sr$ ratio determination (see Table 4.2). For quartz-tempered pottery, a sample of sand was collected extracting some grams of pure sand from a Mesolithic layer of site 16-D-4 at Al Khiday. For Kfs-tempered pottery, it has been necessary to reach the closest source of granite-like rock containing K-feldspar, and in particular the pegmatites associated into the ring complexes occurring at the Jebel Seleitat, that emerge to the east of Sabaloka (IV Cataract, about 60-80 km north of Al Khiday). In figure 4.2 macroscopic image of the rock sample.

Figure 4.2: the rock sample collected at Jebel Seleitat, near Sabaloka.

Table 4.2: raw materials with their location (see Figure 4.1)

SAMPLE	LOCATION	ACRONYM
SAND	Al Khiday	SAND
GRANITE-LIKE ROCK	Jebel Seleitat, near Sabaloka	KFS

4.2 Pottery samples

As previously mentioned, ceramic production of Central-Northern Sudan is basically characterized by two typologies of paste: quartz-rich pottery and K-feldspar-rich pottery (Dal Sasso et al., 2014; Khabir, 1987; 1991a; 1991b; Klein et al., 2004; Zedeño, 2001; De Paepe, 1986; 1988; Jesse, 2003; Klein et al., 2004). The selection of the sherds

started from the former typology since it has been used as a preliminary study addressed to the validation of the application of Sr isotope analysis to pottery analysis. Later, pottery pastes rich in microcline-perthite related to specific decorative motifs (Incised Wavy Line, Alternately Pivoting Stamp,) have been analysed and evaluated. Shown below the selection parameters and the procedures to attain an adequate set of pottery samples.

4.2.1 Quartz-tempered pottery

On the basis of the previous reasoning, a total of twenty-three samples of quartz-tempered pottery were selected among all the potsherds coming from Al Khiday sites that were previously microscopically analysed (Dal Sasso et al., 2014). Data regarding temper and decorative motifs were combined: the so-called decorations Rocker stamp dotted zigzag (AK102, AK165, AK198, AK211 Figure 4.2) and Rocker stamp plain zigzag (AK73, AK136, AK170, AK196 Figure 4.2) were two of the most continuous through time and space and most of the sherds turned out to be tempered with sand (quartz) (Dal Sasso et al, 2014; Salvatori, 2012). The initial set of samples was formed of fourteen Mesolithic sherds. An accurate study at the optical microscopy (see also Dal Sasso et al, 2014), permitted the selection of not contaminated samples, that is to say sherds almost free of Ca-bearing minerals of secondary origin, like calcite and gypsum. In fact, Sr^{2+} easily replaces Ca^{2+} in these minerals and this could bring to a subsequent alteration of the Sr isotope ratio. In order to observe potential changes in pottery paste especially in terms of the base-clay used from Mesolithic to Neolithic period, nine Neolithic sherds were selected. All the chosen samples (marked with the asterisk in Table 4.3) were representative of each prehistoric period. Neolithic sherds are characterized by fine pastes and decorative motifs that have a temporal continuity. AK46 and AK48 are decorated with the Rocker stamp dotted zigzag motif while AK8 is not decorated but presents black semicircles at the rim (see Figure 4.4).

Concerning the comparative study with pottery from other archaeological sites, a selection of samples from Wadi Soba area and Wadi Howar region have been added to the Al Khiday set (see Paragraphs 1.4 and 1.5). From Wadi Soba area two quartz-tempered Neolithic sherds (BN7 and BN8) were chosen, both coming from site Soba-2 (see Fernández et al, 2003b). All the available materials coming from Wadi Howar region were characterized by quartz-tempered ceramic pastes. After a preliminary

comparison of XRF data relative to Al Khiday (this study) and Wadi Howar quartz-tempered pottery (Klein et al., 2004), together with the association in terms of age and decorative motifs, three qtz-tempered fragments turned out to be suitable for the successive analysis of the strontium isotopes:

- sherd No. 24 from Ennedi Erg, Dotted Wavy Line (DWL, Dotted Wavy Line Horizon, c. 5200-4000 BC) (WH24)
- sherd No. 25 from Ennedi Erg, Dotted Wavy Line (DWL, Dotted Wavy Line Horizon, c. 5200-4000 BC) (WH25)
- sherd No. 29 from Ennedi Erg, Halbmondleiterband[1] (Hl, Leiterband Horizon, c.4000-2400 BC) (WH29)

Table 4.3: quartz-tempered pottery with site and stratigraphic unit of provenance (SU); AK= Al Khiday; BN= Blue Nile (Wadi Soba area); WH= Wadi Howar; "*" samples selected for Sr isotope analysis

SAMPLE ID	SELECTED	SITE	SU	DECORATION	PERIOD
AK73	*	16-D-5	455	Rsplzz	Early Mesolithic (EM)
AK102	*	16-D-5	444	Rsdzz	
AK74		16-D-5	455	Rsdrops deep	
AK75		16-D-5	455	Rsdrops deep fan	
AK82		16-D-5	452	Rsplzz	
AK86		16-D-5	452	Rsdrops deep	
AK136	*	16-D-5	420	Rsplzz	Middle Mesolithic (MM)
AK165	*	16-D-5	421	Rsdzz	
AK170	*	16-D-5	421	Rsplzz	
AK173		16-D-5	29	DWL	
AK193		16-D-5	6	Lunula	
AK196	*	10-W-4	9	Rsplzz	Late Mesolithic (LM)
AK198	*	10-W-4	9	Rsdzz	
AK211	*	10-W-4	2c	Rsdzz	
WH24	*	S98/21	Unknown	DWL	
WH25	*	S98/21	Unknown	DWL	
AK8	*	16-D-5	5	Not decorated	Neolithic (NEOL)
AK46	*	16-D-5	5	Rsdzz	
AK48	*	16-D-5	5	Rsdzz	
BN7	*	Soba-2,6	Surface	Rocker impression	
BN8	*	Soba-2,6	Surface	Simple parallel impression	
WH29	*	S99/1	Unknown	Hl	
AK1		16-D-5	5	Not decorated	
AK24		16-D-5	5	Rs unevenly spaced dots	
AK36		16-D-5	5	Rs unevenly spaced dots	
AK47		16-D-5	5	Rsdzz	
AK49		16-D-5	5	Rsdzz	
AK50		16-D-5	5	APS (dotted lines)	

[1] A later variant of the Leiterband pattern (ladder-like impression of the decoration) resulting from the application of a slightly different tool: the first tooth is of crescent shape (Jesse, 2004)

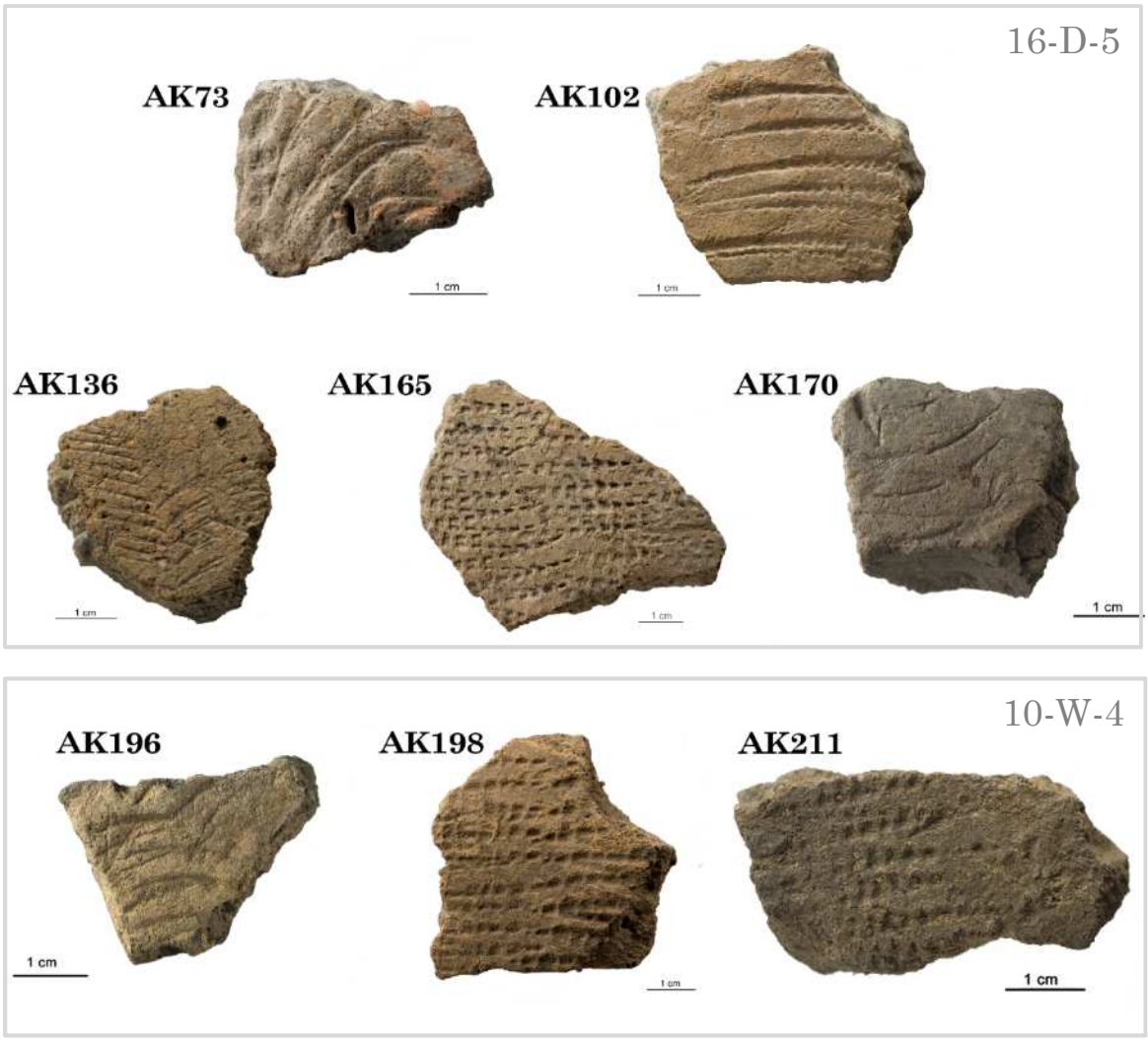

Figure 4.3: qtz-tempered Mesolithic pottery from Al Khiday: Early Mesolithic (AK73, 102) and Middle Mesolithic (AK136,165,170) are from 16-D-5. Late Mesolithic sherds (AK196,198,211) are from 10-W-4

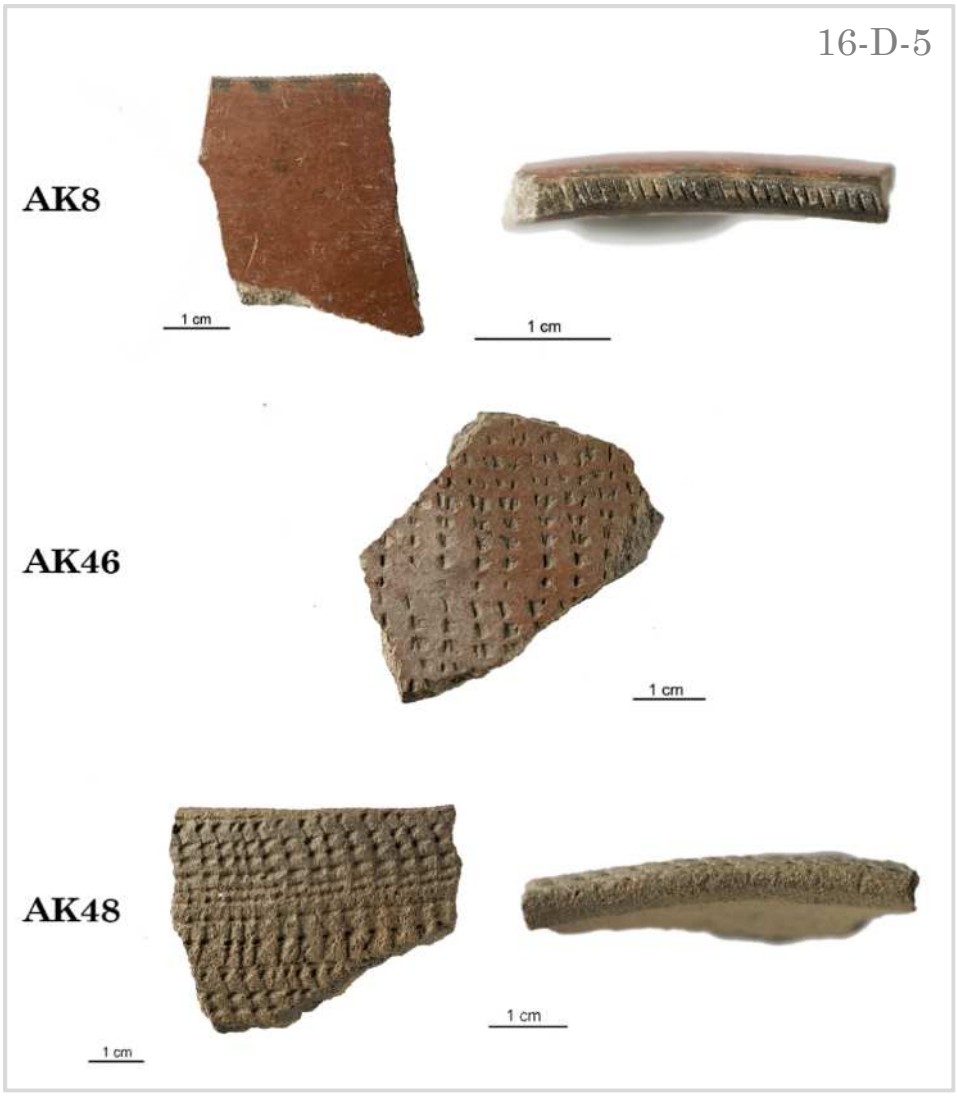

Figure 4.4: qtz-tempered Neolithic pottery from Al Khiday (16-D-5): AK48 (front and rim), burnished with black semicircles at the rim; AK46, Rsdzz; AK48 (front and rim), Rsdzz

4.2.2 K-feldspar tempered pottery

The systematic selection of samples based on widespread decorative motifs was applied also to the Kfs-tempered sherds. Wavy line decoration, together with APS (alternately pivoted stamp), turned out to be common decorative types with the lowest variability in minero-petrographic composition during the Mesolithic period in different areas of the central Sudan (Dal Sasso et al, 2014; Salvatori, 2012). Both were produced exclusively using the recipes rich in alkali feldspar and precisely microcline-perthite (Salvatori, 2012). A total of nine samples were selected (Table 4.4). The samples were analysed under optical microscopy in order to eliminate those with an

excessive amount of Kfs and with temper crystals too small to be mechanically separated from the micromass, representative of the base clay. This approach is based on the fact that it would have been useless to apply Sr isotope analysis to the whole sherd, because of the presence of the feldspar temper, a mineral phase that contains a certain quantity of Sr, the isotope ratio of which may strongly differs from that of the base clay, changing this latter also significantly. The following preparation of the samples concerned only the matrix/micromass (see Paragraph 6.1). The eight selected sherds reported in Figure 4.5 were prepared for Sr isotope analysis.

Concerning the comparative study with pottery coming from other archaeological sites, two Mesolithic sherds were chosen from Wadi Soba area:

- one Kfs-tempered sherd from Sheikh Mustafa-1 (BN5)
- one Kfs-tempered sherd from Al Mahalab (BN10)

Figure 4.5: Mesolithic Kfs-tempered pottery: AK70, AK115, AK116 and AK152 are from 16-D-5. AK204 and AK212 are from 10-W-4.

Table 4.4: Kfs-tempered pottery with site and stratigraphic unit of provenance (SU).

SAMPLE ID	SELECTED	SITE	SU	DECORATION	PERIOD
AK67		16-D-5	455	IWL	Early Mesolithic
AK76		16-D-5	455	Rsdzz	
AK70	*	16-D-5	455	IWL	
AK115	*	16-D-5	441	IWL	Middle Mesolithic
AK116	*	16-D-5	441	IWL	
AK152	*	16-D-5	421	IWL	
AK182		16-D-5	29	Rsdzz	
AK204	*	10-W-4	9	APS	Late Mesolithic
AK212	*	10-W-4	2c	APS	
BN5	*	Sheikh Mustafa 13	Surface	Rocker impression	Mesolithic
BN10	*	Al Mahalab 26	Surface	Rocker impression	

FIFTH CHAPTER

RAW MATERIALS ALONG THE NILE RIVER: CLAY, SAND AND ROCK SAMPLES

5.1 Preparation of the samples

The samples collected along the Nile and in the neighbouring areas (listed in Paragraph 4.1) were prepared following various procedures. As previously mentioned (see Paragraphs 3.2 ~ 3.7) some analytical techniques required the samples to be powdered (XRF, XRPD, TGA-DSC and TIMS) while others (petrographic and SEM observations) necessitated preparing a polished thin section. The map of the locations of the samples is reported in Paragraph 4.1, Figure 4.1.

5.2 Petrographic analysis

The thin sections were analysed under polarizing light microscope following the description protocol mentioned in chapter 3.2, based on Whitbread terminology and descriptive procedure (Whitbread, 1986, 1989, 1995), revised according to Quinn (2013). Some features were omitted (description of the matrix, voids) because we were dealing with soil samples and not with pottery pastes. The petrographic examination of the samples revealed a high variability of the clayey materials due to the different mineralogical and petrographic types of inclusions related to the associated hydrographic basins.

White Nile basin (WN)

The clay samples from the White Nile basin microscopically analysed were clay 1, 2, 30 and 31. They were all characterized by a homogeneous groundmass, containing different proportions of inclusions. Clay 1 (Figure 5.1a), collected at Al Khiday on the

river bank near the archaeological sites, presented small and scarcely abundant inclusions (c:f = 20:80), predominantly composed of quartz with sub-rounded to rounded shape. All the inclusions were poorly sorted. Rare mica, zircon and alkali feldspar were also present. Clay 2 (Figure 5.1b) showed very different features. It was a very sandy clay rich in inclusions (c:f = 50:50) of large size (average size of ~ 400 µm). Quartz inclusions ranged from sub-rounded to rounded and the fracture structure indicated that they have been subjected to alteration (mechanical cracks), probably related to the transport. Rare fragments of limestone and chlorite flakes were present.

Few differences emerged from White Nile clays collected 200 km south of Al Khiday. Clay 30 (Figure 5.1c) showed well-sorted inclusions of different size (c:f = 30:70) represented mainly by rounded to well-rounded quartz grains. Rare mica flakes and occasional small fragments of carbonate rocks were also present. Clay 31 that was collected on the western bank of the White Nile, not far from clay 30, showed more or less the same features as clay 30: the inclusions reached 300 µm in size, showing an average size-fraction around 70-80 µm. Inclusions were in a slightly different relation with the micromass (c:f = 25:75) with predominant sub-rounded to rounded quartz grains together with some sporadic small alkali-feldspar and mica flakes (Figure 5.1d). All the coarse fractions of the clays were mostly sub-rounded in shape, which means they were probably transported from a quite distant source through fluvial action.

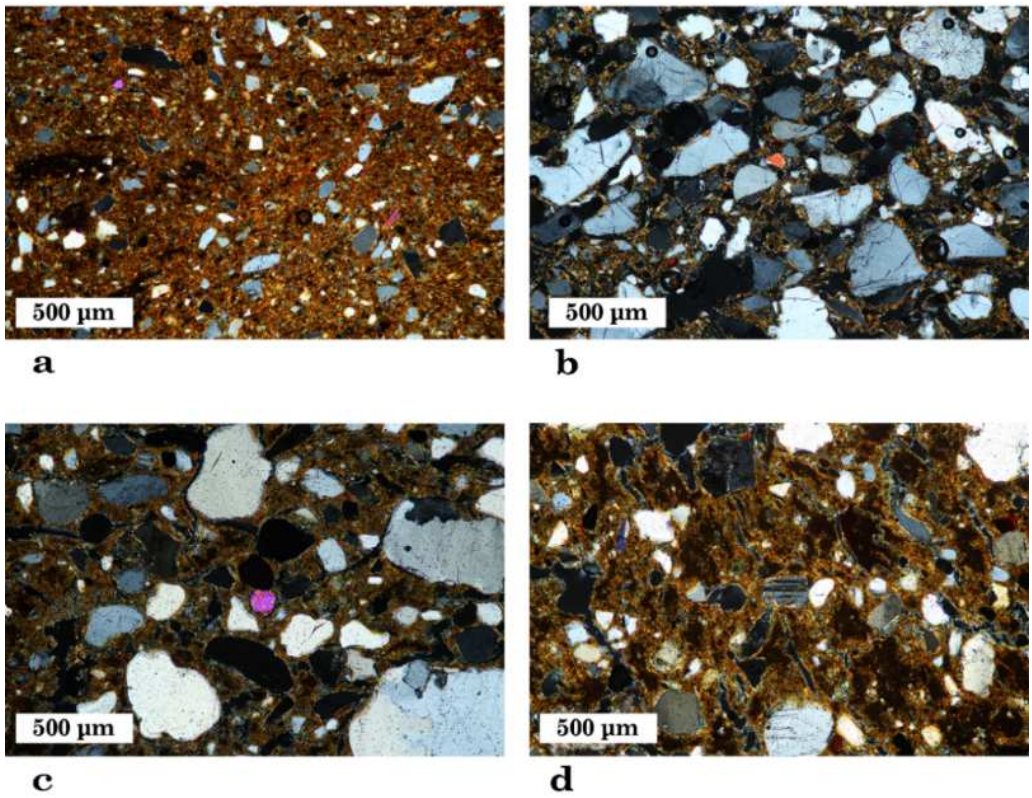

Figure 5.1: photomicrographs (under crossed polars) of selected clay samples analysed in this study belonging to White Nile basin. a) clay 1; b) clay 2; c) clay 30; d) clay 31.

Blue Nile basin (BN)

From the Blue Nile basin, two samples were prepared as thin sections (clay 3 and 15). They show very different features depending on the bank from which they were collected. Clay 15 (Figure 5.2a) came from the western bank of the Blue Nile, that it can be considered part of the Gezira plan. Inclusions occupy at least 25% of the section area (c:f = 25:75) and they are very well sorted. Sizes range from 500-600 µm (coarse fraction) to 50 µm (fine fraction). Inclusions are from sub-rounded to rounded in shape and consist of predominant quartz, and subordinated crystals of amphibole, pyroxene, alkali-feldspar, plagioclase and zircon. Clay 13 (Figure 5.2b), which was sampled on the eastern bank of the river, represents pure Blue-Nile sediments, not blended with that of the White Nile. It is characterized by a brown micromass and the inclusions being about 25-30%, poorly sorted with a size varying from 50 to 100µm. They consist of sub-angular grains of predominant quartz, subordinated plagioclase, mica flakes and abundant plagioclase and considering their fine sand grain size (50-70 µm), they were probably deposited in a low energy environment.

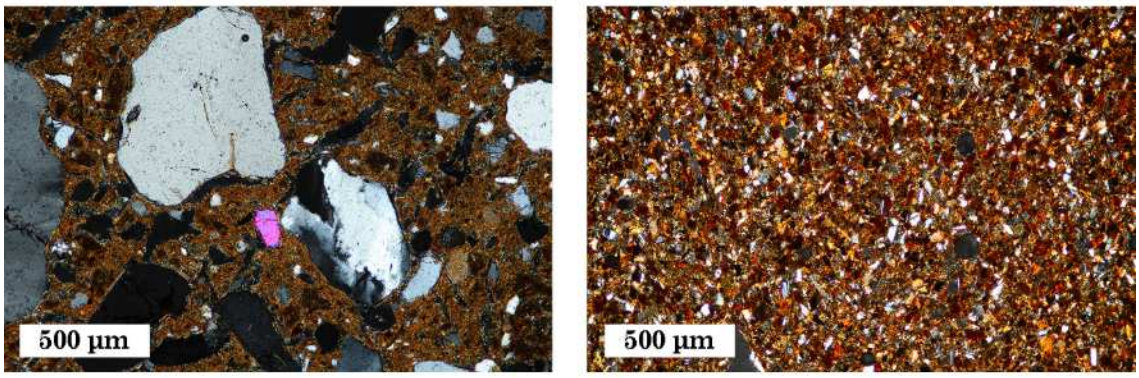

Figure 5.2: microphotographs (under crossed polars) of clay samples analysed in this study belonging to Blue Nile basin. a) clay 15; b) clay 13.

Main Nile "a" basin (MNa)

Sediments collected between Khartoum and Atbara (clay 4 and 6B) show very small quantities of inclusions. Clay 4 (Figure 5.3a) has a brown micromass with about 1% of inclusions, composed mainly of sub-angular to sub-rounded crystals of quartz with average size of about 30-40 µm. Rare opaque minerals and micas are also present. In clay 6B (Figure 5.3b) the quantity of inclusions is higher (c:f = 15:85) as well as the variability of the inclusion types: quartz is still present (angular to sub-angular grains of 200 µ**m**), together with crystals of alkali-feldspar (microcline), plagioclase, olivine, white mica flakes, and rare calcareous rock fragment.

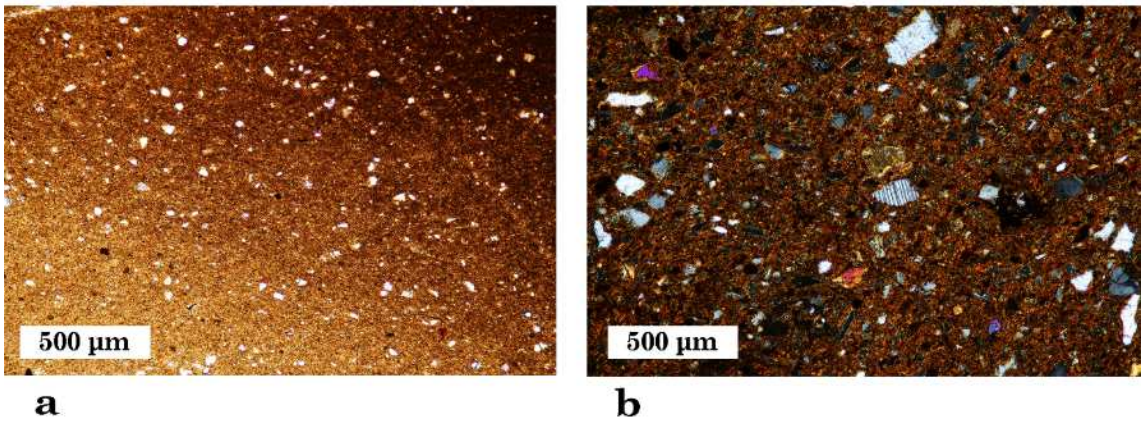

Figure 5.3: microphotographs of selected clay samples analysed in this study belonging to Main Nile "a" basin. a) clay 4 (parallel polars; b) clay 6B (crossed polars).

Main Nile "b" basin (MNb)

Clays collected after the confluence with Atbara River (19, 21, 24, 28 and 8) are characterised by very different inclusions, compositions as well as texture. Clay 19 (Figure 5.4a) shows a prevalence of a brown groundmass (95%) and only few inclusions of opaque minerals and rare quartz. Inclusions in clay 21 (Figure 5.4b) are more abundant (c: f = 15:85) with a larger grain-size (up to 200 µm) and composed of sub-angular to sub-rounded crystals of quartz, microcline, plagioclase, white mica, piroxene, opaque minerals and small fragments of carbonate rocks. Micromass of this clay is brown, but darker than clay 19. Clay 24 (Figure 5.4c) represents the sample collected in the most northern point. Its groundmass is lighter and it covers about 80% of the section area (c:f = 20:80). Inclusions range from 50 to 100 µm and are formed of sub-angular crystals of quartz, microcline and some opaque minerals. Clay 28 (Figure 5.4d) shows almost the same characteristics as clay 21: brown micromass, large and varied inclusions ranging from 40 µm to 200 µm that cover nearly 15% of the section area. Small sub-angular quartz grains, biotite, plagioclase and olivine are present. Clay 8 (Figure 5.4e), collected just after the confluence of the Atbara and Nile Rivers shows the influence of the sediments belonging to the Atbara River. Groundmass is dark brown, with about 30% of small inclusions (30-40 µm), composed of sub-rounded quartz grains, associated to crystals of plagioclase, flakes of chlorite and brown and white mica.

Atbara River

Clay sample (clay 9, Figure 5.4f) comes from Atbara River and is chararacterized by a c:f ratio of about 50:50. The brown micromass surrounds sub-angular to rounded quartz grains (~120 µm wide), abundant crystals of plagioclase, flakes of biotite, white mica and chlorite, and crystals of olivine, pyroxene and opaque minerals.

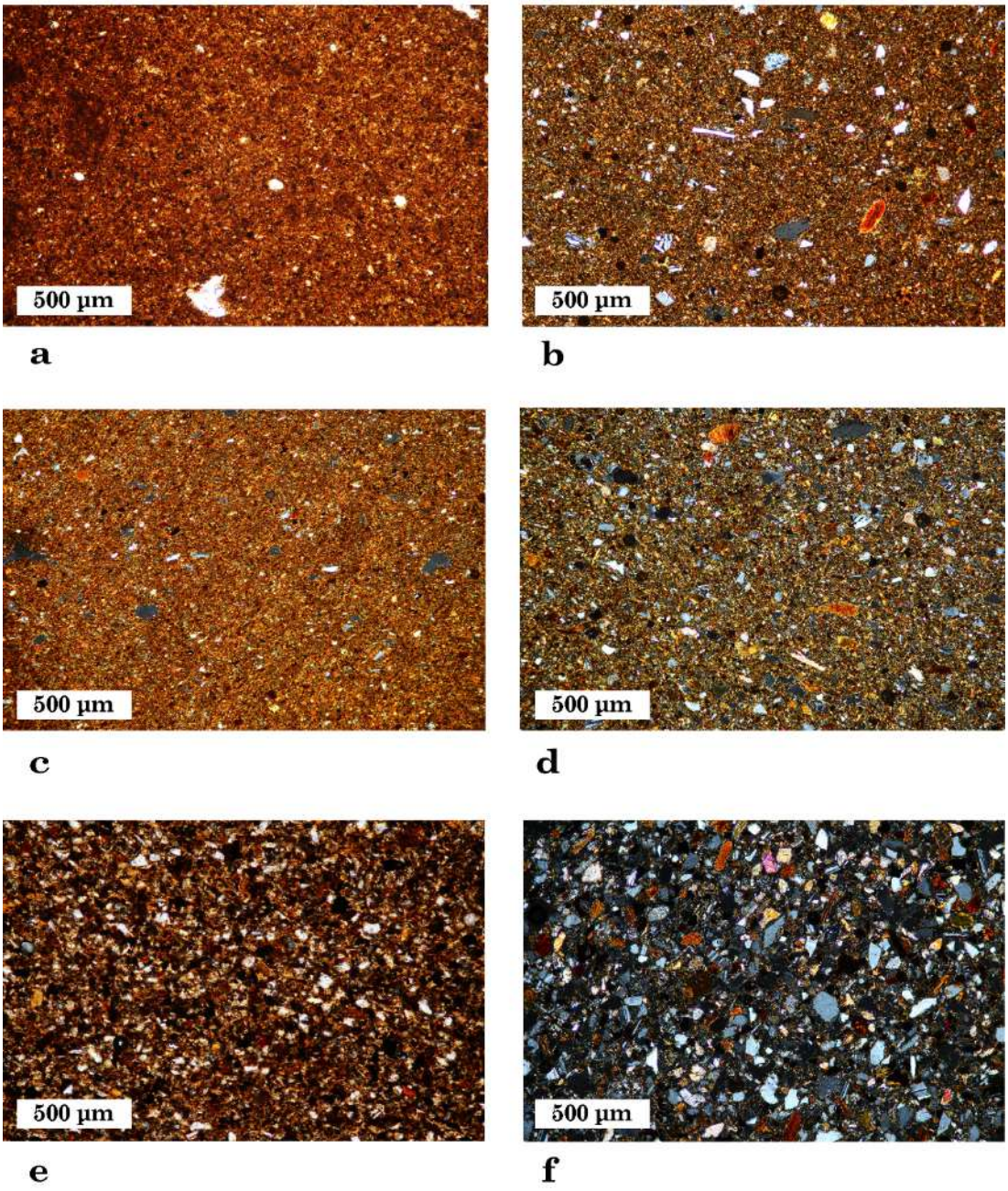

Figure 5.4: photomicrographs of selected clay samples analysed in this study belonging to Nile basin after the confluence with Atbara (clays 19, 21, 24, 28 and 8), and to Atbara (clay 9). a) clay 19; b) clay 21; c) clay 24; d) clay 28; e) clay 8; f) clay 9. Images a) and e) taken in parallel polars, all the others in crossed polars.

5.3 Mineralogical analysis and statistical treatment of data (XRPD)

As mentioned in Paragraphs 3.4, cluster analysis was applied to the diffraction patterns obtained from X-Ray Powder Diffraction (XRPD) of all the studied clay materials, in order to define possible grouping. Handling large amounts of data requires appropriate multivariate statistical methods, in order to compare the scans and sort them into classes. The method used in this research is the agglomerative hierarchical cluster analysis, a statistical procedure that allows to obtain a homogeneous subset (a series of clusters) starting from a set of observations. The result of this elaboration is a tree-like graphic representation (dendrogram) where the height of branches connecting two observations is directly proportional to the degree of dissimilarity between them (Piovesan et al, 2013; Maritan et al, 2015).

This statistical treatment of the diffraction patterns defined homogeneous groups in terms of mineralogical composition. According to the linkage method and measure distance, different dendrograms were obtained using X'Pert HighScore Plus® software. Most of the dendrograms provided concordant results, clustering the same sets of samples. In Figure 5.5 is reported the dendrogram produced applying the Euclidean Distance and Average Linkage as clustering method. The studied clay materials fall into six main clusters:

- cluster 1 (clay 2, 11, 12, Arabian-Nubian Shield): composed of predominant quartz associated to plagioclase, kaolinite, vermiculite and microcline; all these samples were collected on the western bank of the White Nile (clay 2) and in area where there was the Upper Pleistocene lake (Williams et al., 2015) and others small Holocene ponds (Williams et al., 2015; Cremaschi et al., 2007; Williams et al., 2006; Williams and Jacobsen, 2011) in the vicinity of Jebel Baroka. This area is characterised by the presence of the crystalline basement complex (mainly gneiss in amphibolite and granulite facies; Padoan et al, 2011; Abdelsalam et al., 2002; Link et al., 2010) and the of the Nubian Sandstone Formation;
- cluster 2 (clay 15, 16, Blue Nile): composed of quartz, plagioclase, montmorillonite, kaolinite, amphibole, zeolite, and calcite. The presence of montmorillonite and zeolite is related to the weathering of basaltic rocks forming the Ethiopian highlands (Padoan et al, 2011)

- cluster 3 (clay 9, 20, Atbara): characterized by quartz, plagioclase, illite, vermiculite, phillipsite, amphibole and augite;
- cluster 4 (clay 3, 5, 6A, 6B, 7, 8, 10, 13, 14, 26, Main Nile "a"): characterized by quartz, potassic feldspar, montmorillonite, kaolinite, illite and amphibole; these clays mainly belong to the Main Nile after the confluence of the White and the Blue Nile and before the confluence of the Atbara; exceptions are those of the eastern bank of the Blue Nile (clay 13 and 14) and that collected in the island of Sai (clay 26)
- cluster 5 (clay 4, 19, 21, 22, 23, 24, 25, 27, 28, 29, Main Nile "b"): composed of quartz, plagioclase, kaolinite, vermiculite, illite and pyroxene; they were all collected along the Nile, after the confluence of the Atbara, with the exception of clay 4;
- cluster 6 (clay 1, 17, 18, White Nile): composed of quartz, plagioclase, kaolinite, illite and smectite; all these clays were collected along the White Nile.

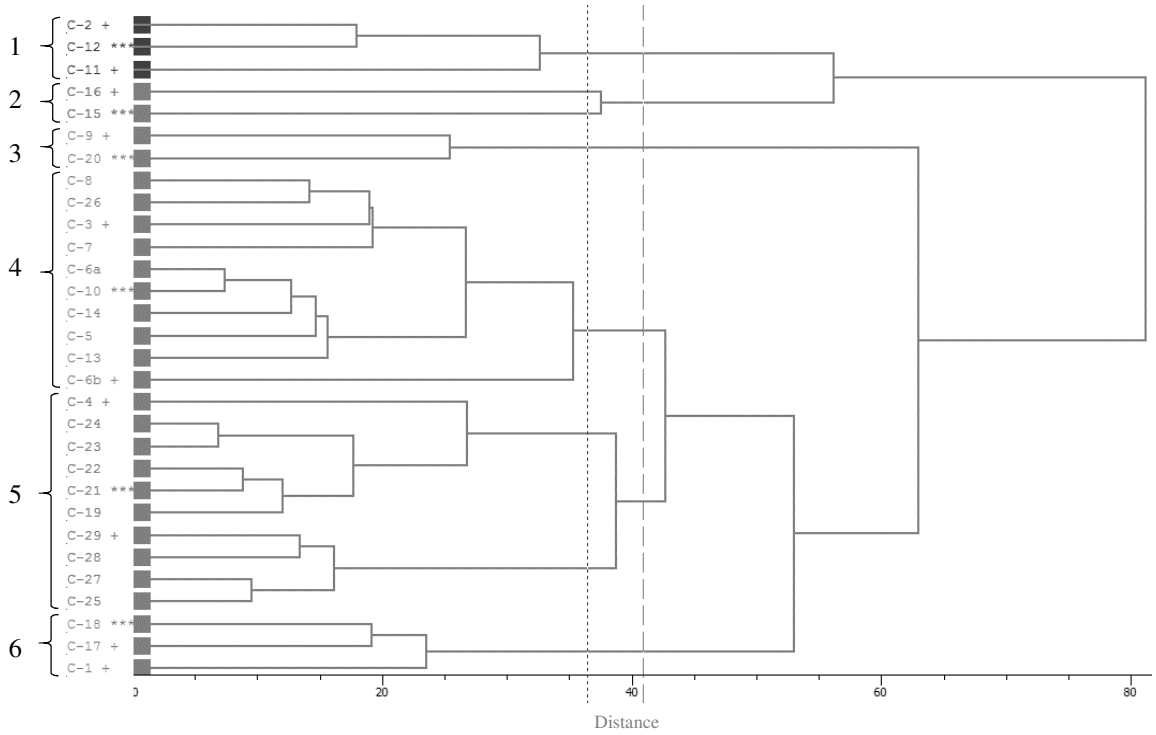

Figure 5.5: Dendrogram obtained from cluster analysis of XRPD data of clay materials according to Euclidean distance and Average linkage method. *** and +: most representative and most different samples within each cluster

In this case study, cluster analysis was capable of discriminating samples characterized by similar mineralogical composition, which almost matched to the hydrographic basin of origin, only with some limited exceptions.

5.4 Chemical analysis and statistical treatment of data (XRF)

As mentioned in Paragraph 3.3, bulk chemical composition was explored using X-Ray Fluorescence Spectroscopy (XRF). For complete chemical data, see APPENDIX. Cluster analysis was applied for the statistical treatment of the chemical data. Combination of different clustering methods and distances supplied similar results. In Figure 5.6 is illustrated a dendrogram obtained using Square Euclidean distance and Average linkage method. A total of six clusters were isolated and samples converge into groups affine to XRPD cluster analysis:

- cluster 1 includes clay 1 and 17, both collected along the White Nile;
- cluster 2 is formed by clay 4, 18, 19, 21, 22, 23, 24, 25, 26, 27, 28, mainly collected along the Nile after the confluence of Atbara, with the exception of clay 4 and 18 coming from the north and south of the confluence between the Blue and the White Nile. The latter (clay 18) belongs to the White Nile group, but lies very close to the confluence between White Nile and Blue Nile. This proximity probably caused the shifting in chemical composition and therefore in the clustering process;
- cluster 3 consists of clay 3, 5, 6A, 6B, 10 from MNa; 7, 8, 20, 29 from MNb; 13 from BN. They show a mixed provenance as they are all affected by the influence of sediments deriving from volcanic rock weathering, both from Atbara and Blue Nile;
- cluster 4 is formed only by clay 9 which represents Atbara sediments;
- cluster 5 includes clay 2, 11 that were collected on the western bank of the White Nile and resulted to be rich in quartz sand, representing the sediments mainly of the Arabian-Nubian Shield;
- cluster 6 is made of clay 15 and 16 that represent the sediments belonging to the Blue Nile.

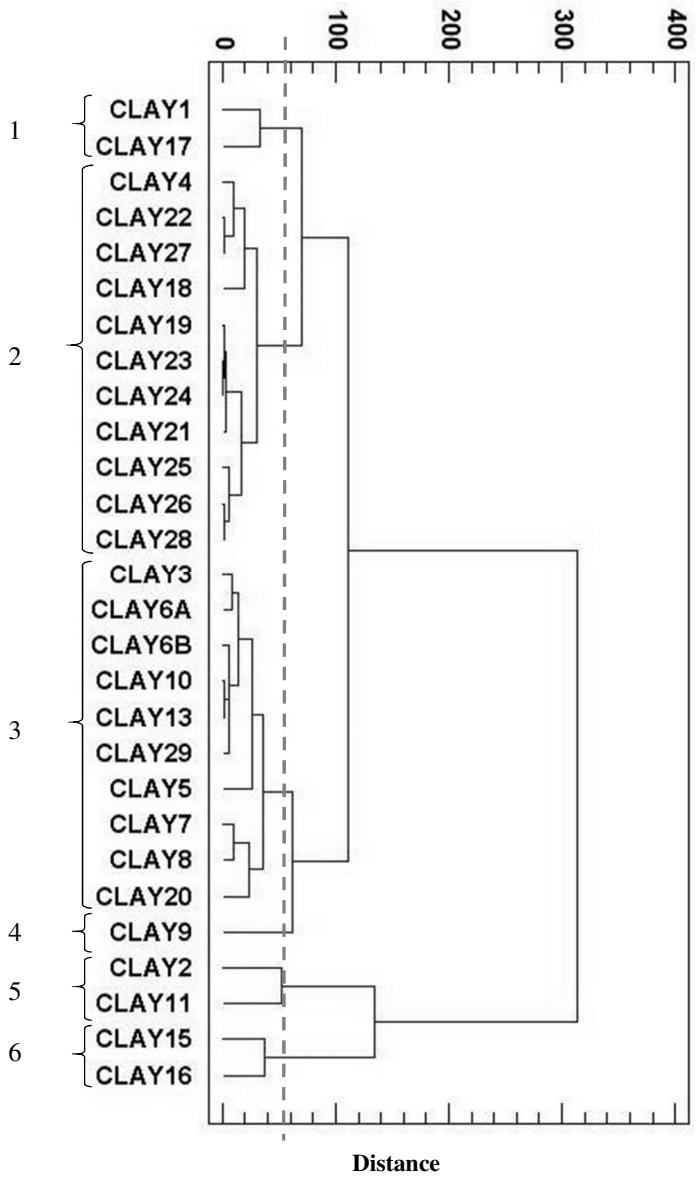

Figure 5.6: dendrogram obtained from cluster analysis of XRF data of clay materials according to Square Euclidean distance and Average linkage method.

In order to find possible parameters to separate clays belonging to Main Nile "a" branch (between Khartoum and Atbara) and Main Nile "b" (after the confluence of the Atbara), the method proposed by Buxeda i Garrigós (1999) was applied. Usually this approach is utilised in the study of the alteration and contamination of archaeological ceramics. It consists in applying specific algorithms for the transformation of chemical data and in studying the covariance structure, which is called the variation matrix (Aitchison, 1986, 1990). The study of elemental concentrations is then based on the variation matrix: there are some components that, when used as divisors in

subsequent log-ratio transformations, impose a low variability on the transformed data without greatly exceeding the total variation of the covariance structure (Buxeda i Garrigós, 1999). The point is that compositions provide information only about the relative magnitudes of the compositional components. The treatment of "closed" dataset by normal statistical methods creates spurious correlations that make the effectiveness of the obtained results low. Instead of processing major oxides independently from trace elements, which is a way to minimize this problem, the transformation of the initial dataset presents a better solution for the processing and interpretation of chemical data. A centred log-ratio is another procedure for removing closure effects and it is suitable for the study of correlation coefficients and subsequent multivariate data analyses. The clr-transform maps a composition in the D-part Aitchison-simplex isometrically to a D-dimensonal euclidian vector subspace. The interpretation of the results is relatively easy since the relation between each original part and a transformed variable is preserved (Aitchison, 1986).

The compositional variation matrix of clay samples is shown in Table 5.1.

Table 5.1: compositional variation matrix of clay samples: vt = total variation, τ_i=total sum of variances in column i, vt/τ.i =percentage of variance in the log-ratio covariance matrix using the component x.i as divisor due to the total variation, $r_{v,\tau.}$=correlation between the values

	SiO_2	TiO_2	Al_2O_3	Fe_2O_3	MnO	MgO	CaO	Na_2O	K_2O	P_2O_5	S	Sc	V	Cr
SiO_2	0	0·3326506	0·22370395	0·34212708	0·3574778	0·4641788	0·5533497	0·4017274	0·2050399	0·4067531	0·679382	0·606532	0·3750696	0·2993815
TiO_2	0·3326506	0	0·07919018	0·03046792	0·1068474	0·0816155	0·2280935	0·1221796	0·1037373	0·0620558	0·756537	0·404413	0·0217476	0·0501143
Al_2O_3	0·2237039	0·0791902	0	0·03210489	0·061147	0·1421578	0·3181382	0·2029847	0·0407182	0·058825	0·721077	0·348935	0·0856545	0·1413503
Fe_2O_3	0·3421271	0·0304679	0·03210489	0	0·0605519	0·0953535	0·273205	0·1724451	0·0932344	0·0360986	0·782931	0·378392	0·0240037	0·0910236
MnO	0·3574778	0·1068474	0·06114705	0·06055193	0	0·1366446	0·3482767	0·230351	0·1035192	0·1267949	0·995151	0·492879	0·0975733	0·1747462
MgO	0·4641788	0·0816155	0·14215782	0·09535348	0·1366446	0	0·096849	0·0522784	0·1384082	0·0960765	0·670821	0·657917	0·0568909	0·0957427
CaO	0·5533497	0·2280935	0·31813819	0·27320501	0·3482767	0·096849	0	0·0733987	0·2749481	0·2177003	0·464607	1·077942	0·1803578	0·2345363
Na_2O	0·4017274	0·1221796	0·20298465	0·17244509	0·230351	0·0522784	0·0733987	0	0·1451643	0·171438	0·528906	0·786065	0·12084	0·1307216
K_2O	0·2050399	0·1037373	0·04071816	0·09323441	0·1035192	0·1384082	0·2749481	0·1451643	0	0·1009806	0·666382	0·463193	0·1369578	0·156056
P_2O_5	0·4067531	0·0620558	0·05882497	0·03609855	0·1267949	0·0960765	0·2177003	0·171438	0·1009806	0	0·644345	0·429667	0·0529987	0·1505188
S	0·6793815	0·7565366	0·72107651	0·78293123	0·9951509	0·6708211	0·4646074	0·5289055	0·6663816	0·6443453	0	1·412616	0·7356949	0·7470234
Sc	0·6065321	0·4044128	0·34893482	0·37839153	0·4928795	0·6579172	1·0779416	0·7860647	0·4631932	0·4296672	1·412616	0	0·5076633	0·5145297
V	0·3750696	0·0217476	0·0856545	0·02400368	0·0975733	0·0568909	0·1803578	0·12084	0·1369578	0·0529987	0·735695	0·507663	0	0·0543312
Cr	0·2993815	0·0501143	0·14135026	0·09102363	0·1747462	0·0957427	0·2345363	0·1307216	0·156056	0·1505188	0·747023	0·51453	0·0543312	0
Co	0·3734481	0·0432144	0·03907177	0·00970265	0·0361972	0·0772837	0·2615384	0·1653926	0·0945166	0·0445926	0·826131	0·41743	0·0311776	0·1046787
Ni	0·3937042	0·0560197	0·05713915	0·0237098	0·0702917	0·0536588	0·2345741	0·1554273	0·1135798	0·0513112	0·795816	0·442956	0·0300827	0·0799444
Cu	0·3915458	0·1184537	0·12013821	0·1158736	0·1679953	0·2012116	0·3765062	0·2466718	0·1500886	0·1530583	0·853188	0·392363	0·1580391	0·201455
Zn	0·3186294	0·0299577	0·02563121	0·01001331	0·0718905	0·0825717	0·2554054	0·1620304	0·0679732	0·0223309	0·722106	0·352452	0·033521	0·0892239
Ga	0·212184	0·0746959	0·00547005	0·04120104	0·0732529	0·1391285	0·3015394	0·2006474	0·0437878	0·0557332	0·6968	0·338087	0·0865606	0·1382535
Rb	0·1677478	0·1803333	0·04581002	0·13635466	0·1218039	0·2259075	0·3743646	0·2483877	0·0261802	0·1466393	0·677039	0·456972	0·2089415	0·2422939
Sr	0·3165346	0·1144697	0·15546851	0·1422529	0·1908914	0·0519813	0·0646276	0·0150529	0·1146261	0·1489601	0·473611	0·776948	0·0997039	0·1140934
Y	0·1863374	0·0940801	0·01092328	0·05723145	0·0760988	0·1720278	0·3403189	0·2342832	0·0454284	0·0774924	0·717081	0·343848	0·1093659	0·1517341

Zr	0·0520896	0·1814276	0·12819785	0·20618932	0·2326183	0·3205912	0·4378553	0·2962728	0·0990772	0·2553936	0·682802	0·479098	0·2410606	0·1781614
Nb	0·3389613	0·0849168	0·04148191	0·05649598	0·0902978	0·1739541	0·3456774	0·2563481	0·0735777	0·0511694	0·78313	0·348288	0·1134532	0·2031495
Ba	0·1542998	0·0787039	0·04571399	0·08114439	0·0728202	0·1444456	0·2860288	0·1463166	0·0257016	0·1291046	0·743956	0·459166	0·1085927	0·1210418
La	0·2439471	0·3197562	0·12722217	0·24581683	0·2176802	0·4311813	0·6084623	0·4902506	0·1530718	0·2542162	0·852199	0·44487	0·3565666	0·4363587
Ce	0·3892312	0·747595	0·38272037	0·60650263	0·5205105	0·8699596	1·0726025	0·8896462	0·40439	0·6059066	1·129607	0·700159	0·783928	0·8909835
Nd	0·123675	0·2174305	0·10084308	0·17449201	0·2436446	0·3694181	0·5230479	0·4147605	0·1698944	0·2058872	0·672896	0·362384	0·2387195	0·249035
Pb	1·8584253	1·7949372	1·53117682	1·65825417	1·6659248	1·7429798	2·0378592	2·0111058	1·6299261	1·5967876	2·242822	1·673519	1·7663021	1·7843873
Th	0·477963	0·9141666	0·85842668	0·96994911	0·9882221	1·1301422	1·1355087	0·9459835	0·7897217	1·084861	1·264502	1·324184	0·9976603	0·917076
U	0·2911823	0·829953	0·56466491	0·76673838	0·6518088	0·9414861	1·0588318	0·8584745	0·511804	0·8710481	1·227936	1·154396	0·8664387	0·8172564
t.i	11·5372788	8·2597604	6·69608589	7·71386067	8·7839095	9·9128632	14·0561507	10·8755511	7·1416841	8·3087452	25·167093	18·547866	8·6798975	9·559202
vt/t.i	0·5445814	0·7606743	0·9383075	0·81450624	0·7152837	0·6338217	0·446992	0·5777167	0·8797627	0·7561897	0·249651	0·338745	0·7238551	0·6572711
R,v,t	0·8677896	0·9751726	0·99434152	0·98152243	0·9829432	0·9372113	0·8961345	0·9333893	0·9968602	0·9685586	0·893608	0·895438	0·965346	0·9630768
vt	6·2829876	0	0	0	0	0	0	0	0	0	0	0	0	0

	Co	Ni	Cu	Zn	Ga	Rb	Sr	Y	Zr	Nb	Ba	La	Ce	Nd	Pb	Th	U
SiO_2	0·3734481	0·3937042	0·391546	0·3186294	0·21218397	0·1677478	0·3165346	0·18633744	0·0520896	0·3389613	0·1542998	0·2439471	0·389231	0·123675	1·858425	0·477963	0·291182
TiO_2	0·04321442	0·0560197	0·118454	0·0299577	0·0746959	0·1803333	0·1144697	0·09408011	0·1814276	0·0849168	0·0787039	0·3197562	0·747595	0·2174305	1·794937	0·914167	0·829953
Al_2O_3	0·03907177	0·0571392	0·120138	0·0256312	0·00547005	0·04581	0·1554685	0·01092328	0·1281979	0·0414819	0·045714	0·1272222	0·38272	0·1008431	1·531177	0·858427	0·564665
Fe_2O_3	0·00970265	0·0237098	0·115874	0·0100133	0·04120104	0·1363547	0·1422529	0·05723145	0·2061893	0·056496	0·0811444	0·2458168	0·606503	0·174492	1·658254	0·969949	0·766738
MnO	0·03619723	0·0702917	0·167995	0·0718905	0·07325292	0·1218039	0·1908914	0·07609878	0·2326183	0·0902978	0·0728202	0·2176802	0·520511	0·2436446	1·665925	0·988222	0·651809
MgO	0·07728374	0·0536588	0·201212	0·0825717	0·13912851	0·2259075	0·0519813	0·17202784	0·3205912	0·1739541	0·1444456	0·4311813	0·86996	0·3694181	1·74298	1·130142	0·941486
CaO	0·26153837	0·2345741	0·376506	0·2554054	0·30153945	0·3743646	0·0646276	0·34031892	0·4378553	0·3456774	0·2860288	0·6084623	1·072602	0·5230479	2·037859	1·135509	1·058832
Na_2O	0·16539259	0·1554273	0·246672	0·1620304	0·20064744	0·2483877	0·0150529	0·23428316	0·2962728	0·2563481	0·1463166	0·4902506	0·889646	0·4147605	2·011106	0·945984	0·858474
K_2O	0·09451663	0·1135798	0·150089	0·0679732	0·04378784	0·0261802	0·1146261	0·04542839	0·0990772	0·0735777	0·0257016	0·1530718	0·40439	0·1698944	1·629926	0·789722	0·511804
P_2O_5	0·04459256	0·0513112	0·153058	0·0223309	0·05573315	0·1466393	0·1489601	0·0774924	0·2553936	0·0511694	0·1291046	0·2542162	0·605907	0·2058872	1·596788	1·084861	0·871048
S	0·82613106	0·7958157	0·853188	0·7221061	0·69679996	0·6770388	0·4736106	0·71708102	0·6828016	0·7831297	0·7439561	0·8521994	1·129607	0·6728959	2·242822	1·264502	1·227936

Sc	0·41743018	0·4429561	0·392363	0·3524521	0·33808678	0·456972	0·776948	0·34384844	0·4790983	0·348288	0·4591662	0·4448704	0·700159	0·362384	1·673519	1·324184	1·154396
V	0·03117764	0·0300827	0·158039	0·033521	0·08656059	0·2089415	0·0997039	0·10936595	0·2410606	0·1134532	0·1085927	0·3565666	0·783928	0·2387195	1·766302	0·99766	0·866439
Cr	0·10467872	0·0799444	0·201455	0·0892239	0·13825348	0·2422939	0·1140934	0·15173415	0·1781614	0·2031495	0·1210418	0·4363587	0·890983	0·249035	1·784387	0·917076	0·817256
Co	0	0·0162266	0·122948	0·0173646	0·04683508	0·1395258	0·139535	0·05975376	0·2313215	0·0603841	0·0855911	0·2559019	0·602916	0·2112505	1·567495	1·062543	0·784556
Ni	0·01622659	0	0·147242	0·0237841	0·06260657	0·1665332	0·130261	0·08191754	0·2563484	0·0991772	0·114608	0·3085965	0·68131	0·2284753	1·547823	1·112136	0·828427
Cu	0·12294831	0·1472419	0	0·1132319	0·13034097	0·1911402	0·2271675	0·14060853	0·242922	0·1195124	0·1468021	0·3419046	0·67994	0·2540982	1·750663	0·978241	0·870101
Zn	0·01736462	0·0237841	0·113232	0	0·02609136	0·1087134	0·133997	0·0406917	0·1793609	0·0382227	0·0727076	0·2194531	0·571902	0·1579272	1·561773	0·98491	0·764057
Ga	0·04683508	0·0626066	0·130341	0·0260914	0	0·0497104	0·1552372	0·00726371	0·117489	0·037908	0·0477863	0·1208629	0·388488	0·0936336	1·496996	0·860307	0·578406
Rb	0·13952583	0·1665332	0·19114	0·1087134	0·04971045	0	0·1893108	0·04091713	0·0947955	0·0824839	0·0491777	0·0727096	0·261862	0·1177637	1·586655	0·743359	0·398592
Sr	0·13953505	0·130261	0·227167	0·133997	0·15523716	0·1893108	0	0·18000586	0·2306946	0·2162138	0·1100367	0·4015733	0·778714	0·3247935	1·924203	0·85277	0·741241
Y	0·05975376	0·0819175	0·140609	0·0406917	0·00726371	0·0409171	0·1800059	0	0·0942818	0·0391468	0·0485252	0·1013048	0·344533	0·0754716	1·410052	0·866111	0·525627
Zr	0·23132152	0·2563484	0·242922	0·1793609	0·11748898	0·0947955	0·2306946	0·09428183	0	0·1783905	0·074421	0·1818136	0·429363	0·0916457	1·721839	0·571143	0·38907
Nb	0·06038413	0·0991772	0·119512	0·0382227	0·03790796	0·0824839	0·2162138	0·03914679	0·1783905	0	0·0896655	0·1343459	0·445527	0·1486332	1·510045	0·994448	0·721638
Ba	0·08559107	0·114608	0·146802	0·0727076	0·04778634	0·0491777	0·1100367	0·04852522	0·074421	0·0896655	0	0·1650725	0·444451	0·151579	1·784231	0·65993	0·470297
La	0·25590192	0·3085965	0·341905	0·2194531	0·12086292	0·0727096	0·4015733	0·10130484	0·1818136	0·1343459	0·1650725	0	0·178458	0·1285495	1·596972	0·805571	0·36857
Ce	0·60291569	0·6813098	0·67994	0·5719023	0·3884877	0·2618622	0·778714	0·34453337	0·4293634	0·4455274	0·4444505	0·1784576	0	0·3379939	1·604927	1·065438	0·403495
Nd	0·21125045	0·2284753	0·254098	0·1579272	0·09363358	0·1177637	0·3247935	0·07547163	0·0916457	0·1486332	0·151579	0·1285495	0·337994	0	1·583439	0·70821	0·448999
Pb	1·56749476	1·5478229	1·750663	1·5617731	1·49699583	1·5866552	1·9242031	1·41005173	1·7218392	1·5100455	1·7842312	1·596972	1·604927	1·5834393	0	4·051299	2·390335
Th	1·0625432	1·1121357	0·978241	0·9849103	0·86030657	0·7433585	0·8527701	0·86611087	0·5711431	0·9944484	0·6599301	0·8055706	1·065438	0·7082097	4·051299	0	0·611182
U	0·78455554	0·8284272	0·870101	0·7640573	0·57840605	0·398592	0·7412409	0·5256273	0·3890698	0·7216375	0·4702969	0·36857	0·403495	0·4489993	2·390335	0·611182	0
t.i	7·92852321	8·3636866	10·103451	7·2579254	6·6273023	7·5520245	9·5149754	6·67246315	8·8757345	7·8766435	7·1119179	10·5632585	19·21306	9·1285907	54·083154	30·725963	22·706612
vt/t.i	0·79245371	0·7512223	0·621866	0·8656727	0·94804603	0·8319607	0·6603262	0·94162942	0·7078837	0·7976732	0·8834449	0·5947964	0·327017	0·6882758	0·116173	0·204485	0·276703
r, v,t	0·97146485	0·9609406	0·98464	0·9802364	0·99462419	0·9749401	0·9403366	0·98836161	0·9485508	0·9811864	0·9876878	0·9028508	0·721942	0·9508105	0·799028	0·858686	0·743373
vt	0	0	0	0	0	0	0	0	0	0	0	0	0	0	0	0	0

The XRF data obtained after the log-transformation were then statistically treated with the cluster analysis (Figure 5.7). The last obtained clusters have better highlighted compositional variability of clay samples but still they do not clarify the problem regarding clays of mixed provenance belonging to MNa (between Khartoum and Atbara) and MNb (after the confluence with Atbara).

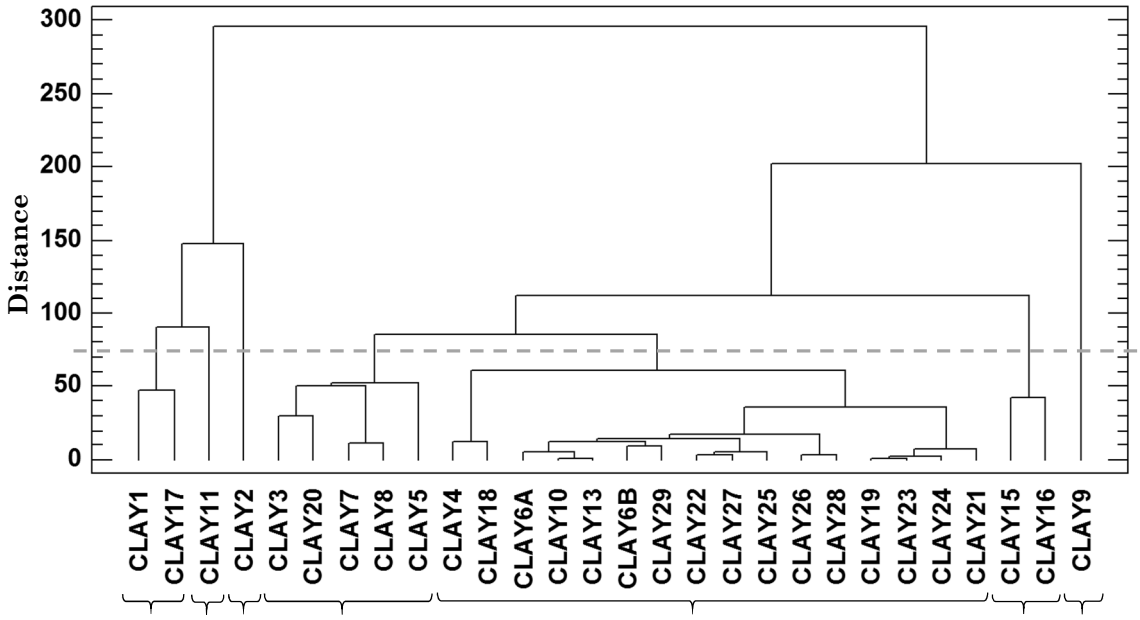

Figure 5.7: dendrogram obtained from cluster analysis of log-transformed XRF data of clay materials, divided by Al_2O_3, according to Square Euclidean distance and Complete linkage method.

From a preliminary observation of the chemical data, it is possible to observe that clays collected along the White Nile (western and eastern bank) are rich in SiO_2 and show a low content in CaO. In Figure 5.8, clay collected at Al Khiday is indicated with a star (☆). Samples coming from Blue Nile, Main Nile "a" and Main Nile "b" show a high CaO content (> 4%) with respect to those from the White Nile. Moreover, all the White Nile clays (WNw and WNe) are characterized by a similar CaO/Sr ratio (Figure 5.9), except for the two quartzose clays that show a high SiO_2 content (see Figure 5.8) and a low Sr content, because of the dilution effect due to the presence of quartz (SiO_2). There seems to be a proportionality between CaO and Sr contents: Blue Nile (BN), Main Nile a (MNa) and Main Nile (MNb) clays show an increasing Sr content in relation to CaO (Figure 5.9). This direct proportionality is not respected when

observing biplot of Rb vs. Sr in Figure 5.10: except for the two quartzose clays (low Rb and Sr contents), clays showing a high Sr content (Atbara clay) have a low Rb content. MNb samples (after the confluence with Atbara) have lower Rb than the White Nile clays, mainly because of major volcanic contribution but also because of local recycling and weathering. In Atbara sediments, low Rb values might reflect dominant volcanic provenance. Al Khiday clay and the three parts of the core drilled underneath the surface show a high Rb content and seem to be one of the end-members, together with Atbara clay, of a mixing curve, describing the Nile system.

When two components of different chemical composition mix in varying proportions, the chemical composition of the resulting mixtures vary systematically depending on the relative abundances of the end-members (Faure, 1986). The concentration of any conservative element in a binary mixture depends on the concentration of that element in both components and on the abundances of those two components in the mixture. Since the concentration of the conservative element in a mixture is calculated as a weighted average, the concentrations of that conservative element in a binary mixture lies on a straight line known as a "mixing line", which includes both end-members. Therefore, a linear relationship between the concentrations of two conservative elements in a suite of natural samples is evidence that they may be the products of mixing (Faure, 1986). In its simplest form, contamination of sediments by the re-mixing process can be regarded as a process of two-component mixing.

However, mixing processes usually have more than one degree of freedom. Therefore, to evaluate mixing relations adequately, it is usually necessary to apply two or more measured variables to the problem. For this reason, XRF data were explored with Principal Component Analysis (PCA).

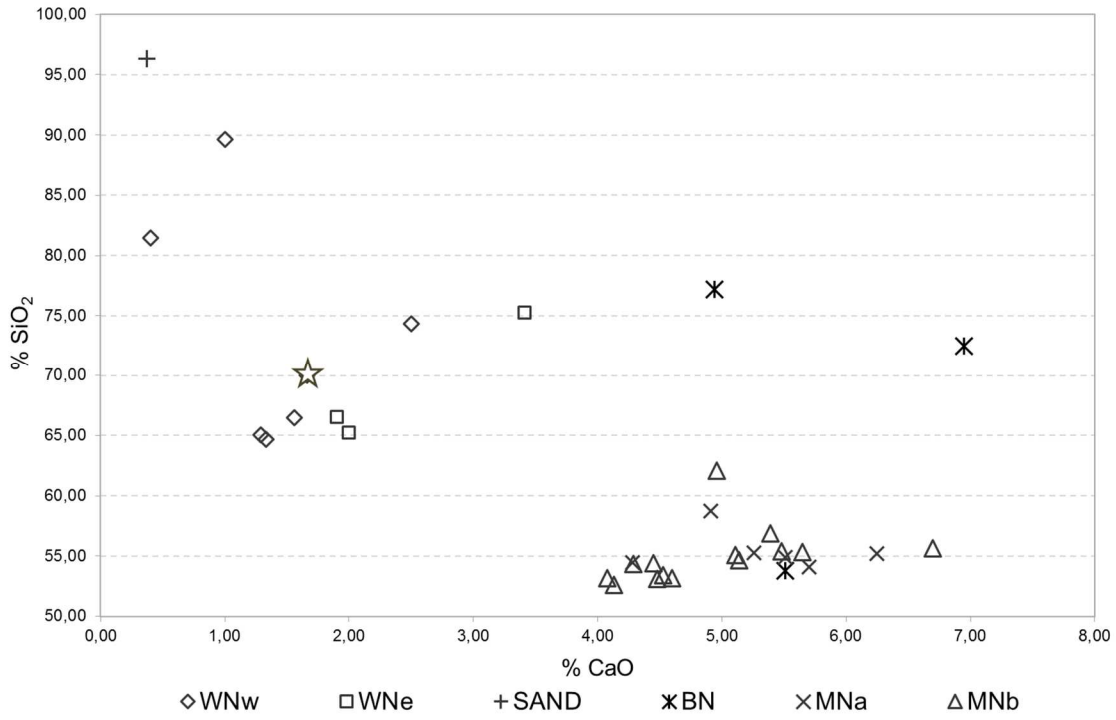

Figure 5.8: biplot of elemental concentration of CaO and SiO_2. The star indicates clay collected at Al Khiday (clay 1). Abbreviations: WNw: White Nile western bank; WNe: White Nile eastern bank; BN: Blue Nile; MNa: Main Nile between Khartoum and Atbara; MNb: Main Nile after the Atbara confluence.

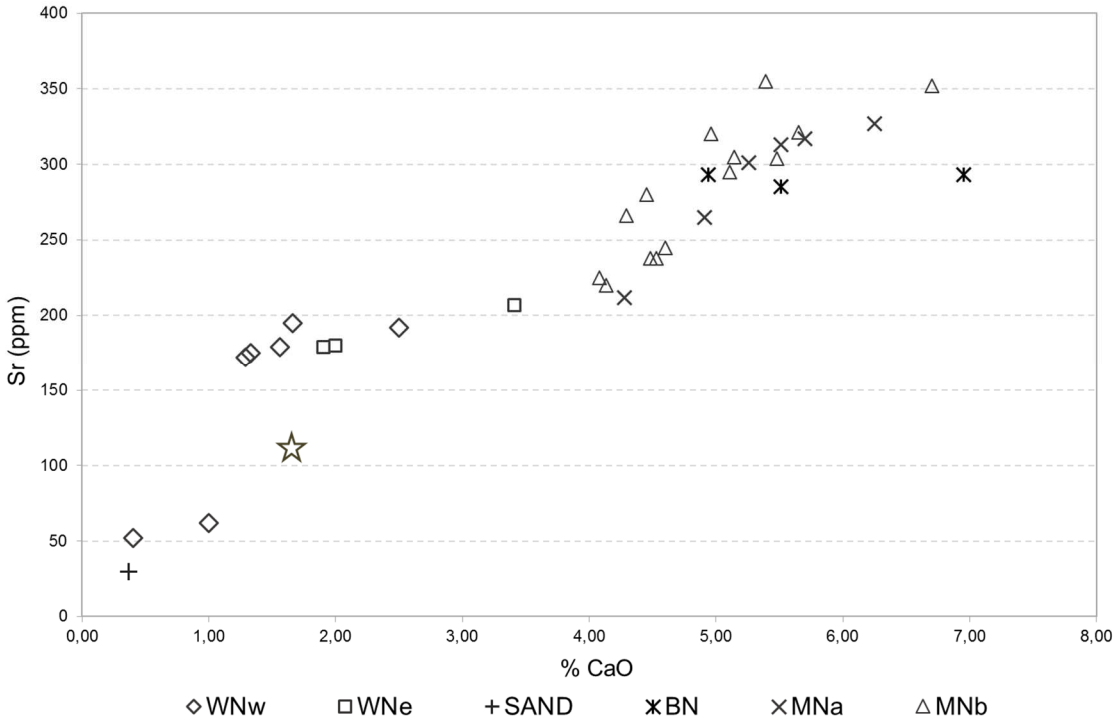

Figure 5.9: biplot of elemental concentration of CaO and Sr. The star indicates clay collected at Al Khiday (clay 1). Abbreviations as in Figure 5.8.

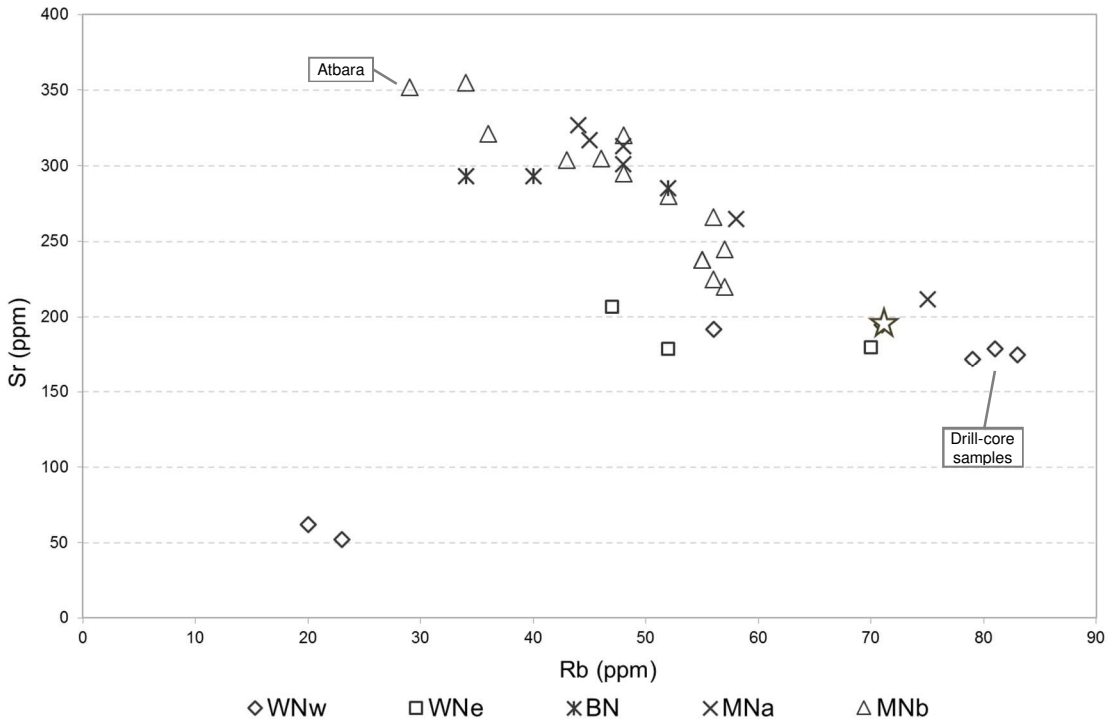

Figure 5.10: biplot of elemental concentration of Rb and Sr. The star indicates clay collected at Al Khiday (clay 1). Abbreviations as in Figure 5.8.

The score plot of the principal component analysis (Figure 5.11) carried out on centered log-ratio transformed data (clr-transformation, from Aitchison, 1986) shows a similar classification as cluster analysis: all the values related to MNa and MNb branches are concentrated at negative values of Component 1 (see also clusters 2, 3, 4 in Figure 5.6). Samples belonging to White Nile (western and eastern bank) and to the Blue Nile (western bank) show positive values of Component 1 (mostly corresponding to clusters 1, 5, 6). Al Khiday clay (clay 1) has a lot in common with samples collected southern along the White Nile (near El Dueim) while clays belonging to the core drilled at Al Khiday show negative values of both Component 1 and Component 2 and are similar to samples collected on the eastern bank of the White Nile. The loading plot (Figure 5.12) indicates that clays at positive values of Component 1 and 2 are aligned toward the direction of high content in SiO_2, Th, U and Zr while clays at positive values of Component 1 and negative values of Component 2 are arranged towards high content in Rb, Ce, La, Nd and Y.

In order to better visualize chemical data characterized by positive values of Component 1, clays after the confluence with Blue Nile and Atbara River were omitted in the PCA, the score plot of which is reported in Figure 5.13. Clays belonging to the western bank of the White Nile mostly lie in the same region (negative values of

Component 1 and positive values of Component 2) towards high content in La, Y Ce and Nd. Clays collected at Al Khiday, both surface (clay 1) and core drill ones (clay 1-35, 1-70 and 1-90), group better in this second PCA, which means that their bulk chemical composition is nearly the same, meaning that only small differences occur among the samples. Blue Nile clays are characterized by negative values of Component 2, as well as the only sample of MNa that usually groups together with WNe clays. They are aligned towards high content of S, Sr, CaO, Na_2O and MgO.

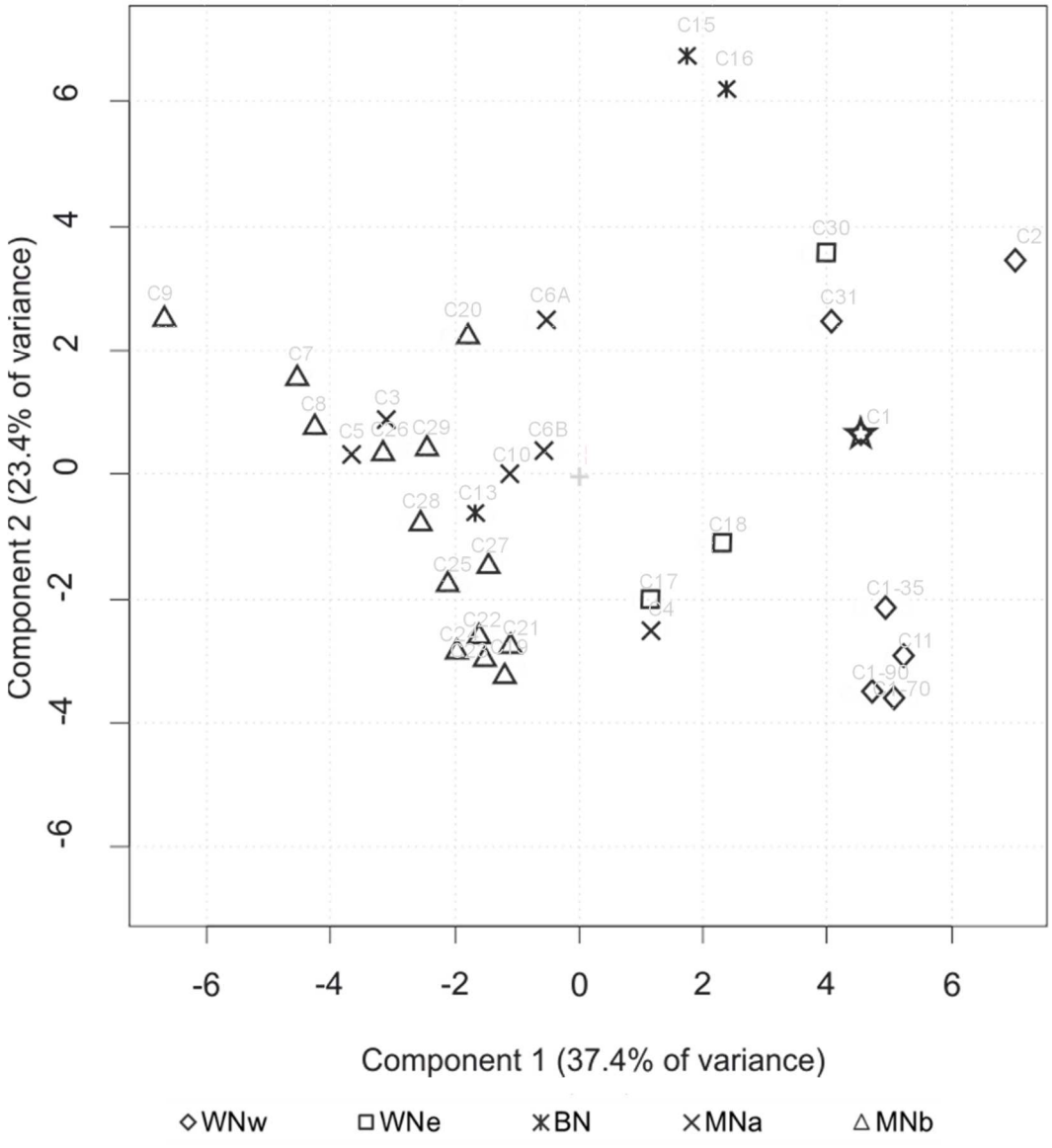

Figure 5.11: Score plot of the Principal component analysis (PCA) of the chemical data with indication of the clay number (C) and brank of the Nile from which they were collected. The star indicates clay collected at Al Khiday (clay 1). Abbreviations as in Figure 5.8.

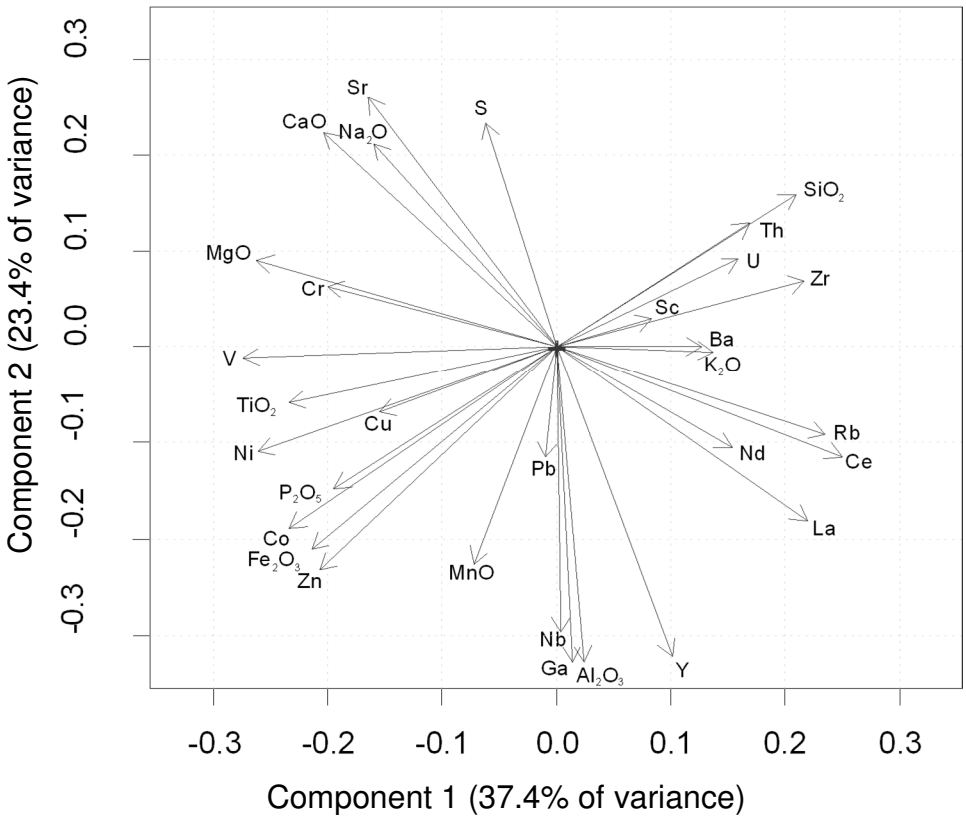

Figure 5.12: Loading plot of the variables considered for the PCA of Figure 5.11, with PC1 and PC2 representing 37.4% and 23.4% of the total variance, respectively.

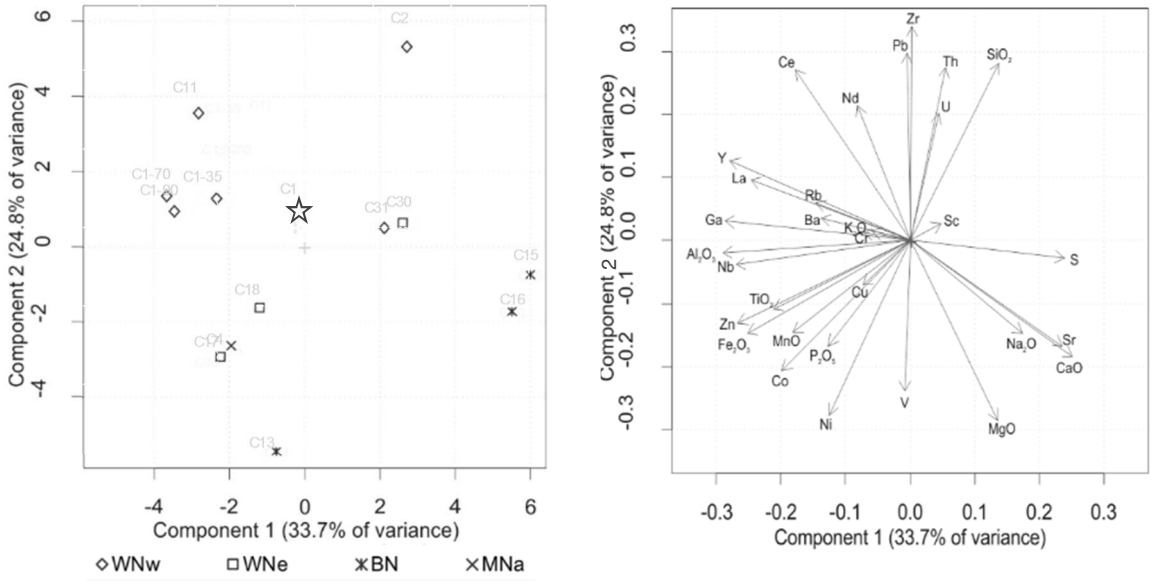

Figure 5.13: score (left) and loading (right) plots obtained from the PCA of chemical data considering clays collected along the White Nile, the Blue Nile and the Main Nile "a" (between Khartoum and Atbara); Main Nile "b" clays (after the confluence with Atbara) were

omitted. The star indicates the clay collected at Al Khiday (clay 1). Abbreviations as in Figure 5.8. PC1 and PC2 represent 37.4% and 23.4% of the total variance, respectively.

Concerning the other geological samples, both sand collected *in situ* at 16-D-4 and granite-like rock collected at Jebel Seleitat were analysed and in Table 5.2 are reported the geochemical composition obtained by XRF.

Table 5.2: geochemical composition of samples SAND and KFS obtained by XRF. Above: major and minor elements expressed in percentage; below: trace elements expressed in ppm.

	SiO_2	TiO_2	Al_2O_3	Fe_2O_3	MnO	MgO	CaO	Na_2O	K_2O	P_2O_5
SAND	96.35	0.2	1.24	0.84	0.01	0.21	0.37	0.1	0.17	0.14
KFS	69.83	0.02	16.49	0.11	0.01	0.05	0.54	3.64	8.37	0.07

S	Sc	V	Cr	Co	Ni	Cu	Zn	Ga	Rb	Sr	Y	Zr	Nb	Ba	La	Ce	Nd	Pb	Th	U
10	13	16	20	3	3	20	13	6	12	30	6	130	2	72	11	12	31	14	8	5
18	13	3	29	2	15	21	38	29	206	140	7	59	2	573	23	32	5	59	2	9

The results obtained from this chemical analysis on raw materials are only partially comparable with those obtained by Padoan et al. (2011) and Garzanti et al. (2015) because of the lack of some data in the aforementioned papers (for example Rb content is absent for some samples as well as many trace elements). However, it is possible to compare some samples collected near the areas of interest.

As regards CaO versus Sr content (Figure 5.14), Blue Nile and Nile values are compatible with those analysed in this study. The average CaO content of samples of both clay and sand from Padoan et al. (2011) and Garzanti et al. (2015) is higher than clay samples of this study. One of the two samples collected on the eastern bank of the White Nile by Padoan et al. (2011) and Garzanti et al. (2015) shows a low content both of CaO and Sr since it is clearly almost a pure sand (94.9% SiO_2, from Garzanti et al, 2015) and it fits quite well with the sand collected in this research at the Al Khiday site. The second sample shows a very high content of both Sr and CaO with respect to those analysed in this study. Also the other clay materials, collected along the Blue Nile and the Main Nile ("a" and "b") have Sr and CaO contents generally higher that those observed in the samples collected for this project.

This may be partially explained by the fact that Padoan et al. (2011) and Garzanti et al. (2015) analysed only the mud fraction, removing any contribute due to the sand size fraction.

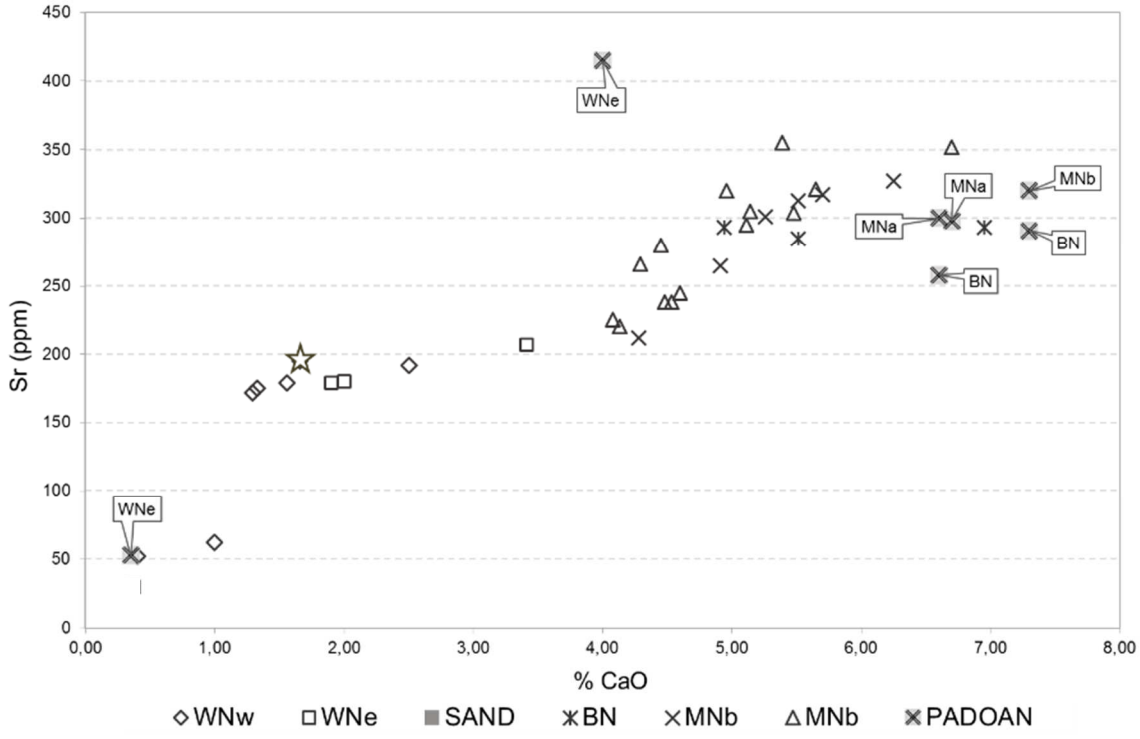

Figure 5.14: biplot of elemental concentration of CaO and Sr of samples from this study and from Padoan et al. (2011) and Garzanti et al. (2015). The star indicates clay collected at Al Khiday (clay 1). Abbreviations as in Figure 5.8.

5.5 Microstructural analysis (SEM)

The microstructural analysis of a clay can supply important information on the composition, structure and texture of the sediment, in terms of provenance and mixing processes.

Thin sections obtained from the *briquettes* were analysed at Scanning Electron Microscope and Back-Scattered Electrons images gave information about the inclusions and the matrix.

Concerning clays originated mainly from the erosion of the basement complex and of the Nubian Sandstone (WNw and WNe), they are characterized by the presence of abundant quartz grains, some micas and a fine matrix with a kaolinitic composition (see Figure 5.15).

- clay 1 (Al Khiday - WNw) is characterised by the presence of abundant quartz grains, small crystals of K-feldspar and plagioclase, few relicts of phyllosilicates (mainly muscovite/illite), rare crystals of ilmenite and amphibole disperse with the sediment, and occasional fragments of ochre (Figure 5.15a)
- clay 2 (near Jebel Aulia dam - WNw) is characterized by the presence of abundant crystals of quartz dispersed in a kaolinitic matrix, where also small flakes of biotite and illite occur with rare crystals of ilmenite and amphibole, occasional fragments of ochre (Figure 5.15b)
- clay 30 (El Dueim, east - WNe) this sediment is characterized, like the previous ones, by the occurrence of abundant grains of quartz dispersed in a kaolinite-rich matrix, where also crystals K-feldspar, plagioclase, amphibole, ilmenite, fragments of ochres and limestone are present (Figure 5.15c)
- clay 31 (El Dueim, west - WNw) this clay material is very similar to the previous, both in term of inclusion and matrix composition (Figure 5.15d)

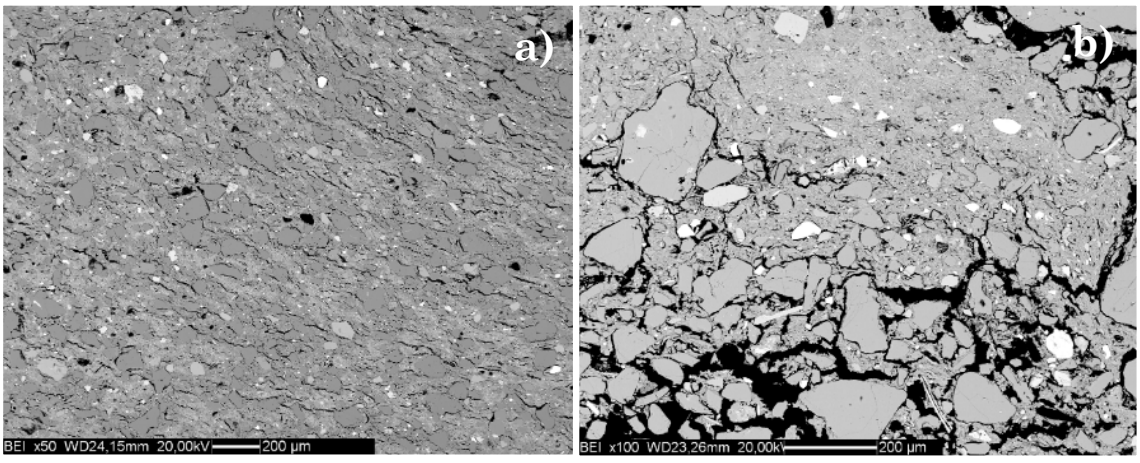

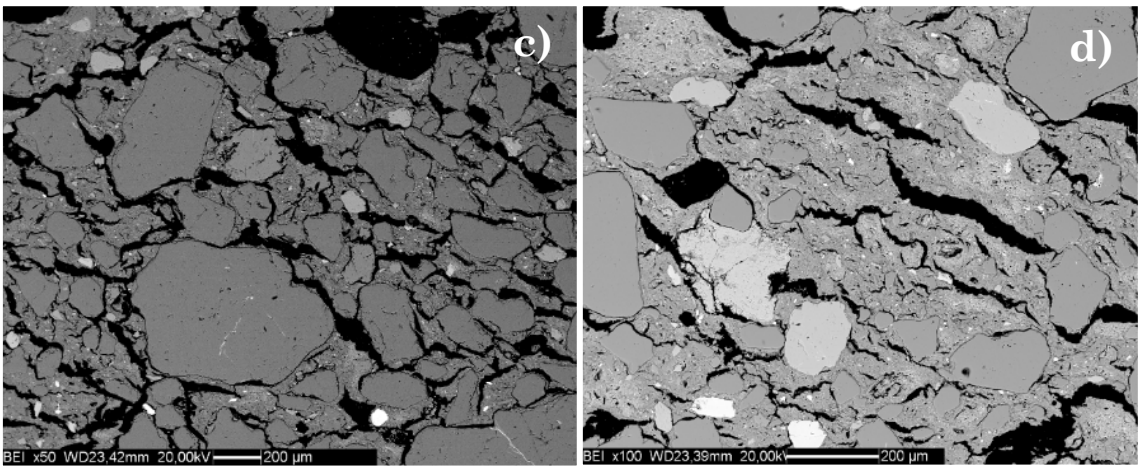

Figure 5.15: BSE images of White Nile clays: a) clay 1; b) clay 2; c) clay 30; d) clay 31

Clays collected along the Blue Nile (clay 13 -near Sheikh Mustafa- and clay 15 -Gezira plan-) (Figure 5.16) are characterized by the presence, in addition to grains of quartz grains, also of crystals of amphibole (Figure 5.16b) and fragments of volcanic rock fragments, in some cases showing intense weathering. The main difference with the sediments of the White Nile clays regards the presence of these rock fragments, as well as the higher amount of femic minerals (especially amphibole, but also pyroxene).

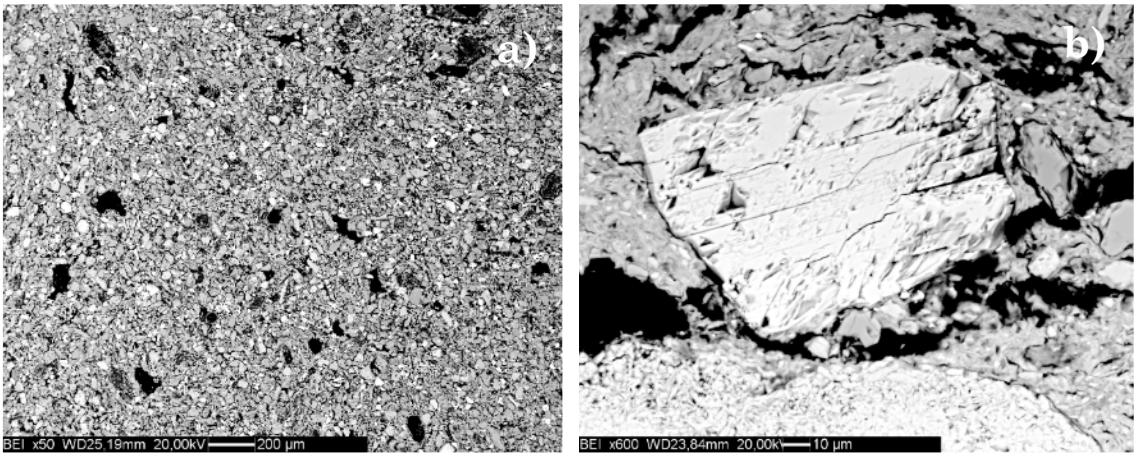

Figure 5.16: BSE images of Blue Nile clays: a) clay 13; b) clay 15: detail of a crystal of amphibole.

The main feature of the clays collected along the MNa branch (clay 4 -near Shendi- and clay 6B -near Meroe-), between Khartoum and Atbara, is the presence of abundant micas (biotite, but also muscovite/illite) and specific clay minerals, such as montmorillonite (Figure 5.17a). The montmorillonite is produced from the alteration

of volcanic mafic rocks, often in association with hydrothermal activity. These minerals are hydrous aluminium silicates in the form of extremely small particles. They are characterized by the general chemical formula $(Na,Ca)_{0,3}(Al,Mg)_2Si_4O_{10}(OH)_2 \cdot n(H_2O)$. Microchemical analysis carried out at the SEM-EDS on montmorillonite aggregates found in clay 4 show that they have a composition with oxides ratio nearly the same than the theoretical one, except for a higher percentage of MgO and FeO, this latter probably due to the presence of weathering product of volcanic rocks, such as iron oxides interlayered in the montmorillonite rich aggregate (Table 5.3).

Table 5.3: chemical composition of montmorillonite expressed in oxides wt% as reported in mindat.org and of that analysed in sample clay 4 (PhiZAF Quantification, Standardless)

Element	Mindat	Clay 4
Na_2O	1.13	1.34
MgO		3.74
CaO	1.02	1.77
Al_2O_3	18.57	23.08
SiO_2	43.77	58.44
K_2O		1.58
TiO_2		0.81
FeO		9.24
H_2O	36.09	-
Total	100.58	100

In fact, they are the first weathering product of basalts. The presence of such minerals highlights the large contribution of the Blue Nile to the total sediment budget of the Main Nile, since these type of inclusions were not detected in the White Nile sediments.

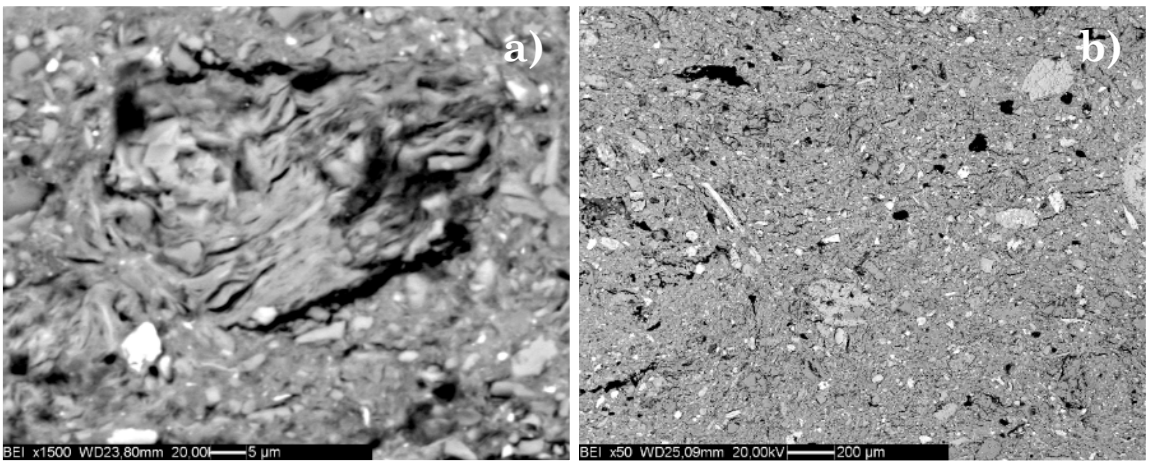

Figure 5.17: BSE images of MNa clays: a) clay 4 (montmorillonite); b) clay 6B

The last clay samples (clay 19 -eastern Bayuda Desert- and clay 8 -just after the confluence with Atbara-) belong to the MNb segment, after the confluence with Atbara. In these clays, montmorillonites are very abundant, especially in that collected just after the confluence of the Atbara (Figure 5.18a) together with volcanic rock fragments. Abundant Fe oxides and chlorites are also present.

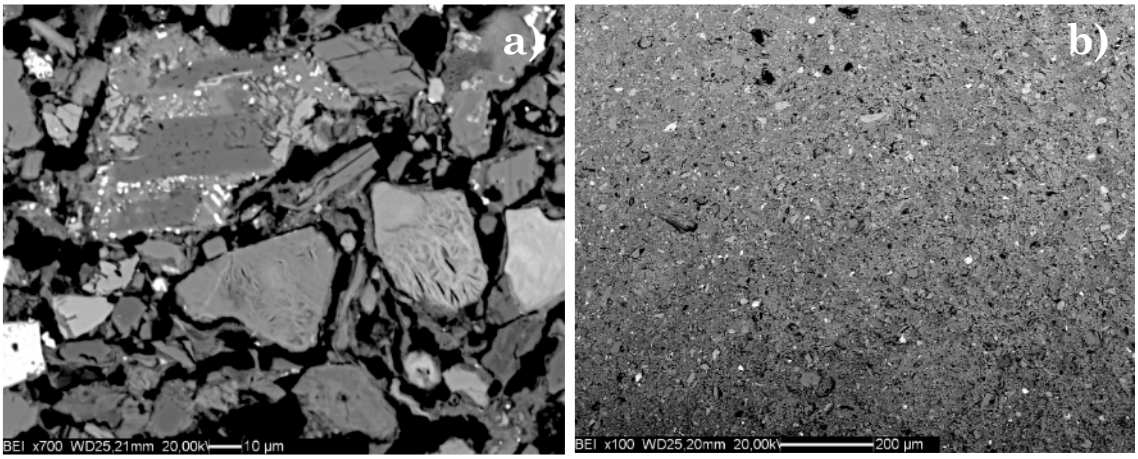

Figure 5.18: BSE images of MNb clays: a) clay 8: detail of montmorillonite-rich fragments; b) clay 19

5.6 Thermal analysis (TGA and DSC)

Thermal analysis methods (differential scanning calorimetry and thermogravimetry) are very powerful tools for investigating the thermal behavior of multi-mineral mixtures such as clays.

At the present moment, the thermal analysis of clay samples has highlighted the presence of abundant organic matter within the mixture, the nature of which is represented by different substances, mainly consisting of nitrogen and carbon compounds, as observed from the infrared spectra of the gas produced form its decomposition.

As examples are reported below the information obtained from this analytical method on some representative clays collected along the Nile River and its tributaries.

White Nile (WNw and WNe): clay 1 (Figure 5.19), clay 1-90 (Figure 5.20) and clay 17 (Figure 5.21) show very similar characteristics. The initial mass loss (up to about 110°C), is related to the loss of the absorbed water. After that, there is the loss of the interlayer water present in the smectite (up to about 200°C), although this phase is present in small quantity in the clay material. Then there is the decomposition of the organic matter, the mass loss of which is mainly confined to the thermal interval included between 200°C and 500°C, as it was also possible to see from the related infrared spectra. Then, around 500°C there is the decomposition of kaolinite. The small mass loss at temperature exceeding 600°C is related to the decomposition of smectite.

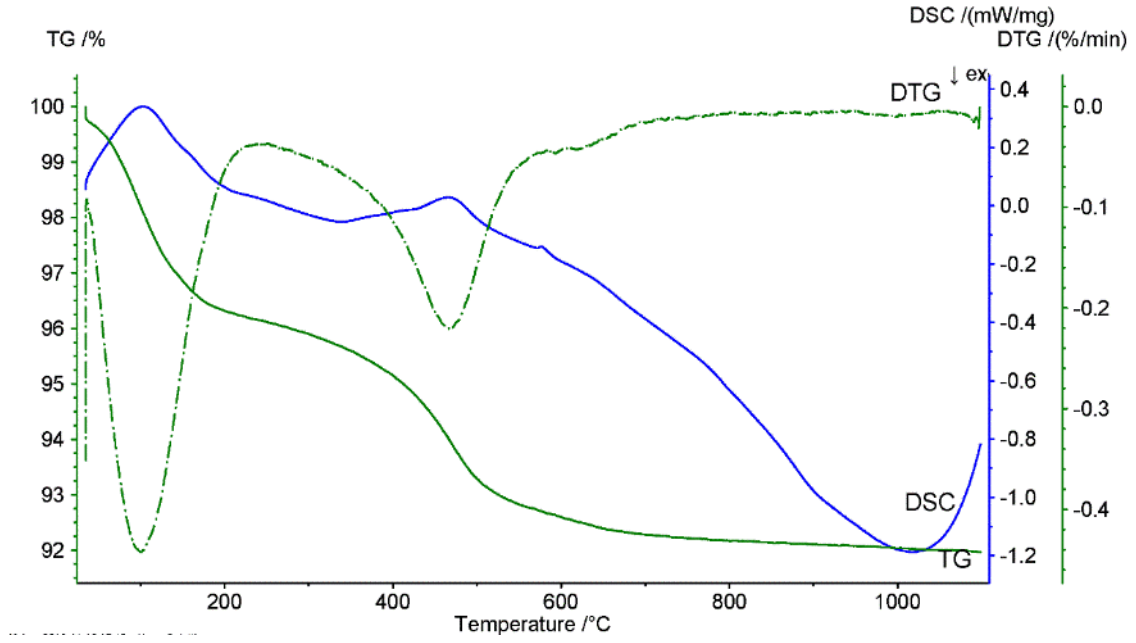

Figure 5.19: thermal analysis of clay 1 (WNw). TG: thermogravimetric curve; DSC: differential scanning calorimetry curve; DTG: 1st derivative of TG curve

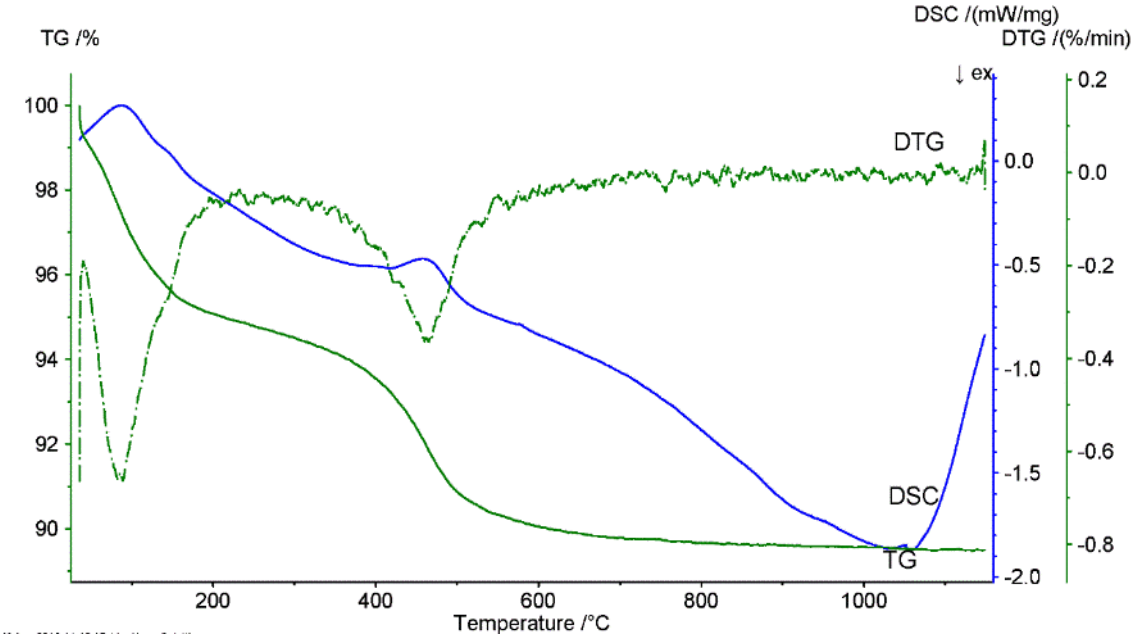

Figure 5.20: thermal analysis of clay 1-90 (WNw). Abbreviations as in Figure 5.19

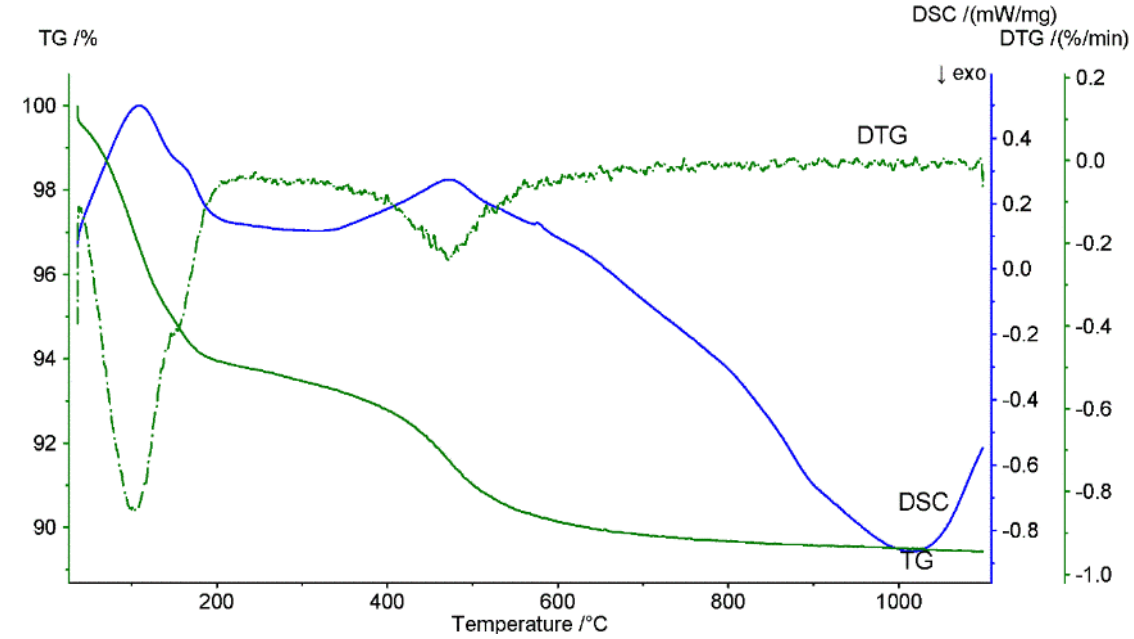

Figure 5.21: thermal analysis of clay 17 (WNe). Abbreviations as in Figure 5.19

The situation is very different for the second group of clays, formed by clay 8 (Figure 5.22), clay 6B (Figure 5.23), clay 24 (Figure 5.24) and clay 30 (Figure 5.25). The amount of their organic content is still high but there is clearly a higher amount of

montmorillonite, the decomposition of which determines an important mass loss at temperature exceeding 600°C.

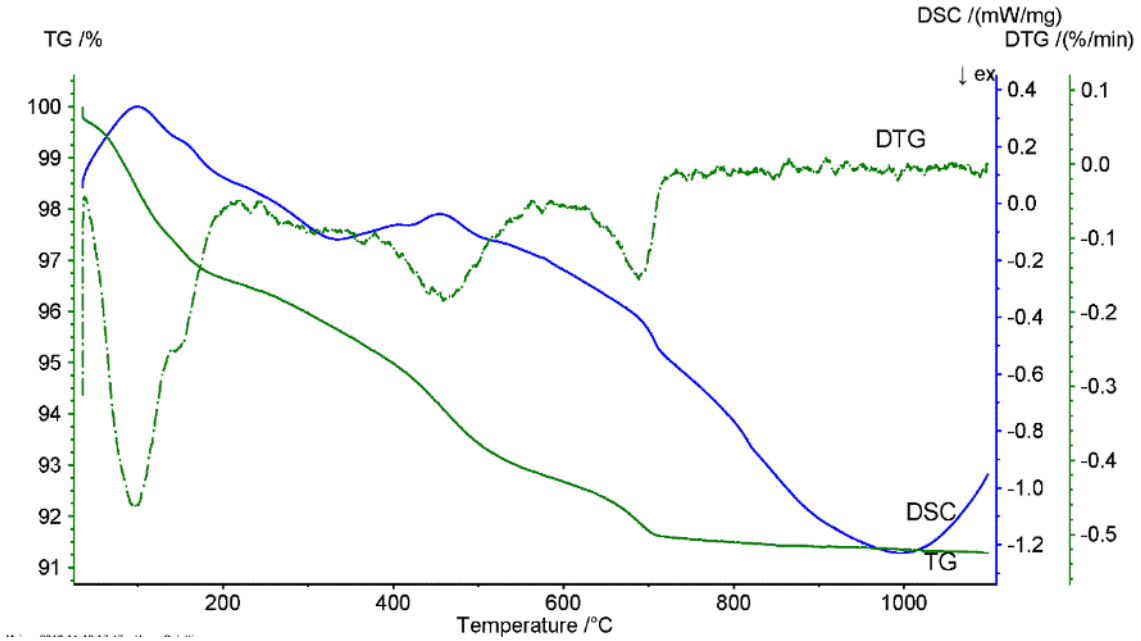

Figure 5.22: thermal analysis of clay 8 (MNb). Abbreviations as in Figure 5.19

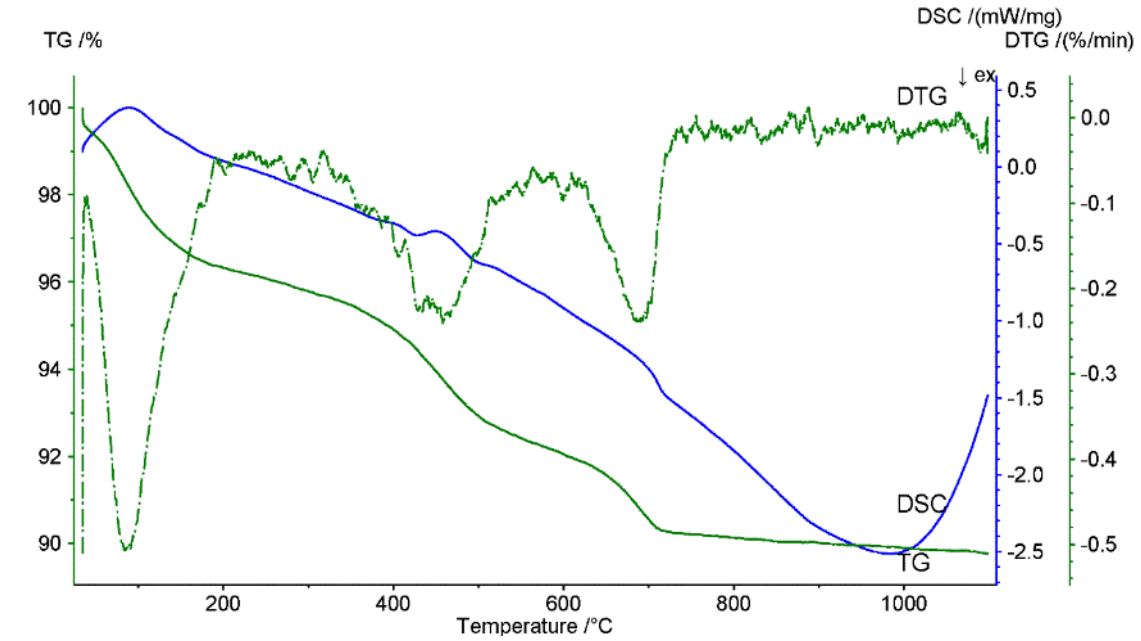

Figure 5.23: thermal analysis of clay 6B (MNa). Abbreviations as in Figure 5.19

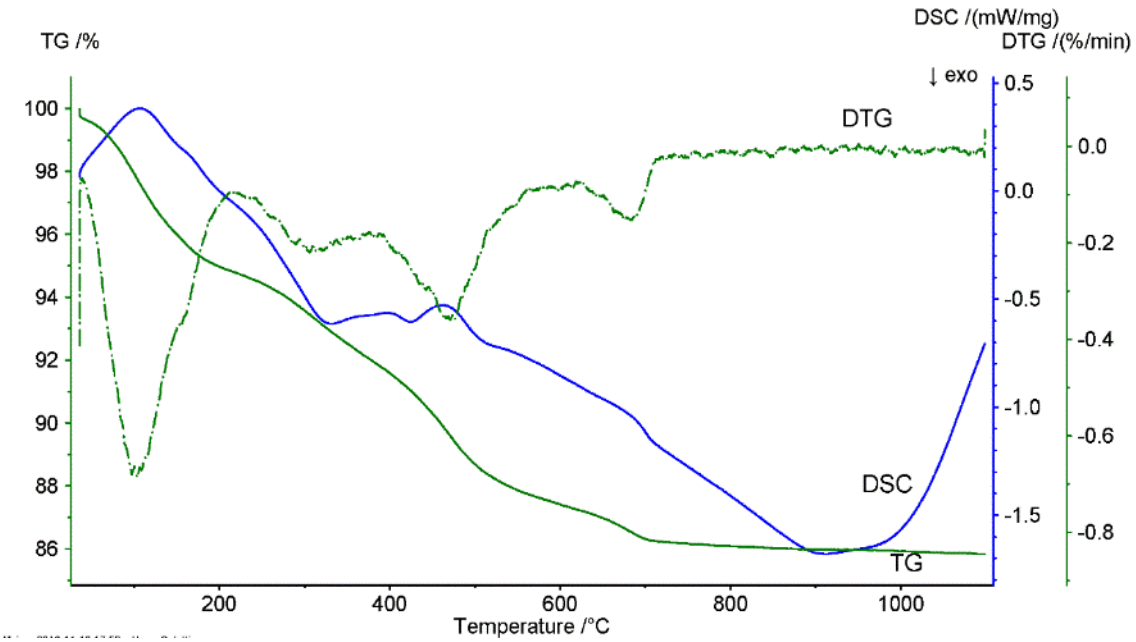

Figure 5.24: thermal analysis of clay 24 (MNb). Abbreviations as in Figure 5.19

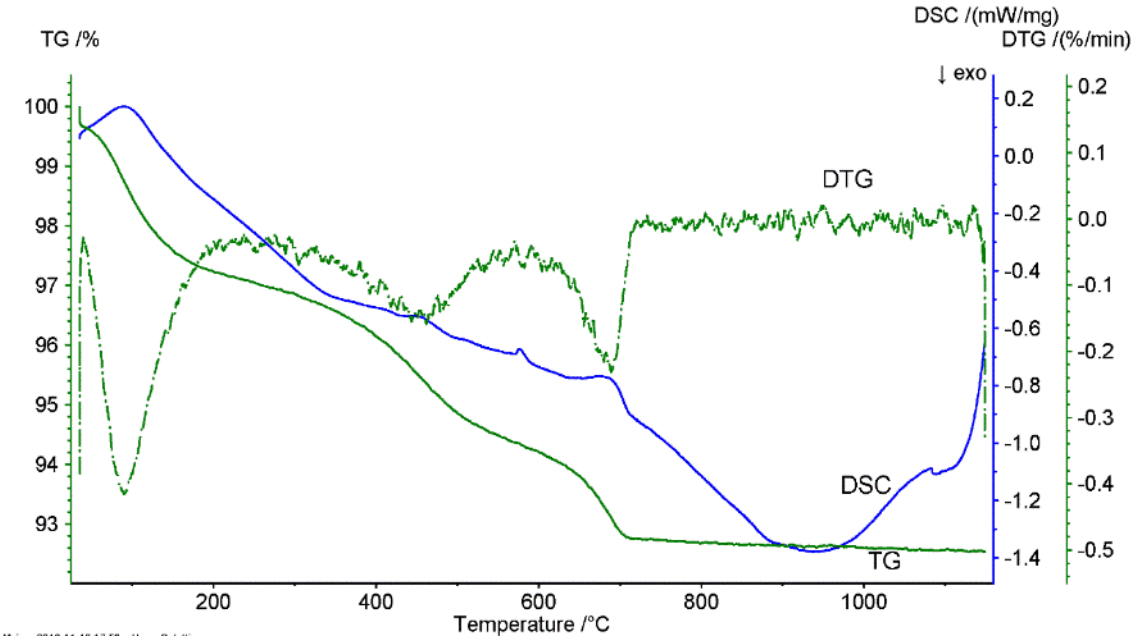

Figure 5.25: thermal analysis of clay 30 (WNe). Abbreviations as in Figure 5.19

Clay 15 (Figure 5.26) that represents Blue Nile sediments shows a high content in clay minerals.

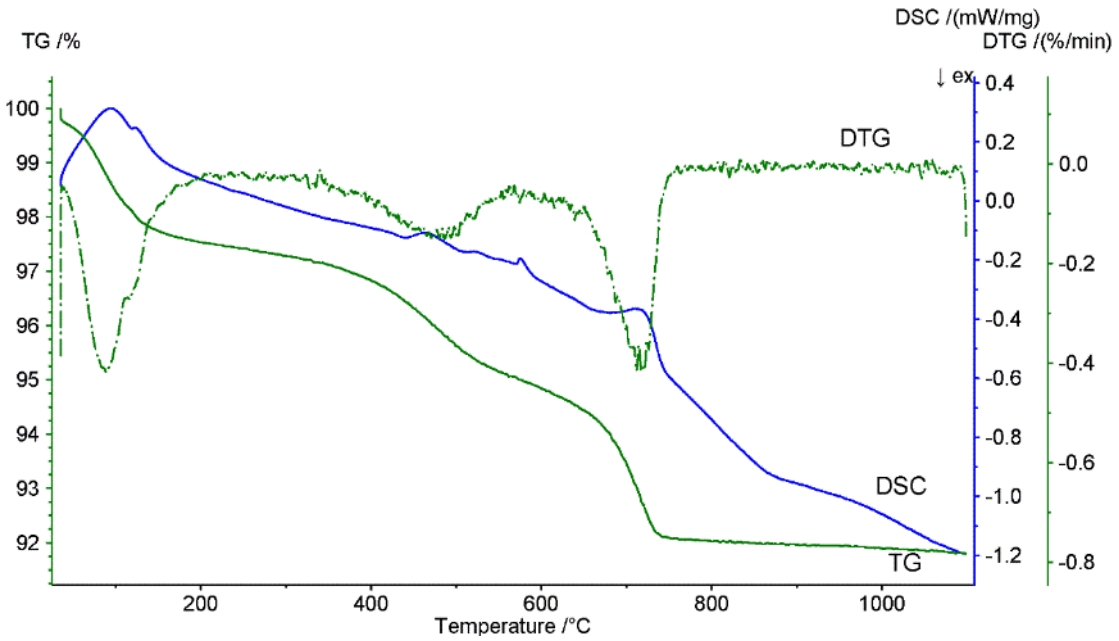

Figure 5.26: thermal analysis of clay 15 (BN). Abbreviations as in Figure 5.19

In order to have a more comprehensive overview of TG curve trends, in Figure 5.27 is illustrated a comparative diagram that shows the different features of the samples. Two main trends can be observed, one grouping clays of White Nile (clay 1, 1-90, 17) and the other one those of the Blue Nile, Main Nile "a" and "b" (clay 15, 30, 8, 6B, 24).

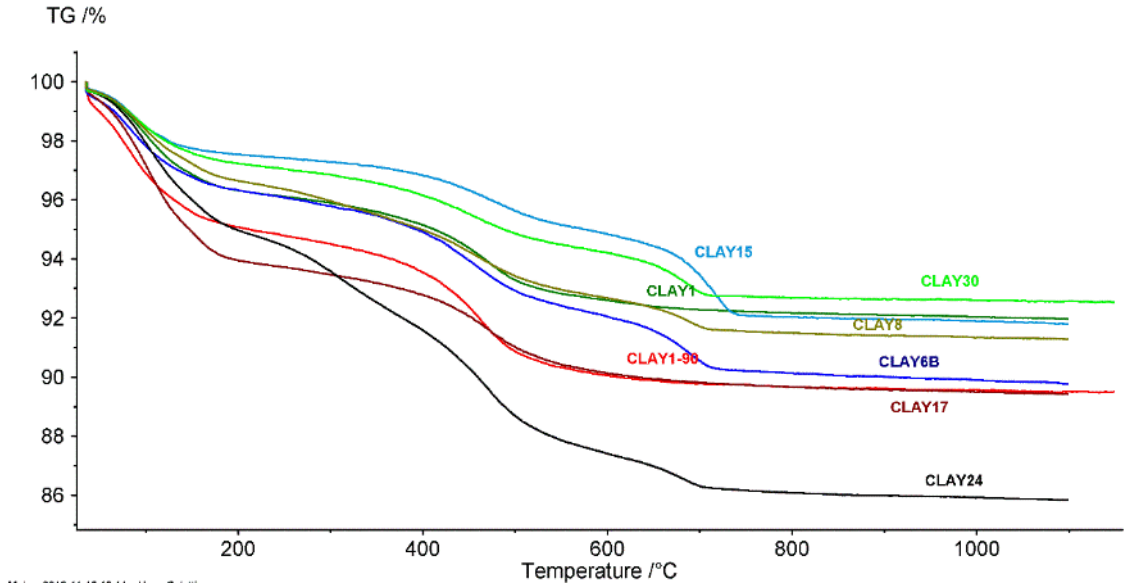

Figure 5.27: Comparative diagram of TG curves of clay samples

5.7 Sr isotope analysis (TIMS)

Isotopic analyses were carried out on the set of samples described in Paragraph 4.1. The isotopic signatures of clay materials can be interpreted as weighted averages of the end-member isotopic signatures of rocks eroded in the drainage basin (Padoan et al, 2011). Through Sr isotopic analysis it has been possible to discriminate between clays derived from volcanic rocks of Ethiopian highlands and clays formed by crystalline basements and Mesozoic sedimentary covers exposed along the western shoulder of the Red Sea and East African rift. In Table 5.4 are listed the measured Sr isotopic ratios and in Figure 5.28 values of $^{87}Sr/^{86}Sr$ are represented in a diagram. Samples collected along the western bank of the White Nile are aligned towards high $^{87}Sr/^{86}Sr$ ratios as they derive from the crystalline basement and the sedimentary clastic sequence (Nubian Sandstone). Samples collected along the Blue Nile are characterized by low $^{87}Sr/^{86}Sr$ ratios underlying their volcanic origin as well as samples from Main Nile "b" after the confluence with Atbara. This affinity resides in the contribution in terms of sediment loads derived from both Blue Nile and Atbara that contribute for more than 90% to the total sediment budget of the Main Nile River (see Paragraph 2.2; Padoan et al, 2011; Garzanti et al, 2015). Clays coming from the eastern bank of the White Nile (Gezira plan) show values that seem to be the average of White Nile and Blue Nile $^{87}Sr/^{86}Sr$ ratios.

Table 5.4: Sr isotopic data of the clay samples

SAMPLE ID	LOCATION	$^{87}Sr/^{86}Sr$	error	Sr (ppm)	TYPE
CLAY 1	near Al Khiday	0.710481	2.0E-05	195	WNw
CLAY 2	near Jebel Aulia dam	0.709396	1.9E-05	62	WNw
CLAY 11	near Jebel Maddaha	0.709757	3.2E-05	52	WNw
CLAY 1-35	near Al Khiday	0.711537	2.9E-05	179	WNw
CLAY 1-70	near Al Khiday	0.711981	1.2E-05	175	WNw
CLAY 1-90	near Al Khiday	0.712120	2.2E-05	172	WNw
CLAY 17	Kalakla Galaa	0.707857	1.7E-05	179	WNe
CLAY 30	near Ed Duiem	0.708218	3.1E-05	207	WNe
SAND	At Al Khiday	0.708924	2.9E-05	30	SAND
CLAY 13	Soba	0.705781	2.3E-05	285	BN
CLAY 15	El Srmir Village	0.707070	1.0E-05	293	BN

CLAY 3	near Saggai	0.705598	1.9E-05	327	MNa
CLAY 4	near Gerri	0.708730	2.0E-05	212	MNa
CLAY 6B	Meroe	0.706371	2.0E-05	265	MNa
CLAY 9	Atbara	0.704777	2.1E-05	352	MNb(A)
CLAY 8	Atbara (after the confluence)	0.705102	1.9E-05	321	MNb
CLAY 21	near Korti	0.706345	1.4E-05	238	MNb
CLAY 24	Amara	0.706539	1.9E-05	225	MNb
CLAY 28	near Kerma	0.705819	1.8E-05	295	MNb

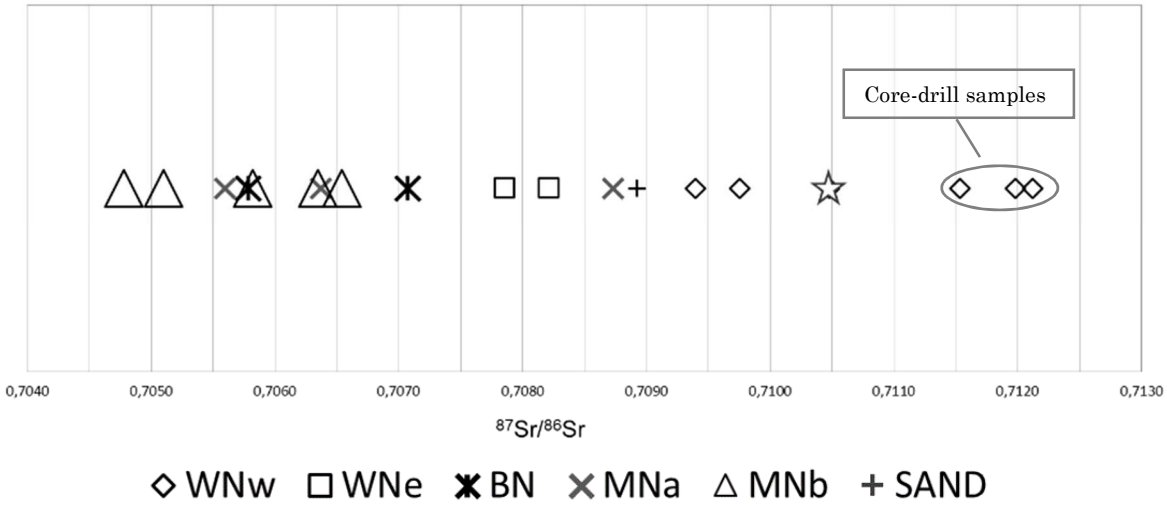

Figure 5.28: diagram of the $^{87}Sr/^{86}Sr$ ratios of clays and sand. The star represents the clay collected near Al Khiday (clay 1). Abbreviation as in Figure 5.8.

Sr isotope ratios are clearly related to geographic areas of origin. Also sandy clays (clay 2 and clay 11) which are characterized by a low Sr content (see Table 5.4), as well as the SAND sample collected from the archaeological site of Al Khiday, show a $^{87}Sr/^{86}Sr$ ratio compatible with the area of origin. As regards the core-drill specimens from Al Khiday, clay 1-90 as well as the other samples (clay 1-70 and clay 1-35) show Sr isotopic ratio higher than clay 1 that was collected in the same location from the surface. The Sr isotopic variability is not reproduced in bulk chemical analysis (see Paragraph 5.4). This is probably due to a superficial mixing of the sediments related to a high flood episode of the Blue Nile occurred a few decades ago. Moreover the core-drill samples are probably more ancient than clay 1 and reflect the situation before the construction of the Jebel Aulia dam in 1937, located 35 km south of Khartoum. At that time, sediments of the White Nile were not halted by any barrier and the crustal fingerprint deriving from the dismantling of the crystalline basement was more evident.

Some ambiguities regards also clay 30 that was collected at El Dueim, 200 km south of Al Khiday along the White Nile. It shows a lower Sr isotopic ratio than White Nile clays of Al Khiday even if it is located away from the Blue Nile course. Although clay 30 was collected along the eastern bank of the White Nile, that is to say inside the Gezira plan, it still shows the influence of the Blue Nile. In fact, 14.500 years ago the White Nile deposited clays along its flood plain and simultaneously reworked pre-existing sands and gravels brought in by the late Pleistocene Blue Nile channels that flowed across the Gezira fan (Williams et al., 2015). It is most likely that actual clay collected at El Dueim still shows the $^{87}Sr/^{86}Sr$ ratio of the reworked mixed sediments present along the eastern bank of the White Nile.

As previously said (Paragraph 5.4) when two components of different chemical composition mix in varying proportions, the chemical compositions of the resulting mixtures vary systematically depending on the relative abundances of the end-members (Faure, 1986). In order to evaluate mixing relations, it is usually necessary to apply two or more measured variables to the problem. These variables are usually isotope ratios, elemental ratios, and elemental abundances (Dickin, 2006). In this context, it is logical to begin examining the behaviour of isotopic tracers as a function of the elemental concentration of the same element. Therefore, $^{87}Sr/^{86}Sr$ ratios as a function of Sr concentration are shown in Figure 5.29. Ideally, initial Sr isotope ratios should be plotted against the abundance of ^{86}Sr but since the decay constant of Rb is low (48–49 billion years), ^{88}Sr makes up the bulk of strontium in most rocks and the abundance of ^{86}Sr can be approximated by total Sr without introducing significant errors (Dickin, 2006). Mixing of components with different isotopic and elemental compositions produces a hyperbolic curve on a diagram of $^{87}Sr/^{86}Sr$ ratio against Sr concentration (Figure 5.29). A bivariate diagram for two ratios with common denominators originates linear mixing lines. Therefore, the hyperbolic mixing curve can be transformed into a straight line by plotting the initial $^{87}Sr/^{86}Sr$ ratio against 1/Sr (approximating $1/^{86}Sr$) (Figure 5.30). Real data sets representing binary mixtures commonly scatter above and below the mixing line. In this case, samples enriched in SiO_2 are characterized by a low amount of Sr because of the dilution effect caused by quartz. However, Sr isotope ratios of those samples are consistent with the area of origin. Sr concentration increases while Sr isotope ratio decreases progressively from clays draining crystalline basement products to clays containing sediments deriving from Ethiopian highlands (Blue Nile and Atbara). The three samples with the highest $^{87}Sr/^{86}Sr$ ratio derive from the core drilled underneath clay 1 and they show the typical

fingerprint of the crystalline basement and sedimentary clastic sequence derived from its disruption.

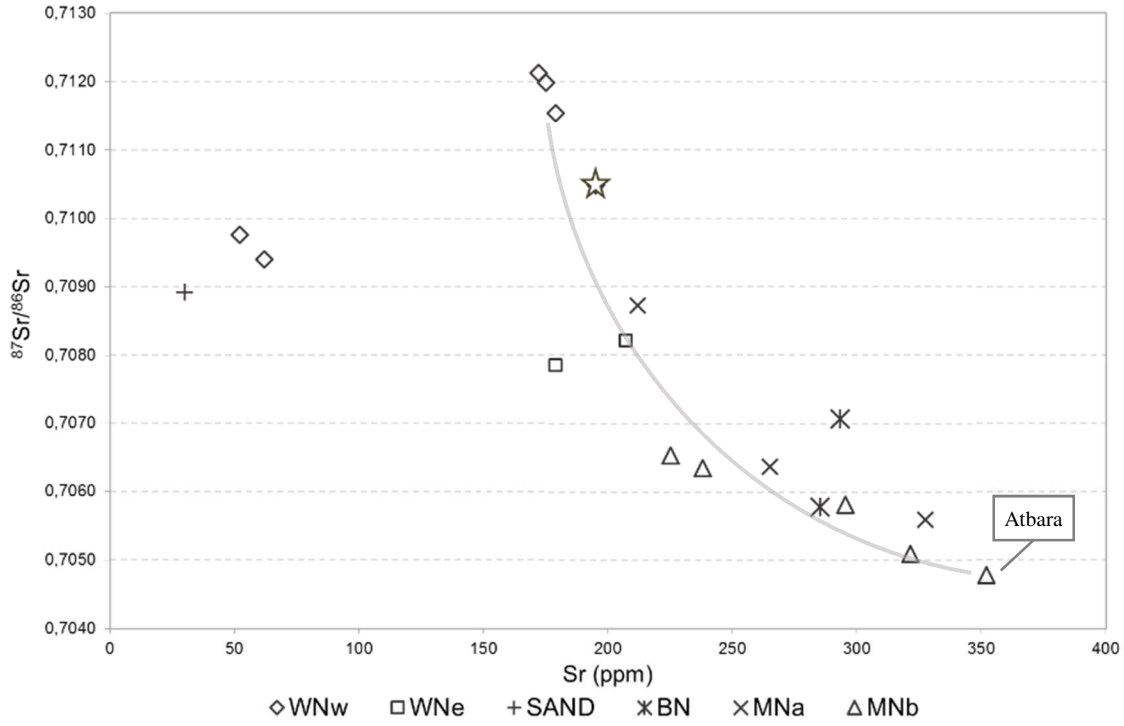

Figure 5.29: strontium concentration versus strontium isotope ratios in Nile clays and Al Khiday sand. The branch of the hyperbola represents the mixing curve. The star indicates the clay collected at Al Khiday (clay 1). Abbreviation as in Figure 5.8.

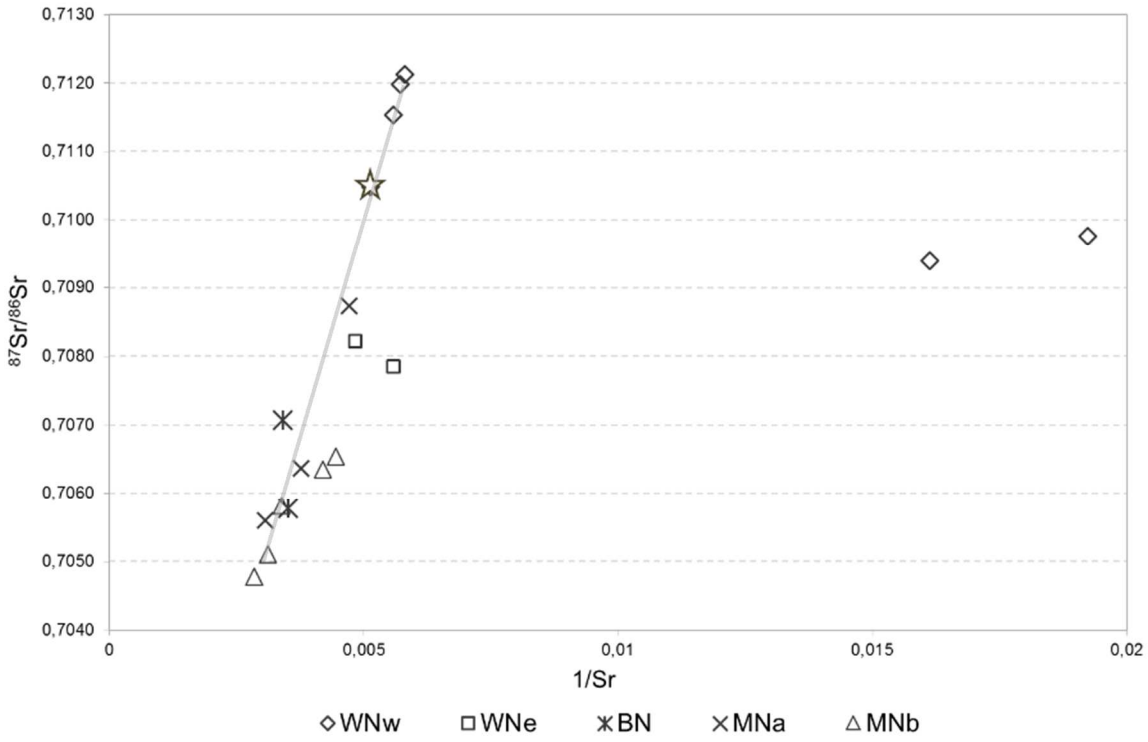

Figure 5.30: inverse of strontium concentration versus strontium isotope ratios in Nile clays. The straight line represents the mixing curve. For graphical reasons the SAND sample was omitted. The star indicates the clay collected at Al Khiday (clay 1). Abbreviations as in Figure 5.8.

The results obtained from this research are only partially consistent with those obtained from Padoan et al. (2011) and Garzanti et al. (2015), since they analysed mud (40-63 μm) and sand (63-2000 μm) size fraction separately. Moreover, the results obtained were expressed as a mean of a series of measures, losing any detail concerning the analysis of the segments of Nile system crossing the Sudan territory, since they consider the whole Nile River from its springs to the delta. However, it is possible to compare data reported in Table 5.5 and plotted in Figure 5.31. Main Nile "a" (MNa), Main Nile "b" (MNb) and Blue Nile (BN) $^{87}Sr/^{86}Sr$ ratios are well-matched with data obtained after this study, as regards both Sr content and isotopic fingerprint. Similarly, clays collected for this study along the White Nile (WNw and WNe) show $^{87}Sr/^{86}Sr$ ratios compatible with levee and sand samples analysed by Padoan et al. (2011) and Garzanti et al. (2015). The variability in Sr content is due to the different analysed grain-size fraction.

These data are quite important since they indicate that Sr isotope ratio is not strongly affected by the grain-size selected, within certain limits. While Padoan et al. (2011) and Garzanti et al. (2015) analysed only the "mud" (silt and clay fractions, < 60 μm or

<40 μm), in this study it has been decided not to make any grain-size selection, since the aim of this research is addressed to define possible isotopic markers to distinguish ancient pottery provenance. In fact, during the ceramic production, especially in prehistoric period but also in historic periods, any possible preparation of the clay material (levigation or tempering) was carried out according to the potters' skills and not using sophisticated separation methods as those used in laboratories. Therefore, the Sr isotopic ratio was here measured taking the clay material available along the riverbanks or in the inner areas, which was possibly exploited by the ancient potters to produce their pottery, without any grain-size selection.

Table 5.5: Sr isotopic data of clay samples from Padoan et al. (2011) and Garzanti et al. (2015) and from this study. S and L in the SAMPLE ID of Padoan et al. (2011) and Garzanti et al. (2015) stand for "sand" and "levee", respectively.

	SAMPLE ID	Location	TYPE	Sr ppm	$^{87}Sr/^{86}Sr$	error
Padoan et al. (2011) and Garzanti et al. (2015)	**30** (<63 μm)	Kosti	WNw	231	0.71097	±5
	2878S (<40 μm)	Rabak	WNe	396	0.71045	±2
	2878S (<40 μm)	Rabak	WNe	415	0.71083	±3
	2878S (125-180 μm)	Rabak	WNe	34	0.71038	±2
	2878S (125-180 μm)	Rabak	WNe	30	0.71116	±3
	2843L (<40 μm)	Khartoum	BN	271	0.70513	±2
	2843L (<40 μm)	Khartoum	BN	258	0.70546	±2
	2843S (125-180 μm)	Khartoum	BN	277	0.70516	±2
	2884L (<40 μm)	6° Cataract	MNa	269	0.70546	±2
	2884L (<40 μm)	6° Cataract	MNa	300	0.70566	±2
	2846L (<40 μm)	Ghaba	MNa	331	0.70516	±2
	2846L (<40 μm)	Ghaba	MNa	320	0.70508	±3
	2899L (<40 μm)	3° Cataract	MNb	330	0.70497	±3
	2899L (<40 μm)	3° Cataract	MNb	315	0.70536	±2
	2899S (125-180 μm)	3° Cataract	MNb	348	0.70614	±3
	2899S (125-180 μm)	3° Cataract	MNb	460	0.70591	±1
This study	**Clay 1**	near Al Khiday	WNw	195	0.710481	2.0E-05
	Clay 2	near Jebel Aulia dam	WNw	62	0.709396	1.9E-05
	Clay 11	near Jebel Maddaha	WNw	52	0.709757	3.2E-05
	Clay 1-35	near Al Khiday	WNw	179	0.711537	2.9E-05
	Clay 1-70	near Al Khiday	WNw	175	0.711981	1.2E-05
	Clay 1-90	near Al Khiday	WNw	172	0.71212	2.2E-05
	Clay 17	Kalakla Galaa	WNe	179	0.707857	1.7E-05

	Clay 30	near Ed Duiem	WNe	207	0.708218	3.1E-05
	SAND	At Al Khiday	SAND	30	0.708924	2.9E-05
	Clay 13	Soba	BN	285	0.705781	2.3E-05
	Clay 15	El Srmir Village	BN	293	0.70707	1.0E-05
	Clay 3	near Saggai	MNa	327	0.705598	1.9E-05
	Clay 4	near Gerri	MNa	212	0.70873	2.0E-05
	Clay 6B	Meroe	MNa	265	0.706371	2.0E-05
	Clay 9	Atbara	A	352	0.704777	2.1E-05
	Clay 8	Nile after Atbara	MNb	321	0.705102	1.9E-05
	Clay 21	near Korti	MNb	238	0.706345	1.4E-05
	Clay 24	Amara	MNb	225	0.706539	1.9E-05
	Clay 28	near Kerma	MNb	295	0.705819	1.8E-05

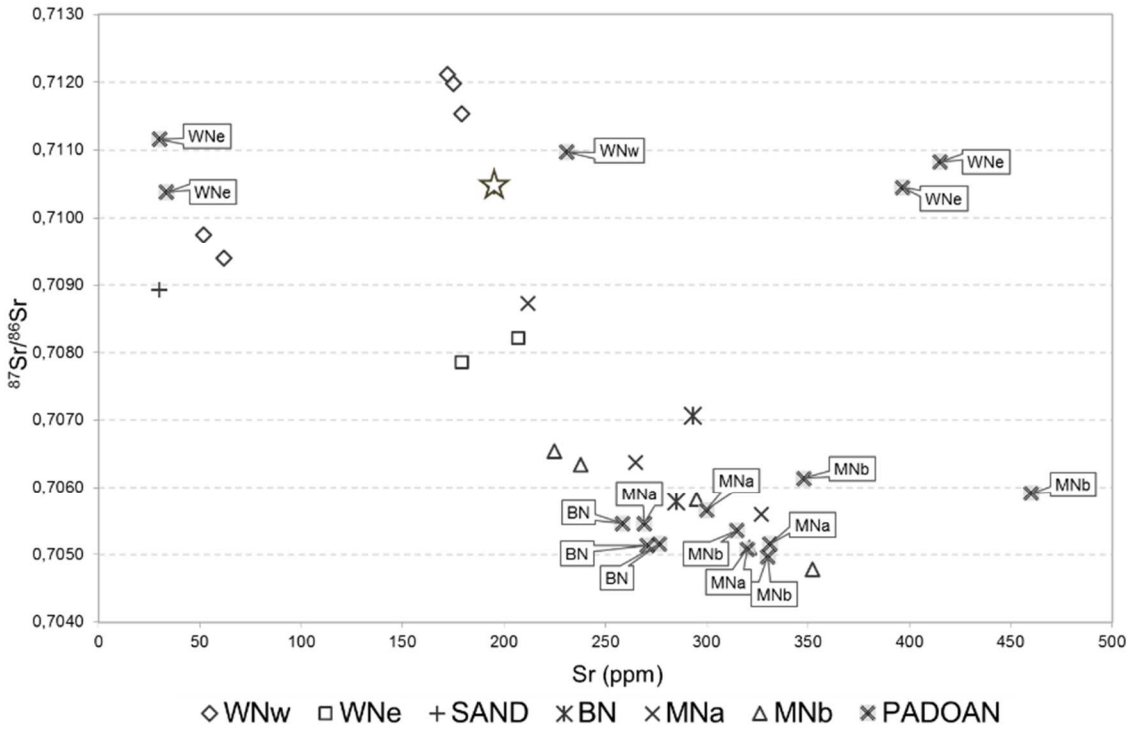

Figure 5.31: strontium concentration versus strontium isotope ratios from this study and from Padoan et al. (2011). The star indicates the clay collected at Al Khiday (clay 1). Abbreviations as in Figure 5.8.

5.8 Discussion and conclusion

Sr isotopic data provide a complementary tool to assess clay provenance since the homogeneity in terms of chemical composition does not allow univocally determining the area of origin.

As regards petrographic and microstructural analyses, the occurrence of big sub-rounded to rounded quartz grains resulted to be more characteristic of the clay samples collected along the White Nile, whereas that of small angular and sub-angular quartz grains is typical of sediments from the basins pertinent to the Ethiopian highlands. Furthermore, the occurrence of other phases such as plagioclase, olivine and pyroxene, contributed to characterize the volcanic origin of these sediments. BSE images highlighted the presence of specific weathering products derived from the weathering of basaltic rocks, montmorillonite-rich aggregates. These phases were found only in clays collected on the Blue Nile and after the confluence with Blue Nile (and Atbara) and might be diagnostic for the discrimination of used raw materials in ceramic production.

As regards the mineralogical analysis, the statistical treatment of data revealed a good clustering of samples collected along the main tributaries (White and Blue Nile, Atbara) but partially failed in discriminating clays coming from the main branch of the Nile River (among Khartoum and Atbara, after Atbara), since the mineral composition of the Nile after the confluence is strongly affected by the contribute of Blue Nile. Some exceptions were explained by the influence of the sediments brought from ancient rivers tributaries of the Nile, the remixing of the sediments of which still affects the mineralogical and chemical composition of the clay materials.

Chemical analysis led more or less to the same results: bivariate statistical treatment revealed a dependence between Sr and Rb contents that might be the result of a mixing process of sediments along the main course of the Nile River. Principal Component Analysis highlighted some interesting similarities among samples collected within the Gezira plan, but only after the omission of clay samples belonging to the MNb segment. The last samples lay all in the same region of the diagram, diametrically opposite to White Nile, Blue Nile and Gezira clays and for a clearer overview of other groups, they were omitted in the second PCA. Clay samples collected at Al Khiday (clay 1, 1-35, 1-70 and 1-90) show an analogue bulk chemical composition.

Isotopic information indicate that the supposed mixing process is a factual phenomenon that involves all the sediments of the Nile River. White Nile clays have

a high $^{87}Sr/^{86}Sr$ ratio: WNw clays range from 0.709396 to 0.712120 and the high values of the core-drill samples probably indicate the stronger contribution of the White Nile before the construction of the Jebel Aulia dam. $^{87}Sr/^{86}Sr$ ratio of clay 1 (superficial clay from Al Khiday) is probably affected by the occurrence of a recent episodic flood event of the Blue Nile. WNe samples are influenced by the presence of the Blue Nile (from 0.707857 to 0.708218). As previously mentioned (Paragraph 2.2) for over a century when the Blue Nile was in overflow it dammed the flow of the White Nile through a network of distributary channels (Figure 5.32) that flowed across the Gezira fan (Williams et al., 2015). Clays collected along the Blue Nile show $^{87}Sr/^{86}Sr$ ratios that vary from 0.705781 to 0.707070 and these values are comparable with Nile River samples (from 0.704777 of Atbara clay to 0.706539 of the northern sample) indicating that Nile River maintains the mixed fingerprint. Main Nile "a" (MNa) isotopic fingerprints vary from 0.705598 to 0.708730 and this is probably due to the high variability of the region between Khartoum and Atbara.

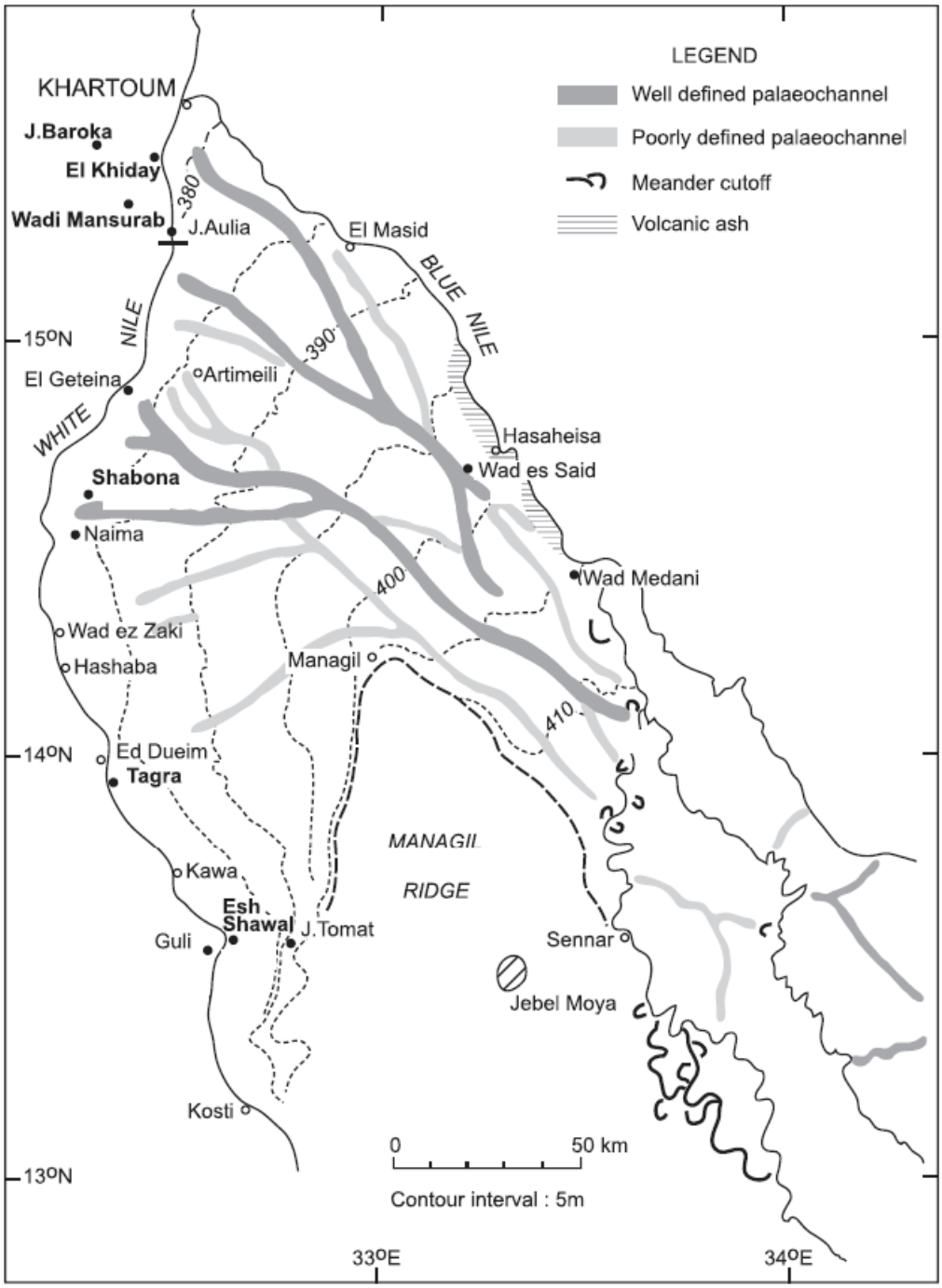

Figure 5.32: simplified map of the Gezira plan and paleochannels between Blue Nile and White Nile (from Williams et al., 2015)

SIXTH CHAPTER

MESOLITHIC AND NEOLITHIC POTTERY FROM CENTRAL - NORTHERN SUDAN

6.1 Preparation of the samples

Thirty-nine ceramic sherds were selected as illustrated in Paragraphs 4.2.1 and 4.2.2. They were transformed in two kinds of samples: thin sections and fine powder. Some of the thin sections were already available while the others were prepared as described above (see Paragraph 3.2).

6.2 Petrographic analysis

Variability of decorative motifs may represents changes in production technology in terms of ceramic paste recipes. Petrographic analysis of the pottery from Al Khiday (Dal Sasso, 2011; Dal Sasso et al, 2014) identified two main types of ceramic recipes (quartz-rich and alkali-feldspar-quartz-rich pastes) in the Mesolithic ceramic assemblage over a time-span of two millennia. Previous studies (Dal Sasso et al, 2014) highlighted that the potsherds show a homogenous, isotropic and often optically active matrix. The 39 ceramic samples studied in this research project were divided into two petrographic groups:

- *Qtz-tempered* (AK73, AK102, AK74, AK75, AK82, AK86, AK67, AK76, AK70, AK136, AK165, AK170, AK173, AK193, AK115, AK116, AK152, AK182, AK196, AK198, AK211, AK204, AK212, WH24, WH25, AK8, AK46, AK48, BN7, BN8, WH29, AK1, AK24, AK36, AK47, AK49, AK50): quartz-rich potsherds are characterized by sub-rounded quartz grains, sandstone fragments (Figure 6.1b), rarely associated with small crystals of alkali feldspar (microclin-perthite) (Figure 6.1d), plagioclase, biotite, chlorite, white mica and opaque minerals. In some cases, ARF (argillaceous rock

fragments) and ochre fragments were also found (Figure 6.1a). Generally speaking, Mesolithic qtz-tempered pottery is characterized by large inclusions. Particularly interesting is the fact that pottery from Wadi Howar region contains also biological remains probably associated to chaff used as a temper and related to the nature of the environment on which the pottery was produced (Figure 6.1e and 6.1f). Also in the pottery from Al Khiday large pores formed from the decomposition of the chaff, but no type of vegetal remain was found in the studied samples. A finer paste characterizes Neolithic qtz-tempered pottery (Figure 6.2) where inclusions are smaller and porosity is mainly typical of medium to high-temperature firing (Figure 6.2a, 6.2b, 6.2d). Also Neolithic pottery from Wadi Howar shows biological remains that are well incorporated in the ceramic paste.

- *Kfs-tempered* (AK67, AK76, AK70, AK115, AK116, AK152, AK182, AK204, AK212, BN5, BN10): feldspar-rich potsherds are characterized by the presence of abundant inclusions of alkali feldspar (Figure 6.3a, 6.3e, 6.3f) (microclin-perthite, Figure 6.3c) associated with quartz, both angular in shape (Figure 6.3c, 6.3d); scarce crystals of plagioclase, biotite (Figure 6.3b), amphibole, clinopyroxene, chlorite and opaque minerals are also present.

Petrographic analysis has been used as a parameter to select the most suitable samples for the succeeding analysis. While concerning qtz-tempered sherds any selection was done by evaluating the c:f ratio, because of their similarities with clay samples, especially for Al Khiday, regarding the Kfs-tempered ceramics it has been possible to select ceramics with an adequate amount of clay matrix and large Kfs inclusions. This way the micro-drilling of the samples got easier and the necessary amount of matrix was extracted.

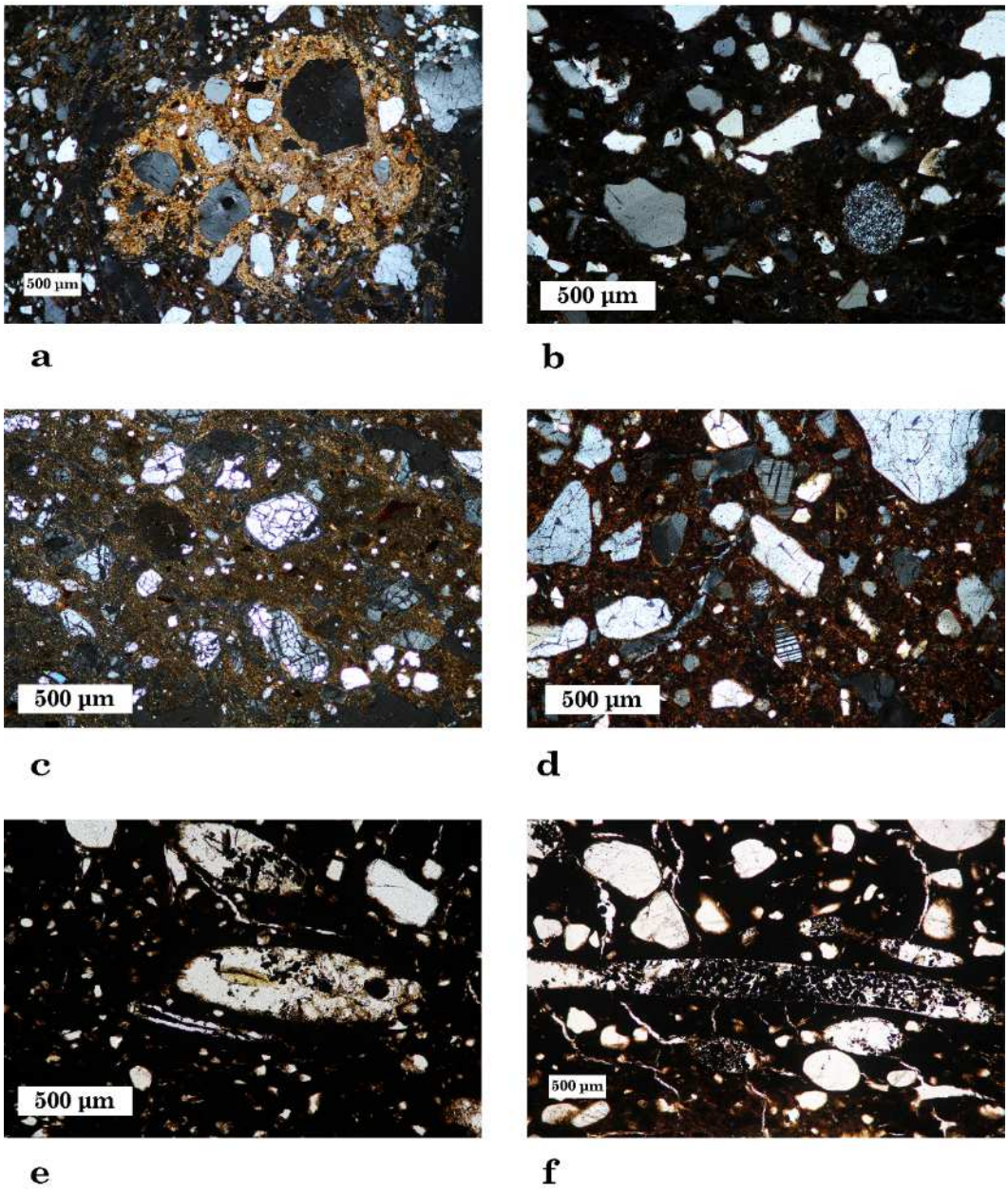

Figure 6.1: Mesolithic quartz-tempered pottery: a) AK73; b) AK102; c) AK136; d) AK198; e) WH24; f) WH25

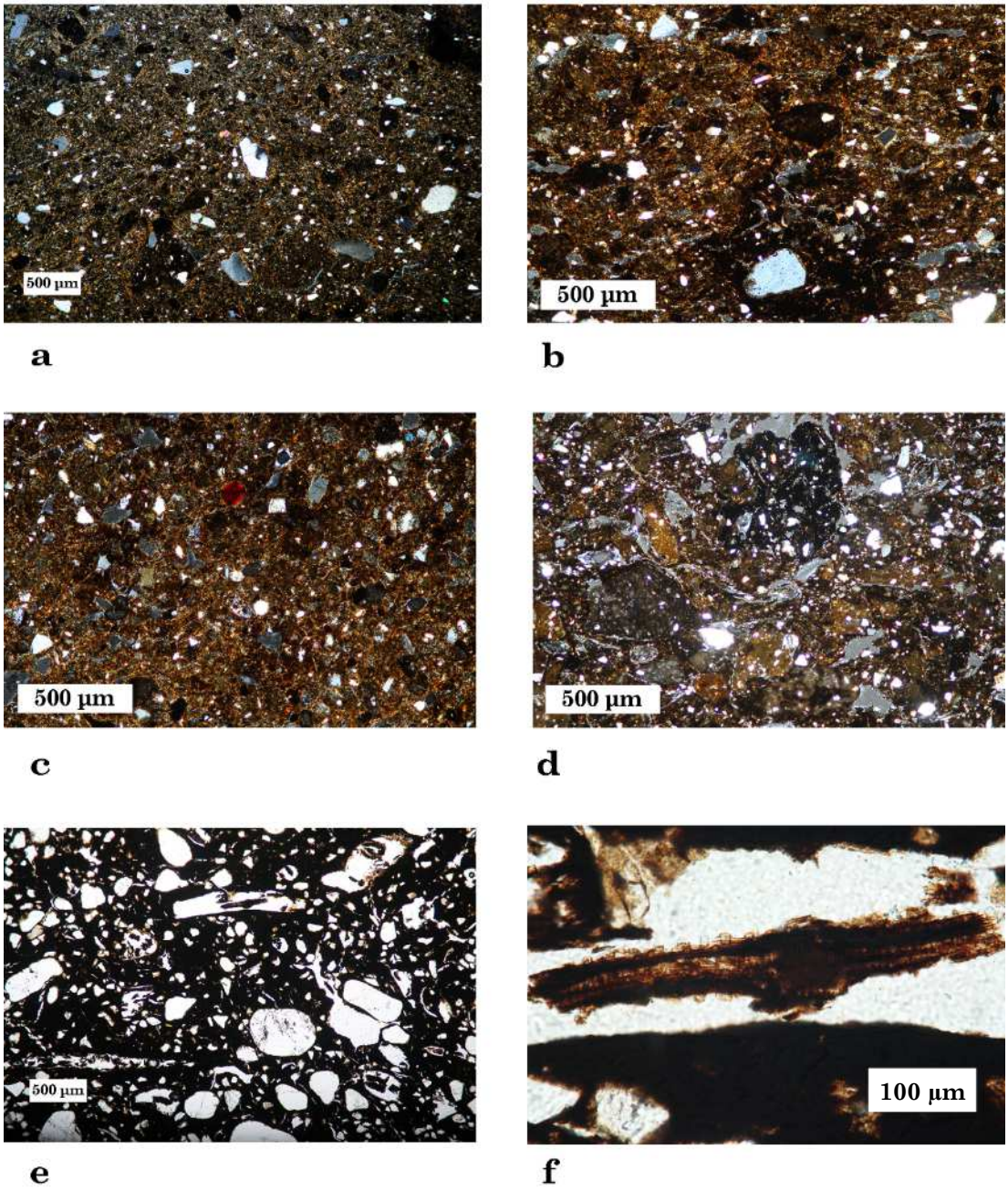

Figure 6.2: Neolithic quartz-tempered pottery: a) AK8, b) AK48; c) BN7; d) BN8; e) WH29; f) WH29

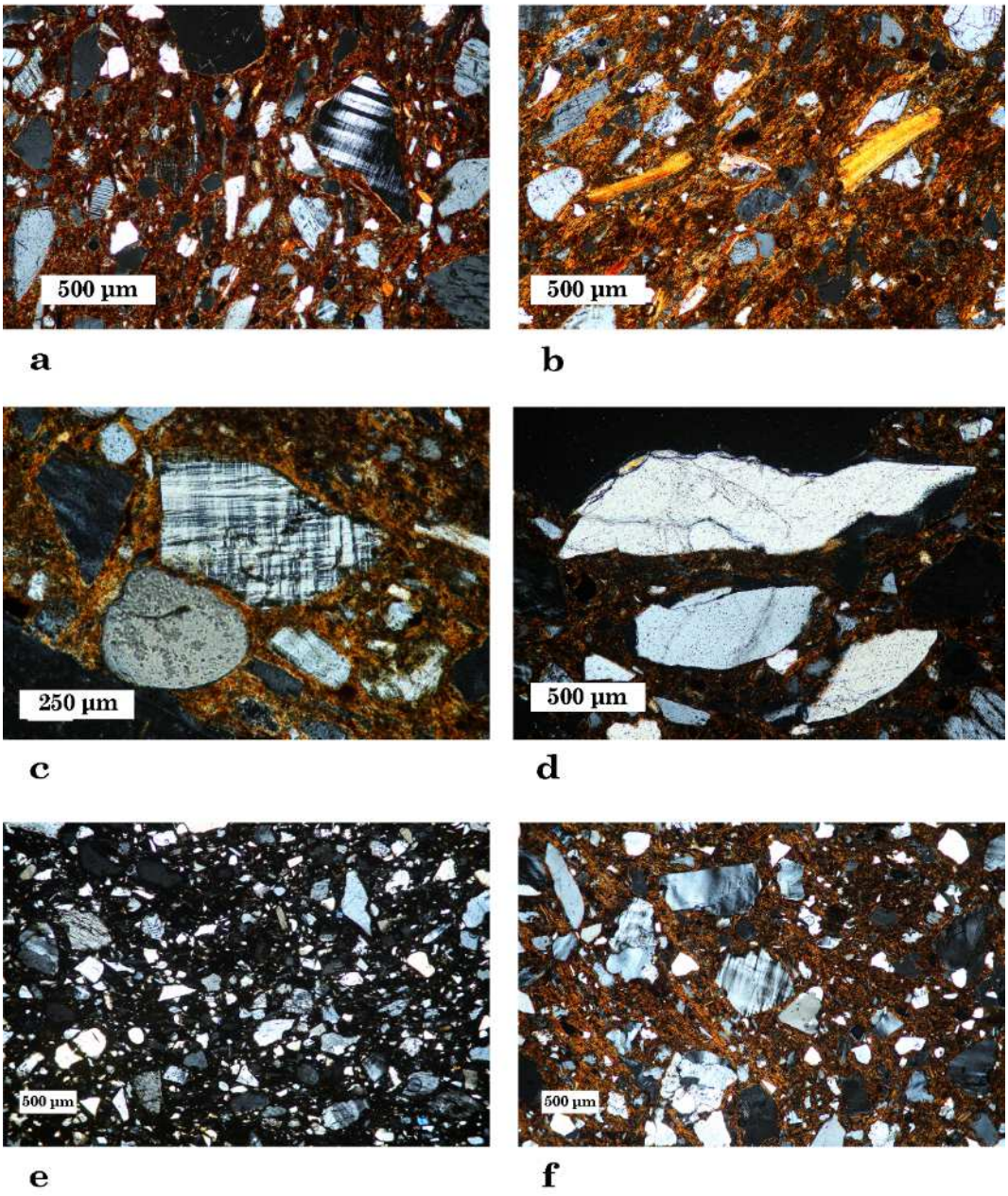

Figure 6.3: Mesolithic Kfs-tempered pottery: a) AK115; b) AK116; c) AK204; d) AK152; e) AK212; f) BN5

6.3 Chemical analysis and statistical treatment of data (XRF)

As previously mentioned, chemical composition has been explored using X-Ray Fluorescence Spectroscopy (XRF). Bulk chemical analysis was conducted on both qtz-

tempered and Kfs-tempered pottery. The first type of paste was grinded as is (see Paragraph 3.3) since the temper used does not contribute to the total amount of Sr. The second paste has been treated as described in Paragraph 3.3: in order to explore the provenance of the used clay without the contribution of Kfs grains, the clayey matrix has been extracted from the sherds using a micro-drill.

The preliminary chemical analyses were based on a descriptive approach on two variables procedures. The results are shown in the successive biplots.

As regards CaO versus SiO_2 content, it is possible to observe that all the pottery is low in CaO and it ranges from 1% to 3% (Figure 6.4). These values are compatible with clays collected along the White Nile. SiO_2 contents are moderately high especially in the Mesolithic pottery, while in the Neolithic pottery SiO_2 contents tend to decrease. The high SiO_2 contents should be related to the added sand-temper while, as regards Kfs-tempered pottery, SiO_2 values are lower because quartz is mainly related to the granite-like rock used as temper. Also ceramic samples from the two other region of interest (Wadi Soba and Wadi Howar) lie in the same region of Al Khiday samples and they show comparable contents of CaO and SiO_2 of the respective period of production.

Regarding the relation of CaO versus Sr, as seen for raw materials, there is a positive correlation between the two elements (Figure 6.5). From the diagram it is clear that the region of interest of clays is included between 1.33-3.41% of CaO and 175-207 ppm of Sr. Almost all of the pottery shows an enrichment in Sr content with respect to the raw materials. Early Mesolithic pottery seems not to convey the influence of this perturbation. Moreover, the two groups of data (pottery and raw materials) seem to show different ratios of CaO/Sr (trend lines in Figure 6.5) and this is not due to the added temper (SAND), since it has very low Sr content. The enrichment in Sr seems to be linked to some external factors. The Neolithic qtz-tempered pottery from Wadi Howar (WH29) is very poor in CaO and Sr and this might be due to the dilution effect caused by the abundant added temper (quartz). The other samples from both Wadi Soba area and Wadi Howar region are consistent with their contemporary samples from Al Khiday.

As regards Rb versus Sr (Figure 6.6), it is possible to notice that there is no correlation and no overlapping of pottery with Al Khiday clays. The high Rb content of Al Khiday clays is probably due to the presence of micas but only one sample of Neolithic pottery relates to these values. As regards pottery from Wadi Howar region, the samples show a low Rb content probably related to the geographical area of provenance. Wadi Soba samples, instead, show high Rb content, which is consistent with that of the Neolithic

samples, containing less quartz inclusions. Obviously, Kfs-tempered pottery is characterized by high Rb contents because of the presence of alkali feldspars (Figure 6.7). Kfs-tempered pottery from Wadi Soba area shows values of Rb/Sr compatible with those from the other sites.

In order to explore possible causes of the enrichment in Sr, its correlation with other elements has been explored. Firstly, since at the Al Khiday sites evidences of fish salting were proven (Maritan et al, submitted), the relation between Na_2O and Sr has been investigated for the studied potsherds. The biplots in Figure 6.8 shows that there is no correlation between the two elements because there is no correspondence between the age of the pottery and its Na_2O content and not even the more recent sherds are high in Na_2O. Therefore, it is possible to exclude that the Sr enrichment is related to the occurrence of halite on fish preserved or cooked in the pottery. We considered this possibility because Sr content in halite can be also very high and its possible presence would have affected the pristine Sr signature of the pottery.

Very interesting is to see that there is a positive correlation between Ba and Sr (Figure 6.9). Low Ba content is observed concerning the Early Mesolithic and Middle Mesolithic pottery and high Ba content for the Late Mesolithic and Neolithic samples, therefore the correlation roughly corresponds to the age of the ceramic. Moreover, clays of White Nile have low content of both Sr and Ba, very proximal to those observed for the oldest pottery. Apart from sample WH29 that is, as previously said, rich in SiO_2, all the other pottery from Wadi Howar shows Ba/Sr ratios comparable to the contemporary samples from Al Khiday. Also ceramic from Wadi Soba area shows values that are compatible with that of Al Khiday.

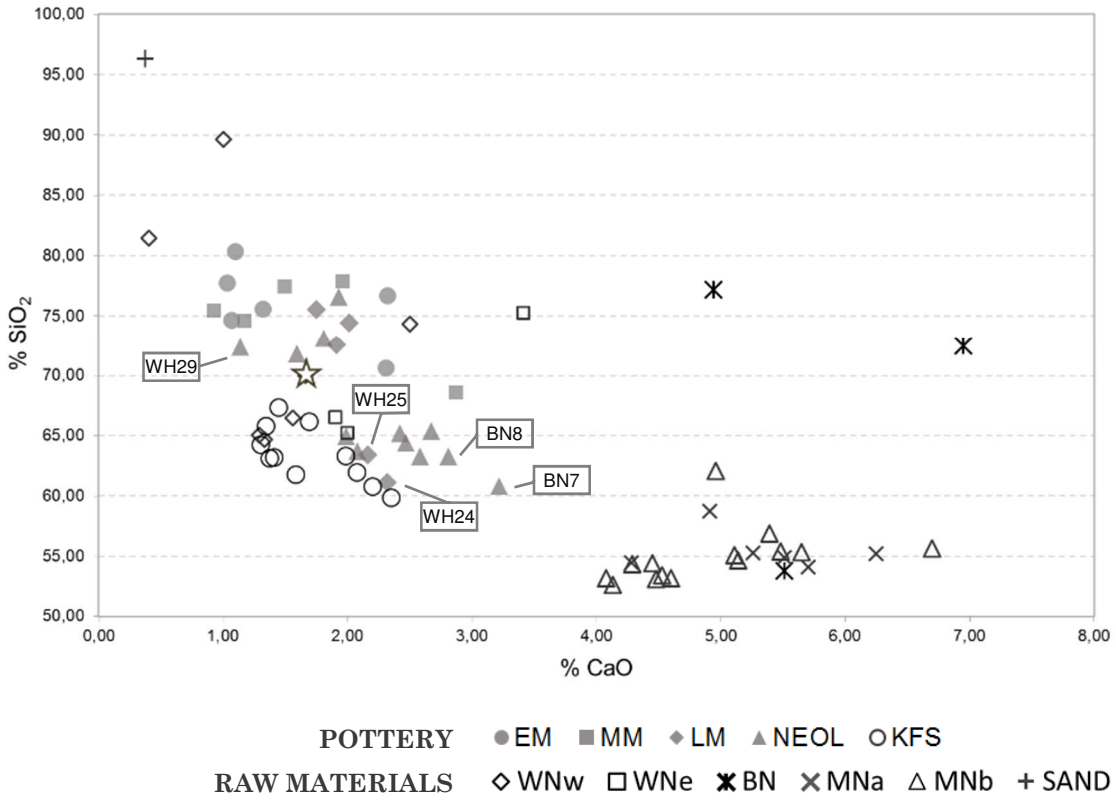

Figure 6.4: biplot of elemental concentration of CaO and SiO_2. The star indicates clay collected at Al Khiday (clay 1). Abbreviations: EM: Early Mesolithic; MM: Middle Mesolithic; LM: Late Mesolithic; NEOL: Neolithic; KFS: K-feldspar tempered pottery. WNw: White Nile western bank; WNe: White Nile eastern bank; BN: Blue Nile; MNa: Main Nile between Khartoum and Atbara; MNb: Nile after the Atbara confluence. Samples from the area of Wadi Howar (WH) and Wadi Soba (BN) are labelled

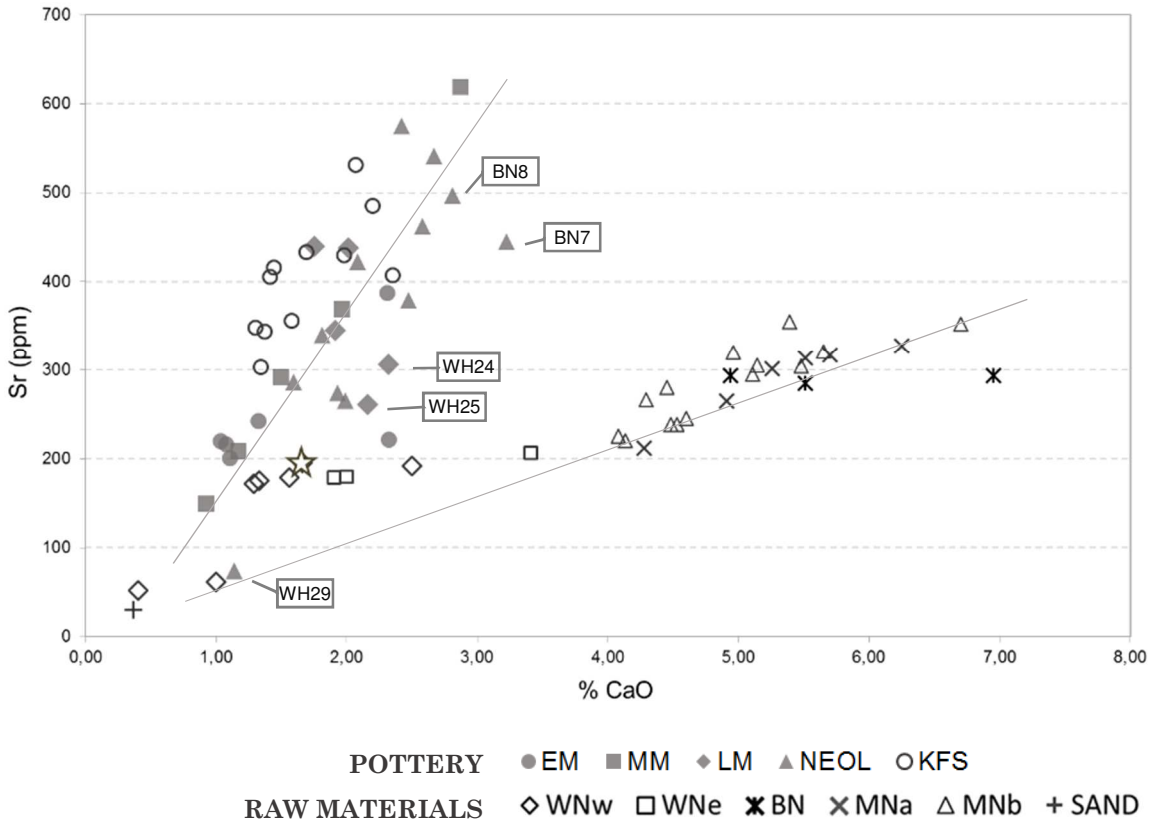

Figure 6.5: biplot of elemental concentration of CaO and Sr. The star indicates clay collected at Al Khiday (clay 1). Abbreviations as in Figure 6.4. Samples from the area of Wadi Howar (WH) and Wadi Soba (BN) are labelled

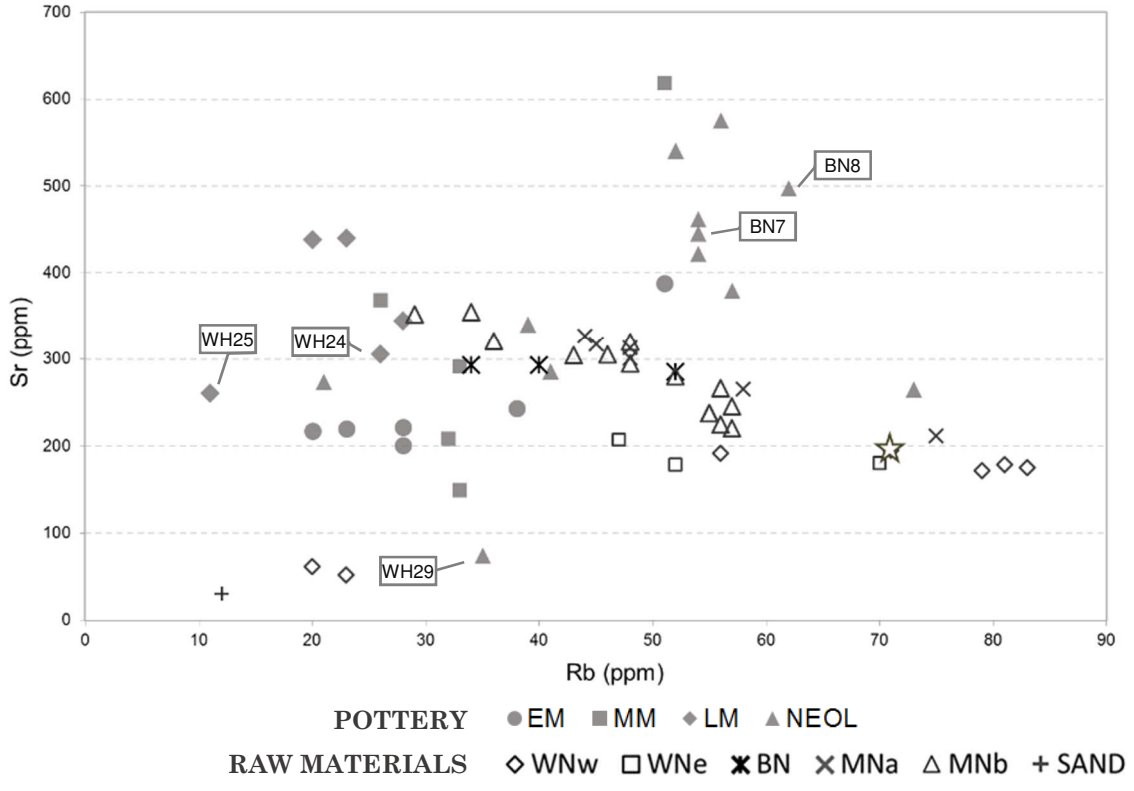

Figure 6.6: biplot of elemental concentration of Rb and Sr for quartz-tempered pottery. The star indicates clay collected at Al Khiday (clay 1). Abbreviations as in Figure 6.4. Samples from the area of Wadi Howar (WH) and Wadi Soba (BN) are labelled

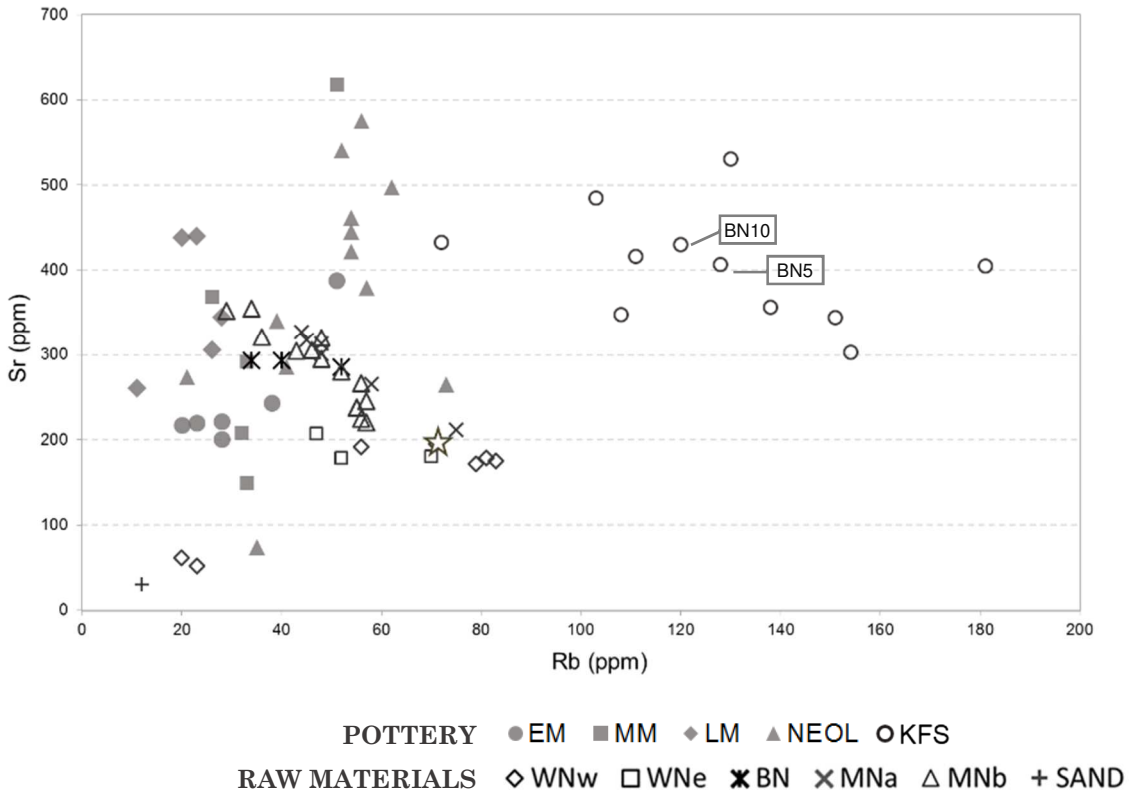

Figure 6.7: biplot of elemental concentration of Rb and Sr for Kfs-tempered pottery. The star indicates clay collected at Al Khiday (clay 1). Abbreviations as in Figure 6.4. Samples from the area of Wadi Soba (BN) are labelled.

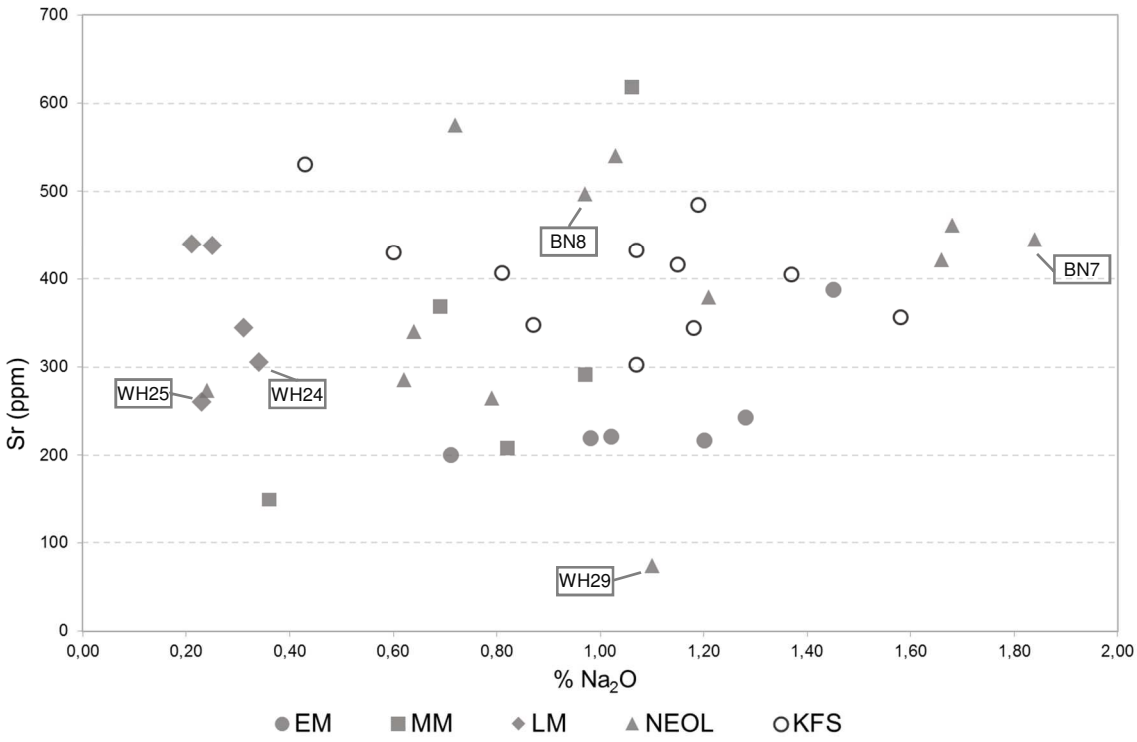

Figure 6.8: biplot of elemental concentration of Na_2O and Sr. The two variables seem to be independent. Abbreviations as in Figure 6.4. Samples from the area of Wadi Howar (WH) and Wadi Soba (BN) are labelled

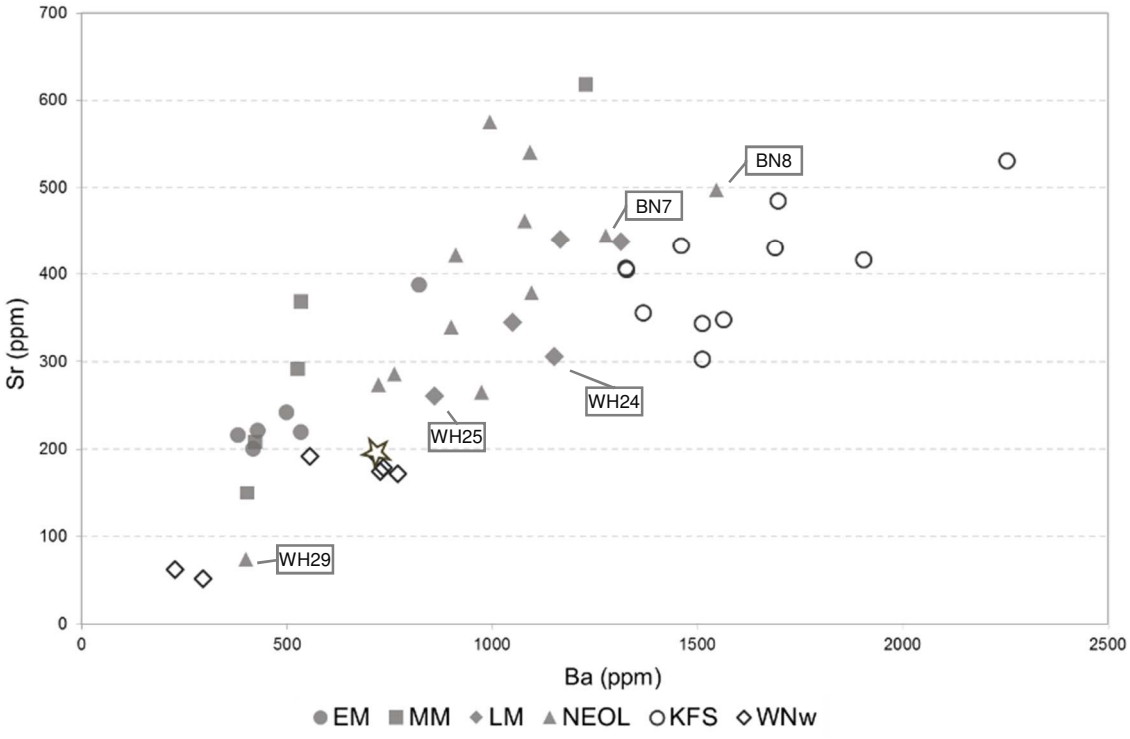

Figure 6.9: biplot of elemental concentration of Ba and Sr. Pottery contents are compared to WNw clay samples. The star indicates clay collected at Al Khiday (clay 1). Abbreviations as in Figure 6.4. Samples from the area of Wadi Howar (WH) and Wadi Soba (BN) are labelled

Multivariate statistical analysis was performed only on quartz-tempered pottery because the bulk chemical analysis of the Kfs-tempered sherds was altered by the presence of the temper. Compared to both the clay materials from the Nile and the quartz-tempered pottery, the rubidium content was too high (Figure 6.7). In order to bypass the problem regarding the other possible added temper (quartz), statistical analysis was carried out on trace elements divided by SiO_2 content (Figure 6.10). In fact, each vessel could have been made with a different mixture of clay and temper and this differentiation manifests in the SiO_2 content, which can vary from one artefact to another. Principal Component 1 explains almost 2/3 of the total variance. Although many Neolithic samples show positive values of PC1 and negative values of PC2, there are two of them that lie close to the Mesolithic ones. The situation regarding Mesolithic pottery is still not clear but almost all the Al Khiday samples (except for one Middle Mesolithic pottery) show negative values of Principal Component 1. Ceramic samples from other regions (WH24, WH25, WH29, BN7 and BN8) seem to lie in the external area of the diagram, denoting an interesting difference with Al Khiday pottery. Wadi Howar pottery (WH) is characterized by positive values of PC2 while Wadi Soba (BN) pottery shows negative values of PC2. The score plot of the principal component analysis (Figure 6.11) carried out on chemical clr-transformed data of raw materials and pottery, highlighted that 9/11 of the Early and Middle Mesolithic samples groups together (positive PC1 and PC2) while Late Mesolithic ceramic shows negative values of PC1 and PC2. Very interesting is to see that the pottery overlaps with the clay materials collected along the White Nile (WNe and WNw), and in some cases lies close to some of the Blue Nile ones. Again, as regards bulk chemical composition, Neolithic pottery from Wadi Soba area (BN) shows similar features to the other Neolithic samples from Al Khiday. Also Late Mesolithic pottery from Wadi Howar region (WH) seems to be very similar to Late Mesolithic pottery from Al Khiday. Sample WH29 groups well with Middle Mesolithic and Early Mesolithic pottery probably because of its high SiO_2 content. Since any pottery samples matches Main Nile values (neither MNa nor MNb), data points related to Nile are no longer considered. From the score plot in Figure 6.12 that shows the PCA

carried out on all the elements (major, minor and trace elements) without Main Nile values, it is clear that there is an overlapping of Early and Middle Mesolithic pottery with both WNe and WNw clay samples. The other clear correspondence regards Neolithic pottery and Al Khiday raw materials. Finally, Late Mesolithic pottery does not show any clear overlapping with the studied raw materials. In order to obtain a complete overview of the chemical system, statistical analysis was carried out also only on trace elements, excluding Main Nile clays (Figure 6.13). It is possible to notice that the situation approximately reflects the score plot in Figure 6.12. There is an overlapping of Neolithic pottery and Al Khiday and two of the Gezira clays. The correspondence between Early and Middle Mesolithic pottery and the other WNw and WNe clays persists. In the case of trace elements, Late Mesolithic samples from Wadi Howar region (WH24 and WH25) are better discerned (compare Figure 6.10 and 6.13). Trace elements seem to be a good method to discern Mesolithic pottery that shows a relatively low content in temper (quartz). All the other external samples are in agreement with Al Khiday values.

Therefore, neither bulk chemical composition nor trace elements are able to add useful information to this complex system and unfortunately, it is still not possible to identify clay sources.

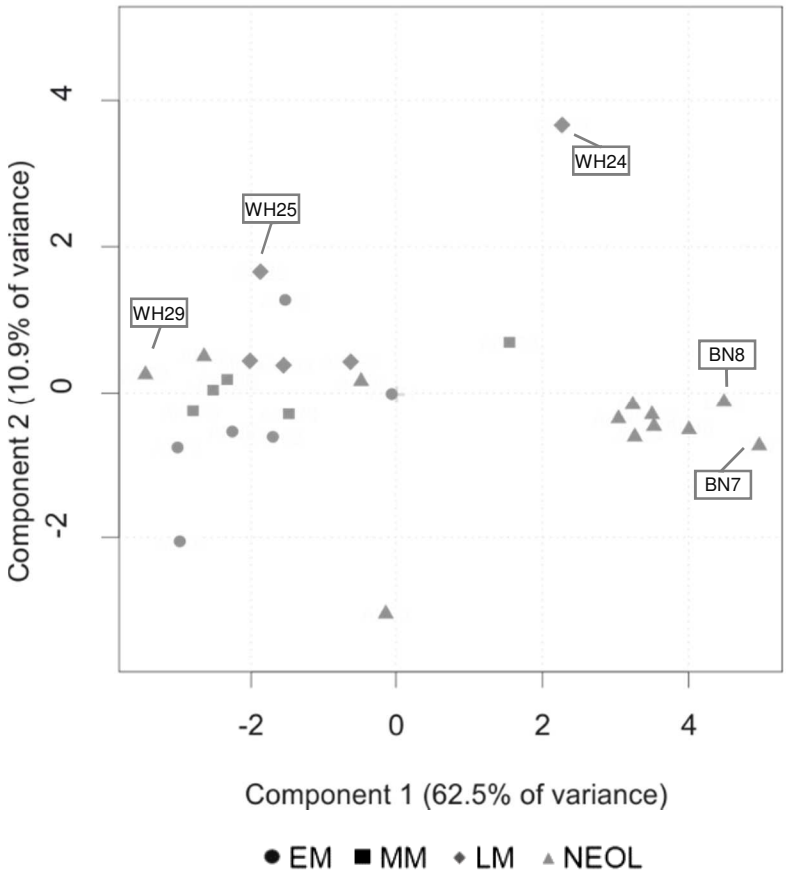

Figure 6.10: score plot of the Principal Component Analysis (PCA) on trace elements divided by the respective SiO_2 content. PC1 and PC2 explain 62.5 % and 10.9% of total variance, respectively. Abbreviations as in Figure 6.4. Samples from the area of Wadi Howar (WH) and Wadi Soba (BN) are labelled

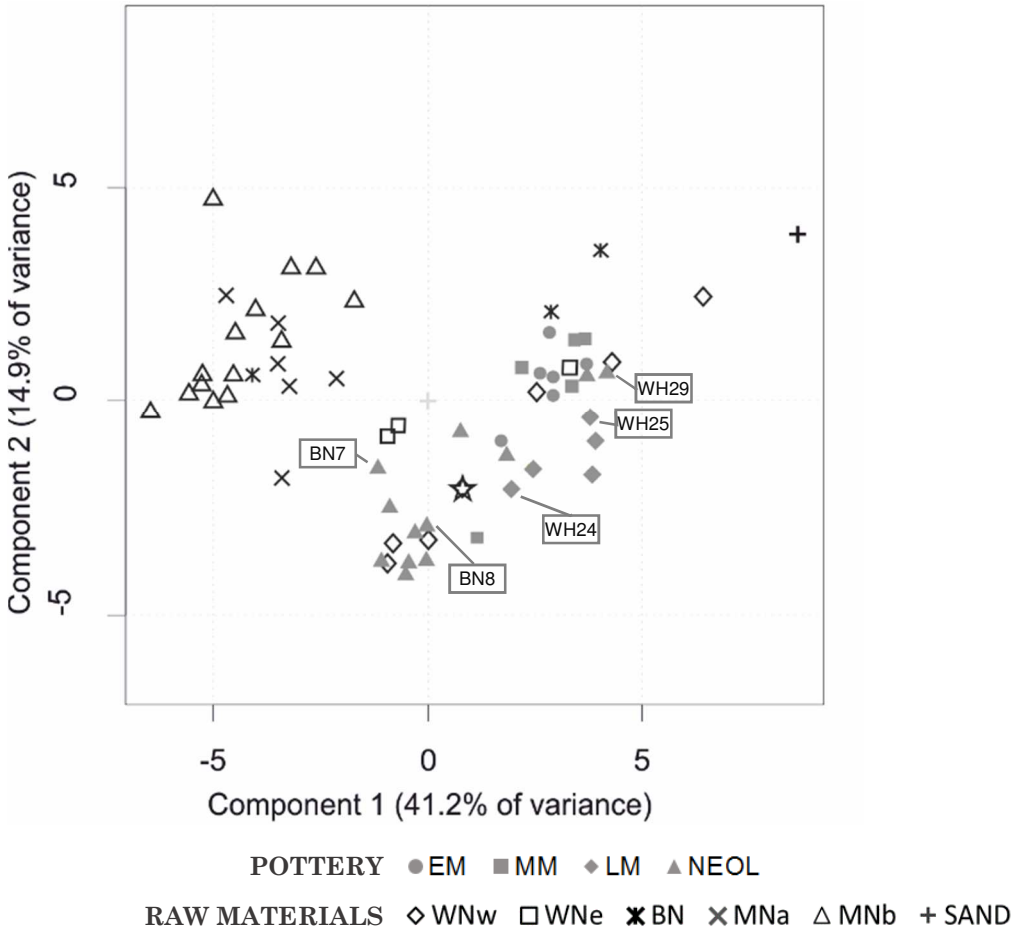

Figure 6.11: score plot of the Principal component analysis (PCA) of the chemical data of all the samples. The star indicates clay collected at Al Khiday (clay 1). PC1 and PC2 explain 41.2% and 14.9% of the total variance, respectively. Abbreviations as in Figure 6.4. Samples from the area of Wadi Howar (WH) and Wadi Soba (BN) are labelled

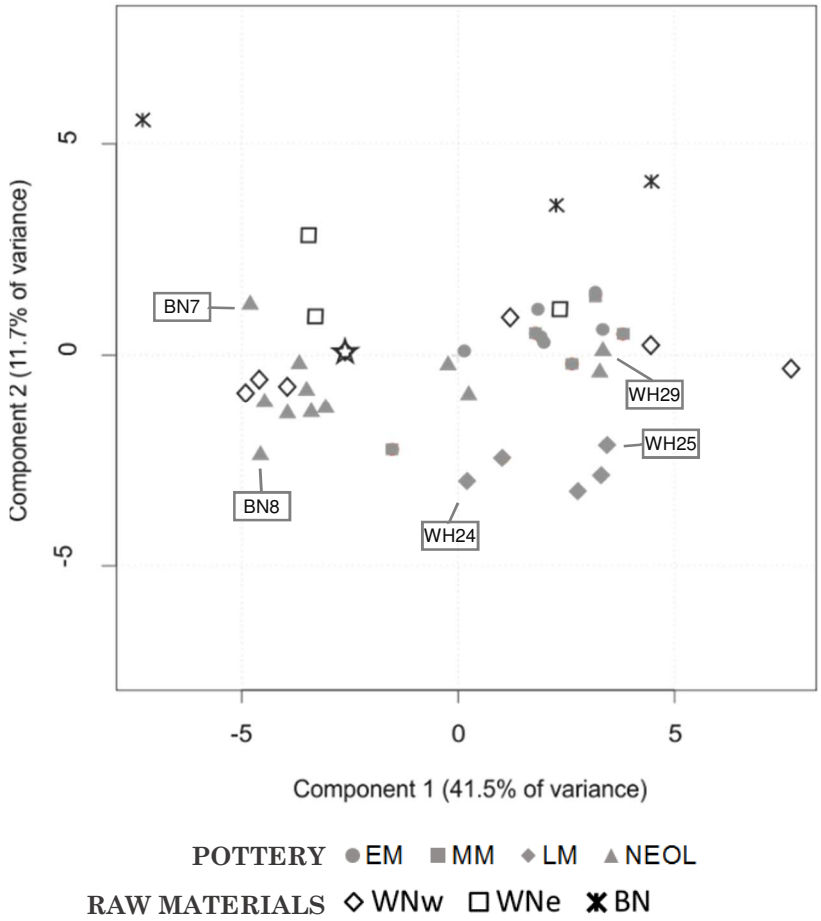

Figure 6.12: score plot of the PCA carried out on all the elements without the samples collected along the Main Nile (MNa and MNb). PC1 and PC2 explain 41.5% and 11.7% of the total variance, respectively. The star indicates clay collected at Al Khiday (clay 1). Abbreviations as in Figure 6.4. Samples from the area of Wadi Howar (WH) and Wadi Soba (BN) are labelled

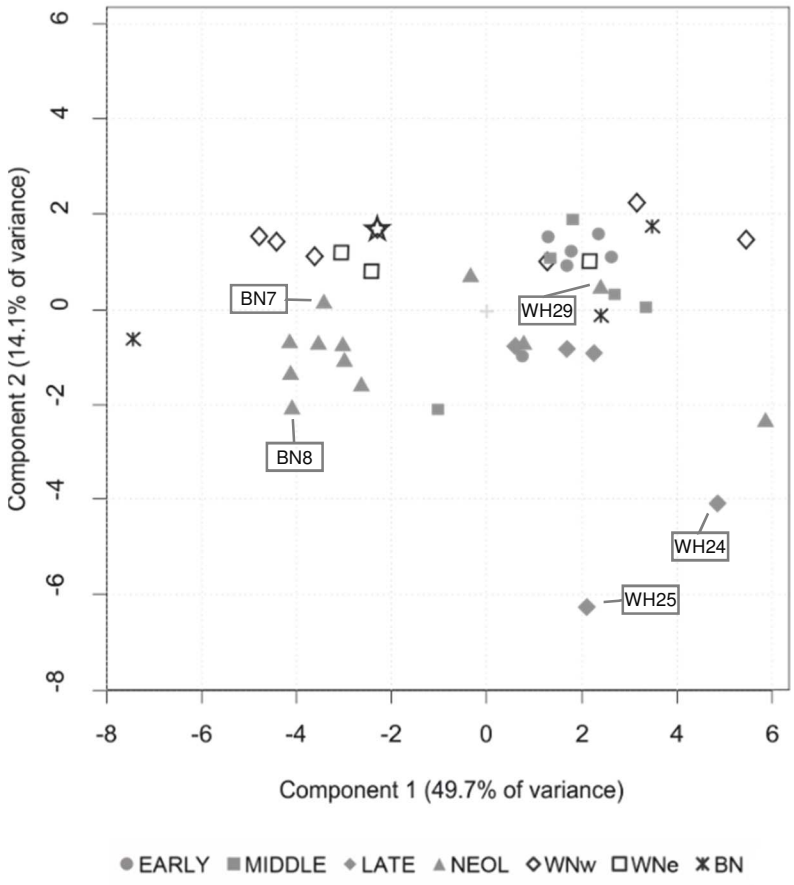

Figure 6.13: score plot of the PCA on trace elements without the samples collected along the Main Nile (MNa and MNb). PC1 and PC2 explain 49.7% and 14.1% of the total variance, respectively. The star indicates clay collected at Al Khiday (clay 1). Abbreviations as in Figure 6.4. Samples from the area of Wadi Howar (WH) and Wadi Soba (BN) are labelled

6.4 Microstructural analysis (SEM)

The microstructural analysis of pottery was addressed to collect information on texture and composition of the ceramic paste and on markers to constrain the provenance and any possible alteration process. In particular, possible occurrence of secondary phases as well as the microstructural diversity between the micromass of pottery produced according to different recipes were analysed.

As regards quartz-tempered pottery, BSE images highlighted several distinctive features of this paste (Figure 6.14). The large presence of rounded quartz grains, some ilmenite, zircon (Figure 6.14b) and ochre inclusions together with a scarce matrix, characterizes this pottery.

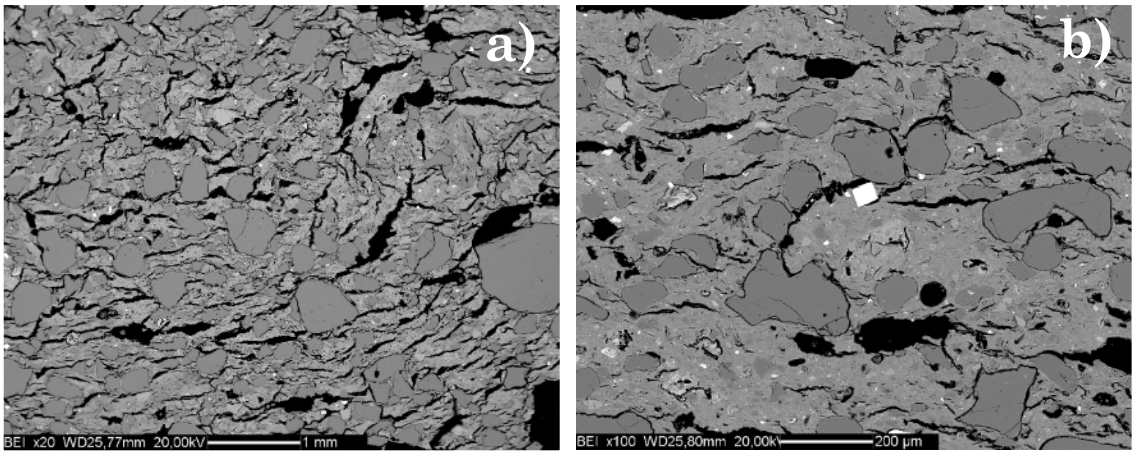

Figure 6.14: BSE image of quartz-tempered pottery: a) AK 165; b) AK 102, detail of a zircon (bright crystal at the center)

The second petrographic group is represented by Kfs-tempered pottery. It is important to highlight that in order to mechanically extract the clay from the sherds, samples with discernable matrix were chosen. Even if large areas of the paste are occupied by clay matrix and not by K-feldspar, in Figure 6.15 it is possible to observe that alkali feldspars are the main mineral phases of the coarse fraction in all samples. Abundant is also the presence of micas and sub-angular to angular quartz grains. However, the main feature of this ceramic paste is the presence of montmorillonite. As seen in Paragraph 5.5, montmorillonite is a common clay mineral that is mainly produced from the alteration of volcanic mafic rocks (Figure 6.16). The finding of such mineral in Kfs-tempered pottery together with its absence in qtz-tempered samples, opens the way for the formulation of some provenance hypothesis. As seen in Paragraph 5.5, montmorillonite was found only in clays collected after the confluence with Blue Nile and Atbara, while is absent in the sediments belonging to the banks of the White Nile. This correspondence heavily links the use of raw materials coming from MNa branch (between Khartoum and Atbara) to the production of K-feldspar-tempered pottery and strengthens the hypothesis that it was produced locally and then exported as a final product from one community to others. Furthermore, it is possible to develop another supposition. It being understood that the production of Kfs-tempered pottery was geographically limited to the area around Jebel Seleitat, where both raw materials were available, different groups of hunter-fisher-gatherers might take this opportunity to aggregate and share more than just "goods". That might have been the context for communal, opportunistic pottery production, in order to contribute to the diffusion of specific decoration motifs as a common meta-language. The importance of

manufacturing ceramic vessels together with different groups lay in the fact that it was a moment of socialization for the purpose of sharing social facts. As previously mentioned, Al Khiday is one of the locations where Kfs-tempered pottery has been found but alkali feldspar-bearing rocks outcrop far away from it. This information might provide an unexpected new perspective on long-range exchanges and relationships between hunter-gatherer-fisher groups in Central Sudan.

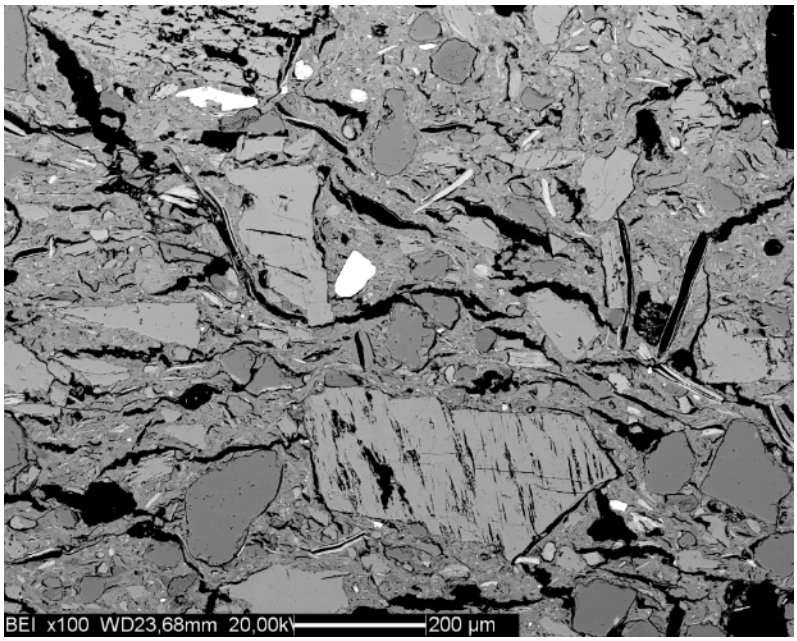

Figure 6.15: BSE image of Kfs-tempered pottery.

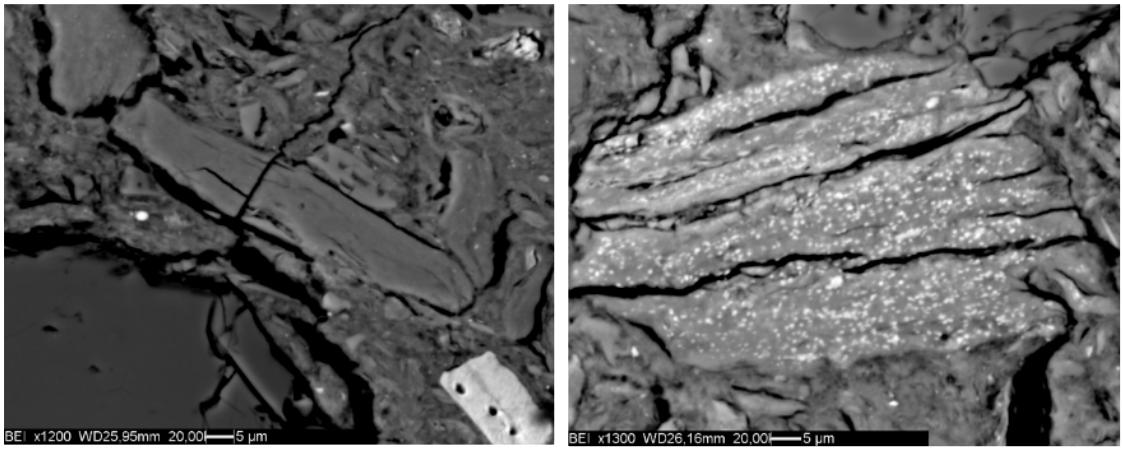

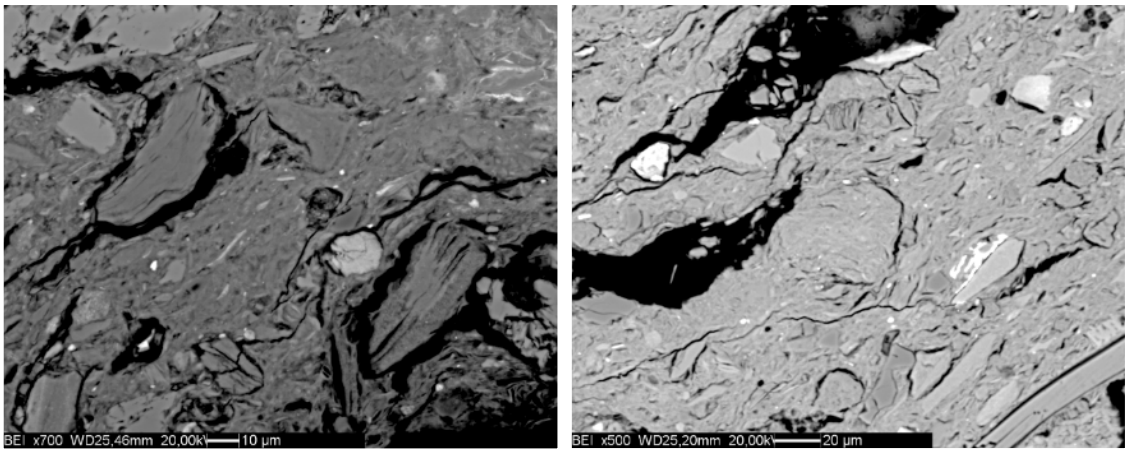

Figure 6.16: BSE images of montmorillonite-rich inclusion in Kfs-tempered pottery.

6.4.1 Secondary phases

A particular subset of quartz-tempered samples is formed by Late Mesolithic pottery found at site 10-W-4 (AK 196, AK 198 and AK 211). They are affected by the presence of secondary phases well recognizable in BSE images. The first phase has been identified as magadiite (Figure 6.17 and 6.18), a hydrous sodium silicate derived from a secondary precipitation of amorphous silica. The precipitation of amorphous silica can result from mineralization of preexisting organic matter, such as fragments of higher plants, membranes, and cell tissue (Sebag et al., 1999). Its general formula is $NaSi_7O_{13}(OH)_3 \cdot 4(H_2O)$. Micro-chemical analysis carried out at the SEM-EDS on a magadiite layer found in potsherd AK196 shows that it has a composition with oxides ratio nearly the same as the theoretical one (Table 6.1).

Magadiite formed in this potsherd a quite compact layer on the internal surface of the pottery and did not penetrate the internal pores. It is may be due to the fact that this mineral phase formed after an original organic residue present in the ceramic vase, which was probably related to the storage or consumption of food. Future analyses on possible phytolite remains (some traces seems to have been identified in Fig. 5.17 left) will be carried out by the CaSEs research team at the Department of Humanities, University Pompeu Fabra and IMF-CSIC, (Barcelona, Spain), coordinated by Marco Madella. This research will allow to identify the possible vegetal species or groups of plants from which this phytolites can come, therefore reconstructing the plants

exploited in the Mesolithic and contributing to what has been also defined for another site located at el Ghaba, north of Khartoum (Out et al., 2016).

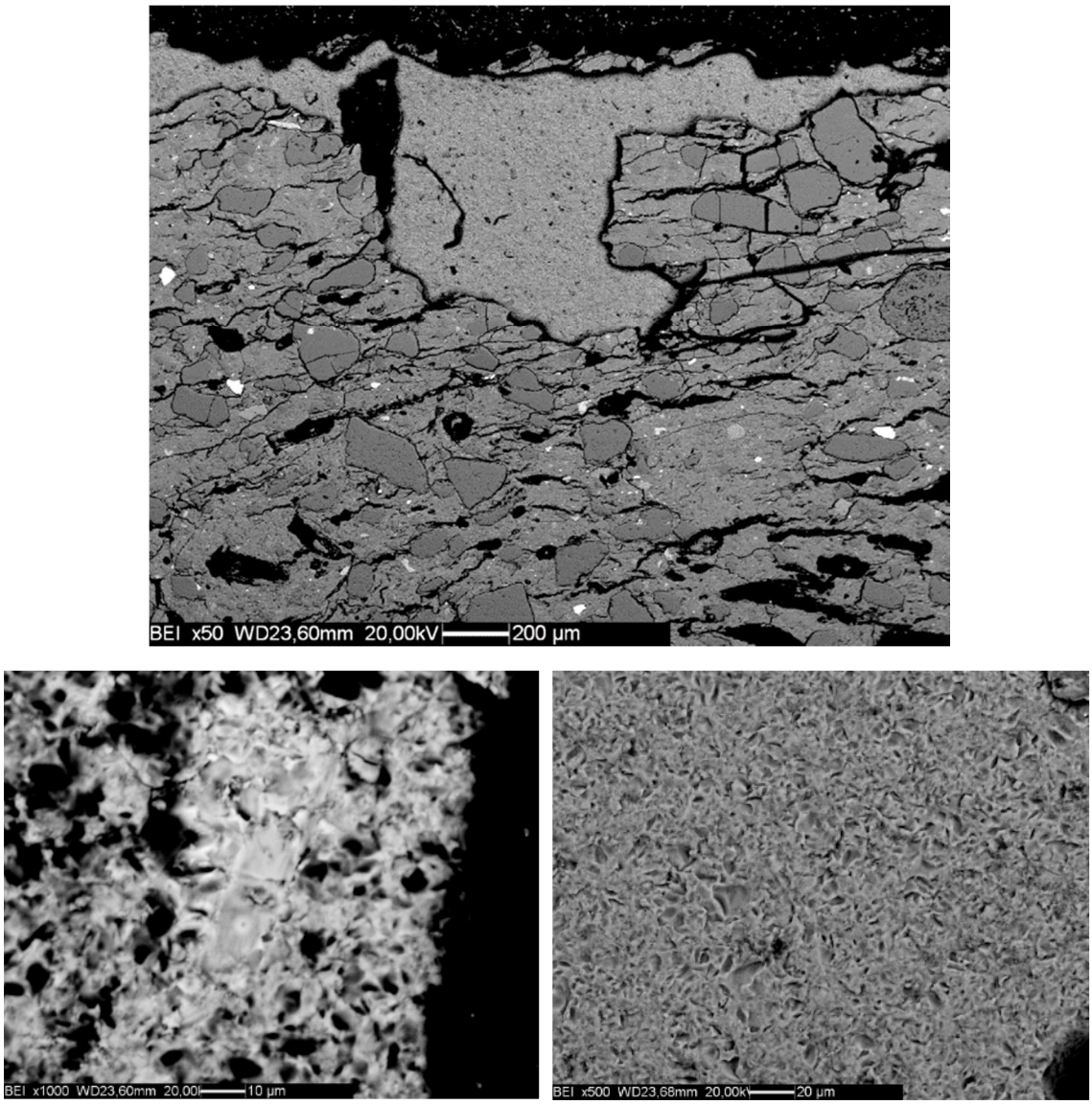

Figure Figure 6.17: BSE images of a fragment of magadiite layer in sample AK 196

Table 6.1: chemical composition of magadiite expressed in oxides wt% as reported in mindat.org and of that analysed in sample AK196 (PhiZAF Quantification, Standardless)

Element	Mindat	AK196
Na_2O	5.63	4.78
MgO		4.67
CaO		8.52
Al_2O_3		2.20
SiO_2	76.38	79.82

H_2O	17.99	
Total	100	100

The second phase that has been found in Late Mesolithic samples is crandallite, a phosphate mineral with the chemical formula $CaAl_3(PO_4)_2(OH)_5 \cdot (H_2O)$. It was observed in sample AK211 as a bright (see its chemical composition in Table 6.2) phase filling the ceramic porosity, especially in most of the outer voids, near the surface. Rodrigues and Costa (2016) highlighted that the formation of crandallite in archaeological ceramics might be facilitated by the presence of shell fragments used as a non-plastic material, which are substituted completely by crandallite during cooking. In other words, the shell might act as a catalyzer, and the sherds containing this material returns high levels of phosphates. Although at the moment we cannot reconstruct the process which determined the phosphate precipitation, it is quite interesting to notice that this phase was only detected in this sample and not in others, likewise to what observed also for other phosphate phases (mitridatite and vivianite) in ancient pottery in north-eastern Italy (Maritan and Mazzoli 2004; Maritan te al, 2009), for which local chemical-physical conditions affected only few samples.

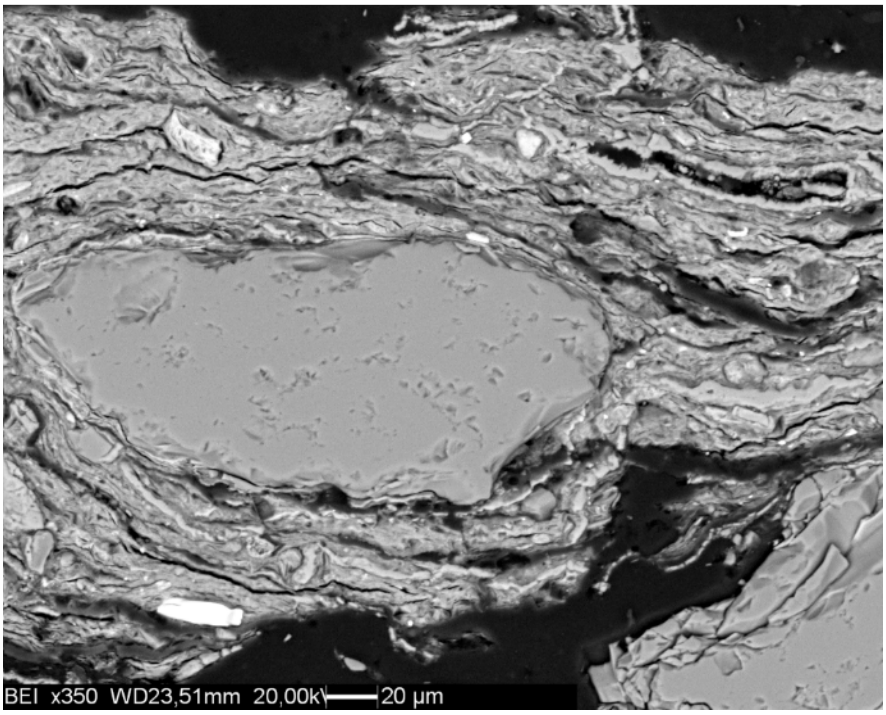

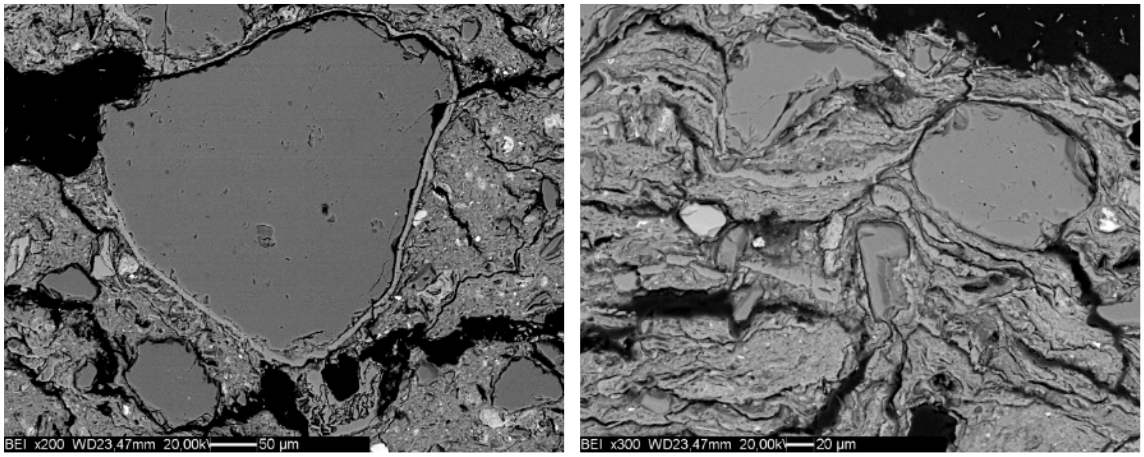

Figure 6.18: BSE images of crandallite in sample AK 211. It shows up like a light-coloured interstitial phase.

Table 6.2: chemical composition of crandallite expressed in oxides wt% as reported in mindat.org and of that analysed in sample AK211 (PhiZAF Quantification, Standardless)

Element	Mindat	AK211
CaO	13.54	14.26
Al_2O_3	36.94	43.94
P_2O_5	34.28	41.80
H_2O	15.23	
Total	100	100

6.4.2 Biological inclusions

The second subset of ceramic samples included pottery from both Wadi Soba area (BN7 and BN8) and Wadi Howar region (WH24, WH25, WH29). The main feature of these samples is the presence of silicified fragments of biological remains (probably Gramineae) very different in shape. In some cases, they show a circular shape (Figure 6.19a) while other remains have a more complex structure, from globular (Figure 6.19c) to reticulated (Figure 6.19d). The sizes vary from 10 µm to 200 µm according as the shape is simple or complex. Some samples seem to contain these biological remains inside the matrix (Figure 6.19a,b), as if they were part of the used base-clay. Other

fragments of biological remains lie inside the voids (Figure 6.19c,d) as if they were part of the temper (*chaff*). The inclusions inside the voids appear to be flaked but this could be due to both the sample preparation and the use of the original pot.
Also in this case, the collaboration with the CaSEs research team will allow to define which type of plants populated those regions. Very interestingly, the pottery from Al Khiday did not show any evidence of biological remains, neither as natural component of the used base-clay.

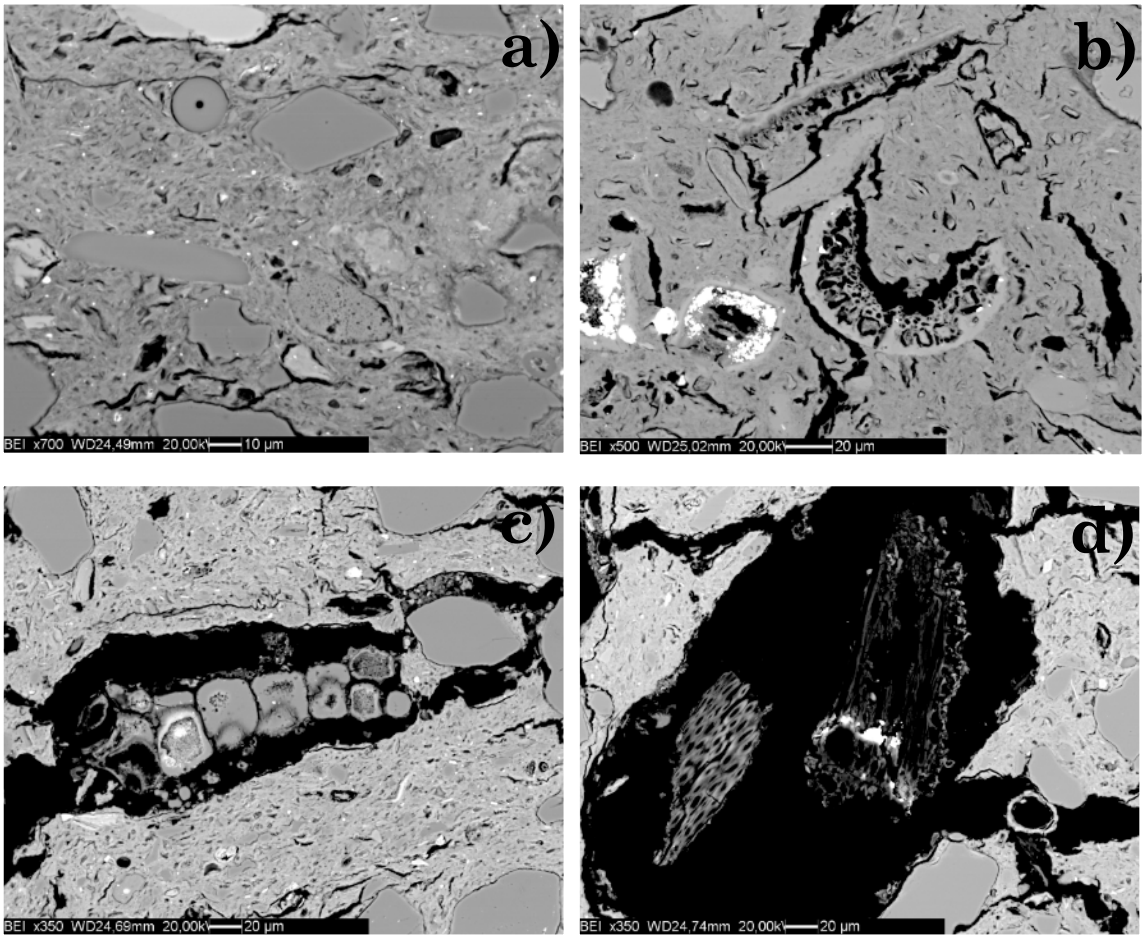

Figure 6.19: BSE images of silicified biological inclusions in Late Mesolithic pottery. a) circular silicified biological remain, BN7; b) slice-shaped silicified biological remain, WH25; c) globular-shaped silicified biological remain, WH29; d) flaked reticular silicified biological remain, WH29

6.5 Sr isotope analysis (TIMS)

Strontium isotopic signature of pottery depends on Sr isotopic compositions of different mineralogical reservoirs of Sr. The contribution of each reservoir is given by both the Sr concentration in the clay mineral and its abundance in the ceramic. Since clay minerals are not the only components in ceramic paste, it is important to evaluate the presence of Rb- and Sr-bearing minerals in the coarse fraction of the paste, in order to understand the significance of the Sr isotopic composition of a ceramic, especially when tempered. If the coarse fraction is composed merely of quartz (SiO_2), which does not contain significant amounts of Rb or Sr, the Sr isotopic ratio of the ceramic is derived almost entirely from the clay fraction.

In Table 6.3 are listed the measured Sr isotopic ratios of quartz-tempered pottery, in Table 6.4 are presented $^{87}Sr/^{86}Sr$ ratios of the matrix mechanically separated of Kfs-tempered pottery and in Figure 6.20 values of $^{87}Sr/^{86}Sr$ ratios are represented in a diagram. Observing Sr concentration values and Sr isotopic ratios of Kfs-tempered pottery matrix, it is clear that the clayey matrix mechanically extracted from these sherds is not representative of the used base-clay because it is enriched in Sr and its Sr isotopic ratios are too high, when compared with those of the qtz-tempered pottery. Moreover, none of the clays that lie close to the Kfs source (MNa clays) show Rb contents as high as those of the matrix collected from Kfs-tempered pottery (see Figure 6.7). Bulk chemical analyses were carried out on Kfs-tempered pottery and the comparison between Sr concentration obtained by XRF and that measured by IDMS (Isotopic Dilution Mass Spectrometry) is reported in Table 6.5. The deviation ranges from 0.67% to a maximum of 18.06%, which would be a very narrow interval if the analysed samples would be typologically different. The strong correspondence of Sr concentrations between bulk and matrix analyses indicates that the mechanical separation of clayey matrix failed; therefore, it is necessary to find other solutions in order to measure the $^{87}Sr/^{86}Sr$ ratios of samples containing Sr-bearing mineral phases. For this reason, the $^{87}Sr/^{86}Sr$ ratios of clay matrix extracted from Kfs-tempered pottery are no longer considered for the succeeding evaluations.

Table 6.3: Sr isotopic data of the quartz-tempered pottery samples. Abbreviations: EM: Early Mesolithic; MM: Middle Mesolithic; LM: Late Mesolithic; NEOL: Neolithic

SAMPLE ID	SITE	$^{87}Sr/^{86}Sr$	error	Sr (ppm)	AGE
AK102	16-D-5	0.708807	2.2E-05	220	EM
AK73	16-D-5	0.708562	3.7E-05	201	EM
AK136	16-D-5	0.708438	2.2E-05	369	MM
AK165	16-D-5	0.708978	1.1E-05	150	MM
AK170	16-D-5	0.707363	2.4E-05	209	MM
AK196	10-W-4	0.708109	1.6E-05	345	LM
AK198	10-W-4	0.708133	1.7E-05	438	LM
AK211	10-W-4	0.708131	1.3E-05	440	LM
WH24	Ennedi Erg	0.709865	2.1E-05	306	LM
WH25	Ennedi Erg	0.709391	1.9E-05	261	LM
AK46	16-D-5	0.709025	3.5E-05	462	NEOL
AK48	16-D-5	0.70917	2.6E-05	379	NEOL
AK8	16-D-5	0.70876	1.7E-05	541	NEOL
BN7	Soba-2	0.706843	2.0E-05	445	NEOL
BN8	Soba-2	0.708344	1.9E-05	497	NEOL
WH29	Ennedi Erg	0.711126	1.3E-05	74	NEOL

Table 6.4: Sr isotopic data of the matrix mechanically separated from Kfs-tempered pottery samples. Abbreviations as in table 6.3. MESO=Mesolithic (unspecified) are referred to samples form the Soba area, eastern of the blue Nile.

SAMPLE ID	SITE	$^{87}Sr/^{86}Sr$	error	Sr (ppm)	AGE
AK70	16-D-5	0.710443	0.000041	433	EM
AK115	16-D-5	0.715172	0.00002	303	MM
AK116	16-D-5	0.716197	0.000024	405	MM
AK152	16-D-5	0.712557	0.000023	416	MM
AK204	10-W-4	0.714906	0.000012	531	LM
AK212	10-W-4	0.711348	0.000027	485	LM
BN5	Sheikh Mustafa	0.712269	0.000031	407	MESO
BN10	Al Mahalab	0.713456	0.000016	430	MESO

Table 6.5: comparison between Sr concentration measured by IDMS technique (Isotopic Dilution Mass Spectrometry) and by XRF (X-Ray Fluorescence)

SAMPLE ID	IDMS on matrix		XRF on bulk	Deviation
	Sr (ppm)	Er ass	Sr (ppm)	
AK70	435.913	1.802	433	0.67%
AK115	340.787	1.327	303	11.09%
AK116	452.741	1.767	405	10.54%
AK152	507.718	1.970	416	18.06%
AK204	453.596	1.739	531	17.06%
AK212	416.422	1.626	485	16.47%
BN5	419.399	1.636	407	2.96%
BN10	400.148	1.601	430	7.46%

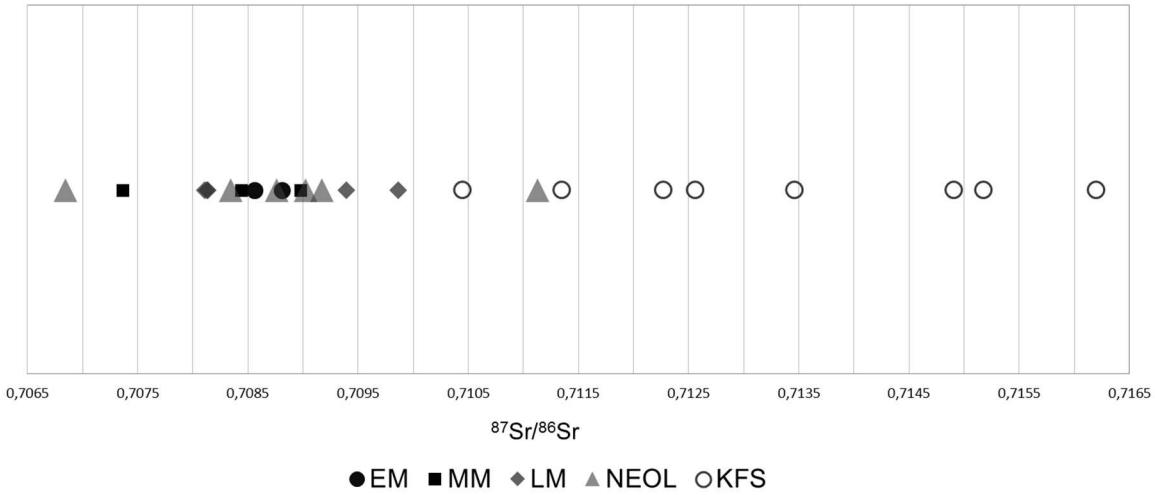

Figure 6.20: diagram of the $^{87}Sr/^{86}Sr$ ratios of pottery samples. Both quartz-tempered (filled symbols) and Kfs-tempered (empty symbols) values are shown.

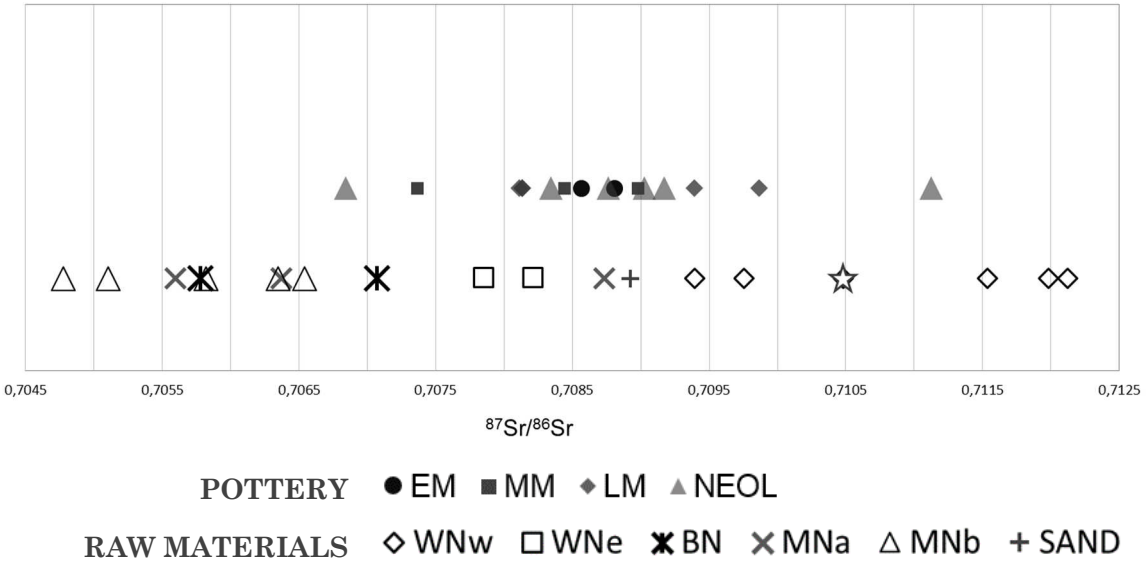

Figure 6.21: diagram of the $^{87}Sr/^{86}Sr$ ratios of quartz-tempered pottery samples versus clay samples. Abbreviations: EM: Early Mesolithic; MM: Middle Mesolithic; LM: Late Mesolithic;

NEOL: Neolithic; KFS: K-feldspar tempered pottery. WNw: White Nile western bank; WNe: White Nile eastern bank; BN: Blue Nile; MNa: Main Nile between Khartoum and Atbara; MNb: Main Nile after the Atbara confluence

As regards quartz-tempered pottery, $^{87}Sr/^{86}Sr$ ratios as a function of Sr concentration are shown in Figure 6.22. $^{87}Sr/^{86}Sr$ ratios of Early Mesolithic pottery range from 0.7085 to 0.7088 and are similar that of the SAND collected *in situ* (0.708924) at Al Khiday. These values are comparable with White Nile values (eastern bank) also as regards Sr content. Middle Mesolithic pottery shows a wide variety of $^{87}Sr/^{86}Sr$ ratios and two samples have a Sr content comparable with that of the White Nile clays. Late Mesolithic pottery maintains a surprising constant $^{87}Sr/^{86}Sr$ ratio but shows an evident increase in Sr content, reaching values unrelated with any of the analysed clays (Sr ppm = 440).

Concerning Neolithic pottery, its Sr isotopic ratios are comparable with that of the White Nile clays but it is particularly enriched in Sr. The exceptions regard one sample that shows high Sr isotopic ratio and low Sr content (WH29) and another sherd which shows low $^{87}Sr/^{86}Sr$ ratio and high Sr content (BN7), both coming from other site than Al Khiday: the former from the area of Wadi Howar and the second from that of Soba, eastern of the Blue Nile.

Sr isotopic ratios of samples from Wadi Howar region (WH24, WH25, WH29) are generally higher than Mesolithic and Neolithic samples from Al Khiday and this is probably due to the fact that raw materials used to produce this pottery belong to a different region in terms of mixture of sediments which, near the site of Ennedi Erg, were influenced only by the flow of Wadi Howar. Unfortunately, because of the absence of raw materials coming from that region, it is difficult to make interesting comparisons.

It is possible to observe that the enrichment in Sr follows a sort of chronological trend that starts from not-enriched Early Mesolithic samples and ends up to highly-enriched Neolithic samples. Also Neolithic samples from Wadi Soba area show an enrichment in Sr content. Moreover, all the $^{87}Sr/^{86}Sr$ ratios of the more recent ceramics seem to lie around a small interval of Sr isotopic ratios that are represented in Figure 6.22 by a grey bar. This bar represents the range of Middle Holocene Sr isotopic ratios measured by Talbot et al. (2000) along the White Nile, near Shabona (100 km south of Al Khiday) (see Figure 6.23). On the base of these measurements, strontium isotope signature of Nile's water at the Mesolithic and Neolithic periods was similar to that of the

sediments close to the modern confluence. The variability of Sr isotope ratios of qtz-tempered pottery is much smaller than that of raw materials'. Together with Sr enrichment, this may be a tangible clue of contamination.

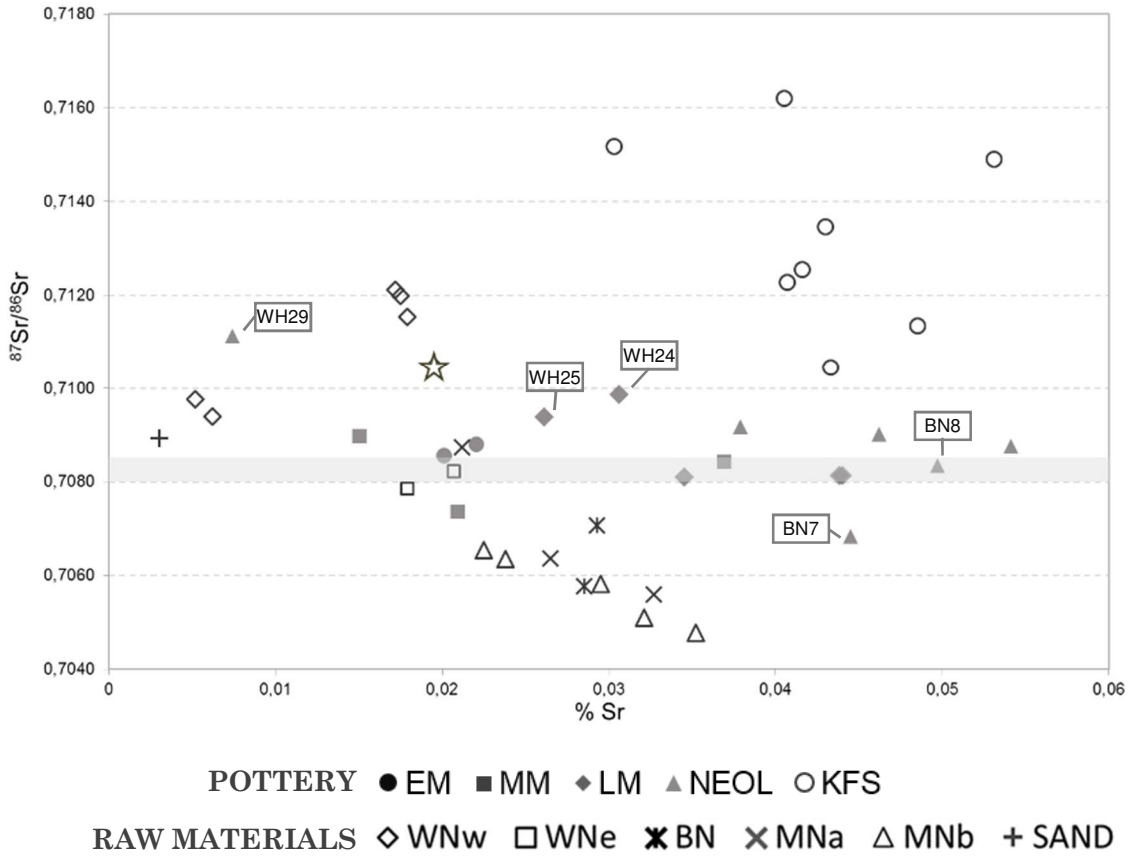

Figure 6.22: strontium concentration versus strontium isotope ratios in qtz-tempered pottery and in Nile clays and Al Khiday sand. Abbreviations as in Figure 6.21. Samples from the area of Wadi Howar (WH) and Wadi Soba (BN) are labelled

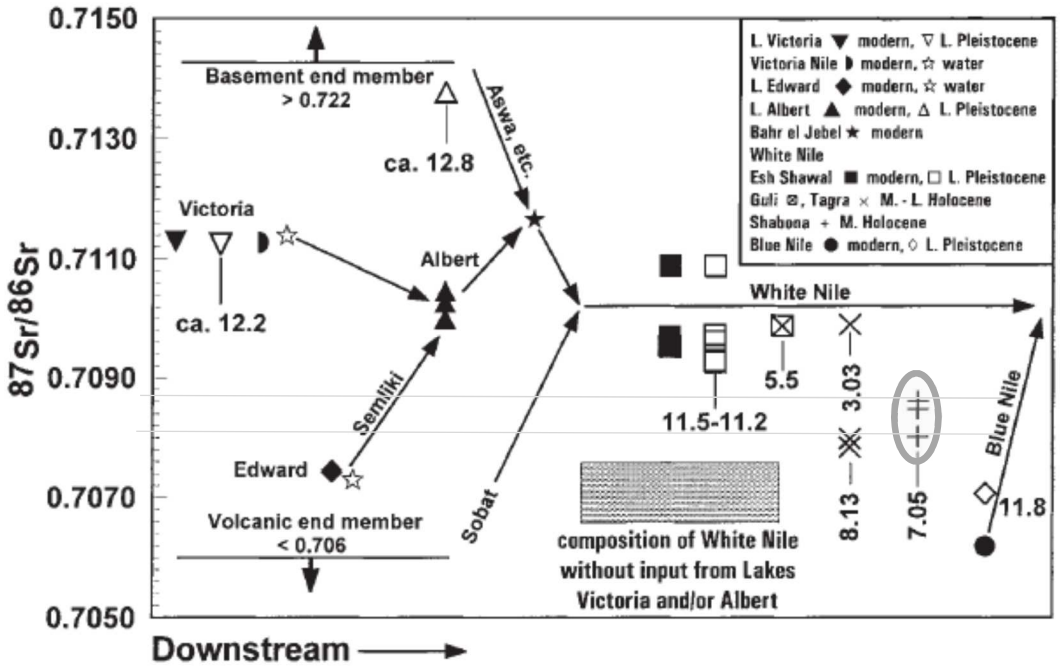

Figure 6.23: Schematic longitudinal profile (variable horizontal scale) along Upper Nile–White Nile from headwater lakes to Khartoum, summarizing Sr isotope composition of main components of drainage system (from Talbot et al., 2000). Long arrows are main water courses. Circled values correspond to the Middle Holocene $^{87}Sr/^{86}Sr$ ratios of the White Nile (from fossils of permanent water species)

6.6 Discussion and conclusion

The multianalytical approach applied in this study allowed the comparison of the main features of both raw materials and archaeological ceramics.

As regards petrographic analysis, it was possible to distinguish two petrographic groups as highlighted by Dal Sasso et al. (2014). The main differences lie in the type of inclusions (quartz and K-feldspar) but also the presence of biological silicised inclusions helps to discriminate pottery found at Al Khiday from pottery coming from the other archaeological sites of interest. In fact, all the pottery from both Wadi Soba area and Wadi Howar region is characterized by the presence of biological remains that were punctuated also by microstructural analysis. SEM-BSE images highlighted that these peculiar inclusions vary in shape and size but they are most likely attributable to the Family of Gramineae grasses.

As regards the microstructural analysis of the ceramic micromass, a surprising feature of Kfs-tempered pottery was observed: nearly all the samples characterized by this paste show the presence of montmorillonite-rich aggregates inside the matrix. On the contrary, they are always absent in qtz-tempered pottery. Therefore, a fundamental correspondence between Kfs-tempered pottery and clays collected along the Main Nile (MNa and MNb) exists. This symmetry might indicate that Kfs-tempered pottery was produced using raw materials coming from Main Nile "a" (MNa) / Main Nile "b" (MNb) clays. Since it seems unlikely that prehistoric populations might had the need to transport clay that was clearly easily accessible as well as K-feldspar (temper) to produce this pottery, K-feldspar-tempered pottery was probably produced along the MNa branch and then exchanged among groups. Therefore, it may be considered as an imported product at Al Khiday. Otherwise, the opportunity to exploit local raw materials for making pottery was associated to an important moment of socialization. Different groups of hunter-fisher-gatherers were probably used to meet in geographic places with symbolic meanings in order to share social facts reflected for example in the use of different decorations.

As regards chemical analyses, it has been highlighted that all the pottery shows a low content in CaO and contents in SiO_2 that vary from nearly 60% to 80%, the latter connected with the added temper (sand). The positive correlation between CaO and Sr observed in the samples is also typical of the pottery, but this latter shows a consistent enrichment in Sr. Since by petrographic and microstructural analyses it has been highlighted the absence of carbonates, Sr is not contained in these Ca-bearing minerals. For this reason, other possible sources of contamination were explored. Firstly, since halite, a possible carrier of high Sr concentration, was detected in fish bones as a record of fish salting and storage (food conservation) (Maritan et al., submitted), the relation between Na_2O and Sr has been studied. The two elements seem to be independent thus it is possible to exclude this cause. Moreover, the correlation between the Sr and Ba content in the pottery indicates that the possible contaminant was carrying both these elements. Quite interestingly, Early Mesolithic and Middle Mesolithic pottery seems to be less involved into this enrichment than Late Mesolithic and Neolithic samples. Bulk chemical features of pottery from Wadi Soba area and Wadi Howar region are comparable with those of Al Khiday ceramic. They are rarely discernable, except for statistical analyses on trace elements that highlighted the possible presence of some markers able to separate especially pottery from Wadi Howar region.

As for the Sr isotope ratio of Kfs-tempered pottery, it was clear from the start that Sr concentrations and its Sr isotopic ratios were too high compared with those of the qtz-tempered pottery. Thus, clayey matrix mechanically extracted from these sherds was not representative of the used base-clay since it was enriched in Sr. For this reason, this type of paste has been not included in the succeeding analyses. Nevertheless, petrographic and microstructural data gave a credible overview of the places involved in the production and suggested long-range exchanges, which seem to explain possible movements of materials as well as potential sharing of social facts along the Nile River in Central Sudan.

Concerning qtz-tempered sherds, Early Mesolithic pottery resulted in having $^{87}Sr/^{86}Sr$ ratios ranging from 0.7085 to 0.7088, which are comparable with those of White Nile values (eastern bank) and sand collected at Al Khiday. Middle Mesolithic pottery showed a wide variety of $^{87}Sr/^{86}Sr$ ratios (from 0.707363 to 0.708978) and an average high content of Sr. Late Mesolithic pottery maintained a constant $^{87}Sr/^{86}Sr$ ratio but showed an evident increase in Sr content, probably due to the presence of the secondary phases highlighted by microstructural analysis. Thus, Late Mesolithic pottery from 10-W-4 might be contaminated and its Sr isotopic ratios might be unusable. Finally, Neolithic pottery resulted in having Sr isotopic ratios comparable with that of the White Nile clays but it was particularly enriched in Sr. Sr isotopic ratios of samples from Wadi Howar region (WH24, WH25, WH29) are generally higher than Mesolithic and Neolithic samples from Al Khiday and this is probably due to the fact that raw materials used to produce this pottery have a higher crustal fingerprint. Unfortunately, because of the unavailability of raw materials coming from that region, it is difficult to make interesting comparisons. Only one sample from Wadi Soba area (BN7) shows a different Sr isotopic ratio compared to Al Khiday clays. Its $^{87}Sr/^{86}Sr$ ratio is much lower than the others, but this sample belongs to a production area located along the Blue Nile and this might explain the discordant value.

The phenomenon of Sr enrichment in pottery samples seems to be related to the age of the pottery: it starts from not-enriched Early Mesolithic samples and ends up to highly-enriched Neolithic samples. The explanation of this phenomenon might be related to the different use of the Mesolithic pots. During Early Mesolithic period, the groups of hunter-gatherer-fishers had a nomadic way of life and were used to frequent the same areas for short periods. It is most likely that the ceramic production was represented by small pots that were used for a short period and then abandoned on the site at the time of leaving the settlement. During Middle and Late Mesolithic

periods, the way of life of these groups changed little, but it converted into semi-sedentary. The latter manifested in the building of structures, in the excavation of pits for different functions (Zerboni, 2011) and in the change of vessels' use and size. Pots were made to be used for longer periods and probably for a larger group of people. The relative intensity of use changed a lot also from Mesolithic to Neolithic period even if hunting, gathering and fishing have been the base of the economy of Central Sudan until the beginning of the fifth millennium BC (Out et al. 2016; Maritan et al, submitted). The repeated seasonal occupation of the same sites increased in terms of duration, thus the ceramic produced within the group was used for longer periods and was more subjected to contamination by solid and liquid food. This might explain the increasing enrichment in Sr of Late Mesolithic and Neolithic pottery. It is plausible to assume that the diet of these populations was based mainly on fish, that was the most accessible and nearest food source. The study of Walther and Thorrold (2006) demonstrated that "Water, not food, contributes the majority of strontium and barium deposited in the otoliths of a marine fish", thus it is possible to assume that fish present at Al Khiday had the same $^{87}Sr/^{86}Sr$ ratio of water flowing in the White Nile. Since from Talbot et al. (2000) $^{87}Sr/^{86}Sr$ ratio of this water was ranging between ~ 0.7080 and ~ 0.7086 in the Middle Holocene, fishes living in this water had the same Sr isotopic ratio, which is the interval all the more recent pottery tends to. Thus, it is possible to state that the process of food preparation and consumption heavily contaminated the whole body of the vessels causing a homogenization of the $^{87}Sr/^{86}Sr$ ratios of the pottery. Unfortunately, at the moment the only reliable information regards Early Mesolithic pottery which does not show any enrichment in Sr content and has a Sr isotope fingerprint comparable with both White Nile clays and SAND used as temper.

CONCLUSION

The research project presented in this thesis concerned the definition of the provenance of Mesolithic and Neolithic pottery found in some prehistoric sites in Central-Sudan. The study aimed at the definition of possible exchanges and contacts through groups of hunter-gatherer-fishers and focused on the analysis of both local raw materials (clay and temper) and ceramic artefacts. In particular, the research was orientated to explore the application of Sr isotope analysis ($^{87}Sr/^{86}Sr$) to pottery characterised by similar pastes in terms of bulk chemical and petrographic composition.

In order to gain these aims, a series of different analytical methods, largely consolidated within provenance studies of ancient pottery were coupled with Sr isotope analysis. The same analyses were conducted on both raw materials and ceramic sherds.

As regards raw materials, the sampling design have been carefully planned in order to cover almost the whole course of the Nile River in the Sudanese territory. Not only the main course also at the connection with the ancient main tributaries have been analysed, but also many samples have been collected inside the confluence areas that are more affected by mixing processes, especially in the Gazira plain between the Blue and the White Nile south of Khartoum.

Petrographic and microstructural analyses highlighted the occurrence of big sub-rounded to rounded quartz grains in clay samples collected along the White Nile, whereas small angular and sub-angular quartz grains are typical of sediments from the basins pertinent to the Ethiopian highlands, these latter associated with plagioclase, olivine and pyroxene, all phases derived from the weathering of volcanic rocks (basalts). SEM-BSE images highlighted the presence of montmorillonite-rich aggregates, that are specific weathering products derived from the weathering of basaltic rocks. These phases have been found only in clays collected along the Blue Nile as well as to the north of the White and Blue Nile confluence and north of the Atbara River confluence, and might be diagnostic for the discrimination of used raw materials in ceramic production. Both mineralogical and chemical analyses

highlighted that clays collected on the western bank of the White Nile (where Al Khiday is located) show identical features that are clearly discernible from those coming from the Blue Nile. Most of the times, clays collected along the eastern bank of the White Nile (inside the Gezira plan) lie between White Nile and Blue Nile values. All the clay samples collected after Khartoum (MNa) and after Atbara (MNb) show almost the same bulk chemical and mineralogical composition. High amounts of organic matter have been found in all the clays, and it gives them a high plasticity. Samples from Blue Nile, Main Nile "a" and Main Nile "b" show a higher content in clay minerals. Sr isotope analysis confirmed the mixing processes occurring along the whole course of the River. Of particular interest for this research, Al Khiday clays (both surface and core-drill ones) have a high $^{87}Sr/^{86}Sr$ ratio reflecting the typical fingerprint of the crystalline basement and sedimentary clastic sequence derived from its disruption. Moreover, by the comparison with data from Padoan et al. (2011) and Garzanti et al. (2015) it was possible to affirm that Sr isotope ratio is not strongly affected by the grain-size selected, within certain limits. This is of great interest for this study because during prehistoric and historic periods, the ceramic production and the preparation of the clay material was carried out according to the potters' skills and not using sophisticated separation methods as those used in laboratories. Thus, the Sr isotopic ratio was here measured in the clay material available at the river banks or in the inner areas, which was most likely exploited by the ancient potters to produce their pottery.

Concerning pottery samples, Mesolithic and Neolithic sherds have been chosen based on their decoration motifs, period (Early, Middle, Late Mesolithic and Neolithic), and temper (quartz or K-feldspar). The petrographic and microstructural analysis on quartz-tempered pottery have been not in help, because of the homogeneity of clay matrix and inclusions. Only samples from both Wadi Howar region and Wadi Soba area presented specific inclusion characterized by silicified biological remains, that were totally absent in sherds from Al Khiday. On the contrary, microstructural analysis of Kfs-temperd pottery revealed an important feature: nearly all the samples were characterized by the presence of montmorillonite-rich aggregates inside the matrix. A fundamental correspondence between Kfs-tempered pottery and clays collected along the Main Nile (MNa and MNb) exists. This symmetry might indicate that Kfs-tempered pottery was produced using raw materials coming at least after the confluence with Blue Nile. Therefore, K-feldspar-tempered pottery was probably produced along the Main Nile "a" and then exchanged among groups. Therefore, it

may be considered as an imported product at Al Khiday as well as in Wadi Howar region. Nevertheless, proved the circumscribed pottery production limited to the Main Nile branch between Khartoum and Atbara, it is plausible to hypothesize that different groups of hunter-fisher-gatherers coming from different regions were used to meet periodically in an established place. The aim of these meetings probably concerned the sharing of social facts, distinctive and identitary traits such as technologies, knowledge or decorations techniques and motifs.

Chemical and isotopic analyses on qtz-tempered pottery showed that a general enrichment in Sr exists. This phenomenon seems to be unrelated to the use of salt for food conserving and seems to be lightly affected by CaO content. Moreover, it is possible to observe that the enrichment in Sr follows a sort of chronological trend that starts from not-enriched Early Mesolithic samples and ends up to highly-enriched Neolithic samples. Also Neolithic samples from Wadi Soba area show an enrichment in Sr content. Moreover, all the $^{87}Sr/^{86}Sr$ ratio of the more recent ceramics seems to trend to a small interval of Sr isotopic ratios which corresponds to the Middle Holocene Sr isotopic ratios measured by Talbot et al. (2000) near Shabona (100 km south of Al Khiday). Since it is plausible to assume that the diet of these populations was based mainly on fish and as is known "Water, not food, contributes the majority of strontium and barium deposited in the otoliths of a marine fish" (Walther and Thorrold, 2006), then it is possible to assume that fish present at Al Khiday had the same $^{87}Sr/^{86}Sr$ ratio of water flowing in the White Nile. Thus, it is possible to state that the process of food preparation and consumption heavily contaminated the whole body of the vessels causing and increasing in Sr content and a homogenization of the $^{87}Sr/^{86}Sr$ ratios of the pottery. Moreover, during Early Mesolithic period, the groups of hunter-gatherer-fishers had a nomadic way of life and were used to frequent the same areas for short periods. Is most likely that the ceramic production was represented by small pots that were used for a short period and then left on the site at the time of leaving the settlement. During Middle and Late Mesolithic period, the way of life of these groups changed little, but it converted into semi-sedentary. Pots were made to be used for longer periods and probably for a large group of people. The repeated seasonal occupation of the same sites increased in terms of duration, thus the ceramics produced within the group was used for longer periods and was more subjected to contamination by solid and liquid food. This might explain the increasing enrichment in Sr of Late Mesolithic and Neolithic pottery.

For this reason, only Sr isotope values related to Early Mesolithic pottery are reliable and they reflect the Sr concentration of Al Khiday clays but a $^{87}Sr/^{86}Sr$ ratio lightly lower than that characteristic of the site.

At the present time, it is possible to make valid hypotheses only about the origin of Kfs-tempered pottery basing on microstructural analysis. However, the method worked well with raw materials but it needs to be applied to a larger number pottery samples trying to select not contaminated sherds. This project must be considered a preliminary step towards the application of Sr isotope analysis on provenance studies but, together with the different authors who have used isotope methods in their research on ceramic provenance, it has shown that further research is needed, particularly concerning methodological approaches, choice of the most promising isotope tool, and refinement of analytical procedures. Moreover, interpretation of the data requires a more interdisciplinary thinking, as especially the study of ceramic provenances provides the opportunity to link between archaeological and geological-geochemical sciences to illuminate interaction of prehistoric humans with natural resources in a more detailed way.

APPENDIX

CHEMICAL DATA OF CLAY SAMPLES, QUARTZ-TEMPERED POTTERY AND K-FEDLSPAR-TEMPERED POTTERY

Table A.1: bulk chemical data of raw materials analyzed by XRF (major and minor elements expressed in %; trace elements expressed in ppm)

LOCATION	near Al Khiday	near Jebel Aulia dam	near Saggai	near Gerri	near Banqa	Meroe	Meroe	Atbara	Atbara	Atbara	Alyab	near Jebel Maddaha
TYPE	WNw	WNw	MNa	MNa	MNa	MNa	MNa	MNb	MNb	MNb	MNa	WNw
SAMPLE ID	CLAY1	CLAY2	CLAY3	CLAY4	CLAY5	CLAY6A	CLAY6B	CLAY7	CLAY8	CLAY9	CLAY10	CLAY11
SiO_2	70,02	89,61	55,21	54,49	54,12	54,88	58,73	56,88	55,32	55,62	55,24	81,49
TiO_2	1,57	0,63	3,30	1,86	3,14	2,71	2,04	2,23	2,77	3,91	2,71	0,90
Al_2O_3	14,39	4,57	14,83	21,35	16,32	17,05	16,38	15,89	15,96	12,26	16,98	9,55
Fe_2O_3	7,26	2,05	13,61	12,51	13,91	13,37	11,12	11,70	12,84	13,59	13,05	6,23
MnO	0,18	0,03	0,19	0,16	0,20	0,19	0,20	0,17	0,19	0,18	0,19	0,09
MgO	1,62	0,49	3,34	2,42	3,09	2,99	2,89	3,91	3,78	4,67	2,92	0,42
CaO	1,66	1,00	6,25	4,28	5,70	5,51	4,91	5,39	5,65	6,70	5,26	0,40
Na_2O	0,99	0,28	1,60	0,83	1,59	1,54	1,49	1,86	1,68	1,65	1,43	0,18
K_2O	1,74	0,43	1,29	1,53	1,27	1,33	1,46	1,10	1,05	0,96	1,35	0,45
P_2O_5	0,10	0,05	0,26	0,30	0,27	0,28	0,27	0,19	0,21	0,20	0,27	0,07

Tot	99,53	99,14	99,88	99,73	99,61	99,85	99,49	99,32	99,45	99,74	99,40	99,78
L.O.I.	8,90	4,22	8,99	15,23	9,73	12,14	10,72	11,08	9,59	6,45	13,12	5,70
S	100	179	241	201	260	269	255	262	201	183	329	37
Sc	25	18	18	28	24	23	20	28	18	18	21	23
V	106	48	338	223	317	286	230	278	328	424	292	103
Cr	112	53	228	134	179	163	166	230	252	587	151	84
Co	29	7	46	39	49	49	44	44	44	48	44	19
Ni	46	14	76	95	82	82	82	105	99	122	79	32
Cu	129	27	73	118	425	79	77	102	101	106	80	38
Zn	78	30	138	137	139	134	117	118	129	143	135	51
Ga	24	11	27	38	27	32	29	28	29	23	31	15
Rb	71	20	44	75	45	48	58	34	36	29	48	23
Sr	195	62	327	212	317	313	265	355	321	352	301	52
Y	38	17	39	51	39	41	42	33	36	33	43	26
Zr	526	335	379	350	341	322	316	238	290	478	333	309
Nb	28	9	34	41	40	38	28	16	23	25	37	12
Ba	715	227	701	575	697	673	639	551	558	584	683	295
La	41	16	31	60	18	25	31	14	14	12	41	21
Ce	76	33	18	72	24	51	57	21	18	4	50	60
Nd	26	26	24	50	32	33	33	19	34	34	38	47
Pb	26	23	15	20	13	15	18	21	11	11	15	19
Th	13	10	9	13	9	12	7	6	8	9	10	10
U	8	2	2	4	1	0	5	1	2	1	3	6

LOCATION	Soba	El Srmir Village	west of El Srmir Village	Kalakla Galaa	Cinese bridge	near Sereger (V cataract)	north of Merowe	near Korti	ner El Debba	near El Ghaba	at Amara	between Amara and Sai
TYPE	BN	BN	BN	WNe	WNe	MNb	MNb	MNb	MNb	MNb	MNb	MNb
SAMPLE ID	CLAY13	CLAY15	CLAY16	CLAY17	CLAY18	CLAY19	CLAY20	CLAY21	CLAY22	CLAY23	CLAY24	CLAY25
SiO_2	53,80	77,19	72,51	66,51	65,24	53,12	62,06	53,40	53,18	52,63	53,16	54,43
TiO_2	2,92	0,81	1,06	1,78	1,55	2,24	2,05	2,36	2,45	2,33	2,32	2,75
Al_2O_3	17,79	8,17	9,27	14,79	16,41	20,35	13,83	19,92	19,91	20,19	20,56	18,71
Fe_2O_3	13,75	4,78	5,27	9,78	9,27	13,67	9,55	13,85	13,91	14,00	14,04	13,57
MnO	0,23	0,07	0,16	0,37	0,15	0,24	0,14	0,26	0,26	0,26	0,26	0,21
MgO	2,99	1,71	2,03	2,51	2,13	3,38	3,31	3,27	3,23	3,22	3,29	3,15
CaO	5,51	4,94	6,95	1,90	2,00	4,48	4,96	4,53	4,60	4,13	4,08	4,45
Na_2O	1,37	1,11	1,09	0,83	0,77	1,03	1,69	0,98	1,11	0,93	0,95	1,39
K_2O	1,29	0,61	1,02	1,06	1,50	1,28	1,59	1,27	1,29	1,27	1,27	1,34
P_2O_5	0,28	0,09	0,10	0,12	0,20	0,26	0,21	0,28	0,29	0,28	0,29	0,28
Tot	99,93	99,48	99,46	99,65	99,22	100,05	99,39	100,12	100,23	99,24	100,22	100,28
L.O.I.	13,99	9,42	9,70	10,52	13,33	13,76	7,29	14,18	14,40	14,03	14,59	10,65
S	367	2096	183	19	326	120	279	249	205	206	259	234
Sc	19	4	0	29	28	29	15	31	27	29	29	26
V	317	113	149	204	161	277	233	282	285	283	283	293
Cr	168	88	104	136	127	172	223	176	170	174	176	172
Co	49	17	23	43	31	57	38	58	56	56	58	53
Ni	86	37	44	80	67	109	89	111	111	114	117	99
Cu	96	40	39	75	66	116	73	115	114	115	119	106
Zn	143	49	56	97	124	148	114	159	157	153	152	147
Ga	33	14	17	26	28	37	23	38	36	36	39	34

Rb	52	34	40	52	70	55	48	55	57	57	56	52
Sr	285	293	293	179	180	238	320	238	245	220	225	280
Y	46	21	26	39	39	54	39	63	54	54	56	47
Zr	352	234	328	282	355	311	372	355	340	331	340	348
Nb	40	11	14	25	30	39	23	48	41	40	41	41
Ba	655	313	537	810	571	570	579	576	587	580	561	616
La	38	20	19	38	39	40	15	47	34	34	39	34
Ce	44	37	35	65	72	56	40	66	72	52	61	55
Nd	38	32	17	26	39	43	24	49	41	46	39	37
Pb	18	16	12	13	39	321	264	729	30	285	379	59
Th	9	12	10	12	6	2	2	2	5	2	2	2
U	3	5	7	6	3	2	2	2	2	2	2	2

LOCATION	**island of Sai (north)**	**III catarct**	**near Kerma**	**near Khantaq**	**near Al Khiday**	**near Al Khiday**	**near Al Khiday**	**near El Dueim**	**near El Dueim**	**Site 16-D-4**	**Jebel Seleitat**
TYPE	MNb	MNb	MNb	MNb	WNw	WNw	WNw	WNe	WNw	SAND	KFS
SAMPLE ID	**CLAY26**	**CLAY27**	**CLAY28**	**CLAY29**	**CLAY 1-35**	**CLAY 1-70**	**CLAY 1-90**	**CLAY 30**	**CLAY 31**	**SAND 16D4**	**JS11**
SiO_2	55,40	54,31	55,07	54,66	66,46	64,68	65,04	75,3	74,32	96,35	69,83
TiO_2	2,81	2,62	2,55	2,71	1,64	1,68	1,64	1,08	1,09	0,20	0,02
Al_2O_3	16,18	19,14	17,71	16,98	16,71	18,22	17,79	10,37	12,17	1,24	16,49
Fe_2O_3	12,59	13,61	12,92	12,84	9,04	9,88	9,85	5,35	5,78	0,84	0,11
MnO	0,19	0,26	0,21	0,18	0,21	0,21	0,22	0,08	0,11	0,01	0,01
MgO	3,60	3,18	3,53	3,75	1,48	1,36	1,27	1,84	1,52	0,21	0,05

CaO	5,48	4,29	5,11	5,14	1,56	1,33	1,29	3,41	2,5	0,37	0,54
Na_2O	1,66	1,26	1,52	1,56	0,9	0,94	1	0,93	1,04	0,10	3,64
K_2O	1,24	1,36	1,30	1,33	1,57	1,53	1,53	1,21	1,42	0,17	8,37
P_2O_5	0,24	0,30	0,25	0,26	0,15	0,17	0,2	0,11	0,17	0,14	0,07
Tot	99,39	100,33	100,17	99,41	99,72	100	99,83	99,68	100,12	99,63	99,13
L.O.I.	8,82	12,79	10,55	9,80	9,56	9,96	9,87	8,31	9,79	1,11	0,36
S	231	413	266	194	68	25	25	114	880	10	18
Sc	25	28	24	22	19	25	27	16	16	13	13
V	302	293	288	294	101	112	113	86	87	16	3
Cr	237	172	201	198	121	126	119	99	90	20	29
Co	48	56	53	49	28	29	36	15	19	3	2
Ni	107	104	102	109	50	51	49	37	37	3	15
Cu	98	111	106	110	52	51	49	40	48	20	21
Zn	134	147	140	138	101	113	109	59	75	13	38
Ga	31	35	34	31	29	31	31	18	21	6	29
Rb	43	56	48	46	81	83	79	47	56	12	206
Sr	304	266	295	305	179	175	172	207	192	30	140
Y	43	51	49	42	47	49	47	24	32	6	7
Zr	316	348	328	303	507	488	500	390	381	130	59
Nb	29	37	34	30	37	40	40	15	22	2	2
Ba	598	618	605	606	734	728	769	454	555	72	573
La	27	41	27	29	58	70	57	28	21	11	23
Ce	32	57	36	32	89	107	86	47	63	12	32
Nd	31	41	34	37	30	48	44	27	26	31	5
Pb	153	17	236	12	28	25	25	21	23	14	59
Th	2	8	2	12	13	14	14	9	10	8	2
U	3	2	2	5	9	6	7	7	5	5	9

Table A.2: bulk chemical data of quartz-tempered pottery (major, minor and trace elements expressed in %). Abbreviations: Rsplzz= Rocker stamp plain zigzag; Rsdzz= Rocker stamp dotted zigzag; RS Drops Deep= Rocker stamp Drops Deep; RS Drops Deep Fun= Rocker stamp Drops Deep Fun; DWL= Dotted Wavy Line; APS= Alternately pivoting stamp; RS unevenly spaced dots= Rocker stamp unevenly spaced dots

	MESOLITHIC QUARTZ-TEMPERED									
AGE	EARLY	EARLY	EARLY	EARLY	EARLY	EARLY	MIDDLE	MIDDLE	MIDDLE	MIDDLE
DEC. MOTIF	Rsplzz	Rsdzz	RS Drops Deep	RS Drops Deep Fun	Rsplzz	RS Drops Deep	Rsplzz	Rsdzz	Rsplzz	DWL
Site	16D5	16D5	16D5	16D5	16D5	16D5	16D5	16D5	16D5	16D5
SAMPLE ID	**AK73**	**AK102**	**AK74**	**AK75**	**AK82**	**AK86**	**AK136**	**AK165**	**AK170**	**AK173**
SiO_2	80,36	77,75	70,64	76,70	74,64	75,58	77,91	75,48	74,65	77,49
TiO_2	0,98	1,00	1,24	0,97	1,04	1,00	0,94	1,09	1,08	0,85
Al_2O_3	9,75	12,53	13,35	11,07	11,24	11,57	9,96	14,61	13,70	10,51
Fe_2O_3	4,44	4,58	7,35	4,87	8,41	6,08	5,81	5,02	6,03	5,40
MnO	0,08	0,13	0,15	0,09	0,13	0,15	0,13	0,06	0,10	0,11
MgO	1,16	0,57	1,25	1,31	0,83	1,08	1,74	0,76	0,82	0,74
CaO	1,10	1,03	2,31	2,32	1,07	1,32	1,96	0,92	1,17	1,49
Na_2O	0,71	0,98	1,45	1,02	1,20	1,28	0,69	0,36	0,82	0,97
K_2O	0,73	0,96	1,43	0,90	0,44	1,05	0,54	0,84	0,66	0,89
P_2O_5	0,10	0,14	0,18	0,12	0,33	0,22	0,18	0,12	0,16	0,65
Tot	99,41	99,67	99,35	99,37	99,33	99,33	99,86	99,26	99,19	99,10
L.O.I.	6,79	5,32	9,69	6,80	6,33	9,00	7,53	2,54	8,25	7,50
S	0,02	0,0249	0,0068	0,0129	0,0081	0,0061	0,0247	0,0048	0,0039	0,006
Sc	0,0024	0,002	0,0018	0,0012	0,0027	0,0018	0,0014	0,0027	0,0028	0,002
V	0,0094	0,0106	0,0115	0,0103	0,0189	0,0095	0,0115	0,0116	0,0122	0,0108

Cr	0,0114	0,0113	0,0102	0,0091	0,0137	0,01	0,0112	0,0104	0,0118	0,0105
Co	0,0015	0,0032	0,002	0,0016	0,0017	0,0017	0,0019	0,0016	0,002	0,0014
Ni	0,0121	0,0053	0,0043	0,0162	0,004	0,0054	0,0049	0,0039	0,0054	0,0038
Cu	0,0043	0,0047	0,0037	0,0039	0,0037	0,0033	0,0057	0,0051	0,006	0,0045
Zn	0,0063	0,0067	0,0084	0,0053	0,0053	0,0075	0,0062	0,0057	0,0079	0,0083
Ga	0,0015	0,002	0,0019	0,0014	0,0016	0,0016	0,0017	0,0022	0,0022	0,0014
Rb	0,0028	0,0023	0,0051	0,0028	0,002	0,0038	0,0026	0,0033	0,0032	0,0033
Sr	0,0201	0,022	0,0388	0,0222	0,0217	0,0243	0,0369	0,015	0,0209	0,0292
Y	0,0024	0,0039	0,0029	0,0028	0,0029	0,0026	0,0022	0,0023	0,0033	0,0023
Zr	0,0397	0,0296	0,0389	0,0276	0,0401	0,0274	0,0332	0,0271	0,0269	0,019
Nb	0,0013	0,0012	0,0026	0,0015	0,0013	0,0022	0,0014	0,0016	0,0017	0,0014
Ba	0,0417	0,0533	0,0821	0,0428	0,0379	0,0497	0,0532	0,0402	0,0422	0,0525
La	0,0024	0,002	0,0036	0,0034	0,0028	0,004	0,0012	0,0031	0,0027	0,0012
Ce	0,0041	0,0053	0,0058	0,0052	0,0055	0,005	0,004	0,0049	0,0043	0,0045
Nd	0,003	0,0025	0,0015	0,0038	0,0047	0,0033	0,0024	0,0034	0,0036	0,0021
Pb	0,0018	0,0022	0,0012	0,0016	0,002	0,0022	0,0017	0,0019	0,0019	0,001
Th	0,0011	0,001	0,0008	0,001	0,0011	0,001	0,0008	0,0013	0,0009	0,0008
U	0,0009	0,0006	0,0004	0,0002	0,0006	0,0006	0,0007	0,0005	0,0003	0,0002

	MESOLITHIC QUARTZ-TEMPERED							
AGE	MIDDLE	LATE	LATE	LATE	LATE	LATE	LATE	LATE
DEC. MOTIF	Lunula	Rsplzz	Rsdzz	Rsdzz	APS	APS	DWL	DWL
Site	16D5	10W4	10W4	10W4	10W4	10W4	S98/21	S98/21
SAMPLE ID	**AK193**	**AK196**	**AK198**	**AK211**	**AK204**	**AK212**	**WH24**	**WH25**
SiO_2	68,61	72,57	74,42	75,58	62,01	60,84	61,1	63,4

TiO_2	1,36	1,17	1,09	1,02	0,69	0,84	1,11	0,56
Al_2O_3	14,43	13,94	13,82	13,00	21,31	22,28	17,5	17,3
Fe_2O_3	7,52	6,47	4,06	4,28	4,97	5,13	3,33	1,31
MnO	0,11	0,04	0,05	0,04	0,04	0,06	0,02	0
MgO	1,19	1,13	0,54	0,76	0,55	0,74	0,53	0,37
CaO	2,87	1,91	2,01	1,75	2,07	2,2	2,32	2,16
Na_2O	1,06	0,31	0,25	0,21	0,43	1,19	0,34	0,23
K_2O	1,84	0,92	0,75	0,67	5,43	3,86	0,89	0,75
P_2O_5	0,09	1,47	2,14	1,82	2,11	2	0,79	0,67
Tot	99,08	99,93	99,13	99,13	99,61	99,14		
L.O.I.	11,29	11,13	8,97	9,86	10,71	7,37		
S	0,0061	0,0026	0,0035	0,0034	0,0021	0,0029		
Sc	0,0022	0,0025	0,0018	0,0018	0,0011	0,0018		
V	0,0112	0,0121	0,0097	0,0091	0,0057	0,0052	0,0127	0,007
Cr	0,0096	0,0122	0,0103	0,0103	0,0055	0,0073	0,0152	0,013
Co	0,0021	0,0018	0,002	0,0014	0,0016	0,0009	0,001	0,0006
Ni	0,0038	0,0065	0,0051	0,0055	0,0036	0,0037	0,0029	0,0044
Cu	0,0036	0,0048	0,005	0,0048	0,0041	0,0028		
Zn	0,0077	0,0065	0,0052	0,0052	0,0051	0,0067	0,0045	0,0028
Ga	0,002	0,002	0,002	0,0018	0,0029	0,0035	0,0024	0,0018
Rb	0,0051	0,0028	0,002	0,0023	0,013	0,0103	0,0026	0,0011
Sr	0,0619	0,0345	0,0438	0,044	0,0531	0,0485	0,0306	0,0261
Y	0,0035	0,0034	0,0025	0,0025	0,0016	0,0024	0,0037	0,0022
Zr	0,0519	0,0348	0,0295	0,0305	0,0262	0,0324	0,0627	0,0245
Nb	0,0031	0,0018	0,0014	0,0013	0,0011	0,0009	0,003	0,0024
Ba	0,1226	0,105	0,1313	0,1165	0,2254	0,1697	0,115	0,086
La	0,0041	0,0042	0,0034	0,0025	0,0025	0,0071		

Ce	0,0092	0,0068	0,0054	0,0052	0,0084	0,0156		
Nd	0,0005	0,0007	0,0005	0,0005	0,0005	0,0005		
Pb	0,002	0,0022	0,0019	0,0019	0,0048	0,0047		
Th	0,0011	0,0009	0,0007	0,0008	0,0004	0,0028		
U	0,0002	0,0003	0,0008	0,0005	0,0006	0,0012		

	NEOLITHIC QUARTZ-TEMPERED											
AGE	NEOL	NEOL	NEOL	NEOL	NEOL	NEOL	NEOL	NEOL	NEOL	NEOL	NEOL	NEOL
Site	16D5	16D5	16D5	Soba-2,6	Soba-2,6	S99/1	16D5	16D5	16D5	16D5	16D5	16D5
DEC. MOTIF	Not decorated	Rsdzz	Rsdzz	Rocker impression	Parallel impression	Not specified	Not decorated	RS unevenly spaced dots	RS unevenly spaced dots	Rsdzz	Rsdzz	APS
SAMPLE ID	**AK8**	**AK46**	**AK48**	**BN7**	**BN8**	**WH29**	**AK1**	**AK24**	**AK36**	**AK47**	**AK49**	**AK50**
SiO_2	65,39	63,27	64,41	60,79	63,31	72,4	65,18	64,97	73,12	76,61	63,70	71,82
TiO_2	1,46	1,58	1,55	1,91	1,65	0,59	1,48	1,59	1,46	1,03	1,55	1,24
Al_2O_3	16,20	18,23	17,41	16,11	17,21	9,3	16,49	17,02	13,51	13,12	17,67	13,16
Fe_2O_3	9,39	9,78	9,53	10,40	9,28	4,74	9,85	9,58	6,38	4,82	10,10	8,61
MnO	0,16	0,20	0,17	0,13	0,16	0,04	0,23	0,14	0,20	0,04	0,22	0,22
MgO	1,35	1,23	1,28	2,51	1,36	1,19	1,18	1,35	0,86	0,73	1,19	0,83
CaO	2,67	2,58	2,47	3,22	2,81	1,14	2,42	1,99	1,81	1,93	2,08	1,59
Na_2O	1,03	1,68	1,21	1,84	0,97	1,1	0,72	0,79	0,64	0,24	1,66	0,62
K_2O	1,55	1,31	1,63	2,20	2,21	1,79	1,59	1,53	1,41	0,60	1,40	1,08
P_2O_5	0,21	0,27	0,26	0,38	0,62	0,11	0,31	0,23	0,21	0,06	0,25	0,30
Tot	99,41	100,13	99,92	99,49	99,58		99,45	99,19	99,60	99,18	99,82	99,47
L.O.I.	10,26	11,60	8,56	6,29	8,05		7,48	1,97	6,82	7,35	10,43	3,43
S	0,0056	0,0085	0,0147	0,0524	0,0224		0,0107	0,024	0,0209	0,0052	0,011	0,006

Sc	0,002	0,0024	0,0022	0,0026	0,002		0,002	0,0026	0,0017	0,0013	0,002	0,0024
V	0,0112	0,0114	0,0104	0,0165	0,0107	0,0054	0,0139	0,0143	0,01	0,0101	0,014	0,0101
Cr	0,0114	0,0114	0,0115	0,014	0,0126	0,0095	0,0115	0,0121	0,0092	0,0109	0,0119	0,0105
Co	0,0026	0,0027	0,0028	0,0034	0,0027	0,0014	0,0031	0,0028	0,0022	0,0011	0,0031	0,0025
Ni	0,0053	0,0057	0,005	0,007	0,0057	0,0017	0,0047	0,0067	0,0037	0,0037	0,0054	0,0209
Cu	0,0053	0,0052	0,0048	0,0071	0,006		0,0033	0,0041	0,0065	0,0091	0,0036	0,0036
Zn	0,0117	0,0124	0,0118	0,0147	0,013	0,0047	0,01	0,0101	0,0065	0,0058	0,0105	0,0082
Ga	0,0028	0,0031	0,0028	0,0029	0,0029	0,0009	0,0023	0,0025	0,0016	0,0013	0,0025	0,0018
Rb	0,0052	0,0054	0,0057	0,0054	0,0062	0,0035	0,0056	0,0073	0,0039	0,0021	0,0054	0,0041
Sr	0,0541	0,0462	0,0379	0,0445	0,0497	0,0074	0,0575	0,0265	0,034	0,0274	0,0422	0,0286
Y	0,0042	0,0046	0,0046	0,0038	0,0044	0,0026	0,0042	0,0042	0,0038	0,0035	0,0043	0,0039
Zr	0,0381	0,0396	0,0409	0,0296	0,0408	0,0331	0,0394	0,0466	0,044	0,0279	0,038	0,0356
Nb	0,0037	0,0041	0,0039	0,0028	0,0036	0,0016	0,0036	0,0039	0,0032	0,0014	0,0039	0,0029
Ba	0,1092	0,1078	0,1095	0,1277	0,1545	0,04	0,0994	0,0973	0,09	0,0722	0,0911	0,0762
La	0,003	0,0046	0,0057	0,0039	0,0042		0,0058	0,0049	0,0037	0,0026	0,0052	0,0022
Ce	0,0104	0,0109	0,01	0,0061	0,0106		0,0102	0,0095	0,0053	0,0055	0,0089	0,008
Nd	0,001	0,0021	0,0016	0,0005	0,0005		0,0018	0,003	0,0011	0,0024	0,0034	0,0029
Pb	0,0021	0,0024	0,0021	0,0023	0,0029		0,0021	0,0019	0,0018	0,002	0,0024	0,0023
Th	0,001	0,001	0,0011	0,0007	0,001		0,001	0,0015	0,0011	0,0009	0,0009	0,001
U	0,0005	0,0007	0,0006	0,0007	0,0004		0,0006	0,0003	0,0002	0,0004	0,0002	0,0005

Table A.3: bulk chemical data of Mesolithic K-feldspar-tempered pottery (major, minor and trace elements expressed in %). Abbreviations as in Table A.2

MESOLITHIC K-FELDSPAR-TEMPERED											
AGE	EARLY	EARLY	EARLY	MIDDLE	MIDDLE	MIDDLE	MIDDLE	LATE	LATE	MESO	MESO
Site	16D5	16D5	16D5	16D5	16D5	16D5	16D5	10W4	10W4	Sheikh Mustafa 13	Al Mahalab 26
DEC. MOTIF	WL	Rsdzz	WL	WL	WL	WL	Rsdzz	APS	APS	Rocker impression	Not specified
SAMPLE ID	**AK67**	**AK76**	**AK70**	**AK115**	**AK116**	**AK152**	**AK182**	**AK204**	**AK212**	**BN5**	**BN10**
SiO_2	64,26	63,15	66,23	65,8	63,25	67,37	61,78	62,01	60,84	59,87	63,32
TiO_2	0,76	0,97	0,82	0,79	0,78	0,51	1,17	0,69	0,84	0,59	0,36
Al_2O_3	19,93	19,44	19,73	17,69	19,34	19,63	18,93	21,31	22,28	23,82	22,51
Fe_2O_3	5,78	8,31	5,87	6,64	6,22	3,51	9,00	4,97	5,13	5,3	3,88
MnO	0,17	0,14	0,17	0,11	0,08	0,08	0,13	0,04	0,06	0,04	0,02
MgO	0,80	0,77	0,53	0,84	0,8	0,55	0,76	0,55	0,74	0,79	0,89
CaO	1,30	1,37	1,69	1,34	1,41	1,44	1,58	2,07	2,2	2,35	1,98
Na_2O	0,87	1,18	1,07	1,07	1,37	1,15	1,58	0,43	1,19	0,81	0,6
K_2O	4,52	4,78	3,14	4,96	5,43	5,24	4,00	5,43	3,86	4,11	6,11
P_2O_5	0,23	0,10	0,33	0,22	0,51	0,36	0,19	2,11	2	2,18	0,15
Tot	98,62	100,21	99,58	99,46	99,19	99,84	99,12	99,61	99,14	99,86	99,82
L.O.I.	6,54	8,39	8,49	7,98	8,07	7,13	6,17	10,71	7,37	12,3	6,58
S	0,0023	0,0188	0,0084	0,0027	0,0075	0,0042	0,0056	0,0021	0,0029	0,0049	0,0089
Sc	0,0019	0,0023	0,0017	0,0026	0,0022	0,0018	0,0023	0,0011	0,0018	0,0015	0,0014

V	0,0116	0,0079	0,0076	0,003	0,008	0,0033	0,0093	0,0057	0,0052	0,0049	0,0031
Cr	0,0071	0,0037	0,0077	0,0035	0,008	0,0039	0,0053	0,0055	0,0073	0,0036	0,0035
Co	0,0015	0,0019	0,0021	0,0012	0,0012	0,0008	0,0018	0,0016	0,0009	0,0007	0,0006
Ni	0,015	0,0028	0,0046	0,002	0,0048	0,0032	0,0031	0,0036	0,0037	0,0057	0,0027
Cu	0,0038	0,0039	0,0052	0,0031	0,004	0,0035	0,0043	0,0041	0,0028	0,0041	0,0042
Zn	0,008	0,0145	0,0065	0,0134	0,0091	0,0052	0,0164	0,0051	0,0067	0,0079	0,0042
Ga	0,0025	0,004	0,0029	0,0037	0,0031	0,0028	0,0041	0,0029	0,0035	0,0034	0,0031
Rb	0,0108	0,0151	0,0072	0,0154	0,0181	0,0111	0,0138	0,013	0,0103	0,0128	0,012
Sr	0,0348	0,0344	0,0433	0,0303	0,0405	0,0416	0,0356	0,0531	0,0485	0,0407	0,043
Y	0,002	0,0088	0,0017	0,0096	0,0019	0,002	0,0114	0,0016	0,0024	0,0025	0,0017
Zr	0,0305	0,0876	0,0237	0,0856	0,0234	0,0254	0,1209	0,0262	0,0324	0,0299	0,0134
Nb	0,0011	0,004	0,0012	0,0029	0,0014	0,0006	0,0048	0,0011	0,0009	0,0006	0,0006
Ba	0,1564	0,1512	0,1459	0,1511	0,1327	0,1904	0,1367	0,2254	0,1697	0,1326	0,1688
La	0,0062	0,0088	0,0027	0,0088	0,0023	0,0055	0,0119	0,0025	0,0071	0,0066	0,0013
Ce	0,012	0,033	0,0104	0,0313	0,0052	0,0121	0,0307	0,0084	0,0156	0,0171	0,0047
Nd	0,0005	0,0043	0,0005	0,0047	0,0005	0,0005	0,008	0,0005	0,0005	0,0011	0,0005
Pb	0,0038	0,0036	0,004	0,0035	0,0044	0,0043	0,0034	0,0048	0,0047	0,0032	0,0051
Th	0,0021	0,0014	0,0012	0,0017	0,0002	0,002	0,0018	0,0004	0,0028	0,0033	0,0002
U	0,0004	0,0005	0,0009	0,0009	0,0007	0,0008	0,0006	0,0006	0,0012	0,0008	0,0005

REFERENCES

Abdelsalam, M.G., Liégeois, J.P. and Stern, R.J. (2002) The Saharan Metacraton. Review. J. Afr. Earth Sci. 34, 119–136.

Aikens, C.M. (1995). First in the world: The Jomon pottery of early Japan. In Barnett, W. K., and Hoopes, J. W. (eds.), The Emergence of Pottery. Technology and Innovation in Ancient Societies, Smithsonian Institution Press, Washington, DC, 11-21.

Aitchison, J. (1986) The Statistical Analysis of Compositional Data. Monographs on Statistics and Applied Probability, Chapman & Hall Ltd., London, (Reprinted in 2003 with additional material by The Blackburn Press), 416 p.

Aitchison, J. (1990) Relative variation diagrams for describing patterns of compositional variability. Mathematical Geology, 22 (4), 487–511.

Alex, B.A., Nichols, D.L., and Glascock, M.D. (2012) Complementary Compositional Analysis of Formative Period Ceramics from the Teotihuacan Valley. Archaeometry 54: 821–834.

Ali Hakem, A.M., Khabir, A. M. (1989) Sarourab 2: a new contribution to the Early Khartoum tradition from Bauda site. Late Prehistory of the Nile Basin and the Sahara, (eds.) Krzyżania L, Kroeper K, Kobusiewicz M (Poznań Archaeological Museum, Poznań), 381-385.

Arkell, A.J. (1947) Early Khartoum. Antiquity, 21, 172–181

Arkell, A.J. (1949) Early Khartoum. An Account of the Excavation of an Early Occupation Site carried out by the Sudan Government Antiquities service in 1944-5. Oxford: Oxford University Press.

Barrows, T.T., Williams, M.A.J., Mills, S.C., Duller, G.A.T., Fifield, L.K., Haberlah, D., Tims, S.G., Williams, F.M. (2014) A White Nile megalake during the last interglacial period. Geology 42, 163-166.

Baxter, M.J., and Buck C.E. (2000) Data Handling and Statistical Analysis. In Modern Analytical Methods in Art and Archaeology, edited by E. Ciliberto and G. Spoto, pp. 681–746. John Wiley & Sons, New York.

Bentley, R.A. (2006) Strontium Isotopes from the Earth to the Archaeological Skeleton: A Review. J. Archaeol. Method and Theory, 13, 135-187.

Betancourt, P.P. and Peterson, S.E. (2009) Thin-section Petrography of Ceramic Materials. Institute for Aegean Prehistory, Archaeological Excavation Manual 2. INSTAP Academic Press, Philadelphia.

Bimson, M. (1969) The examination of ceramics by X-ray powder diffraction. Stud. Conserv. 14, 85-89.

Bowser, B.J. (2000) From pottery to politics: an ethnoarchaeological case study of political factionalism, ethnicity, and domestic pottery style in the Ecuadorian Amazon. J. Archaeol. Method Theory 7, 219-248.

Brems, D., Ganio, M., Latruwe, K., Balcaen, L., Carremans, M., Gimeno, D., Silvestri, A. Vanhaecke, F., Muchez, P., Degryse, P. (2013) Isotopes on the beach, part 1: strontium isotopic analysis for the provenancing of Roman glass-making. Archaeometry, 55, 214–234.

Brilli, M., Cavazzini, G., Turi, B. (2005) New data of $^{87}Sr/^{86}Sr$ ratio in classical marble: an initial database for marble provenance determination. J. Archaeol. Sci., 32, 1543-1551.

Budja, M. (2006) The transition to farming and the ceramic trajectories in Western Eurasia: from ceramic figurines to vessels. Documenta Praehistorica 33, 183-201.

Bullok, P.N., Neferoff, A., Jongerius, A. et al. (1985) The handbook of soil thin section description. Wayne Research, Wolverhampton.

Buxeda i Garrigós, J. (1999) Alteration and Contamination of Archaeological Ceramics: The Perturbation Problem, Journal of Archaeological Science, Volume 26, Issue 3, 295-313

Buxeda i Garrigós, J., Cau Ontiveros, M.A., Madrid i Fernández, M., Toniolo, A. (2005) Roman amphorae from the Iulia Felix shipwreck: alteration and provenance. In: Hars, H., Burke, E. (eds.), Proceedings of the 33rd International Symposium on ArchaeometryGeoarchaeological and Bioarchaeological Studies Vol. 3. Institute for Geo- and Bio-archaeology, Vrije Universiteit, Amsterdam, pp. 149–151.

Buxeda i Garrigós, J., Mommsen, H., Tsolakidou, A. (2001) Alteration of Na, K and Rb concentrations in Mycenaean pottery and a proposed explanation using X-ray diffraction. Archaeometry 44, 187–198.

Cairo, A., Messiga, B. and Riccardi, M.P. (2001) Technological features of the 'Cotto Variegato': a petrological approach. Journal of Cultural Heritage 2, 133-142.

Caneva, I. (1983) Pottery using gatherers and hunters at Saggai (Sudan): Preconditions for food production. Origini, 12, 7–271.

Caneva, I. (1983a) Excavating Saggai 1. In: I. Caneva (eds.), Pottery using gatherers and hunters at Saggai (Sudan): Preconditions for food production. Origini, 12, 7-29

Caneva, I. (1983b) “Wavy Line” pottery from Saggai I: An essay of classification. In Caneva, I. (eds.), Pottery Using Gatherers and Hunters at Saggai (Sudan): Preconditions for Food Production, Origini 12, 155–189.

Caneva, I. (1986) Recent field works in the Northern Khartoum Province. Nyame Akuma, 27, 42–44.

Caneva, I. (1988) El Geili: the history of a Middle Nile environment 7000 BP-AD 1500. Oxford: British Archaeological Reports International series S424.

Caneva, I. (1991) Jebel Moya revisited: a settlement of the 5th millennium BC in the middle Nile Basin. Antiquity 65: 262-8.

Caneva, I., and Marks, A. (1990) More on the Shaqadud pottery: Evidence for Saharo-Nilotic connections during the 6th–4th millennium B.C. Archéologie du Nil Moyen, 4, 11–36.

Carter, W.S., Wiegang, B., Mahood, G.A., Dudas, F.O., Wooden, J.L., Sullivan, A.P. III, Bowring, S.A. (2011) Strontium isotopic evidence for prehistoric transport of Gray-ware ceramic materials in the Eastern Grand Canion region, USA. Geoarcheology: An International Journal, 26, 189-218.

Cau Ontiveros, M.A., Day, P.M. and Montana, G. (2002) Secondary calcite in archaeological ceramics: evaluation of alteration and contamination processes by thin section study. In: Kilikoglou, V., Hein, A. and Maniatis, Y. (eds.) Modern trends in scientific studies on ancient ceramics. British Archaeological Reports, 101. Archaeopress, Oxford, 9-18.

Charalambous, A.C., Sakalis, A.J., Kantiranis, N.A., Papadopoulou, L.C., Tsirliganis, N.C., Stratis, J.A. (2010) Cypriot Byzantine glazed pottery: the study of Paphos workshops. Archaeometry 52, 628-643.

Clark, J.D. (1989) Shabona: an Early Khartoum settlement on the White Nile. Late Prehistory of the Nile Basin and the Sahara, (eds.) Krzyżaniakm L, Kobusiewicz M (Poznań Archaeological Museum, Berlin), 387-410.

Close, A.E. (1995) Few and far between: Early ceramics in North Africa. In Barnett, W. K., and Hoopes, J. W. (eds.), The Emergence of Pottery. Technology and Innovation in Ancient Societies, Smithsonian Institution Press, Washington, DC, 23-37.

Courty, M.A. and Roux, V. (1995) Identification of wheel throwing on the basis of ceramic surface features and microfabrics. Journal of Archaeological Science 22, 17-50.

Cremaschi, M., Salvatori, S., Usai, D., Zerboni, A. (2007) A Further "tessera" to the Huge "mosaic": Studying the Ancient Settlement Patterns of the El Salha Region (South-west of Omdurman, Central Sudan). Archaeology of Early Northeastern Africa, (eds.) Kroeper K, Chłodnicki M, Kobusiewicz M (Poznań Archaeological Museum, Berlin), 39-48.

Cremaschi, M., and Zerboni, A. (2009) Early to Middle Holocene landscape exploitation in a drying environment: Two case studies compared from the central Sahara (SW Fezzan, Libya). C. R. Geoscience, 341, 689–702.

Cuomo Di Caprio, N. and Vaughan, S.J. (1993) An experimental study in distinguishing grog (chamotte) from argillaceous inclusions in ceramic thin sections. Archeomaterials 7, 21-40.

Dal Sasso, G. (2011) Modelling the Mesolithic and Neolithic Pottery Production from Al Khiday (Khartoum, Sudan) through a Multianalytical Approach. Unpublished Master's thesis in Sciences and Technology Applied to Archaeological and Artistic Heritage. University of Padova.

Dal Sasso, G., Maritan, L., Salvatori, S., Mazzoli, C., and Artioli, G. (2014) Discriminating pottery production by image analysis: a case study of Mesolithic and Neolithic pottery from Al Khiday (Khartoum, Sudan). Journal of Archaeological Science, 46, 125-143.

De Paepe, P.P. (1986) Etude mineralogique et chimique de la ceramique Neolithique d'el Kadada et se simplications archeologiques. Archeologie du Nil Moyen, 1, 113-137.

De Paepe, P.P. (1988) Analyse microscopique et chimique de la céremique et inventaire de l'outillage lithique du site de Kerma (Soudan). Kerma – Soudan, GENEVA XXXVI, 31-35.

De Paepe, P., Rutten, K., Vrydaghs, L. et al. (2003) Petrographic, chemical and phytolith analysis of late Preislamic ceramic from ed-Dur, Um el-Kawein (U.A.E.). In: Potts, D., Hasan Al Naboodah, H. & Hellyer, P. (eds.) Archaeology of the United Arab Emirates. Trident Press, London, 207-229.

Dickin, A.P. (2005) Radiogenic Isotope Geology 2nd (eds.) Cambridge University Press

Eberhardt, A., Delwiche, R. and Geiss, J. (1964) Isotopic effects in single filament thermal ion sources. Z. Naturf. 19a, 736–40.

Eckert, S.L. (2008) Pottery and Practice: the Expression of Identity at Pottery Mound and Hummingbird Pueblo. University of New Mexico Press, Albuquerque.

Eckert, S.L. (2012) Choosing clays and painting pots in the Fourteenth-Century Zuni region. In: Cordell, L.S., Habicht-Mauche, J.H. (eds.), Potters and Communities of Practice: Glaze Paint and Polychrome Pottery in the American Southwest, AD 1250 to 1700, Anthropological Papers of the University of Arizona, vol. 75. The University of Arizona Press, Tucson, 55-64.

Eckert, S.L., Schleher, K. L., and James, W. D. (2015) Communities of identity, communities of practice: Understanding Santa Fe black-on-white pottery in the Española basin of new Mexico. Journal of Archaeological Science, 63, 1-12

El-Anwar, E.S. (1981) Archaeological Excavations on the west bank of the River Nile in the Khartoum Area. NyameAkuma 18: 42-45.

Elamin, Y.M., Mohammed-Ali, A.S. (2004) Umm Marrahi. An early Holocene ceramic site, north of Khartoum (Sudan). Sahara 15: 97-110.

Faure, G. (1986) Principles of isotope geology (2nd ed.) New York: John Wiley & Sons

Faure, G. and Mensing, T.M. (2005) Isotopes: Principles and Applications. John Wiley & Sons. 897 pp

Faure G., Powell J.L. (1972) Strontium isotope geology, Springer-Verlag, New York.

Fernández, V.M., Jimeno, A., Menéndez, M. (2003a) Archaeological excavations in prehistoric sites of the Blue Nile area, Central Sudan. Complutum, 14, 273-344.

Fernández, V.M., Jimeno, A., Menendez, M., and Lario, J. (1997) The Mesolithic sites of Sheikh Mustafa and Al Mahalab (Central Sudan): A preliminary report. CRIPEL, 17(2), 21–27.

Fernández, V.M., Jimeno, A., Menéndez, M., Lario, J. (2003b) Archaeological survey in the Blue Nile area, Central Sudan. Complutum, 14, 201-272.

Fernández, V.M., Jimeno, A., Menéndez, M., Trancho, G. (1989) The Neolithic Site of Haj Yousif (Central Sudan). Trabajos de Prehistoria, 46, 261-269.

Freestone, I. (1995) Ceramic Petrography. American Journal of Archaeology 99, 111-115.

Freestone, I.C. (2001) Post-depositional changes in archaeological ceramics and glasses. In: Brothwell, D.R. & Pollard, A.M. (eds.) Handbook of archaeological sciences, John Wiley, Chichester, 615-625.

Freestone, I.C., Leslie, K.A., Thirlwall, M. and Gorin-Rosen, Y. (2003) Strontium isotopes in the investigation of early glass production: Byzantine and early Islamic glass from the Near East. Archaeometry 45, 19-32

Gale, N.H. (1981) Mediterranean obsidian source characterization by strontium isotope analysis. Archaeometry, 23, 41-51.

Garcea, E.A.A., and Hildebrand, E.A. (2009) Shifting social networks along the Nile: Middle Holocene ceramic assemblages from Sai Island, Sudan. Journal of Anthropological Archaeology, 28(3), 304–322.

Garzanti, E., Andò S., Padoan, M., Vezzoli, G., and El Kammar, A. (2015) The modern Nile sediment system: Processes and products. Quaternary Science Reviews, 130, 9-56

Garzanti, E., Andò, S., Vezzoli, G., Ali Abdel Megid, A., and El Kammar, A. (2006) Petrology of Nile River sands (Ethiopia and Sudan): Sediment budgets and erosion patterns. Earth and Planetary Science Letters, 252(3–4), 327-341

Gatto, M.C. (2006) The Most Ancient Pottery from the Dongola Reach (Northern Sudan): New Data from the SFDAS Survey Related to the Construction of the Merowe Dam. Archéologie du Nil Moyen 10: 73-86.

Gilpin, D., Hays-Gilpin, K. (2012) Polychrome pottery of the Hopi Mesas. In: Cordell, L.S., Habicht-Mauche, J.H. (eds.), Potters and Communities of Practice: Glaze Paint and Polychrome Pottery in the American Southwest, AD 1250 to 1700, Anthropological Papers of the University of Arizona, vol. 75. The University of Arizona Press, Tucson, 45-54.

Govindaraju, K. (1994) Compilation ofworking values and sample description for 383 geostandards. Geostand. Newslett. 18 (Special Issue), 1-158.

Grattan-Bellew, P.E., Litvan, G.G. (1978) X-ray diffraction method for determining the firing temperature of clay brick. American Ceramic Society Bulletin 57, 493-495.

Haaland, R. (1993) Aqualithic sites of the Middle Nile. Azania, 28, 47–86.

Haaland, R., Magid, A. (1995) Aqualithic Sites along the Rivers Nile and Atbara, Sudan (Alma Mater, Forlag).

Heimann, R.B., Franklin, U.M. (1972) Archaeo-thermometry: the assessment of firing temperatures of ancient ceramics. J. Int. Inst. Conserv. 4, 23-45.

Heimann, R.B., Maggetti, M. (1981) Experiment on simulated burial of calcareous Terra Sigillata (mineralogical change). Preliminary Results. British Museum Occasional Paper, 163-177.

Hinkel, F. (1977) The Archaeological Map of the Sudan. A Guide to its Use and Explanations of its Principles. Berlin: Akademie Verlag.

Hoelzmann, P., Keding, B., Berke, H., Kröpelin, S., and Kruse, H.-J. (2001) Environmental change and archaeology: lake evolution and human occupation in the

eastern Sahara during the Holocene, Palaeogeography, Palaeoclimatology, Palaeoecology, 169, 193–217.

Hommel, P., Day, P.M., Jordan, P., and Vetrov V.M. (2016) Context is Everything: Early Pottery, Hunter-gatherers and the Interpretation of Technological Choices in Eastern Siberia. In E. Sibbesson, B. Jervis, and S. Coxon (eds.), Insight from Innovation: New Light on Archaeological Ceramics. Papers in Honour of Professor David Peacock. Southampton: Southampton Monographs, 1-18.

Honegger, M. (2005) El-Barga: un site clé pour la compréhension du Mésolithique et du début du Néolithique en Nubie. Revue de Paléobiologie, 10, 95–104.

Honegger, M. (2010) La Nubie et le Soudan: un bilan des vingt dernières années de recherche sur la pré-et protohistoire. ARCHÉO-NIL, 20, 77–86.

Honegger, M. (2014) Recent Advances in Our Understanding of Prehistory in Northern Sudan. In: Anderson J.R. and Welsby D.A. (eds). The Fourth Cataract and Beyond. Proceedings of the 12th International Conference for Nubian Studies. Leuven, Peeters: 19-30.

Hoopes, J.W., and Barnett, W.K. (1995) The shape of early pottery studies. In Barnett, W.K., and Hoopes, J. W. (eds.), The Emergence of Pottery. Technology and Innovation in Ancient Societies, Smithsonian Institution Press, Washington, DC, 1-7.

Huysecom, E., Rasse, M., Lespez, L. et al. (2009) The emergence of pottery in Africa during the tenth millennium cal BC: new evidence from Ounjougou (Mali). Antiquity 83, 905-917.

Ingham, J.P. (2010) Geomaterials under the microscope: a colour guide. Manson Publishing Ltd, London.

Jesse, F. (2000) Early Khartoum Ceramics in the Wadi Howar, Nothwest Sudan. Recent Research into the Stone Age of Northeastern Africa, (eds.) Krzyżaniak L, Kroeper K, M. Kobusiewicz M (Poznań Archaeological Museum, Berlin), pp. 77-87.

Jesse, F. (2003) Rahib 80/87. Ein Wavy-Line-Fundplatz im Wadi Howar und die früheste Keramik in Nordafrika. (Africa Praehistorica 16). Köln: Heinrich-Barth-Institut.

Jesse, F. (2004) The development of pottery design styles in the Wadi Howar Region (Northern Sudan). Préhistoire Anthropologie Méditerranéennes, 13, 97–107.

Jesse, F. (2010) Early pottery in Northern Africa. Journal of African Archaeology 8, 219-238.

Jiang, L. and Liu, L. (2006) New evidence for the origins of sedentism and rice domestication in the Lower Yangzi River, China. Antiquity 80, 355-361.

Khabir, A.M. (1985) A note on the excavation of a Neolithic site in the Sarurab Area, Khartoum Province. Nyame Akuma, 26, 40.

Khabir, A.M. (1987) New Radiocarbon Dates for Sururab 2 and the Age of the Early Khartoum Tradition. Current Anthropology 28: 377-380.

Khabir, A.M. (1987) Petrographic and X-ray analyses of Neolithic pottery from Sarurab. Nyame Akuma, 28, 45-46.

Khabir, A.M. (1991a) The firing index of Neolithic pottery from Central Nile. Nyame Akuma, 35, 33-35.

Khabir, A.M. (1991b) A qualitative change in the texture of temper of Neolithic ceramics from the Central Nile Valley, Sahara, 4, 145-147.

Klein, M., Jesse, F., Kasper, H.U., Gölden, A. (2004) Chemical characterization of ancient pottery from Sudan by X-ray fluorescence spectrometry (XRF), electron microprobe analysis (EMPA) and inductively coupled plasma mass spectrometry (ICP-MS). Archaeometry, 46, 339-356.

Knacke-Loy, O. (1994) Isotopengeochemische, chemische und petrographische Untersuchungen zur Herkunfstbestimmung der bronzezeitlichen Keramik von Troia. Heidelberger Geowissenschaftliche Abhandlungen 77: 1–193.

Kreiter, A., Riebe, D.J, Parkinson, W.A. et al. (2014) Unique in its chaîne opératoire, unique in its symbolism: undressing a figurine from the 6th Millennium BC Körös culture, Hungary. Journal of Archaeological Science 44, 136-147.

Kröpelin, S. (1993) Zur Rekonstruktion der spätquartären Umwelt am Unteren Wadi Howar (Südöstliche Sahara/NWSudan), Selbstverlag des Geomorphologischen Laboratoriums der Freien Universität Berlin.

Krzyżaniak, L. (2002) Early Khartoum Pottery from Kadero in Tides of the Desert - Gezeiten der Wüste. Contributions to the Archaeology and Environmental History of Africa in Honour of Rudolph Kuper (Heinrich-Barth-Institut, Köln), pp. 199-201.

Li, B.P., Zhao, J.X., Greig, A., Collerson, K.D., Zhuo, Z.X., Feng, Y.X. (2005) Potential of Sr isotopic analysis in ceramic provenance studies: characterization of Chinese stoneware. NIMB, 240, 726-732.

Link, K., Koehn, D., Barth, M.G., Tiberindwa, J.V., Barifaijo, E., Aanyu, K. and Foley, S.F. (2010) Continuous cratonic crust between the Congo and Tanzania blocks in western Uganda. Int. J. Earth Sci. 99, 1559–1573.

Ludwig, K.R. (1993) Analyst (Version 2.20), A computer program for control of a thermal-ionization, single-collector mass-spectrometer, USGS Open File Report 92-543, 1-92.

Ma, H., Henderson, J., Evans, J. (2014) The exploration of Sr isotopic analysis applied to Chinese glazes: part one. Journal of Archaeological Science 50, 551-558.

Maggetti, M. (1982) Phase analysis and its significance for technology and origin. In: Olin, J.S. & Franklin A.D. (eds.) Archaeological ceramics. Smithsonian Institution Press, Washington. 121-133.

Maggetti, M., Westley, H., Olin, J. (1984) Provenance and technical studies of Mexican majolica using elemental and phase analysis. In: Lambert, J.B. (Ed.), ACS Advances in Chemistry Series, No.205. Archaeological Chemistry III. American Chemical Society, 151–191

Mange, M.A. and Bezeczky, T. (2007) The provenance of paste and temper in Roman amphorae from the Istrian Peninsula, Croatia. In: Mange, M.A. & Wright, D.T. (eds) Heavy minerals in use: Developments in Sedimentology, 58, Elsevier, Amsterdam, 1007-1033.

Mangueira, G.M., Toledo, R., Teixeira, S., Franco, R.W.A. (2011) A study of the firing temperature of archaeological pottery by X-ray diffraction and electron paramagnetic resonance. Journal of Physics and Chemistry Solids 72, 90-96.

Manzo, A. (2016) Italian archaeological expedition to the eastern Sudan of the University of Naples "L'Orientale". Preliminary report of the 2015 field season. Newsletter di Archeologia CISA 7: 191-202.

Maritan, L. (2004) Archaeometric study of Etruscan-Padan type pottery from the Veneto region: petrographic, mineralogical and geochemical–physical characterisation. European Journal of Mineralogy 16, 297-307.

Maritan, L., Angelini, I., Artioli, G., Mazzoli, C., Saracino, M. (2009) Secondary phosphates in the ceramic materials from Frattesina (Rovigo, North-Eastern Italy). Journal of Cultural Heritage, 10, 144-151.

Maritan, L., Holakooei, P., Mazzoli, C. (2015) Cluster analysis of XRPD data in ancient ceramics: What for? Applied Clay Science 114, 540-549.

Maritan L., Iacumin P., Zerboni A., Venturelli G., Dal Sasso G., Linseele V., Salvatori S., Usai D. (submitted) The oldest evidence of fish salting along the Nile (7th millennium BC). Submitted to Journal of Archaeological Science

Maritan, L. and Mazzoli, C. (2004) Phosphates in archaeological finds: implications for environmental conditions of burial. Archaeometry 46, 673-683.

Maritan, L., Secco, M., Mazzoli, C., Artioli, G. (2012) Secondary phases in archaeological and historical materials: a microstructural approach for interpreting the correct sequences of crystallization. In "SEM and microanalysis in the study of historical technology, materials and conservation" Eds. N. Meeks, C. Cartwright, A. Meek and A. Mongiatti, Archetype Publications.

Maritan, L., Secco, M., Mazzoli, C., Mantovani, V., Bonetto, J. (2013) The decorated Padan terra sigillata from the site of Retratto, Adria (north-eastern Italy): provenance and production technology. Applied Clay Science 82, 62-69.

Mariotti Lippi, M., Gonnelli, T., Pallecchi, P. (2011) Rice chaff in ceramics from the archaeological site of Sumhuram (Dhofar, Southern Oman), Journal of Archaeological Science, Volume 38, Issue 6, 1173-1179

Marks, A.E., Mohammed-Ali, A. (1991) The Late Prehistory of the Eastern Sahel. The Mesolithic and the Neolithic of Shaqadud, Sudan (Southern Methodist University Press Dallas).

Martin-Socas, D., Camalich-Massieu, M.D., Tejedor-Salguero, M.L., Rodriguez-Rodriguez, A. (1989) Mineralogical composition and evaluation of firing temperatures of the Purchena pottery (Almeria, Spain). In: Maniatis, Y. (Ed.), Proceedings of the 25th International Symposium of AmsterdamArchaeometry. Elsevier, Amsterdam, 149–157.

Mills, B.J. (2007) Performing the feast: visual display and suprahousehold commensalism in the Puebloan southwest. Am. Antiq. 72, 210-239.

Moore, A.M.T. (1995) The inception of potting in western Asia and its impact on economy and society. In Barnett, W. K., and Hoopes, J. W. (eds.), The Emergence of Pottery. Technology and Innovation in Ancient Societies, Smithsonian Institution Press, Washington, DC, 39-53.

Neumann, K. (1989) Holocene vegetation of the eastern Sahara: charcoal from prehistoric sites, African Archaeological Review, 7, 97–116.

Nodari, L., Maritan, L., Mazzoli, C., Russo, U. (2004) Sandwich structures in the Etruscan-Padan type pottery. Applied Clay Science 27, 119-128.

Nordström, H.Å. (1972) Neolithic and A-Group Sites, Vols. 3:1-2, Uppsala/Lund.

Nyssen, J., Poesen, J., Moeyersons, J., Deckers, J., Haile, M., Lang, A. (2004) Human impact on the environment in the Ethiopian and Eritrean highlands — a state of the art, Earth-Sci. Rev. 273–320.

Obenauer, K. (1933) Die Verwendug Petrographischer Methoden in der Vorgeschichte. Nachr. Blatt f. Deutsch Vorseit 9, 10, 88-90.

Out, W.A., Ryan, P., García-Granero, J.J., Barastegui, J., Maritan, L., Madella, M., Usai, D. (2016) Plant exploitation in Neolithic Sudan: New insights from the cemeteries R12 and Ghaba in a wider perspective. Quaternary International, 412, 36-53.

Pachur, H.J., and Kröpelin, S. (1987) Wadi Howar: paleoclimatic evidence from an extinct river system in the southeastern Sahara, Science, 237, 298–300.

Padoan, M., Garzanti, E., Harlavan, Y., Villa, I.M. (2011) Tracing Nile sediment sources by Sr and Nd isotope signatures (Uganda, Ethiopia, Sudan). Geochim. Cosmochim. Acta,75, 3627-3644.

Papadopoulou, D.N., Lalia-Kantouri, M., Kantiranis, N., Stratis, J.A. (2006) Thermal and mineralogical contribution to the ancient ceramics and natural clays characterization. Journal of Thermal Analitical Calorimetry 84, 39-45.

Philpotts, A.R., Wilson, N. (1994) Application of petrofabric and phase equilibria analysis to the study of a potsherd. Journal of Archaeological Science 21, 607-618.

Pinter, F. (2005) Provenance Study of the Early Iron Age Knobbed Ware in Troia, NW Turkey and the Balkans. Petrographic And Geochemical Evidence. Dissertation, Eberhard-Karls-University of Tübingen, Germany.

Piovesan, R., Dalconi, C., Maritan, L., Mazzoli, C. (2013) X-ray powder diffraction diagram clustering and quantitative phase analysis on historic mortars. European Journal of Mineralogy 25, 165-175.

Pradell, T., Vendrell-Saz, M., Krumbein, W., Picon, M. (1996) Altérations de céramiquesen milieu marin: les amphores de l'épave romaine de la Madrague de Giens (Var). Revue d'Archéométrie 20, 47–56.

Price, T.D., Burton, J.H., Bentley, R.A. (2002) The Characterization of Biologically Available Strontium Isotope Ratios for the Study of Prehistoric Migration. Archaeometry, 44, 117-135.

Prudêncio, M.I., Dias, M.I., Gouveia, M.A., Marques, R., Franco, D., Trindade, M.J. (2009) Geochemical signatures of Roman amphorae produced in the Sado River estuary, Lusitania (Western Portugal). Journal of Archeological Science 36, 873-883.

Prudêncio, M.I., Oliveira, F., Dias M.I., Sequeira Braga, M.A., Delgado, M., Martins, M. (2006) Raw materials identification used for the manufacture of Roman "Bracarense" ceramics from NW Iberian Peninsula. Clay and Clay Minererals 54, 639-651.

Quinn, P.S. (2009) Interpreting Silent Artefacts: Petrographic Approaches to Archaeological Ceramics. Oxford, England: Archaeopress.

Quinn, P.S. (2013) Ceramic petrography: the interpretation of archaeological pottery and related artefacts in thin-sections. Archaeopress, Oxford.

Reedy, C.L. (1994) Thin-section petrography in studies of cultural materials. Journal of the American Institute of Conservation 33, 115-129.

Reedy, C.L. (2008) Thin-section Petrography of Stone and Ceramic Materials. Archetype, London.

Rice, P.M (1999) On the Origins of Pottery. Journal of Archaeological Method and Theory, 6-1, 1-54

Rodrigues, S.S.F. and Costa, M.L. (2016) Phosphorus in archaeological ceramics as evidence of the use of pots for cooking food. Applied Clay Science 123, 224-231.

Roosvelt, A.C., Lima da Costa, M., Lopes Machado, C., et al. (1996) Paleo-Indian Cave Dwellers in Amazon: The Peopling of the Americas. Science 272, 373-384.

Rye, O.S. (1981) Pottery Technology. Principles and Reconstruction (Manuals in Archaeology 4). Washington D.C.

Salvatori, S. (2012) Disclosing archaeological complexity of the Khartoum Mesolithic: New data at the site and regional level. African Archaeological Review, 29(4), 399-472.

Salvatori, S., Usai, D. (2007) The oldest representation of a Nile boat. Antiquity, 81 ,314

Salvatori, S., Usai, D. (2008) El Salha Project 2005: New Khartoum Mesolithic Sites from Central Sudan. Kush 19: 87-96.

Salvatori, S., and Usai, D. (2006) Archaeological research south of Omdurman. A preliminary assessment on ceramic and lithic materials from 10-X-6 multistratified mound site along the western bank of the White Nile in Central Sudan. Archéologie du Nil Moyen, 10, 203–220.

Salvatori, S. and Usai, D. (2016) Ghaba in Context. In: S. Salvatori, D. Usai, Y. Lecointe (eds), Ghaba: An Early Neolithic Cemetery in Central Sudan. Africa Magna Verlag. Frankfurt a.M.: 121-134.

Salvatori, S., Usai D., Faroug, M.A., Di Matteo, A., Iacumin, P., Lindseele, V., Magzoub, M.K. (2014) Archaeology at Al Khiday: New insight on the prehistory and history of Central Sudan. The Fourth Cataract and Beyond, (eds.) Anderson J.R., Welsby D.A. (Peeters, Leuven), 243-247

Salvatori, S., Usai, D., Zerboni, A. (2011) Mesolithic Site Formation and Palaeoenvironment along the White Nile (Central Sudan). African Archaeol. Rev., 28, 177-211.

Sampeck, K.E., (2011) Understanding identity: archaeological insights from colonial and post colonial North America and the Caribbean. SAA Archaeol. Rec. 4, 38-42.

Schwedt, A., Mommsen, H., Zacharias, N., Buxeda i Garrigós, J. (2006) Analcime crystallization and compositional profile-comparing approaches to detect post-depositional alteration in archaeological pottery. Archaeometry 48, 237–251.

Sebag D., Verrecchia E.P., Durand A. (1999) Biogeochemical cycle of silica in an apolyhaline interdunal holocene lake (Chad, N'Guigmi region, niger). Naturwissenschaften, 86 (10), 475-8

Secco, M., Maritan, L., Mazzoli, C. et al. (2011) Alteration processes of pottery in lagoon-like environments. Archaeometry 43, 809-829.

Secco, M., Maritan, L., Mazzoli, C., Lampronti, G.I., Zorzi, F., Nodari, L., Russo, U., Pesavento Mattioli, S. (2011) Alteration processes of pottery in lagoon-like environments. Archaeometry, 43, 809-829.

Shepard, A.O. (1942) Rio Grande glaze paint ware, a study illustrating the place of ceramic technological analysis in archaeological research. Carnegie Inst. Washington.

Shelach, G. (2012) On the invention of pottery. Science 336, 1644-1645.

Shiner, J.L. (1968) The Cataract tradition. In: Fred Wendorf (eds.), The Prehistory of Nubia, Dallas, 535-629.

Shirai, N. (2013) What makes the Neolithic in northeastern Africa? A new debate over an old issue for eliminating neighbourly ignorance. Neolithisation of Northeastern Africa, (eds.) Shirai N (Ex Oriente, Berlin), 1-3.

Stark, M.T. (2006) Glaze Ware technology, the social lives of pots, and communities

of practice in the late prehistoric southwest. In: Habicht-Mauche, J.A., Eckert, S.L., Huntley, D.L. (eds.), The Social Life of Pots: GlazeWares and Cultural Dynamics in the Southwest, A.D. 1250-1680. University of Arizona Press, Tucson.

Steiger, R.H., Jäger, E. (1977) Subcommission on geochronology: Convention on the use of decay constants in geo- and cosmochronology, Earth and Planetary Science Letters, Volume 36, Issue 3, Pages 359-362

Stoops, G. (2003) Guidelines for analysis and description of soil and regolith thin sections. Soil Science Society of America. Wisconsin.

Suková, L., Varadzin, L. (2012) Preliminary report on the exploration of Jebel Sabaloka (West Bank), 2009-2012. Sudan & Nubia 16: 118-131.

Sutcliffe, J.V., Parks, Y.P. (1999) The hydrology of the Nile, Int. Assoc. Hydrol. Sci. Spec. Publ. 5, 179 pp.

Talbot, M.R., Williams M.A.J. and Adamson D.A. (2000) Strontium isotope evidence for late Pleistocene re-establishment of an integrated Nile drainage network. Geology 28: 343–346.

Tite, M.S. (1995) Firing Temperature Determination: How and Why? In: Lindahl, A., Stilberg, O. (eds.), Konfrenser, Stockholm, 37-42.

Tite, M.S., Freestone, I.C., Meeks, N.D., Bimson, M. (1982) The use of scanning electron miscorscope iin the technological examination of ancient ceramics. In "Archaeological ceramics" (eds.) Olin J.S. and Franklin A.D., Smithsonian Institute, Washington, 109-120.

Tite, M.S. and Maniatis, Y. (1975) Examination of ancient pottery using the scanning electron microscope. Nature 257, 122-123.

Tomber, R., Cartwright, C. and Gupta, S. (2011) Rice temper: technological solutions and source identification in the Indian Ocean. Journal of Archaeological Science 38, 360-366.

Underhill, A.P. (1997) Current issues in Chinese Neolithic archaeology. Journal of World Prehistory, 11, 103-160.

Usai, D. (2014) Recent advances in understanding the prehistory of Central Sudan. In: The Fourth Cataract and Beyond. Proceedings of the 12th International Conference for Nubian Studies, edited by J. R. Anderson and D. A. Welsby, 31–44.

Usai, D., and Salvatori, S. (2002). The IsIAO El-Salha archaeological project. Sudan & Nubia, 6, 67–72.

Usai, D., Salvatori, S. (2005) The IsIAO Archaeological Project in the el Salha Area (Omdurman South, Sudan): Results and Perspectives. Africa 60: 474-493.

Usai, D., Salvatori, S., Iacumin, P., Di Matteo, A., Jakob, T., Zerboni, A. (2010) Excavating a unique pre-Mesolithic cemetery in central Sudan. Antiquity, 84, 323.

Velraj, G., Mohamed Musthafa, A., Janaki, K., Deenadayalan, K., Basavaiah, N. (2010) Estimation of firing temperature and ancient geomagnetic field intensity of archaeological potteries recently excavated from Tamilnadu, India. Applied Clay Science 50, 148-153.

Verpoorte, A. (2001) Places of art, traces of fire: A contextual approach to anthropomorphic figurines in the Pavlovian (Central Europe, 29-24 kyr BP). Archaeological Studies of Leiden University 8, Leiden.

Vitali, V. and Franklin, U. (1986) New approaches to the characterization and classification of ceramics on the basis of their elemental composition. Journal of Archaeological Science 13: 161-170.

Walther, B.D., and Thorrold, S.R. (2006) Water, not food, contributes the majority of strontium and barium deposited in the otoliths of a marine fish. Marine Ecology Progress Series, 311: 125–130.

Welsby, D. (1997) Early pottery in the middle Nile valley. In Freestone, I., and Gaimster, D. (eds.), Pottery in the Making. Ceramic Traditions, Smithsonian Institution Press, Washington, DC, 26-31.

Whitbread, I.K. (1986) The characterisation of argillaceous inclusions in ceramic thin sections. Archaeometry 28, 79-88.

Whitbread, I.K. (1989) A proposal for the systematic description of thin sections towards the study of ancient ceramic technology. In: Maniatis, Y. (eds.), Proceedings of the 25th International Symposium of Archaeometry. Elsevier, Amsterdam, 127-138

Whitbread, I.K. (1995) Greek transport of amphorae – A petrological and archaeological study. British School at Athens, Fitch laboratory occasional paper, 4.

Whiteman, A.J. (1971) The Geology of the Sudan Republic. London (Clarendon Press: Oxford University Press).

Williams, D.F. (1983) Petrology of ceramics. In: D.R.C. Kempe, A.P. Harvey (eds.) The Petrology of Archaeological Artefacts. Claredon Press, Oxford. 301-329.

Williams, M.A.J. (2012) Geomorphology and Quaternary Geology of the Region Between Wadi El-Arab and Kerma. Documents de la mission archéologique Suisse au Soudan 4: 10-15.

Williams, M.A.J., Adamson, D. (1980) Late Quaternary depositional history of the Blue and White Nile rivers in central Sudan. In: M.A.J. Williams, H. Faure (eds.), The Sahara and the Nile, Rotterdam, Balkema, Rotterdam, 281–304

Williams, M.A.J., Adamson, D., Cock, B., McEvedy, R. (2000) Late Quaternary environments in the White Nile region, Sudan. Global and Planetary Change 26: 305-316.

Williams, M.A.J., Adamson, D., Prescott, J.R. and Williams, F.M. (2003) New light on the age of the White Nile. Geology 31, 1001–1004.

Williams, M.A.J., Jacobsen, G.E.A. (2011) A wetter climate in the desert of northern Sudan 9900–7600 years ago. Sahara 22: 7-14.

Williams, M.A.J., Talbot, M., Aharon, P., Salaam, Y.A., Williams, F. and Brendeland, K.I. (2006) Abrupt return of the summer monsoon 15,000 year ago: new supporting evidence from the lower White Nile valley and Lake Albert. Quat. Sci. Rev. 25, 2651–2665.

Williams, M.A.J., Usai, D., Salvatori, S., Williams, F.M., Zerboni, A., Maritan, L., Linseele, V. (2015) Late Quaternary environments and prehistoric occupation in the lower White Nile valley, central Sudan, Quaternary Science Reviews, Volume 130, 72-88

Woodward, J.C., Macklin, M.G., Krom, M.D., Williams, M.A.J. (2007) The Nile: evolution, Quaternary river environments and material fluxes. In: A. Gupta (eds.), Large Rivers: Geomorphology and Management. John Wiley & Sons, Chichester, 261-292.

Woodward, J., Macklin, M., Fielding, L., Millar, I., Spencer, N., Welsby, D., and Williams, M. (2015) Shifting sediment sources in the world's longest river: A strontium isotope record for the Holocene Nile. Quaternary Science Reviews, 130, 124-140

Woodward, J.C., Williams, M.A.J., Garzanti, E., Macklin, M.G., and Marriner, N. (2015) From source to sink: Exploring the quaternary history of the Nile. Quaternary Science Reviews, 130, 3-8

Xu, X., Zhang, C., Goldberg, P., Cohen, D., Pan, Y., Arpin, T. and Bar-Yosef, O. (2012) Early pottery at 20.000 years ago in Xianrendong Cave, China. Science 336, 1696-1700.

Zedeño, M.N. (2001) The pottery of Nabta Playa. Holocene settlement of the Egyptian Sahara, Vol. 2 (eds. K- Nelson), New York, 51-64.

Zerboni, A. (2011) Micromorphology Reveals in Situ Mesolithic Living Floors and Archaeological Features in Multiphase Sites in Central Sudan. Geoarchaeology: An International Journal, 26, 365-391.

Zerboni, A. (2013) Early Holocene palaeoclimate in North Africa: An overview. In: N. Shirai (eds.), Neolithisation of Northeastern Africa. ex oriente, Berlin, 65-82.